University of California
Los Angeles

Informationally Efficient Multi-User Communication

A dissertation submitted in partial satisfaction
of the requirements for the degree
Doctor of Philosophy in Electrical Engineering

by

Yi Su

2010

The dissertation of Yi Su is approved.

Lixia Zhang

Gregory J. Pottie

Jason L. Speyer

Mihaela van der Schaar, Committee Chair

University of California, Los Angeles

2010

To my parents

Table of Contents

List of Figures

List of Tables

Acknowledgments

Foremost, I would like to thank my family for their love, endless support, and encouragement during my Ph.D. study at UCLA. Words cannot describe my immense gratitude for my parents whose kindness and inspiration have helped me pursue my life long dreams.

I would like to express my sincere appreciation and deepest gratitude to my advisor Professor Mihaela van der Schaar for her constant support and invaluable guidance throughout the past four years. I really appreciate her integral vision of research and her strive for high-quality work. I have benefited tremendously from her unique blend of enthusiasm, energy, and technical insights. I feel very fortunate to have had the opportunity to work under her supervision.

I have had the good fortune to have learned from and have worked with so many incredible individuals at UCLA during my Ph.D. study. I would like to thank all my friends for the great time we had together. In particular, I would like to thank all my colleagues of the Multimedia Communications and Systems Lab in the Electrical Engineering Department at UCLA.

Finally I would like to acknowledge that my Ph.D work was supported in part by the National Science Foundation under grants CCF-0830556 and CCF-0541867 and in part by grants from UC Micro and ONR.

Vita

1982	Born, Guilin, China.
2004	B.E. in Electronic Engineering Department, Tsinghua University, Beijing, China.
2006	M.E. in Electronic Engineering Department, Tsinghua University, Beijing, China.
2006–2010	Research Assistant, Electrical Engineering Department, University of California, Los Angeles, Los Angeles, California.
2009	Summer Intern, Qualcomm, Santa Clara, California.

Publications

Y. Su and M. van der Schaar, "Dynamic conjectures in random access networks using bio-inspired learning," to appear in *IEEE Journal on Selected Areas in Communications (JSAC), Special Issue on Bio-Inspired Networking*, vol. 28, no. 4, pp. 587-601, May 2010.

Y. Su and M. van der Schaar, "Conjectural equilibrium in multiuser power control games," *IEEE Transactions on Signal Processing*, vol. 57, no. 9, pp. 3638-3650, September, 2009.

Y. Su and M. van der Schaar, "A new perspective on multi-user power control games in interference channels," *IEEE Transactions on Wireless Communications*, vol. 8, no. 6, pp. 2910-2919, June 2009.

Y. Su and M. van der Schaar, "Minimum required learning and impact of information feedback delay for cognitive users," *IEEE Transactions on Vehicular Technology*, vol. 58, no. 6, pp. 2825-2834, July 2009.

Y. Su and M. van der Schaar, "Multi-user multimedia resource allocation over multi-carrier wireless networks," *IEEE Transactions on Signal Processing*, vol. 56, no. 5, pp. 2102-2116, May 2008.

Y. Su and M. van der Schaar, "A simple characterization of strategic behaviors in broadcast channels," *IEEE Signal Processing Letters*, vol. 15, pp. 37-40, 2008.

Y. Su and M. van der Schaar, "Conjectural equilibrium in water-filling games," in *Proc. IEEE Global Telecommunications Conference (Globecom)*, pp. 1-7, Honolulu, Hawaii, December 2009.

Y. Su and M. van der Schaar, "From competition to coopetition: Stackelberg equilibrium in multi-user power control games," in *Proc. International Conference on Game Theory for Networks (Gamenets)*, pp. 107-116, Istanbul, Turkey, May 2009.

Y. Su and M. van der Schaar, "Learning for cognitive wireless users," in *Proc. IEEE Symposia on New Frontiers in Dynamic Spectrum Access Networks (DyS-*

PAN), pp. 1-5, Chicago, Illinois, October 2008.

Y. Su and M. van der Schaar, "How much learning is sufficient for interference games?" in *Proc. 1st IAPR Workshop on Cognitive Information Processing (CIP)*, pp. 12-17, Santorini, Greece, June 2008.

Y. Su and M. van der Schaar, "Resource allocation for multi-user video transmission over multi-carrier networks," in *Proc. IEEE International Conference on Communications (ICC)*, pp. 4138-4143, Beijing, China, May 2008.

Y. Su and M. van der Schaar, "A new look at multi-user power control games," in *Proc. IEEE International Conference on Communications (ICC)*, pp. 1072-1076, Beijing, China, May 2008.

Abstract of the Dissertation

Informationally Efficient Multi-User Communication

by

Yi Su

Doctor of Philosophy in Electrical Engineering

University of California, Los Angeles, 2010

Professor Mihaela van der Schaar, Chair

The rapid increase in the demand for data rate over wired and wireless communication networks has led to a rethinking of the traditional network architecture and design principles. In fact, communication systems are inherently informationally decentralized competitive environments, where multiple devices executing a variety of applications and services need to locally adapt their transmission strategies based on their available information and compete for scarce networking resources. The concepts and techniques that have dominated multi-user communication research in recent years are not well suited for these informationally decentralized environments. Specifically, most existing research has focused on two extreme multi-user interaction scenarios, the complete information scenario with a common system-wide objective (e.g. Pareto optimality) and the private information scenario with conflicting objectives (e.g. Nash equilibrium (NE)).

The objective of this dissertation is to characterize users' optimal strategies to improve their performance subject to varying degrees of informational constraints. We mainly focus on fully distributed solutions without any real-time information exchange between different users. In particular, we investigate three key problems

in information-constrained multi-user communication systems. First, when will a distributed algorithm (e.g. best response dynamics) converge to a NE? And how fast? Second, if information is constrained and no real-time information exchange between users is allowed, how to improve an inefficient NE without message passing? Last, assuming no real-time information exchange between users, can we still achieve Pareto optimality? We propose and analyze two new classes of games named additively coupled sum constrained games and linearly coupled games, in which we individually address these three questions. In particular, we provide sufficient conditions under which a unique NE exists and best response dynamics linearly converges to the NE. We also provide conjectural equilibrium based solutions that can substantially improve the performance of inefficient NE and fully recover Pareto optimality without any real-time information exchange between users. The proposed game models apply to a variety of realistic applications in multi-user communication systems, including multi-channel power control, flow control, and wireless random access.

CHAPTER 1

Introduction

Mathematical communications theory that started with Shannon's seminal paper "A mathematical theory of communication" is a fairly young, but rapidly maturing science just over sixty years old. Shannon's original work focused on communication scenarios between a single transmitter and receiver pair [Sha48]. These communication models are referred to as single-user channels for which the capacities are now well-investigated. Practical communication systems are inherently competitive environments, where multiple transmitters and receivers executing a variety of applications and services share the same transmission medium and compete for limited network resources. As opposed to its single-user counterpart, the characterization of multi-user environments is much more complicated. This is because in resource-constrained communication networks, a user's utility is usually not only affected by its own action but also by the actions taken by all the other users sharing the same resources. Due to the mutual coupling among users, the performance optimization of multi-user communication systems becomes quite challenging.

1.1 Game Theory in Multi-user Communication

Game theory provides a formal framework for describing and analyzing the interactions of multiple decision makers. Recently, there has been a surge in research

activities that adopt game theoretic tools to investigate a wide range of problems in multi-user communication theory, such as flow and congestion control, network routing, load balancing, power control, peer-to-peer content sharing, etc [ABE06, MW01, FH06, NRT07, JLL09]. The majority of the existing game theoretic research works formalize the multi-user interactions in various communication scenarios as a strategic game, which is a suitable model for the analysis of a game where all users act independently and simultaneously according to their own self-interests and a priori knowledge of the other users' strategies. This can be formally defined as a tuple

$$\Gamma = \langle \mathcal{N}, \mathcal{A}, u \rangle. \tag{1.1}$$

In particular, $\mathcal{N} = \{1, 2, \ldots, N\}$ is the set of communication devices, which are the rational decision makers in the system. Define $\mathcal{A}$ to be the joint action set $\mathcal{A} = \times_{n \in \mathcal{N}} \mathcal{A}_n$, with $\mathcal{A}_n \subseteq \mathcal{R}^K$ being the action set available for user n. The vector utility function $u = \times_{n \in \mathcal{N}} u_n$ is a mapping from the individual users' joint action set to real numbers, i.e. $u : \mathcal{A} \rightarrow \mathcal{R}^N$. In particular, $u_n(\mathbf{a}) : \mathcal{A} \rightarrow \mathcal{R}$ is the utility of the nth user that generally depends on the strategies $\mathbf{a} = (\mathbf{a}_n, \mathbf{a}_{-n})$ of all users, where $\mathbf{a}_n \in \mathcal{A}_n$ denotes a feasible action of user n, and $\mathbf{a}_{-n} = \times_{m \neq n} \mathbf{a}_m$ is a vector of the actions of all users except n. We also denote by $\mathcal{A}_{-n} = \times_{m \neq n} \mathcal{A}_m$ the joint action set of all users except n. To capture the multi-user performance tradeoff, the utility region is defined as $\mathcal{U} = \{(u_1(\mathbf{a}), \ldots, u_N(\mathbf{a})) | \ \exists \ \mathbf{a} = (a_1, a_2, \ldots, a_N) \in \mathcal{A}\}$. Depending on the characteristics of different applications, numerous game-theoretical models have been proposed to characterize the multi-user interactions and optimize the users' decisions in communication networks. A variety of game theoretic solutions, such as Nash equilibrium (NE) and Pareto optimality [FT91], have been developed to characterize the resulting performance of the multi-user interactions. Depend-

ing on the feasibility of real-time information exchange among users, significant research efforts have been devoted in the literature to constructing operational algorithms in order to achieve NE and Pareto optimality in various games with special structures of action set $\mathcal{A}_n$ and utility function u_n.

1.1.1 Nash Equilibrium

To avoid the overhead associated with exchanging information between users in real-time, network designers may prefer fully decentralized solutions in which the participating users simply compete against other users by choosing actions $\mathbf{a}_n \in \mathcal{A}_n$ to selfishly maximize their individual utility functions $u_n(\mathbf{a}_n, \mathbf{a}_{-n})$, given the actions $\mathbf{a}_{-n} \in \mathcal{A}_{-n}$. Most of these approaches focus on investigating the existence and properties of NE.

Definition 1.1 *A profile* $\mathbf{a}$ *of actions constitutes a Nash equilibrium of* Γ *if* $u_n(\mathbf{a}_n^*, \mathbf{a}_{-n}^*) \geq u_n(\mathbf{a}_n, \mathbf{a}_{-n}^*)$ *for all* $\mathbf{a}_n \in \mathcal{A}_n$.

At NE, given the other users' actions, no user can increase its utility alone by changing its action. For an extensive discussion of the methodologies studying the existence, uniqueness, and convergence of various equilibria in communication networks, we refer the readers to [LDA09].

For example, to establish the existence of and convergence to a pure NE, we can examine whether $\mathcal{A}$ and u satisfy the conditions of concave games, supermodular game, potential game, etc. Specifically, to apply the existence result of a pure NE in concave games [FT91, Ros65], we need to check the following conditions: i) each player's action set $\mathcal{A}_n$ is convex and compact; and ii) the utility function $u_n(\mathbf{a}_n, \mathbf{a}_{-n})$ is continuous in $\mathbf{a}$ and quasi-concave[1] in $\mathbf{a}_n$ for any fixed

[1] A real-valued function f is quasi-concave if $\mathrm{dom} f$ is convex and $\{x \in \mathrm{dom} f | f(x) \geq \alpha\}$ is convex for all α.

$\mathbf{a}_{-n}$. As additional examples of games that guarantee the convergence to NE, it is well-known that, in supermodular games [Top98, AA03] and potential games [MS96, SBP06], the best response dynamics can be used to search for a pure NE. Suppose that utility function u_n is twice continuously differentiable, $\forall n \in \mathcal{N}$. If $\mathcal{A}_n$ is a compact subset of $\mathcal{R}$ (or more generally $\mathcal{A}_n$ is a nonempty and compact sublattice[2] of $\mathcal{R}^K$), $\forall n \in \mathcal{N}$, establishing that game Γ is a supermodular game is equivalent to showing that u_n satisfies

$$\forall (m,n) \in \mathcal{N}^2, m \neq n, \frac{\partial^2 u_n}{\partial \mathbf{a}_n \partial \mathbf{a}_m} \geq 0. \tag{1.2}$$

If action set $\mathcal{A}$ in game Γ is an interval of real numbers, we can show that game Γ is a potential game by verifying

$$\forall (m,n) \in \mathcal{N}^2, m \neq n, \frac{\partial^2 (u_n - u_m)}{\partial \mathbf{a}_n \partial \mathbf{a}_m} = 0. \tag{1.3}$$

1.1.2 Pareto Optimality

It is important to note that operating operating at a Nash equilibrium will generally limit the performance of the user itself as well as that of the entire network, because the available network resources are not always effectively exploited due to the conflicts of interest occurring among users. As opposed to the NE-based approaches, there exists a large body of literature that focuses on studying how users can *jointly* improve the system performance by optimizing a certain common objective function $f(u_1(\mathbf{a}), u_2(\mathbf{a}), \ldots, u_N(\mathbf{a}))$. This function represents the fairness rule based on which the system-wide resource allocation is performed. Different objective functions, e.g. sum utility maximization in which $f(u_1(\mathbf{a}), u_2(\mathbf{a}), \ldots, u_N(\mathbf{a})) = \sum_{n=1}^{N} u_n(\mathbf{a})$, can provide reasonable allocation outcomes by jointly considering fairness and efficiency. A profile of actions is Pareto

[2] A real K-dimensional set $\mathcal{V}$ is a *sublattice* of $\mathcal{R}^K$ if for any two elements $a, b \in \mathcal{V}$, the component-wise minimum, $a \wedge b$, and the component-wise maximum, $a \vee b$, are also in $\mathcal{V}$.

optimal if there is no other profile of actions that makes every user at least as well off and at least one user strictly better off.

The majority of these approaches focus on studying how to efficiently or distributedly find the optimum joint policy. There exists a large body of literature that investigates how to compute Pareto optimal solutions in large-scale networks where centralized solutions are infeasible. Numerous convergence results have been obtained for various generic distributed algorithms. An important example is the NUM framework that develops distributed algorithms to solve network resource allocation problems [CLC07]. The majority of the results in the existing NUM literature are based on convex optimization theory, in which the investigated problems share the following structures: the objective function $f(u_1(\mathbf{a}), u_2(\mathbf{a}), \ldots, u_N(\mathbf{a}))$ is convex[3], inequality resource constraint functions are convex, and equality resource constraint functions are affine. It is well-known that, for convex optimization problems, users can collaboratively exchange price signals that reflect the "cost" for consuming the constrained resources between each other and the Pareto optimal allocation that maximizes the network utility can be determined in a fully distributed manner [PC06].

Summarizing, these general structural results without and with real-time message exchange turn out to be very useful when analyzing various multi-user interactions in communication networks. The majority of the existing game theoretic research works in communication networking applications usually depend on these specific structures and inter-user coupling of their action sets and utility functions. By considering or even architecting these specific structures, the associated games become analytically tractable and possess various important convergence properties. Numerous existing works are devoted to constructing or shaping the

[3] $f : \mathrm{R}^n \to \mathrm{R}$ is convex if $\mathrm{dom} f$ is a convex set and $f(\theta x + (1-\theta)y) \leq \theta f(x) + (1-\theta) f(y)$, $\forall x, y \in \mathrm{dom} f, 0 \leq \theta \leq 1$.

multi-user coupling such that it fits into these frameworks and the corresponding generic solutions can be directly applied.

1.2 Motivation

The rapid increase in the demand for data rate over wired and wireless communication networks has led to a rethinking of the traditional network architecture and design principles. In fact, communication systems are inherently informationally decentralized competitive environments, where multiple devices executing a variety of applications and services need to locally adapt their transmission strategies based on their available information and compete for scarce networking resources. The concepts and techniques that have dominated multi-user communication research in recent years are not well suited for these informationally decentralized environments. Specifically, most existing research has focused on two extreme multi-user interaction scenarios:

- the complete information scenario with a common system-wide objective. This scenario assumes either that all participating users transmit their private information to a trusted moderator or peer (e.g. access point, base station, selected network leader etc.), to which it is given the authority to fairly divide the wireless resources among the participating users or that, in a distributed environment, users exchange information between each other such that the information required for achieving the common objective is obtained. These solutions can lead to Pareto efficient allocations at the cost of a large amount of information exchange.

- the private information scenario with conflicting objectives, where selfish users interact by assuming no or limited information about each other (e.g. infor-

mation about the other users' channel or traffic characteristics) , usually resulting in inefficient solutions such as NE.

Both aforementioned communications scenarios encourage a passive participation of the users in the multi-user interaction, because they assume that users cannot proactively influence the resource division. However, such multi-user network designs do not take advantage of the transceivers' "smartness" (i.e. their ability to acquire information, learn and reason about their opponents). Interestingly, these passive interactions among users may lead in practice to inefficient resource usage. Even in fully collaborative communications scenarios, some users may not be able to exchange certain desired information. This is because they are not able to make optimal decisions on which information to exchange due to their bounded rationality (e.g. limited memory or complexity constraints), or because they cannot transmit their complete private information due to their communication constraints.

1.3 Overview of Dissertation

The objective of this dissertation is to characterize users' optimal strategies to improve their performance subject to varying degrees of informational constraints in several classes of multi-user communication environments. We will mainly focus on fully distributed solutions without any real-time information exchange between different users, which perfectly satisfy the informationally efficient requirement in communication systems. In particular, to achieve the coordination purpose without real-time information exchange, we will fully explore the structures of the investigated inter-user coupling, enable the devices to proactively accumulate information via observed outcomes of the historical interactions with other devices and, based on this information, build their beliefs about the competing

devices and the environment to optimize their transmission strategies.

In order to capture the characteristics of mutual coupling among multiple users and classify various communication games, we need to introduce two new elements $\mathcal{S}$ and s into the traditional strategic game formulation [FT91] and redefine the multi-user game in various communication scenarios as a tuple

$$\Gamma = \langle \mathcal{N}, \mathcal{A}, u, \mathcal{S}, s \rangle. \tag{1.4}$$

Specifically, $\mathcal{S}$ is the *state space* $\mathcal{S} = \times_{n\in\mathcal{N}}\mathcal{S}_n$, where $\mathcal{S}_n$ is the part of the state relevant to user n. The state is defined to capture the effects of the multi-user coupling such that each user's utility solely depends on its own state and action. In other words, the utility function $u = \times_{n\in\mathcal{N}}u_n$ is a mapping from the individual users' state space and action space to real numbers, $u_n : \mathcal{S}_n \times \mathcal{A}_n \to \mathcal{R}$. The state determination function $s = \times_{n\in\mathcal{N}}s_n$ maps joint actions to states for each component $s_n : \mathcal{A}_{-n} \to \mathcal{S}_n$ in which $\mathcal{A}_{-n} = \times_{m\neq n}\mathcal{A}_m$. Note that traditional strategic games simply assume $\mathcal{S}_n = \mathcal{A}_{-n}$.

Based on the formulation above, we derive several important structural results for several special classes of multi-user interaction scenarios in communication networks under the informationally efficient constraint. In particular, we want to investigate three key problems in information-constrained multi-user communication systems:

Question 1: When will a distributed algorithm (e.g. best response dynamics) converge to a NE? And how fast?

Question 2: If information is constrained and no information exchange between users is allowed, how to improve an inefficient NE without message passing?

Question 3: Assuming no real-time information exchange between users,

can we still achieve Pareto optimality ?

First of all, to address Question 1, Chapter 2 proposes and analyzes a broad family of games played by resource-constrained players, which are referred to as *Additively Coupled Sum Constrained Games* (ACSCG) and are characterized by the following central features: 1) each user has a multi-dimensional action space $\mathcal{A}_n$, subject to a single sum resource constraint; 2) user n's utility in a particular dimension k depends on an additive coupling between user n's action in the same dimension and a state determined by the actions of the other users; and 3) each user's total utility u_n is the sum of the utilities obtained in each dimension. Familiar examples of such multi-user environments in communication systems include power control over frequency-selective Gaussian interference channels and flow control in Jackson networks. In settings where users cannot exchange messages in real-time, we study how users can adjust their actions based on their local observations. We derive sufficient conditions under which a unique Nash equilibrium exists and the best-response algorithm converges globally and linearly to the Nash equilibrium. In settings where users can exchange messages in real-time, we focus on user choices that optimize the overall utility in distributed manner. We provide the convergence conditions of two distributed action update mechanisms, gradient play and Jacobi update.

As the first step to address Question 2, Chapter 3 considers the problem of how to allocate power among competing users sharing a frequency-selective interference channel. The multi-channel power control game is a special case of ACSCG in which user n's state represents its experienced interference in different channels. We model the interaction between selfish users as a non-cooperative game. As opposed to the existing iterative water-filling algorithm that studies the myopic users, this chapter studies how a foresighted user, who knows the

channel state information and response strategies of its competing users, should optimize its transmission strategy. To characterize this multi-user interaction, the Stackelberg equilibrium is introduced, and the existence of this equilibrium for the investigated non-cooperative game is shown. We analyze this interaction in more detail using a simple two-user example, where the foresighted user determines its transmission strategy by solving as a bi-level program which allows him to account for the myopic user's response. It is analytically shown that a foresighted user can improve its performance, if it has the necessary information about its competitors. Since the optimal solution of Stackelberg equilibrium is computationally prohibitive, we propose a practical low-complexity approach based on Lagrangian duality theory. Surprisingly, numerical simulations show that, in most of the simulation settings, the Stackelberg equilibrium results in higher rates for both the foresighted and the myopic users.

To further address Question 2, Chapter 4 discusses how a foresighted user in multi-channel power control games can acquire its desired information by modeling its experienced interference as a function of its own power allocation. To characterize the outcome of the multi-user interaction, the conjectural equilibrium is introduced, and the existence of this equilibrium for the investigated power control game is proved. Interestingly, both the Nash equilibrium and the Stackelberg equilibrium are shown to be special cases of the generalization of conjectural equilibrium. We also develop practical algorithms to form accurate beliefs and search desirable power allocation strategies. We show that a foresighted user without any a priori knowledge of its competitors' private information can effectively learn the required information through repeated interaction with its competitors, and induce the entire system to an operating point that improves both its own achievable rate as well as the rates of the other participants in the power control game.

Finally, to answer Question 3, Chapter 5 and 6 discuss another special type of multi-user communication scenarios named linearly coupled games, in which users' states s_n are linearly impacted by their competitors' actions $\mathbf{a}_{-n}$. We characterize the inherent structures of the utility functions u_n for the linearly coupled games and define two basic types of linearly coupled games. Both the investigated Type I and Type II games apply to a variety of realistic applications encountered in the multiple access design, including wireless random access and rate control. For both Type I and Type II linearly coupled games, to improve the inefficient NE, we investigates the properties of conjectural equilibrium, in which individual users compensate for their lack of information by forming internal beliefs about their competitors. In both games, it is analytically shown that all the achievable operating points in the throughput region are essentially stable conjectural equilibria corresponding to different conjectures. Moreover, it is shown that the Pareto boundaries of the investigated linearly coupled games can be sustained as stable conjectural equilibria without real-time information exchange among users, if the belief functions are properly initialized. Specifically, Chapter 5 investigates Type II games and analyzes the necessary and sufficient condition that guarantees the global convergence of the best response and Jacobi update dynamics. Chapter 6 investigates Type I games using the wireless random access game as an illustrative example. We enables nodes to proactively gather information, form internal conjectures on how their competitors would react to their actions, and update their beliefs according to their local observations. In this way, nodes are capable to autonomously "learn" the behavior of their competitors, optimize their own actions, and eventually cultivate reciprocity in the random access network. Two distributed conjecture-based action update mechanisms, including best response and gradient play, are proposed to stabilize the random access network. The sufficient conditions that guarantee the

proposed conjecture-based algorithms to converge are derived. We also investigate how the conjectural equilibrium can be selected in heterogeneous networks and how the proposed methods can be extended to ad-hoc networks. Numerical simulations verify that the system performance significantly outperforms existing protocols, such as IEEE 802.11 Distributed Coordination Function (DCF) protocol and priority-based fair medium access control (P-MAC) protocol, in terms of throughput, fairness, convergence, and stability.

Chapter 7 summarizes the main points of the dissertation. In informationally decentralized multi-user environment, by exploring the structures of inter-user coupling and designing appropriate belief functions, conjectural equilibrium based solutions can achieve satisfactory performance without any real-time information exchange between users.

CHAPTER 2

Additively Coupled Sum Constrained Games

2.1 Introduction

Power control is one of the first few communication problems in which researchers started to apply game theoretic tools to formalize the multi-user interaction and characterize its properties. An interesting and important topic that has been extensively investigated recently is how to optimize multiple devices' power allocation when sharing a common frequency-selective interference channel. In [YGC02], Yu et. al. first defined such a power control game from a game-theoretic perspective, proposed a best-response algorithm in which all users iteratively update their power allocations using the water-filling solution, and proved several sufficient conditions under which the algorithm globally converges to a unique pure NE. Many follow-up papers further establish various sufficient convergence conditions with or without real-time information exchange for power control in communication networks [CSK03, CHC07, SPB08, HBH06, SBH08]. The purpose of this chapter is to introduce and analyze a general framework that abstracts the common characteristics of this family of multi-user interaction scenarios, which includes, but is not limited to the power control scenario. In particular, the main contributions of this paper are as follows.

First of all, we define the class of *Additively Coupled Sum Constrained Games* (ACSCG), which captures and characterizes the key features of several communi-

cation and networking applications. In particular, the central features of ACSCG are: 1) each user has a multi-dimensional strategy that is subject to a single sum resource constraint; 2) each user's payoff in each dimension is impacted by an additive combination of its own action in the same dimension and a function of the other users' actions; 3) users' utilities are separable across different dimensions and each user's total utility is the sum of the utilities obtained within each dimension.

Second, based on the feasibility of real-time information exchange, we provide the convergence conditions of various generic distributed algorithms in different scenarios. When no message exchanges between users are possible and every user maximizes its own utility, it is essential to determine whether a NE exists and if yes, how to achieve such an equilibrium. In ACSCG, a pure NE exists in ACSCG because ACSCG belongs to concave games [FT91, Ros65]. Our key contribution in this context is that we investigate the uniqueness of pure NE and consider the best response dynamics to compute the NE. We explore the properties of the additive coupling among users given the sum constraint and provide several sufficient conditions under which best response dynamics converges linearly[1] to the unique NE, for any set of feasible initialization with either sequential or parallel updates. We also explain the relationship between our results and the conditions previously developed in the game theory literature [Ros65, GM80]. When users can collaboratively exchange messages with each other in real-time, we present the sufficient convergence conditions of two alternative distributed pricing algorithms, including gradient play and Jacobi update, to coordinate users' action and improve the overall system efficiency. The proposed convergence conditions generalize the results that have been previously

[1]A sequence $x^{(k)}$ with limit x^* is linearly convergent if there exists a constant $c \in (0,1)$ such that $|x^{(k)} - x^*| \leq c|x^{(k-1)} - x^*|$ for k sufficiently large [BV04].

obtained in [YGC02, CSK03, CHC07, SPB08, HBH06, SBH08] for the multi-user power control problem and they are immediately applicable to other multi-user applications in communication networks that fulfill the requirements of ACSCG.

The rest of this chapter is organized as follows. Section 2.2 defines the model of ACSCG. For ACSCG models, Sections 2.3 and 2.4 present several distributed algorithms without and with real-time information exchanges, respectively, and provide sufficient conditions that guarantee the convergence of the proposed algorithms. Section 2.5 presents the numerical examples and concluding remarks are drawn in Section 2.6.

2.2 Game Model and Examples

In this section, we present the definition of ACSCG and subsequently, we present several exemplary multi-user scenarios which appertain to this new class of game.

2.2.1 Definition of ACSCG

Definition 2.1 *A multi-user interaction* $\Gamma = \langle \mathcal{N}, \mathcal{A}, u, \mathcal{S}, s \rangle$ *is a ACSCG if it satisfies the following assumptions:*

A1: $\forall n \in \mathcal{N}$*, action set* $\mathcal{A}_n \subseteq \mathcal{R}^K$ *is defined to be*[2]

$$\mathcal{A}_n = \Big\{ (a_n^1, a_n^2, \cdots, a_n^K) \;\Big|\; a_n^k \in [a_{n,k}^{\min}, a_{n,k}^{\max}] \text{ and } \sum_{k=1}^{K} a_n^k \leq M_n \Big\}. \tag{2.1}$$

A2: *There exist* $h_n^k : \mathcal{R} \to \mathcal{R}$, $f_n^k : \mathcal{A}_{-n} \to \mathcal{R}$, *and* $g_n^k : \mathcal{A}_{-n} \to \mathcal{R}$, $k =$

[2] *We consider a sum constraint throughout the chapter rather than a weighted-sum constraint, because a weighted-sum constraint can be easily converted to a sum constraint by rescaling* $\mathcal{A}_n$*. Besides, we nontrivially assume that* $\sum_{k=1}^{K} a_{n,k}^{\max} \geq M_n$*.*

$1, \ldots, K$, *such that*

$$u_n(\mathbf{a}) = \sum_{k=1}^{K} \Big[h_n^k\big(a_n^k + f_n^k(\mathbf{a}_{-n})\big) - g_n^k(\mathbf{a}_{-n}) \Big], \tag{2.2}$$

for all $\mathbf{a} \in \mathcal{A}$ *and* $n \in \mathcal{N}$. $h_n^k(\cdot)$ *is an increasing, twice differentiable, and strictly concave function.* $f_n^k(\cdot)$ *and* $g_n^k(\cdot)$ *are both twice differentiable functions which correspond to the state determination functions associated with user* n *in dimension* k.

The ACSCG model defined by assumptions A1 and A2 covers a broad class of multi-user interactions. Assumption A1 indicates that each player's action set is a K-dimensional vector set and its action vector is sum-constrained. This represents the communication scenarios in which each user needs to determine its multi-dimensional action in various channels or networks while the total amount of resources it can consume is constrained. Assumption A2 implies that each user's utility is separable and can be represented by the summation of concave functions h_n^k minus "penalty" functions g_n^k across the K dimensions. In particular, within each dimension, the input of h_n^k is an additive combination of user n's action a_n^k and state determination function $f_n^k(\mathbf{a}_{-n})$ that depends on the remaining users' joint action $\mathbf{a}_{-n}$. Since a_n^k only appears in the concave function h_n^k, it implies that each user's utility is concave in its own action, i.e. diminishing returns per unit of user n's invested action $\mathbf{a}_n$, which is common for many application scenarios in communication networks.

Summarizing, the key features of the game model defined by A1 and A2 include: each user's action is subject to a *sum constraint*; users' utilities are impacted by *additive combinations* of a_n^k and $f_n^k(\mathbf{a}_{-n})$ through concave functions h_n^k. Therefore, we term the game Γ that satisfies assumptions A1 and A2 as ACSCG. In the following section, we present several illustrative multi-user interaction ex-

amples that belong to ACSCG.

2.2.2 Examples of ACSCG

We present four examples that satisfy assumptions A1 and A2 and belong to ACSCG. The details of functions $h_n^k(\cdot)$, $f_n^k(\cdot)$ and $g_n^k(\cdot)$ in each example are summarized in Table 2.1. For each example, Table 2.1 also summarizes the applicable convergence conditions that will be provided in the remaining parts of the chapter.

Example 2.1 *We first consider a simple two-user game with two-dimension action spaces, i.e.* $N = K = 2$. *The utility functions are given by*[3]

$$u_n(\mathbf{a}) = -\exp\Big\{-a_n^1 - \sqrt{(a_{-n}^1)^2+1} + \sqrt{(a_{-n}^2)^2+1}\Big\} \\ -\exp\Big\{-a_n^2 + \sqrt{(a_{-n}^1)^2+1} - \sqrt{(a_{-n}^2)^2+1}\Big\},$$

for $n = 1, 2$. *The resource constraints are* $\sum_{k=1}^{2} a_n^k \le M_n$ *in which* $M_n > 0$ *and* $a_n^k \ge 0$ *for* $\forall n, k$.

Example 2.2 (Power control in frequency-selective Gaussian interference channel [YGC02, SPB08]) *There are* N *transmitter and receiver pairs in the system. The entire frequency band is divided into* K *frequency bins. In frequency bin* k, *the channel gain from transmitter* i *to receiver* j *is denoted as* H_{ij}^k, *where* $k = 1, 2, \cdots, K$. *Similarly, denote the noise power spectral density (PSD) that receiver* n *experiences as* σ_n^k *and player* n*'s transmit PSD as* P_n^k. *The action of user* n *is to select its transmit power* $\mathbf{P}_n = [P_n^1\ P_n^2 \cdots P_n^K]$ *subject to its power constraint:* $\sum_{k=1}^{K} P_n^k \le P_n^{\max}$. *For a fixed* $\mathbf{P}_n$, *if treating its interference as noise,*

[3] *In this example, since there are only two users, the subindex* $-n$ *denotes the user but* n.

user n can achieve the following data rate:

$$\begin{aligned} r_n(\mathbf{P}) &= \sum_{k=1}^{K} \log_2 \Big(1 + \frac{H_{nn}^k P_n^k}{\sigma_n^k + \sum_{m\neq n} H_{mn}^k P_m^k}\Big) \\ &= \sum_{k=1}^{K} \Big(\log_2(\sigma_n^k + \sum_{m=1}^{N} H_{mn}^k P_m^k) - \log_2(\sigma_n^k + \sum_{m\neq n} H_{mn}^k P_m^k)\Big). \end{aligned} \tag{2.3}$$

Example 2.3 *(*Delay minimization in Jackson Networks [CY01]*) As an additional example, we consider a network of N nodes. A Poisson stream of external packets arrive at node n with rate ψ_n and the input stream is split into K traffic classes, which are individually served by exponential servers. Denote node n's input rate and service rate for class k as ψ_n^k and μ_n^k respectively. Therefore, the action of node n is to determine the rates for different traffic classes $\Psi_n = [\psi_n^1\ \psi_n^2 \cdots \psi_n^K]$ and the total rate is subject to the minimum rate constraint: $\sum_{k=1}^{K} \psi_n^k \geq \psi_n^{\min}$. The packets of the same traffic class constitute a Jackson network in which Markovian routing is adopted: packets of class k completing service at node m are routed to node n with probability r_{mn}^k or exit the network with probability $r_{m0}^k = 1 - \sum_{n=1}^{N} r_{mn}^k$. Denote the arrival rate for class k at node n as η_n^k. By Jackson's Theorem, we have $\eta_n^k = \psi_n^k + \sum_{m=1}^{N} \eta_m^k r_{mn}^k, n = 1, 2, \cdots, K$. Denote $[R^k]_{mn} = r_{nm}^k$, $\Upsilon^k = (I - R^k)^{-1}$, and $\upsilon_{mn}^k = [\Upsilon^k]_{nm}$. Equivalently, we have $\eta_n^k = \sum_{m=1}^{N} \upsilon_{mn}^k \psi_m^k$. Each node aims to minimize its total M/M/1 queueing delay incurred by accommodating its traffic:*

$$d_n(\mathbf{\Psi}) = \sum_{k=1}^{K} \frac{1}{\mu_n^k - \sum_{m=1}^{N} \upsilon_{mn}^k \psi_m^k}. \tag{2.4}$$

Example 2.3 can be shown to be a special case of ACSCG by slightly transforming the action sets and utilities. We can define user n's action as $-\Psi_n$. For user n, the sum constraint becomes $\sum_{k=1}^{K} -\psi_n^k \leq -\psi_n^{\min}$ and minimizing $d_n(\mathbf{\Psi})$ is equivalent to maximizing $-d_n(\mathbf{\Psi})$.

Table 2.1: Examples 2.1-2.4 as ACSCG.

Examples	$f_n^k(\mathbf{a}_{-n})$	$h_n^k(x)$	$g_n^k(\mathbf{a}_{-n})$	Convergence conditions
Example 2.1	$f_n^1(\mathbf{a}_{-n}) = \sqrt{(a_{-n}^1)^2+1} - \sqrt{(a_{-n}^2)^2+1}$ $f_n^2(\mathbf{a}_{-n}) = \sqrt{(a_{-n}^2)^2+1} - \sqrt{(a_{-n}^1)^2+1}$	$-e^{-x}$	0	(C4)
Example 2.2	$\sum_{m\neq n} \frac{H_{mn}^k}{H_{nn}^k} P_m^k$	$\log_2(\sigma_n^k + H_{nn}^k x)$	$\log_2(\sigma_n^k + \sum_{m\neq n} H_{mn}^k P_m^k)$	(C1)-(C8)
Example 2.3	$\sum_{m\neq n} \frac{\upsilon_{mn}^k}{\upsilon_{nn}^k} \psi_m^k$	$-\frac{1}{\mu_n^k - \upsilon_{nn}^k x}$	0	(C1)-(C8)
Example 2.4	$\sum_{m\neq n} (\sum_{j=1}^{K} \frac{\gamma(k-j)H_{mn}^k}{H_{nn}^k} P_m^k)$	$\log_2(\sigma_n^k + H_{nn}^k x)$	$\log_2\big(\sigma_n^k + H_{nn}^k f_n^k(\mathbf{a}_{-n})\big)$	(C4)-(C8)

Example 2.4 (Asynchronous transmission in digital subscriber lines network [CHC07]) *The basic setting of this example to similar as that of Example 2.2 except that inter-carrier interference (ICI) exist among different frequency bins. Due to the loss of the orthogonality, the interference that user n experiences in frequency bin k is*

$$f_n^k(\mathbf{P}_{-n}) = \sum_{m \neq n} \Big(\sum_{j=1}^{K} \gamma(k-j) H_{mn}^j P_m^j \Big), \tag{2.5}$$

in which $\gamma(j)$ is the ICI coefficient that represents the relative interference transmitted signal in a particular frequency bin generates to its jth neighbor bin. In particular, it takes the form

$$\gamma(j) = \begin{cases} 1, & \text{if } j = 0 \\ \frac{2}{K^2 \sin^2(\frac{\pi}{K} j)}, & -\frac{K}{2} \leq j \leq \frac{K}{2} \ j \neq 0. \end{cases} \tag{2.6}$$

It satisfies the symmetric and circular properties, i.e. $\gamma(-j) = \gamma(j) = \gamma(K-j)$. User n's achievable rate in the presence of ICI is given by

$$r_n(\mathbf{P}) = \sum_{k=1}^{K} \log_2 \left[1 + \frac{H_{nn}^k P_n^k}{\sigma_n^k + \sum_{m \neq n} \Big(\sum_{j=1}^{K} \gamma(k-j) H_{mn}^j P_m^j \Big)} \right]. \tag{2.7}$$

2.2.3 Issues Related to ACSCG

Since the ACSCG model represents a good abstraction of numerous multi-user resource allocation problems, we aim to investigate the convergence properties of various distributed algorithms in ACSCG without and with real-time message passing.

ACSCG is a concave game [FT91, Ros65] and therefore, it admits at least one pure NE. In practice, we want to provide the sufficient conditions under which best response dynamics provably and globally converges to a pure NE. However, the existing literature, e.g. the diagonal strict concavity (DSC) conditions in

[Ros65] and the supermodular game theory [Top98, Yao95, AA03], does not provide such convergence conditions for the general ACSCG model. For example, the DSC conditions developed for general concave games do not guarantee the convergence of best response dynamics [Ros65]. Even if the utility functions in ACSCG possess the supermodular type structure, due to the sum constraint, the action set of each user is generally not a sublattice[4] of $\mathcal{R}^K$. Therefore, the convergence results based on supermodular games cannot be directly applied in ACSCG. On the other hand, if we want to maximize the sum utility by enabling real-time message passing among users, we also note that, the utility u_n is not necessarily jointly concave in $\mathbf{a}$ because of the existence of $g_n^k(\cdot)$. Therefore, the existing algorithms developed for the convex NUM are not immediately applicable either.

In fact, a unique feature of the ACSCG is that different users' actions are *additively coupled* in $h_n^k(\cdot)$ and each user's action space is *sum-constrained*. In the following sections, we will fully explore these specific structures and address the convergence properties of various distributed algorithms in two different scenarios. Specifically, Section 2.3 investigates the scenarios in which each user n can only observe $\{f_n^k(\mathbf{a}_{-n})\}_{k=1}^K$ and cannot exchange any information with any other user. Section 2.4 focuses on the scenarios in which each user n is able to announce and receive information in real-time to and from the remaining users about $\frac{\partial u_n(\mathbf{a})}{\partial a_m^k}$ and $\frac{\partial u_m(\mathbf{a})}{\partial a_n^k}$, $\forall m \neq n, k = 1, \ldots, K$.

[4] In supermodular games, for each player, the action set is a nonempty and compact sublattice of $\mathcal{R}^K$. We can verify that with the sum constraint, $\mathcal{A}_n$ is usually not a sublattice of $\mathcal{R}^K$ by taking the component-wise maximum.

2.3 Scenario I: No Message Exchange among Users

In communication scenarios where users cannot exchange messages to achieve coordination, the participating users can simply choose actions to selfishly maximize their individual utility functions $u_n(\mathbf{a})$ without taking into account the utility degradation caused to the other users. In particular, each user individually solves the following optimization program:

$$\max_{\mathbf{a}_n \in \mathcal{A}_n} u_n(\mathbf{a}). \tag{2.8}$$

The steady state outcome of such a multi-user interaction is usually characterized as a NE, at which given the other users' actions, no user can increase its utility alone by unilaterally changing its action. It is worth pointing out that, since there is no coordination signal among users, NE generally does not lead to a Pareto-optimal solution. Section IV will discuss distributed algorithms in which users exchange coordination signals in order to improve the system efficiency.

2.3.1 Properties of Best Response Dynamics in ACSCG

To better understand the key properties of the ACSCG, in this subsection, we first focus on the scenarios in which $f_n^k(\mathbf{a}_{-n})$ is the linear combination of the remaining users' action in the same dimension k, i.e.

$$f_n^k(\mathbf{a}_{-n}) = \sum_{m \neq n} F_{mn}^k a_m^k \tag{2.9}$$

and $F_{mn}^k \in \mathcal{R}$, $\forall m, n, k$. Specifically, both Example 2.2 and 2.3 in Table 2.1 belong to this category. In Section 2.3.2, we will extend the results derived for the functions $f_n^k(\mathbf{a}_{-n})$ defined in (2.9) to general $f_n^k(\mathbf{a}_{-n})$.

Since $h_n^k(\cdot)$ is concave, the objective in (2.8) is a concave function in a_n^k when the other users' actions $\mathbf{a}_{-n}$ are fixed. To find the globally optimal solution of

the problem in (2.8), we can first form its Lagrangian

$$L_n(\mathbf{a}_n, \lambda) = u_n(\mathbf{a}) + \lambda(M_n - \sum_{k=1}^{K} a_n^k), \tag{2.10}$$

in which $a_n^k \in [a_{n,k}^{\min}, a_{n,k}^{\max}]$. By taking the first derivatives of (2.10), we have

$$\frac{\partial L_n(\mathbf{a}_n, \lambda)}{\partial a_n^k} = \frac{\partial h_n^k(a_n^k + \sum_{m \neq n} F_{mn}^k a_m^k)}{\partial a_n^k} - \lambda = 0. \tag{2.11}$$

Denote

$$l_n^k(\mathbf{a}_{-n}, \lambda) \triangleq \Big[\Big\{\frac{\partial h_n^k}{\partial x}\Big\}^{-1}(\lambda) - \sum_{m \neq n} F_{mn}^k a_m^k\Big]_{a_{n,k}^{\min}}^{a_{n,k}^{\max}}, \tag{2.12}$$

in which $\big\{\frac{\partial h_n^k}{\partial x}\big\}^{-1}$ is the inverse function[5] of $\frac{\partial h_n^k}{\partial x}$ and $[x]_b^a = \max\{\min\{x, a\}, b\}$. The optimal solution of (2.8) is given by $a_n^{*k} = l_n^k(\mathbf{a}_{-n}, \lambda^*)$, where the Lagrange multiplier λ^* is chosen to satisfy the sum constraint $\sum_{k=1}^{K} a_n^{*k} = M_n$.

We define the best response operator $B_n^k(\cdot)$ as

$$B_n^k(\mathbf{a}_{-n}) = l_n^k(\mathbf{a}_{-n}, \lambda^*). \tag{2.13}$$

We consider the dynamic adjustment process in which users revise their actions over time based on their observations about their opponents. A well-known candidate for such adjustment processes is the so-called best response dynamics. In the best response algorithm, each user updates its action using the best response strategy that maximizes its utility function in (2.2). We consider two types of update orders, including sequential update and parallel update. Specifically, in sequential update, individual players iteratively optimize in a circular fashion with respect to their own actions while keeping the actions of their opponents fixed. Formally, at stage t, user n chooses its action according to

$$a_n^{k,t} = B_n^k([\mathbf{a}_1^t, \ldots, \mathbf{a}_{n-1}^t, \mathbf{a}_{n+1}^{t-1}, \ldots, \mathbf{a}_N^{t-1}]). \tag{2.14}$$

[5] If $\nexists\ x = x^*$ such that $\frac{\partial h_n^k}{\partial x}|_{x=x^*} = \lambda$, we let $\big\{\frac{\partial h_n^k}{\partial x}\big\}^{-1}(\lambda) = -\infty$.

On the other hand, players adopting the parallel update their actions revise at stage t according to

$$a_n^{k,t} = B_n^k(\mathbf{a}_{-n}^{t-1}). \tag{2.15}$$

We obtain several sufficient conditions under which best response dynamics converges. Similar convergence conditions are proved in [CSK03, CHC07, SPB08] for Example 2.2 in which $h_n^k(x) = \log_2(\sigma_n^k + H_{nn}^k x)$. We consider more general functions $h_n^k(\cdot)$ and further extend the convergence conditions in [CSK03, CHC07, SPB08]. The key differences among all the sufficient conditions which will be provided in this section are summarized in Table 2.2.

2.3.1.1 General $h_n^k(\cdot)$

The first sufficient condition is developed for the general cases in which the functions $h_n^k(\cdot)$ in the utilities $u_n(\cdot)$ are specified in assumption A2. Define

$$[\mathbf{T}^{\max}]_{mn} \triangleq \begin{cases} \max_k |F_{mn}^k|, & \text{if } m \neq n \\ 0, & \text{otherwise.} \end{cases} \tag{2.16}$$

and let $\rho(\mathbf{T}^{\max})$ denote the spectral radius of the matrix $\mathbf{T}^{\max}$.

Theorem 2.1 *If*

$$\rho(\mathbf{T}^{\max}) < \frac{1}{2}, \tag{C1}$$

then there exists a unique NE in game Γ *and best response dynamics converges linearly to the NE, for any set of initial conditions belonging to* $\mathcal{A}$ *with either sequential or parallel updates.*

Proof: This theorem is proved by showing that the best response dynamics defined in (2.14) and (2.15) is a contraction mapping under (C1). See Appendix A for details. ■

Table 2.2: Comparison among conditions (C1)-(C6).

Conditions	Assumptions about $f_n^k(\mathbf{a}_{-n})$	$h_n^k(x)$	Measure of residual error $\mathbf{a}_n^{t+1} - \mathbf{a}_n^t$	Contraction factor
(C1)	(2.9)	A2	1-norm	$2\rho(\mathbf{T}^{\max})$
(C2)	(2.9) and F_{mn}^k have the same sign for $\forall k, m \neq n$	A2	1-norm	$\rho(\mathbf{T}^{\max})$
(C3)	(2.9)	(2.18)	weighted Euclidean norm	$\rho(\mathbf{S}^{\max})$
(C4)	general	A2	1-norm	$2\rho(\bar{\mathbf{T}}^{\max})$
(C5)	$\frac{\partial f_n^k(\mathbf{a}_{-n})}{\partial a_m^{k'}}$ have the same sign for $\forall \mathbf{a} \in \mathcal{A}, k, k', m \neq n$	A2	1-norm	$\rho(\bar{\mathbf{T}}^{\max})$
(C6)	general	(2.18)	weighted Euclidean norm	$\rho(\bar{\mathbf{S}}^{\max})$

In multi-user communication applications, it is common to have games of *strategic complements* (or *strategic substitutes*), i.e. the marginal returns to any one component of the player's action rise with increases (or decreases) in the components of the competitors' actions [BGK85]. For instance, in Examples 2.2 and 2.4, increasing user n's transmitted power creates stronger interference to the other users and decreases their marginal achievable rates. Similarly, in Example 2.3, increasing node n's input traffic rate congests all the servers in the network and increases the marginal queueing delay. Mathematically, if u_n is twice differentiable, strategic complementarities (or strategic substitutes) can be described as

$$\frac{\partial^2 u_n(\mathbf{a}_n, \mathbf{a}_{-n})}{\partial a_n^j \partial a_m^k} \geq 0, \ \forall m \neq n, j, k, (\text{or } \frac{\partial^2 u_n(\mathbf{a}_n, \mathbf{a}_{-n})}{\partial a_n^j \partial a_m^k} \leq 0, \ \forall m \neq n, j, k). \quad (2.17)$$

We can verify that Examples 2.2, 2.3, and 2.4 are games with strategic substitutes. For the ACSCG models that exhibit strategic complementarities (or strategic substitutes), the following theorem further relaxes condition (C1).

Theorem 2.2 *Let Γ be an ACSCG with strategic complementarities (or strategic substitutes), i.e. $F_{mn}^k \leq 0$, $\forall k, m \neq n$, (or $F_{mn}^k \geq 0$, $\forall k, m \neq n$). If*

$$\rho(\mathbf{T}^{\max}) < 1, \quad (C2)$$

then there exists a unique NE in game Γ and best response dynamics converges linearly to the NE, for any set of initial conditions belonging to $\mathcal{A}$ with either sequential or parallel updates.

Proof: This theorem is proved by adapting the proof of Theorem 2.1. See Appendix B. ■

Remark 2.1 *(Implications of conditions (C1) and (C2)) Theorem 2.1 and Theorem 2.2 give sufficient conditions for best response dynamics to globally converge*

to a unique fixed point. Specifically, $\max_k |F_{mn}^k|$ *can be regarded as a measure of the strength of the mutual coupling between user* m *and* n*. The intuition behind (C1) and (C2) is that, the weaker the coupling among different users is, the more likely that best response dynamics converges. Consider the extreme case in which* $F_{mn}^k = 0, \forall k, m \neq n$*. Since each user's best response is not impacted by the remaining users' action* $\mathbf{a}_{-n}$*, the convergence is immediately achieved after a single best-response iteration. If no restriction is imposed on* F_{mn}^k*, Theorem 2.1 specifies a mutual coupling threshold under which best response dynamics provably converge. The proof of Theorem 2.1 can be intuitively interpreted as follows. We regard every best response update as the users' joint attempt to approach the NE. Due to the linear coupling structure in (2.9), user* n*'s best response in (2.12) contains a term* $\sum_{m\neq n} F_{mn}^k a_m^k$ *that is a linear combination of* $\mathbf{a}_{-n}$*. As a result, the residual error* $\left|\mathbf{a}_n^{t+1} - \mathbf{a}_n^t\right|_1$*, which is the 1-norm distance between the updated action profile* $\mathbf{a}_n^{t+1}$ *and the current action profile* $\mathbf{a}_n^t$*, can be upper-bounded using linear combinations of* $\left|\mathbf{a}_m^t - \mathbf{a}_m^{t-1}\right|_1$ *in which* $m \neq n$*. Recall that* F_{mn}^k *can be either positive or negative. We also note that, if* $\mathbf{a}_m^t \neq \mathbf{a}_m^{t-1}$*,* $\mathbf{a}_m^t - \mathbf{a}_m^{t-1}$ *contains both positive and negative terms due to the sum-constraint. In the worst case, the distance* $\left|\mathbf{a}_n^{t+1} - \mathbf{a}_n^t\right|_1$ *is maximized if* $\left\{F_{mn}^k\right\}$ *and* $\left\{a_m^{k,t} - a_m^{k,t-1}\right\}$ *are co-phase multiplied and additively summed, i.e.* $F_{mn}^k\left(a_m^{k,t} - a_m^{k,t-1}\right) \geq 0$*, for* $\forall k = 1, \ldots, K, m \neq n$*. After an iteration, all users except* n *contributes to user* n*'s residual error at stage* $t+1$ *up to* $\sum_{m\neq n} 2\max_k \left|F_{mn}^k\right|\left|\mathbf{a}_m^t - \mathbf{a}_m^{t-1}\right|_1$*. Under condition (C1), it is guaranteed that the residual error contracts with respect to the special norm defined in (2.63). Theorem 2.2 focuses on the situations in which the signs of* F_{mn}^k *are the same,* $\forall m \neq n, k$*. In this case,* $\left\{F_{mn}^k\right\}$ *and* $\left\{a_m^{k,t} - a_m^{k,t-1}\right\}$ *cannot be co-phase multiplied. Therefore, the region of convergence enlarges and hence, condition (C2) stated in Theorem 2.2 is weaker than condition (C1) in Theorem 2.1.*

Remark 2.2 *(Relation to the results in references [CSK03, CHC07, SPB08]) Similar to [CSK03, CHC07], our proofs choose 1-norm as the distance measure for the residual errors* $\mathbf{a}_n^{t+1} - \mathbf{a}_n^t$ *after each best-response iteration. However, by manipulating the inequalities in a different way, condition (C2) is more general than the results in [CSK03, CHC07], where they require* $\max_k F_{mn}^k < \frac{1}{N-1}$*. Interestingly, condition (C2) recovers the result obtained in [SPB08] where it is proved by choosing the Euclidean norm as the distance measure for the residual errors* $\mathbf{a}_n^{t+1} - \mathbf{a}_n^t$ *after each best-response iteration. However, the approach in [SPB08] using the Euclidean norm only applies to the scenarios in which* $h_n^k(\cdot)$ *is a logarithmic function. We prove that condition (C2) applies to any* $h_n^k(\cdot)$ *that is increasing and strictly concave.*

2.3.1.2 A special class of $h_n^k(\cdot)$

In addition to conditions (C1) and (C2), we also develop a sufficient convergence condition for a family of utility functions parameterized by a negative number θ. In particular, $h_n^k(\cdot)$ satisfies[6]

$$h_n^k(x) = \begin{cases} \log(\alpha_n^k + F_{nn}^k x), & \text{if } \theta = -1, \\ \frac{(\alpha_n^k + F_{nn}^k x)^{\theta+1}}{\theta+1}, & \text{if } -1 < \theta < 0 \text{ or } \theta < -1. \end{cases} \tag{2.18}$$

and $\alpha_n^k \in \mathcal{R}$ and $F_{nn}^k > 0$. The interpretation of this type of utilities has been addressed in [MW00]. It is shown that varying the parameter θ leads to different types of fairness across $\alpha_n^k + F_{nn}^k(a_n^k + \sum_{m \neq n} F_{mn}^k a_m^k)$ for all k. In particular, $\theta = -1$ corresponds to the proportional fairness; if $\theta = -2$, then harmonic mean fairness; and if $\theta = -\infty$, then max-min fairness. We can see that, Examples 2.2 and 2.3 are special cases of this type of utility functions. In these cases, best

[6] If $\alpha_n^k + F_{nn}^k x \leq 0$, we let $h_n^k(x) = -\infty$. We assume for this class of $h_n^k(\cdot)$ that for $\forall \mathbf{a}_{-n} \in \mathcal{A}_{-n}$, there exists $\mathbf{a}_n \in \mathcal{A}_n$ such that $\alpha_n^k + F_{nn}^k x > 0$ for $\forall n, k$.

response dynamics in equation (2.12) is reduced to

$$l_n^k(\mathbf{a}_{-n},\lambda)=\Big[\big(\frac{1}{F_{nn}^k}\big)^{1+\frac{1}{\theta}}\lambda^{\frac{1}{\theta}}-\frac{\alpha_n^k}{F_{nn}^k}-\sum_{m\neq n}F_{mn}^k a_m^k\Big]_{a_{n,k}^{\min}}^{a_{n,k}^{\max}}, \tag{2.19}$$

Define

$$[\mathbf{S}^{\max}]_{mn}\triangleq\begin{cases}\frac{\sum_{k=1}^K(F_{mm}^k)^{1+\frac{1}{\theta}}}{\sum_{k=1}^K(F_{nn}^k)^{1+\frac{1}{\theta}}}\max_k\Big\{|F_{mn}^k|\Big(\frac{F_{nn}^k}{F_{mm}^k}\Big)^{1+\frac{1}{\theta}}\Big\}, & \text{if } m\neq n\\ 0, & \text{otherwise.}\end{cases} \tag{2.20}$$

For the class of utility functions in (2.18), Theorem 2.3 gives a sufficient condition that guarantees the convergence of the best response dynamics defined in (2.19).

Theorem 2.3 *For $h_n^k(\cdot)$ defined in (2.18), if*

$$\rho(\mathbf{S}^{\max})<1, \tag{C3}$$

then there exists a unique NE in game Γ and best response dynamics converges linearly to the NE, for any set of initial conditions belonging to $\mathcal{A}$ and with either sequential or parallel updates.

Proof: It can be proved by showing that the best response dynamics defined in (2.19) is a contraction mapping with respect to the weighted Euclidean norm. See Appendix C for details. ■

Remark 2.3 *(Relation between conditions (C3) and the results in reference [SPB08]) For aforementioned Example 2.2, Scutari et al. established in [SPB08] a sufficient condition under which the iterative water-filling algorithm converges. The iterative water-filling algorithm essentially belongs to best response dynamics. Specifically, in [SPB08], Shannon's formula leads to $\theta=-1$ and cross channel coefficients satisfy $F_{mn}^k\geq 0,\forall k,m\neq n$. Equation (2.19) reduces to the water-filling formula*

$$l_n^k(\mathbf{a}_{-n},\lambda)=\Big[\frac{1}{\lambda}-\frac{\alpha_n^k}{F_{nn}^k}-\sum_{m\neq n}F_{mn}^k a_m^k\Big]_{a_{n,k}^{\min}}^{a_{n,k}^{\max}}, \tag{2.21}$$

and $[\mathbf{S}^{\max}]_{mn} = \max_k F^k_{mn}$. *By choosing the weighted Euclidean norm as the distance measure for the residual errors* $\mathbf{a}_n^{t+1} - \mathbf{a}_n^t$ *after each best-response iteration, Theorem 2.3 generalizes the results in [SPB08] for the family of utility functions defined in (2.18).*

Remark 2.4 *(Relation between conditions (C1), (C2) and (C3)) The connections and differences between conditions (C1), (C2) and (C3) are summarized in Table 2.2. We have addressed the implications of (C1) and (C2) in Remark 2.1. Now we discuss their relation with (C3). First of all, condition (C1) is proposed for general* $h_n^k(\cdot)$ *and condition (C3) is proposed for the class of utility functions defined in (2.18). However, Theorem 2.1 and Theorem 2.3 individually establish the fact that best response dynamics is a contraction map by selecting different vector and matrix norms. Therefore, in general, (C1) and (C3) do not immediately imply each other. Note that* $[\mathbf{S}^{\max}]_{mn} \leq \zeta_{mn} \cdot \max_k |F^k_{mn}|$ *in which* ζ_{mn} *satifies*

$$\zeta_{mn} = \frac{\sum_{k=1}^K (F^k_{mm})^{1+\frac{1}{\theta}}}{\sum_{k=1}^K (F^k_{nn})^{1+\frac{1}{\theta}}} \cdot \max_k \frac{(F^k_{nn})^{1+\frac{1}{\theta}}}{(F^k_{mm})^{1+\frac{1}{\theta}}} \in \Big[1, \frac{\max_k (F^k_{nn}/F^k_{mm})^{1+\frac{1}{\theta}}}{\min_k (F^k_{nn}/F^k_{mm})^{1+\frac{1}{\theta}}}\Big]. \tag{2.22}$$

The physical interpretation of ζ_{mn} *is the similarity between the preferences of user* m *and* n *across the total* K *dimensions of their action spaces. Recall that both* $\mathbf{S}^{\max}$ *and* $\mathbf{T}^{\max}$ *are non-negative matrices and* $\mathbf{S}^{\max}$ *is element-wise less than or equal to* $\max_{m\neq n} \zeta_{mn} \mathbf{T}^{\max}$. *By the property of non-negative matrix and condition (C1), we can conclude* $\rho(\mathbf{S}^{\max}) \leq \rho(\max_{m\neq n} \zeta_{mn} \mathbf{T}^{\max}) < \max_{m\neq n} \frac{\zeta_{mn}}{2}$. *The relation between (C1) and (C3) is pictorially illustrated in Fig. 2.1. Specifically, if users have similar preference in their available actions and the upper bound of* ζ_{mn} *that measures the difference of their preferences is below the following threshold:*

$$\frac{\max_{k,m\neq n} (F^k_{nn}/F^k_{mm})^{1+\frac{1}{\theta}}}{\min_{k,m\neq n} (F^k_{nn}/F^k_{mm})^{1+\frac{1}{\theta}}} < 2, \tag{2.23}$$

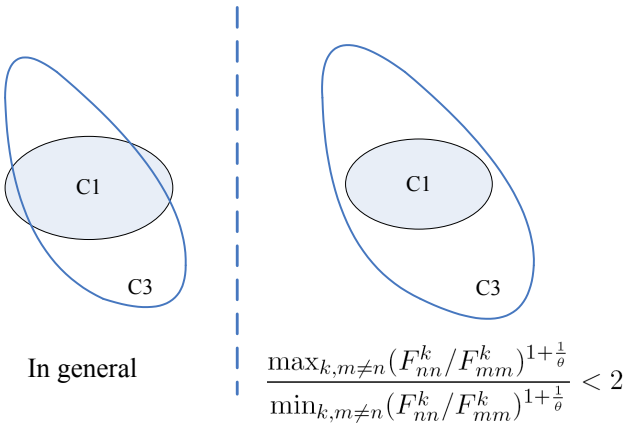

Figure 2.1: Relation between (C1) and (C3).

we know that (C1) implies (C3) in this situation because $\rho(\mathbf{S}^{\max}) < \max_{m,n}\zeta_{mn} \cdot \rho(\mathbf{T}^{\max}) < 2 \cdot \frac{1}{2} = 1$. *We also would like to point out that, the LHS of (2.23) is a function of* θ *and the LHS* $\equiv 1$ *if* $\theta = -1$. *When* $\theta = -1$, $\mathbf{T}^{\max}$ *coincides with* $\mathbf{S}^{\max}$. *Mathematically, in this case, (C3) is actually more general than (C2), because it still holds even if coefficients* F^k_{mn} *have different signs.*

2.3.2 Extensions to General $f^k_n(\cdot)$

As a matter of fact, the results above can be extended to the more general situations in which $f^k_n(\cdot)$ is a nonlinear differentiable function, $\forall n, k$ and its input $\mathbf{a}_{-n}$ consists of the remaining users' action from all the dimensions. Accordingly, equation (2.12) becomes

$$l^k_n(\mathbf{a}_{-n}, \lambda) \triangleq \left[\left\{\frac{\partial h^k_n}{\partial x}\right\}^{-1}(\lambda) - f^k_n(\mathbf{a}_{-n})\right]_{a^{\min}_{n,k}}^{a^{\max}_{n,k}}. \tag{2.24}$$

The conclusions in Theorem 2.1, 2.2, and 2.3 can be further extended as Theorem 2.4, and 2.5, 2.6 that are listed below. We only provide the proof of Theorem 2.4

in Appendix D. The detailed proofs of Theorem 2.5 and 2.6 are omitted because they can be proven similarly as Theorem 2.4.

For general $f_n^k(\cdot)$, we denote

$$[\bar{\mathbf{T}}^{\max}]_{mn} \triangleq \begin{cases} \max_{\mathbf{a}\in\mathcal{A},k'} \sum_{k=1}^{K} \left| \frac{\partial f_n^k(\mathbf{a}_{-n})}{\partial a_m^{k'}} \right|, & \text{if } m \neq n \\ 0, & \text{otherwise.} \end{cases} \tag{2.25}$$

Besides, for $h_n^k(\cdot)$ defined in (2.18), we define

$$[\bar{\mathbf{S}}^{\max}]_{mn} \triangleq \begin{cases} \frac{\sum_{k=1}^{K}(F_{mm}^k)^{1+\frac{1}{\theta}}}{\sum_{k=1}^{K}(F_{nn}^k)^{1+\frac{1}{\theta}}} \max_{\mathbf{a}\in\mathcal{A},k'} \left\{ \sum_{k=1}^{K} \left| \frac{\partial f_n^k(\mathbf{a}_{-n})}{\partial a_m^{k'}} \right| \left(\frac{F_{nn}^{k'}}{F_{mm}^{k'}} \right)^{1+\frac{1}{\theta}} \right\}, & \text{if } m \neq n \\ 0, & \text{otherwise.} \end{cases} \tag{2.26}$$

Theorem 2.4 *If*

$$\rho(\bar{\mathbf{T}}^{\max}) < \frac{1}{2}, \tag{C4}$$

then there exists a unique NE in game Γ *and best response dynamics converges linearly to the NE, for any set of initial conditions belonging to* $\mathcal{A}$ *with either sequential or parallel updates.*

Proof: This theorem can be proved by combining the proof of Theorem 2.1 and the mean value theorem for vector-valued functions. See Appendix D for details. ■

Similarly as in Theorem 2.2, for the general ACSCG models that exhibit strategic complementarities (or strategic substitutes), we can further relax condition (C4).

Theorem 2.5 *For* Γ *with strategic complementarities (or strategic substitutes), i.e.* $\frac{\partial f_n^k(\mathbf{a}_{-n})}{\partial a_m^{k'}} \geq 0, \forall m \neq n, k, k', \mathbf{a} \in \mathcal{A}$, *(or* $\frac{\partial f_n^k(\mathbf{a}_{-n})}{\partial a_m^{k'}} \leq 0, \forall m \neq n, k, k', \mathbf{a} \in \mathcal{A}$*), if*

$$\rho(\bar{\mathbf{T}}^{\max}) < 1, \tag{C5}$$

then there exists a unique NE in game Γ *and best response dynamics converges linearly to the NE, for any set of initial conditions belonging to* $\mathcal{A}$ *with either sequential or parallel updates.*

Theorem 2.6 *For* $h_n^k(\cdot)$ *defined in (2.18), if*

$$\rho(\bar{\mathbf{S}}^{\max}) < 1, \tag{C6}$$

then there exists a unique NE in game Γ *and best response dynamics converges linearly to the NE, for any set of initial conditions belonging to* $\mathcal{A}$ *with either sequential or parallel updates.*

Remark 2.5 *(Implications of conditions (C4), (C5), and (C6)) Based on the mean value theorem, we know that the upper bound of the additive sum of first derivatives* $\sum_{k=1}^{K} \left| \frac{\partial f_n^k(\mathbf{a}_{-n})}{\partial a_m^{k'}} \right|$ *governs the maximum impact that user* m*'s action can make over user* n*'s utility. As a result, Theorem 2.4, Theorem 2.5, and Theorem 2.6 indicate that* $\sum_{k=1}^{K} \left| \frac{\partial f_n^k(\mathbf{a}_{-n})}{\partial a_m^{k'}} \right|$ *can be used to develop similar sufficient conditions for the global convergence of best response dynamics. Table 2.2 summarizes the connections and differences among all the aforementioned conditions from (C1) to (C6). We can verify that, for the linear function* $f_n^k(\cdot)$ *that is defined in (2.9) and studied in Section 2.3.1,* $\forall \mathbf{a} \in \mathcal{A}, m \neq n$*, it satisfies*

$$\frac{\partial f_n^k(\mathbf{a}_{-n})}{\partial a_m^{k'}} = \begin{cases} F_{mn}^k, & \text{if } k' = k \\ 0, & \text{otherwise.} \end{cases} \tag{2.27}$$

In addition, we can see that, in Example 2.4, $f_n^k(\cdot)$ *is actually an affine function with*

$$\frac{\partial f_n^k(\mathbf{P}_{-n})}{\partial P_m^{k'}} = \begin{cases} \gamma(k-k')H_{mn}^{k'}, & \text{if } k' = k \\ 0, & \text{otherwise.} \end{cases} \tag{2.28}$$

and $\bar{\mathbf{S}}^{\max}$ *is reduced to*

$$[\bar{\mathbf{S}}^{\max}]_{mn} \triangleq \begin{cases} \max_{k'} \sum_{k=1}^{K} \gamma(k-k') H_{mn}^{k'}, & \text{if } m \neq n \\ 0, & \text{otherwise.} \end{cases} \tag{2.29}$$

As an immediate result of Theorem 2.6, we have the following corollary which specifies a sufficient condition that guarantees the convergence of the iterative water-filling algorithm for asynchronous transmissions in multi-carrier systems [CHC07].

Corollary 2.1 *In Example 2.4, if the matrix* $\bar{\mathbf{S}}^{\max}$ *defined in (2.29) satisfies*

$$\rho(\bar{\mathbf{S}}^{\max}) < 1, \tag{2.30}$$

then there exists a unique NE in game Γ *and the iterative water-filling algorithm converges linearly to the NE, for any set of initial conditions belonging to* $\mathcal{A}$ *and with either sequential or parallel updates.*

Remark 2.6 *(Impact of sum constraints) An interesting phenomenon that can be observed from the analysis above is that, the convergence condition may depend on the maximum constraints* $\{M_n\}_{n=1}^N$*. This differs from the observation in [SPB08] that the presence of the transmit power and spectral mask constraints does not affect the convergence capability of the iterative water-filling algorithm. This is because when functions* $f_n^k(\mathbf{a}_{-n})$ *are affine, e.g. in Example 2.2, 2.3, and 2.4, the elements in* $\bar{\mathbf{T}}^{\max}$ *and* $\bar{\mathbf{S}}^{\max}$ *are independent of the values of* $\{M_n\}_{n=1}^N$*. Therefore, (C1)-(C6) are independent of* M_n *for affine* $f_n^k(\mathbf{a}_{-n})$*. However, for non-linear* $f_n^k(\mathbf{a}_{-n})$*, the values of* $\{M_n\}_{n=1}^N$ *specify the range of users' joint feasible action set* $\mathcal{A}$*, and this will affect* $\bar{\mathbf{T}}^{\max}$ *and* $\bar{\mathbf{S}}^{\max}$ *accordingly. In other words, in the presence of non-linearly coupled* $f_n^k(\mathbf{a}_{-n})$*, convergence may depend on the players' maximum sum constraints* $\{M_n\}_{n=1}^N$*.*

2.3.3 Connections to the Results of Rosen and Gabay

In [Ros65], Rosen proposed a continuous-time gradient projection based iterative algorithm to obtain a pure NE under the assumption of DSC conditions. Here we present a discrete version of the algorithm in [Ros65], named "*gradient play*". Specifically, at stage t, each user first determines the gradient of its own utility function $u_n(\mathbf{a}_n, \mathbf{a}_{-n}^{t-1})$. Then each user updates its action a_n^t using gradient projection according to

$$a_n^{'k,t} = a_n^{k,t-1} + \kappa_n \frac{\partial u_n(\mathbf{a}_n, \mathbf{a}_{-n}^{t-1})}{\partial a_n^k} \tag{2.31}$$

and

$$\mathbf{a}_n^t = [a_n^{1,t} a_n^{2,t} \cdots a_n^{K,t}] = \left[a_n^{'1,t} a_n^{'2,t} \cdots a_n^{'K,t}\right]_{\mathcal{A}_n}^{\|\cdot\|_2}, \tag{2.32}$$

where κ_n is the stepsize and $[\mathbf{v}]_{\mathcal{A}_n}^{\|\cdot\|_2}$ denotes the projection of the vector $\mathbf{v}$ onto user n's action set $\mathcal{A}_n$ with respect to the Euclidean norm $\|\cdot\|_2$. If κ_n is chosen to be sufficiently small, gradient play approximates the continuous-time gradient projection algorithm. For each nonnegative vector $\boldsymbol{\kappa} = [\kappa_1 \dots \kappa_N]$, define

$$g(\mathbf{a}, \boldsymbol{\kappa}) = [\kappa_1 \nabla_1 u_1(\mathbf{a}) \ \kappa_2 \nabla_2 u_2(\mathbf{a}) \ \dots \ \kappa_N \nabla_N u_N(\mathbf{a})]^T. \tag{2.33}$$

The definition of DSC in [Ros65] is that, for fixed $\boldsymbol{\kappa} > 0$ and every $\mathbf{a}^0, \mathbf{a}^1 \in \mathcal{A}$, we have

$$(\mathbf{a}^1 - \mathbf{a}^0)^T g(\mathbf{a}^0, \boldsymbol{\kappa}) + (\mathbf{a}^0 - \mathbf{a}^1)^T g(\mathbf{a}^1, \boldsymbol{\kappa}) > 0. \tag{2.34}$$

A sufficient condition for DSC is that the symmetric matrix $G(\mathbf{a}, \boldsymbol{\kappa}) + G^T(\mathbf{a}, \boldsymbol{\kappa})$ be negative definite for $\mathbf{a} \in \mathcal{A}$, where $G(\mathbf{a}, \boldsymbol{\kappa})$ is the Jacobian with respect to $\mathbf{a}$ of $g(\mathbf{a}, \boldsymbol{\kappa})$.

However, when using gradient play to search for a pure NE, the stepsize κ_n needs to be carefully chosen and set to be sufficiently small, which usually slows down the rate of convergence. As an alternative distributed algorithm, for

Table 2.3: A summary of various convergence conditions in concave games.

Algorithms	Sufficient conditions and the applicable games
Gradient play	Rosen's DSC conditions for concave games [Ros65]
Best response	Gabay's dominance solvability condition for concave games with $\mathcal{A}_n = \mathcal{R}_+$ [GM80], conditions (C1)-(C6) for ACSCG

concave games with $\mathcal{A}_n = \mathcal{R}_+$, $\forall n \in \mathcal{N}$, Gabay and Moulin provided in [GM80] a dominance solvability condition under which best response dynamics globally converges to a unique NE. Specifically, the dominance solvability condition is given by

$$-\frac{\partial^2 u_n}{\partial^2 a_n} \geq \sum_{m \neq n} \Big| \frac{\partial^2 u_n}{\partial a_n \partial a_m} \Big|. \tag{2.35}$$

The sufficient conditions provided in this section and Gabay's dominance solvability condition specify the convergence conditions of best response dynamics in different subclasses of concave games. Specifically, our results are developed for concave games in which every user has a multi-dimensional action space subject to a single sum-constraint and Gabay's dominance solvability condition is proposed for concave games with single dimensional strategy.

2.4 Scenario II: Message Exchange among Users

In this section, our objective is to coordinate the users' actions in ACSCG to maximize the overall performance of the system, measured in terms of their total utilities, in a distributed fashion. Specifically, the optimization problem we want to solve is

$$\max_{\mathbf{a} \in \mathcal{A}} \sum_{n=1}^{N} u_n(\mathbf{a}). \tag{2.36}$$

We will study two distributed algorithms in which the participating users exchange price signals that indicate the "cost" or "benefit" that its action causes to the other users. Allocating network resources via pricing has been well-investigated for convex NUM problems [CLC07], where the original NUM problem can be decomposed into distributedly solvable subproblems by setting price for each constraint resource, and each subproblem has to decide the amount of resources to be used depending on the charged price. However, unlike in the conventional convex NUM, pricing mechanisms may not be immediately applicable in ACSCG if the objective in (2.36) is not jointly concave in $\mathbf{a}$. Therefore, we are interested in characterizing the convergence condition of different pricing algorithms in ACSCG.

We know that for any local maximum $\mathbf{a}^*$ of problem (2.36), there exist Lagrange multipliers $\lambda_n, \nu_n^1, \cdots, \nu_n^N$ and $\nu_n'^1, \cdots, \nu_n'^N$ such that the following Karush-Kuhn-Tucker (KKT) conditions hold for all $n \in \mathcal{N}$:

$$\frac{\partial u_n(\mathbf{a}^*)}{\partial a_n^k} + \sum_{m \neq n} \frac{\partial u_m(\mathbf{a}^*)}{\partial a_n^k} = \lambda_n + \nu_n^k - \nu_n'^k, \ \forall n \tag{2.37}$$

$$\lambda_n \Big(\sum_{k=1}^{K} a_n^{k*} - M_n \Big) = 0, \ \lambda_n \geq 0 \tag{2.38}$$

$$\nu_n^k (a_n^{k*} - a_{n,k}^{\max}) = 0, \ \nu_n'^k (a_{n,k}^{\min} - a_n^{k*}) = 0, \ \nu_n^k, \nu_n'^k \geq 0. \tag{2.39}$$

Denote π_{mn}^k user m's marginal fluctuation in utility per unit decrease in user n's action a_n^k within the kth dimension

$$\pi_{mn}^k (a_m^k, \mathbf{a}_{-m}^k) = -\frac{\partial u_m(\mathbf{a})}{\partial a_n^k}, \tag{2.40}$$

which is announced by user m to user n and can be viewed as the cost charged (or compensation paid) to user n for changing user m's utility. Using (2.40),

equation (2.37) can be rewritten as

$$\frac{\partial u_n(\mathbf{a}^*)}{\partial a_n^k} - \sum_{m \neq n} \pi_{mn}^k(a_m^{k*}, \mathbf{a}_{-m}^{k*}) = \lambda_n + \nu_n^k - \nu_n'^k. \tag{2.41}$$

If we assume fixed prices $\{\pi_{mn}^k\}$ and action profile $\mathbf{a}_{-n}^k$, condition (2.41) gives the necessary and sufficient KKT condition of the following problem:

$$\max_{\mathbf{a}_n \in \mathcal{A}_n} \; u_n(\mathbf{a}) - \sum_{k=1}^{K} a_n^k \cdot \Big(\sum_{m \neq n} \pi_{mn}^k \Big). \tag{2.42}$$

At an optimum, a user behaves as if it maximizes the differences between its utility minus its payment to the other users in the network due to its impact over the other users' utilities. Different distributed pricing mechanisms can be developed based on the individual objective function in (2.42) and the convergence conditions may also vary based on the specific action update equation.

When optimization program (2.36) is not convex, the pricing algorithms developed for convex NUM, e.g. gradient and subgradient algorithms, cannot be directly applied. In the next two subsections, we will investigate two distributed pricing mechanisms for non-convex ACSCG and provide two sufficient conditions that guarantee their convergence. Specifically, under these sufficient conditions, both algorithms guarantee that the total utility is monotonically increasing until it converges to a feasible operating point that satisfies the KKT conditions. Similarly as in Section 2.3.1, we first assume $f_n^k(\mathbf{a}_{-n})$ takes the form in (2.9) and users update their actions in parallel.

2.4.1 Gradient Play

The first distributed pricing algorithm that we consider is gradient play. The update iterations of gradient play need to be properly redefined in presence of real-time information exchange. Specifically, at stage t, users adopting this algorithm exchange price signals $\{\pi_{mn}^{k,t-1}\}$ using the gradient information at stage

$t-1$. Within each iteration, each user first determines the gradient of the objective in (2.42) based on the price vectors $\{\pi_{mn}^{k,t-1}\}$ and its own utility function $u_n(\mathbf{a}_n, \mathbf{a}_{-n}^{t-1})$. Then each user updates its action a_n^t using gradient projection algorithm according to

$$a_n^{'k,t} = a_n^{k,t-1} + \kappa\Big(\frac{\partial u_n(\mathbf{a}_n, \mathbf{a}_{-n}^{t-1})}{\partial a_n^k} - \sum_{m\neq n} \pi_{mn}^{k,t-1}\Big). \tag{2.43}$$

and

$$\mathbf{a}_n^t = [a_n^{1,t} a_n^{2,t} \cdots a_n^{K,t}] = \Big[a_n^{'1,t} a_n^{'2,t} \cdots a_n^{'K,t}\Big]_{\mathcal{A}_n}^{\|\cdot\|_2}. \tag{2.44}$$

in which the stepsize $\kappa > 0$. The following theorem provides a sufficient condition under which gradient play will converge monotonically provided that we choose small enough constant stepsize κ.

Theorem 2.7 *If* $\forall n, k, \mathbf{x}, \mathbf{y} \in \mathcal{A}_{-n}$,

$$\inf_x \frac{\partial^2 h_n^k(x)}{\partial^2 x} > -\infty, \text{ and } \Big\| \bigtriangledown\, g_n^k(\mathbf{x}) - \bigtriangledown g_n^k(\mathbf{y})\Big\| \leq L'\big\|\mathbf{x}-\mathbf{y}\big\|, \tag{C7}$$

gradient play converges for a small enough stepsize κ.

Proof: This theorem can be proved by showing the gradient of the objective function in (2.36) is Lipschitz continuous and applying Proposition 3.4 in [BT97]. See Appendix E for details. ■

Remark 2.7 *(Application of condition (C7)) A sufficient condition that guarantees the convergence of distributed gradient projection algorithm is the Lipschitz continuity of the gradient of the objective function in (2.36). For example, in the power control problem in multi-channel networks [HBH06], we have* $h_n^k(x) = \log_2(\alpha_n^k + H_{nn}^k x)$ *and* $g_n^k(\mathbf{P}_{-n}) = \log_2(\sigma_n^k + \sum_{m\neq n} H_{mn}^k P_m^k)$. *For this configuration, we can immediately verify that condition (C7) is satisfied. Therefore,*

gradient play can be applied. Moreover, as in [HBH06], if we can further ensure that the problem in (2.36) is convex for some particular utility functions, gradient play converges to the unique optimal solution of (2.36) at which achieving KKT conditions implies global optimality.

2.4.2 Jacobi Update

We consider another alternative strategy update mechanism called Jacobi update [LA02]. In Jacobi update, every user adjusts its action gradually towards the best response strategy. Specifically, the maximizer of problem (2.42) takes the following form

$$B_n^{'k}(\mathbf{a}_{-n}) = \Big\{\frac{\partial h_n^k}{\partial x}\Big\}^{-1}\big(\lambda_n + \nu_n^k - \nu_n^{'k} + \sum_{m\neq n}\pi_{mn}^k\big) - \sum_{m\neq n} F_{mn}^k a_m^k, \tag{2.45}$$

in which λ_n, ν_n^k, and $\nu_n^{'k}$ are the Lagrange multipliers that satisfy complementary slackness in (2.38) and (2.39), and π_{mn}^k is defined in (2.40). In Jacobi update, at stage t, user n chooses its action according to

$$a_n^{k,t} = a_n^{k,t-1} + \kappa\big[B_n^{'k}(\mathbf{a}_{-n}^{t-1}) - a_n^{k,t-1}\big], \tag{2.46}$$

in which the stepsize $\kappa \in (0, 1]$. The following theorem establishes a sufficient convergence condition for Jacobi update.

Theorem 2.8 *If* $\forall n, k, \mathbf{x}, \mathbf{y} \in \mathcal{A}_{-n}$,

$$\inf_x \frac{\partial^2 h_n^k(x)}{\partial^2 x} > -\infty,\ \sup_x \frac{\partial^2 h_n^k(x)}{\partial^2 x} < 0,\ \textit{and}\ \Big\| \bigtriangledown g_n^k(\mathbf{x}) - \bigtriangledown g_n^k(\mathbf{y})\Big\| \leq L'\big\|\mathbf{x}-\mathbf{y}\big\|, \tag{C8}$$

Jacobi update converges if the stepsize κ is sufficiently small.

Proof: This can be proved using the descent lemma and the mean value theorem. The details of the proof are provided in Appendix F. ■

Remark 2.8 *(Relation between condition (C8) and the result in [SBH08]) Shi et al. considered the power allocation for multi-carrier wireless networks with non-separable utilities. Specifically, $u_n(\cdot)$ takes the form*

$$u_n(\mathbf{P}) = r_i\left(\sum_{k=1}^{K}\log_2\left(1+\frac{H_{nn}^k P_n^k}{\sigma_n^k+\sum_{m\neq n}H_{mn}^k P_m^k}\right)\right), \tag{2.47}$$

in which $r_i(\cdot)$ is an increasing and strictly concave function. Since the utilities are non-separable, the distributed pricing algorithm proposed in [SBH08], which in fact belongs to Jacobi update, requires only one user to update its action profile at each stage while keeping the remaining users' action fixed. The condition in (C8) gives the convergence condition of the same algorithm in ACSCG. We prove in Theorem 2.7 that, if the utilities are separable, convergence can still be achieved even if these users update their actions at the same time. Therefore, we do not need an arbitrator to select the single user that updates its action at each stage.

Remark 2.9 *(Complexity of signaling) The complexity of message exchange measured in terms of the number of price signals to update in (2.40) is generally of the order of $O(KN^2)$. It is worth mentioning that the amount of signaling can be further reduced to $O(KN)$ in the scenarios where $g_n^k(\cdot)$ are functions of $\sum_{m\neq n}F_{mn}^k a_m^k$. In this case, each user only needs to announce one price signal π_n^k for each dimension of its action space:*

$$\pi_n^k(a_n^k, \boldsymbol{a}_{-n}^k) = -\frac{\partial u_n(\mathbf{a})}{\partial\big(\sum_{m\neq n}F_{mn}^k a_m^k\big)} \tag{2.48}$$

Consequently, π_{mn}^k can be determined based on $\pi_{mn}^k = F_{nm}^k\pi_m^k$, which greatly reduces the overhead of signaling requirement. It is straightforward to check that only $O(KN)$ messages need to be generated and exchanged per iteration in both utility functions (2.3) and (2.4).

Remark 2.10 *(Extension to general cases) As a matter of fact, conditions (C7) and (C8) apply to a broader class of multi-user interaction scenarios, including the general model defined in (2.2). Specifically, as addressed in Remark 2.7, the Lipschitz continuity of the gradient of* $\sum_{n=1}^{N} u_n(\mathbf{a})$ *is sufficient to guarantee that gradient play with a small enough stepsize achieves an operating point at which KKT conditions are satisfied. In addition, we can use the same technique in Appendix F to show the convergence of Jacobi update given that* $\sup_x \frac{\partial^2 h_n^k(x)}{\partial^2 x} < 0$, $\forall n, k$, *and the gradient of* $\sum_{n=1}^{N} u_n(\mathbf{a})$ *is Lipschitz continuous.*

2.5 Numerical Examples

In Section 2.2.2, we present several illustrative examples of ACSCG. This section uses Examples 2.1 and 2.3 to illustrate the various distributed algorithms discussed in the chapter.

We start with Example 2.1 to verify the proposed convergence conditions of best response dynamics. Even though it is a simple two-user game with $\mathcal{A}_n \subseteq \mathcal{R}^2$, existing results in the literature cannot immediately determine whether or not the best response dynamics in this simple game can globally converge to a NE. Specifically, in Example 2.1, we have

$$\begin{aligned} \frac{\partial f_n^1(\mathbf{a}_{-n})}{\partial a_{-n}^1} &= \frac{a_{-n}^1}{\sqrt{(a_{-n}^1)^2+1}}, \frac{\partial f_n^1(\mathbf{a}_{-n})}{\partial a_{-n}^2} = -\frac{a_{-n}^2}{\sqrt{(a_{-n}^2)^2+1}}, \\ \frac{\partial f_n^2(\mathbf{a}_{-n})}{\partial a_{-n}^1} &= -\frac{a_{-n}^1}{\sqrt{(a_{-n}^1)^2+1}}, \frac{\partial f_n^2(\mathbf{a}_{-n})}{\partial a_{-n}^2} = \frac{a_{-n}^2}{\sqrt{(a_{-n}^2)^2+1}}. \end{aligned} \tag{2.49}$$

According the definition of (2.25), we have

$$\begin{aligned} [\bar{\mathbf{T}}^{\max}]_{12} &= \max\left\{ \max_{\mathbf{a}\in\mathcal{A}} \sum_{k=1}^{K} \left|\frac{\partial f_2^k(\mathbf{a}_{-n})}{\partial a_1^1}\right|, \max_{\mathbf{a}\in\mathcal{A}} \sum_{k=1}^{K} \left|\frac{\partial f_2^k(\mathbf{a}_{-n})}{\partial a_1^2}\right| \right\} \\ &= \max\left\{ \max_{\mathbf{a}_1\in\mathcal{A}_1} \frac{2a_1^1}{\sqrt{(a_1^1)^2+1}}, \max_{\mathbf{a}_1\in\mathcal{A}_1} \frac{2a_1^2}{\sqrt{(a_1^2)^2+1}} \right\} = \frac{2M_1}{\sqrt{M_1^2+1}}. \end{aligned} \tag{2.50}$$

Similarly, we can obtain $[\bar{\mathbf{T}}^{\max}]_{21} = \frac{2M_2}{\sqrt{M_2^2+1}}$. Therefore, $\rho(\bar{\mathbf{T}}^{\max}) = \sqrt{\frac{4M_1M_2}{\sqrt{M_1^2+1}\sqrt{M_2^2+1}}}$.

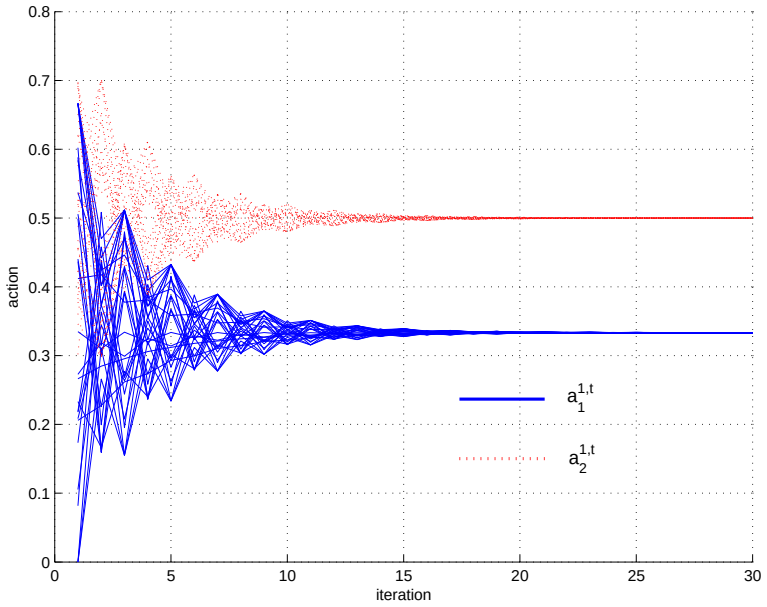

Figure 2.2: Actions versus iterations in Example 2.1.

It is easy to show that $\rho(\bar{\mathbf{T}}^{\max}) < 1 \Leftrightarrow (M_1^2 - \frac{1}{3})(M_1^2 - \frac{1}{3}) < \frac{4}{9}$. By condition (C4), we know that if $(M_1^2 - \frac{1}{3})(M_1^2 - \frac{1}{3}) < \frac{4}{9}$, the best response dynamics is guaranteed to converge to a unique NE. We numerically simulate a scenario with parameters $M_1 = \frac{2}{3}$ and $M_2 = 1$ in which condition (C4) holds. We generate multiple initial action profiles of $\mathbf{a}_1^0$ and $\mathbf{a}_2^0$, iterate the best response dynamics, and obtain the action sequences $\mathbf{a}_1^t$ and $\mathbf{a}_2^t$. Fig. 2.2 shows the trajectories of $a_1^{1,t}$ and $a_2^{1,t}$ for different realizations. We can see that, best response dynamics converges to a unique NE. If we set $M_1 = 2$ and $M_2 = 1$, condition (C4) does not hold any more. We observe from simulations that in many circumstances the best response dynamics will not converge, which agrees with our analysis in Remark 2.6.

Now we consider Example 2.3, which is the problem of minimizing queueing delays in a Jackson network. In particular, we consider a network with $N = 5$ nodes and $K = 3$ traffic classes. The total routing probability $1 - r_{m0}^k$ that node m

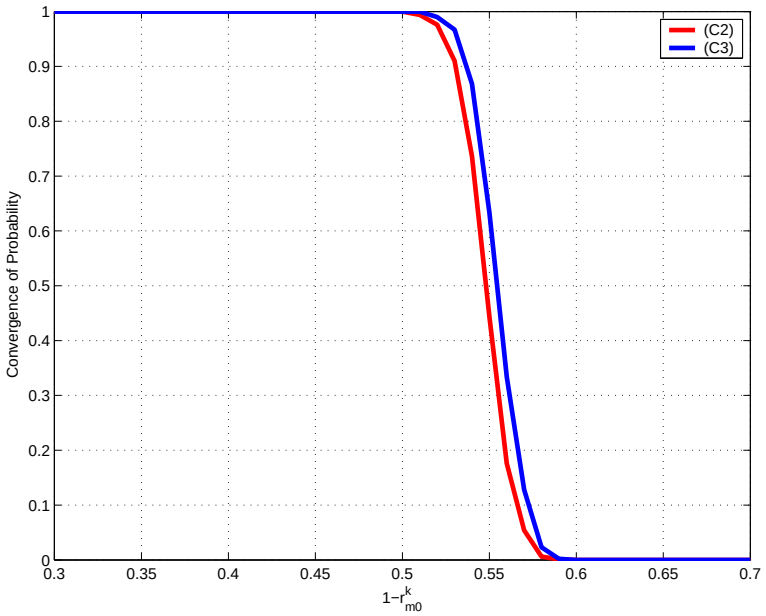

Figure 2.3: Probability of (C2) and (C3) versus $1 - r_{m0}^k$ for $\forall m, k$, $N = 5$, $K = 3$.

will route packets of class k completing service to other nodes is the same for $\forall m \in \mathcal{N}$. We varied the total routing probability $1 - r_{m0}^k$ and generated multiple sets of network parameters in which r_{mn}^k are uniformly distributed for $n = 1, 2, \cdots, N$, μ_n^k are uniformly selected in $[4, 5]$ for $\forall n, k$, and $\psi_n^{\min}$ are uniformly chosen in $[0.6, 1]$ for $n = 1, 2, \cdots, N$.

First of all, we compare the range of validity of the proposed convergence conditions. As we mentioned before, we have $F_{mn}^k = \frac{[(\mathrm{I}-\mathrm{R}^k)^{-1}]_{nm}}{[(\mathrm{I}-\mathrm{R}^k)^{-1}]_{nn}}$ in this example. Note that $(\mathrm{I}-\mathrm{R}^k)^{-1} = \mathrm{I}+\sum_{i=1}^{\infty}(\mathrm{R}^k)^i$ and R^k is a non-negative matrix. Therefore, we can conclude $F_{mn}^k \geq 0, \forall m \neq n, k$. Moreover, since $h_n^k(x) = -\frac{1}{\mu_n^k - \upsilon_{nn}^k x}$, we choose to compare conditions (C2) and (C3). In Fig. 2.3, we plot the probability that conditions (C2) and (C3) are satisfied versus the total routing probability $1 - r_{m0}^k$. From Fig. 2.3, we can see that the probability of guaranteeing convergence decreases as the routing probability $1 - r_{m0}^k$ increases and condition (C3) shows a similar but slightly broader validity than (C2). Fig. 2.4 shows the delay

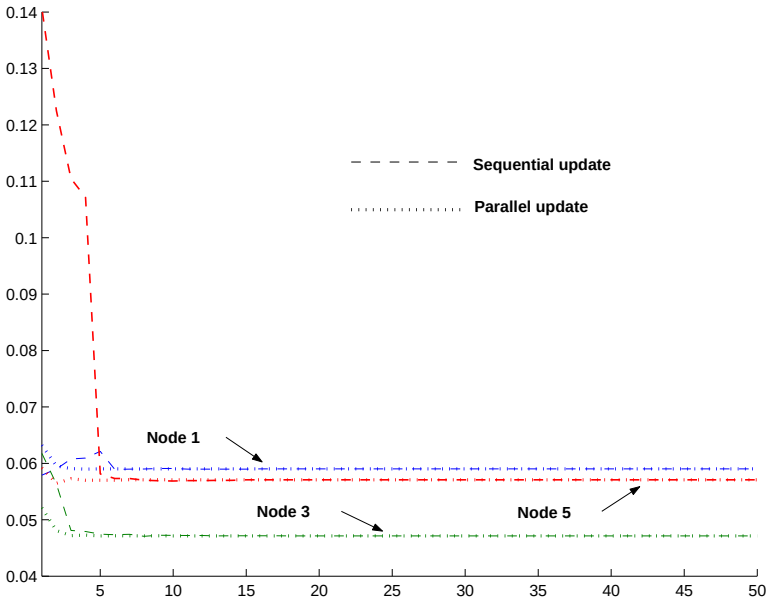

Figure 2.4: Delays of nodes versus iterations.

trajectories of three nodes using both sequential and parallel updates in a certain network realization in which (C2) and (C3) are satisfied. We can see that, the parallel update converges faster than the sequential update.

In Fig. 2.3, we also note that the probability that (C2) or (C3) is satisfied transits very quickly from the almost certain convergence to the non-convergence guarantee as $1-r_{m0}^k$ varies from 0.5 to 0.58. Similar observations have been drawn in the multi-channel power control problem [SPB08], where $\theta = -1$ in (2.18) and the probability that condition (C3) is satisfied exhibits a neat threshold behavior as the ratio between the source-interferer distance and the source-destination distance varies. In Jackson networks, this threshold can be roughly estimated. Define $[\mathbf{S}^k]_{mn} = F_{mn}^k$ for $m \neq n$ and $[\mathbf{S}^k]_{nn} = 0$ for $n \in \mathcal{N}$. If we fix $1 - r_{m0}^k$ for $\forall m, k$, we prove in Appendix G that $\rho(\mathbf{S}^k) \leq \frac{1}{r_{m0}^k} - 1$ for $\forall k$. Therefore, $\rho(\mathbf{S}^k) < 1$ when $r_{m0}^k > 0.5$. We would like to estimate $\rho(\mathbf{T}^{\max})$ and $\rho(\mathbf{S}^{\max})$ based on $\rho(\mathbf{S}^k)$. Note that $\mathbf{T}^{\max}$ defined in (2.16) is the element-wise maximum over $\mathbf{S}^k$

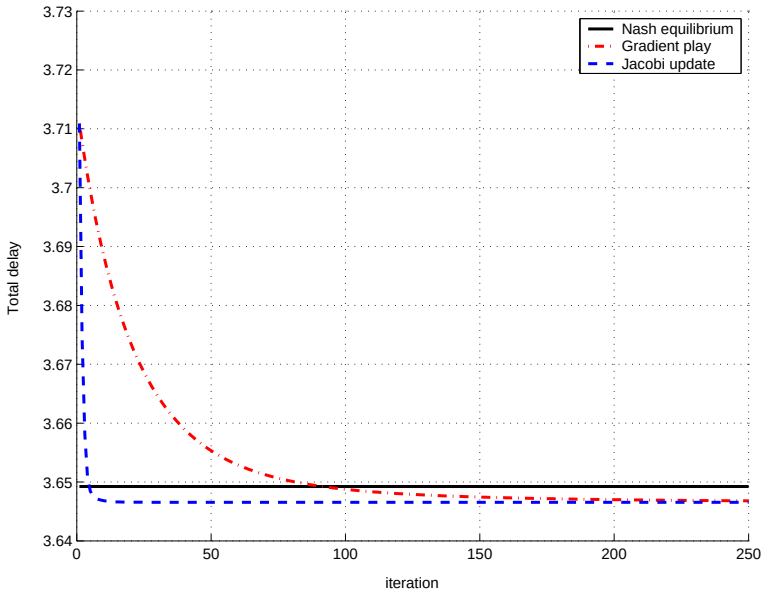

Figure 2.5: Illustration of convergence for gradient play and Jacobi update.

for $k = 1, 2, \ldots, K$. Since $\mathbf{T}^{\max}$ and $\mathbf{S}^k$ are all non-negative matrices, we know that $\rho(\mathbf{T}^{\max}) \geq \max_k \rho(\mathbf{S}^k)$. In addition, recall the effect of $\max_{m,n} \zeta_{mn}$ discussed in Remark 2.4. We can approximate $\rho(\mathbf{S}^{\max})$ defined in (2.20) using $\rho(\mathbf{S}^{\max}) \approx \max_{m,n} \zeta_{mn} \max_k \rho(\mathbf{S}^k)$. Therefore, we expect that $\rho(\mathbf{T}^{\max})$ and $\rho(\mathbf{S}^{\max})$ exceeds 1 for $r_{m0}^k < 0.5$, which agrees with our observation from Fig. 2.3. The physical interpretation is that, if the packets exit the network with a probability less than 50% after completing its service, i.e. more than half of the served packets will be routed to other nodes, the strength of the mutual coupling among users becomes too strong and the multi-user interaction in Jackson networks will gradually lose its convergence guarantee.

In addition, we numerically compare two distributed algorithms in which users pass coordination messages in real time, including Jacobi update and gradient play. Fig. 2.5 shows the delay evolution of both distributed solutions for a particular simulated network in which we set $\kappa = 0.2$. We initialize the system

parameters such that $\inf_{n,k} \mu_n^k - \sum_{m=1}^N \upsilon_{mn}^k \psi_m^k > 0$ and both conditions (C7) and (C8) are satisfied. We can verify that for Example 2.3, problem (2.36) is in fact a convex program. Therefore, there exists a unique operating point at which KKT conditions (2.37)-(2.39) are satisfied. We can see that, both algorithms cause the total delay to monotonically decrease until it reaches the same performance limit that is strictly better than NE. Using the same stepsize κ, Jacobi update converges more quickly than gradient play in this example. Similar observations are drawn in the other simulated examples. This is because the update directions of these two algorithms are different. Jacobi update moves directly towards the optimal solution of (2.42), which is a local approximation of the original optimization program in (2.36), whereas the gradient play algorithm simply updates the actions along the gradient direction of (2.36).

2.6 Concluding Remarks

In this chapter, we propose and investigate a new game model, which we refer to as additively coupled sum constrained games, in which each player is subject to a sum constraint and its utility is additively impacted by the remaining users' actions. The convergence properties of various generic distributed adjustment algorithms, including best response, gradient play, and Jacobi update, have been investigated. The sufficient conditions obtained in this chapter generalize the existing results developed in the multi-channel power control problem and can be extended to other applications that belong to ACSCG.

2.7 Appendix A: Proof of Theorem 2.1

The following lemma is needed to prove Theorem 2.1.

Lemma 2.1 *Consider any non-decreasing function $p(x)$ and non-increasing function $q(x)$. If there exists a unique x^* such that $p(x^*) = q(x^*)$, and the functions $p(x)$ and $q(x)$ are strictly increasing and strictly decreasing at $x = x^*$ respectively, then $x^* = \arg\min_x\{\max\{p(x), q(x)\}\}$.*

Proof of Lemma 2.1: See Lemma 1 in [CHC07]. ■

Denote $a_n^{k,t}$ as the action of user n in the kth dimension after iteration t. Recall that $\left[h_n^k\right]'(\cdot) > 0$, for $\forall n, k$. Therefore, $\sum_{k=1}^K a_n^{k,t} = M_n$ is satisfied at the end of any iteration t for any user n. Define $[x]^+ = \max\{x, 0\}$ and $[x]^- = \max\{-x, 0\}$. It is straightforward to see that

$$\sum_{k=1}^{K}[a_n^{k,t} - a_n^{k,t'}]^+ = \sum_{k=1}^{K}[a_n^{k,t} - a_n^{k,t'}]^-, \forall n, t, t'. \tag{2.51}$$

We also define

$$p^{n,t}(x) \triangleq \sum_{k=1}^{K}\left[l_n^k(\mathbf{a}_{-n}^t, x) - a_n^{k,t}\right]^- \tag{2.52}$$

and

$$q^{n,t}(x) \triangleq \sum_{k=1}^{K}\left[l_n^k(\mathbf{a}_{-n}^t, x) - a_n^{k,t}\right]^+, \tag{2.53}$$

in which $l_n^k(\cdot)$ is defined in (2.12). Since $h_n^k(\cdot)$ is a continuous increasing and strictly concave function, it is clear that $\left\{\frac{\partial h_n^k}{\partial x}\right\}^{-1}(\cdot)$ is a continuous decreasing function. If $p^{n,t}(\lambda_n^{t+1}) \neq 0$ (i.e. it has not converged), $p^{n,t}(x)$ ($q^{n,t}(x)$, respectively) is non-decreasing (non-increasing) in x, and strictly increasing (strictly decreasing) at $x = \lambda_n^{t+1}$. From (2.51) it is always true that $p^{n,t}(\lambda_n^{t+1}) = q^{n,t}(\lambda_n^{t+1})$. We first prove the convergence of the parallel update case in (2.15). For $\forall n$, we

have

$$\sum_{k=1}^{K}[a_n^{k,t+1}-a_n^{k,t}]^+$$

$$=\max\Big\{\sum_{k=1}^{K}[a_n^{k,t+1}-a_n^{k,t}]^+,\sum_{k=1}^{K}[a_n^{k,t+1}-a_n^{k,t}]^-\Big\} \tag{2.54}$$

$$=\max\{p^{n,t}(\lambda_n^{t+1}),q^{n,t}(\lambda_n^{t+1})\} \tag{2.55}$$

$$\leq\max\{p^{n,t}(\lambda_n^{t}),q^{n,t}(\lambda_n^{t})\} \tag{2.56}$$

$$\leq\max\Big\{\sum_{k=1}^{K}\Big[\sum_{m\neq n}F_{mn}^k(a_m^{k,t}-a_m^{k,t-1})\Big]^+,\sum_{k=1}^{K}\Big[\sum_{m\neq n}F_{mn}^k(a_m^{k,t}-a_m^{k,t-1})\Big]^-\Big\} \tag{2.57}$$

$$\leq\max\Big\{\sum_{k=1}^{K}\sum_{m\neq n}\Big[F_{mn}^k(a_m^{k,t}-a_m^{k,t-1})\Big]^+,\sum_{k=1}^{K}\sum_{m\neq n}\Big[F_{mn}^k(a_m^{k,t}-a_m^{k,t-1})\Big]^-\Big\} \tag{2.58}$$

$$=\max\Big\{\sum_{m\neq n}\sum_{k=1}^{K}\Big[F_{mn}^k(a_m^{k,t}-a_m^{k,t-1})\Big]^+,\sum_{m\neq n}\sum_{k=1}^{K}\Big[F_{mn}^k(a_m^{k,t}-a_m^{k,t-1})\Big]^-\Big\} \tag{2.59}$$

$$\leq\sum_{m\neq n}\max_k|F_{mn}^k|\cdot\Big\{\sum_{k=1}^{K}\Big[a_m^{k,t}-a_m^{k,t-1}\Big]^+\!+\sum_{k=1}^{K}\Big[a_m^{k,t}-a_m^{k,t-1}\Big]^-\Big\} \tag{2.60}$$

$$=\sum_{m\neq n}2\max_k|F_{mn}^k|\cdot\sum_{k=1}^{K}\Big[a_m^{k,t}-a_m^{k,t-1}\Big]^+, \tag{2.61}$$

where (2.54) and (2.61) follows from (2.51), (2.55) follows from the definition of $p^{n,t}$ and $q^{n,t}$ in (2.52) and (2.53), (2.56) is due to Lemma 1 in which $x=\lambda_n^t$, (2.57) follows from the definition of $p^{n,t}$ and $q^{n,t}$, the expression of $a_n^{k,t}$ in (2.15), and the fact that $\big[[x]_a^b-[y]_a^b\big]^+\leq[x-y]^+$ and $\big[[x]_a^b-[y]_a^b\big]^-\leq[x-y]^-$, (2.58) is due to the fact that $[x+y]^+\leq[x]^++[y]^+$ and $[x+y]^-\leq[x]^-+[y]^-$, (2.60) follows by using $[\sum_k x_k y_k]^+\leq\sum_k|x_k||y_k|=\sum_k|x_k|([y_k]^++[y_k]^-)\leq\max_k|x_k|\sum_k([y_k]^++[y_k]^-)$. For user n, we define that $e_n^t=\Big[a_m^{k,t}-a_m^{k,t-1}\Big]^+$. Inequality (2.61) can be written as $e_n^{t+1}\leq\sum_{m\neq n}[\mathbf{T}^{\max}]_{mn}e_m^t$ in which $\mathbf{T}^{\max}$ is defined in (2.16).

Since $\mathbf{T}^{\max}$ is a nonnegative matrix, by the Perron-Frobenius Theorem [BT97], there exists a positive vector $\bar{\mathbf{w}} = [\bar{w}_1 \dots \bar{w}_N]$ such that

$$\|\mathbf{T}^{\max}\|^{\bar{\mathbf{w}}}_{\infty,\text{mat}} = \rho(\mathbf{T}^{\max}), \tag{2.62}$$

where $\|\cdot\|^{\bar{\mathbf{w}}}_{\infty,\text{mat}}$ is the weighted maximum matrix norm defined as

$$\|\mathbf{A}\|^{\bar{\mathbf{w}}}_{\infty,\text{mat}} \triangleq \max_{i=1,2,\cdots,N} \frac{1}{\bar{w}_i} \sum_{j=1}^{N} [\mathbf{A}]_{ij} \bar{w}_j, \quad \mathbf{A} \in \mathcal{R}^{N\times N}. \tag{2.63}$$

Define the vectors $\mathbf{e}^{t+1} \triangleq [e_1^{t+1}, e_2^{t+1}, \dots, e_N^{t+1}]^T$ and $\mathbf{e}^t \triangleq [e_1^t, e_2^t, \dots, e_N^t]^T$. The set of inequalities in (2.61) can be expressed in the vector form as $\mathbf{0} \leq \mathbf{e}^{t+1} \leq \mathbf{T}^{\max}\mathbf{e}^t$. By choosing the vector $\bar{\mathbf{w}}$ that satisfies $\|\mathbf{T}^{\max}\|^{\bar{\mathbf{w}}}_{\infty,\text{mat}} = \rho(\mathbf{T}^{\max})$ and applying the infinity norm $\|\cdot\|^{\bar{\mathbf{w}}}_{\infty}$, we obtain the following

$$\|\mathbf{e}^{t+1}\|^{\bar{\mathbf{w}}}_{\infty} \leq 2\|\mathbf{T}^{\max}\mathbf{e}^t\|^{\bar{\mathbf{w}}}_{\infty} \leq 2\|\mathbf{T}^{\max}\|^{\bar{\mathbf{w}}}_{\infty,\text{mat}} \|\mathbf{e}^t\|^{\bar{\mathbf{w}}}_{\infty}, \tag{2.64}$$

Finally, based on (2.61) and (2.64), it follows that

$$\begin{aligned} \max_{n\in\mathcal{N}} \frac{e_n^{t+1}}{\bar{w}_n} &= \|\mathbf{e}^{t+1}\|^{\bar{\mathbf{w}}}_{\infty} \leq 2\|\mathbf{T}^{\max}\|^{\bar{\mathbf{w}}}_{\infty,\text{mat}} \|\mathbf{e}^t\|^{\bar{\mathbf{w}}}_{\infty} \\ &\leq 2\|\mathbf{T}^{\max}\|^{\bar{\mathbf{w}}}_{\infty,\text{mat}} \cdot \max_{n\in\mathcal{N}} \frac{e_n^t}{\bar{w}_n} = 2\rho(\mathbf{T}^{\max}) \cdot \max_{n\in\mathcal{N}} \frac{e_n^t}{\bar{w}_n} \end{aligned} \tag{2.65}$$

Therefore, if $\|\mathbf{T}^{\max}\|^{\bar{\mathbf{w}}}_{\infty,\text{mat}} = \rho(\mathbf{T}^{\max}) < \frac{1}{2}$, the best response dynamics in (2.15) is a contraction with the modulus $\|\mathbf{T}^{\max}\|^{\bar{\mathbf{w}}}_{\infty,\text{mat}}$ with respect to the norm $\max_{n\in\mathcal{N}} \frac{\|\cdot\|_2^{\mathbf{w}_n}}{\bar{w}_n}$. We can conclude that, the best response dynamics has a unique fixed point $\mathbf{a}^*$ and, given any initial value $\mathbf{a}^0$, the update sequence $\{\mathbf{a}^t\}$ converges to the fixed point $\mathbf{a}^*$.

In the sequential update case, the convergence result can be established by using the proposition 1.4 in [BT97]. The key step is to obtain

$$\max_{n\in\mathcal{N}} \frac{e_n^{t+1}}{\bar{w}_n} \leq 2\rho(\mathbf{T}^{\max}) \cdot \max\Big\{ \max_{j<n} \frac{e_j^{t+1}}{\bar{w}_j}, \max_{j\geq n} \frac{e_j^t}{\bar{w}_j} \Big\}. \tag{2.66}$$

A simple induction on n yields

$$\max_{n\in\mathcal{N}} \frac{e_n^{t+1}}{\bar{w}_n} \leq 2\rho(\mathbf{T}^{\max}) \cdot \max_{n\in\mathcal{N}} \frac{e_n^t}{\bar{w}_n} \tag{2.67}$$

for all n. Therefore, inequality (2.61) also holds for the sequential update and the contraction iteration globally converges to a unique equilibrium. ■

2.8 Appendix B: Proof of Theorem 2.2

If $F_{mn}^k \geq 0, \forall m \neq n, k$, the inequalities after (2.59) become

$$\max\Big\{ \sum_{m\neq n}\sum_{k=1}^{K} \Big[F_{mn}^k(a_m^{k,t} - a_m^{k,t-1})\Big]^+, \sum_{m\neq n}\sum_{k=1}^{K} \Big[F_{mn}^k(a_m^{k,t} - a_m^{k,t-1})\Big]^-\Big\} \tag{2.68}$$

$$\leq \sum_{m\neq n} \max_k F_{mn}^k \cdot \max\Big\{ \sum_{k=1}^{K} \Big[a_m^{k,t} - a_m^{k,t-1}\Big]^+, \sum_{k=1}^{K} \Big[a_m^{k,t} - a_m^{k,t-1}\Big]^-\Big\} \tag{2.69}$$

$$= \sum_{m\neq n} \max_k F_{mn}^k \cdot \sum_{k=1}^{K} \Big[a_m^{k,t} - a_m^{k,t-1}\Big]^+. \tag{2.70}$$

Similarly, for $F_{mn}^k \leq 0, \forall m \neq n, k$, we have

$$\max\Big\{ \sum_{m\neq n}\sum_{k=1}^{K} \Big[F_{mn}^k(a_m^{k,t} - a_m^{k,t-1})\Big]^+, \sum_{m\neq n}\sum_{k=1}^{K} \Big[F_{mn}^k(a_m^{k,t} - a_m^{k,t-1})\Big]^-\Big\} \tag{2.71}$$

$$\leq \sum_{m\neq n} \max_k\big\{-F_{mn}^k\big\} \cdot \max\Big\{ \sum_{k=1}^{K} \Big[a_m^{k,t} - a_m^{k,t-1}\Big]^+, \sum_{k=1}^{K} \Big[a_m^{k,t} - a_m^{k,t-1}\Big]^-\Big\} \tag{2.72}$$

$$= \sum_{m\neq n} \max_k\big\{-F_{mn}^k\big\} \cdot \sum_{k=1}^{K} \Big[a_m^{k,t} - a_m^{k,t-1}\Big]^+. \tag{2.73}$$

Therefore, if $F_{mn}^k \geq 0, \forall m \neq n, k$ or $F_{mn}^k \leq 0, \forall m \neq n, k$, given (C2), the sequence $\{\mathbf{a}_n^t\}$ contracts with the modulus $\rho(\mathbf{T}^{\max}) < 1$ under the norm $\max_{n\in\mathcal{N}} \frac{\sum_k [x_n^k]^+}{\bar{w}_n}$ and the convergence follows readily. ■

2.9 Appendix C: Proof of Theorem 2.3

Let $\|\cdot\|_2^{\mathbf{w}}$ denote the weighted Euclidean norm with weights $\mathbf{w} = [w_1 \dots w_K]^T$, i.e. $\|\mathbf{x}\|_2^{\mathbf{w}} \triangleq (\sum_i w_i |x_i|^2)^{1/2}$ [HJ81]. Define the simplex

$$\mathcal{S} \triangleq \Big\{ \mathbf{x} \in \mathcal{R}^K : \frac{1}{K} \sum_{k=1}^{K} x_k = 1, x_k^{\min} \leq x_k \leq x_k^{\max}, \ \forall k = 1, 2, \dots, K \Big\}. \tag{2.74}$$

in which $\sum_k x_k^{\max} \geq 1$. The following lemma is needed to prove Theorem 2.3.

Lemma 2.2 *The projection with respect to the weighted Euclidean norm with weights $\boldsymbol{w}$, of the K-dimensional real vector $-\mathbf{x}_0 \triangleq -[x_{0,1}, \dots, x_{0,K}]^T$ onto the simplex $\mathcal{S}$ defined in (2.74), denoted by $[-\mathbf{x}_0]_{\mathcal{S}}^{\boldsymbol{w}}$, is the optimal solution to the following convex optimization problem:*

$$[-\mathbf{x}_0]_{\mathcal{S}}^{\boldsymbol{w}} \triangleq \arg\min_{\mathbf{x} \in \mathcal{S}} \big\| \mathbf{x} - (-\mathbf{x}_0) \big\|_2^{\boldsymbol{w}} \tag{2.75}$$

and takes the following form:

$$x_k^* = \Big[\frac{\lambda}{w_k} - x_{0,k} \Big]_{x_k^{\min}}^{x_k^{\max}}, k = 1, \dots, K \tag{2.76}$$

where $\lambda > 0$ is chosen in order to satisfy the constraint $\frac{1}{K} \sum_{k=1}^{K} x_k^* = 1$.

Proof of Lemma 2.2: See Corollary 2 in [SPB08]. ■

For $h_n^k(\cdot)$ defined in (2.18), user n updates its action according to

$$a_n^{*k} = l_n^k(\mathbf{a}_{-n}, \lambda^*) = \Big[\big(\frac{1}{F_{nn}^k} \big)^{1+\frac{1}{\theta}} \cdot (\lambda^*)^{\frac{1}{\theta}} - \frac{\alpha_n^k}{F_{nn}^k} - \sum_{m \neq n} F_{mn}^k a_m^k \Big]_{a_{n,k}^{\min}}^{a_{n,k}^{\max}}. \tag{2.77}$$

and λ^* is chosen to satisfy $\sum_{k=1}^{K} a_n^{*k} = M_n$. Define the vector update operator as $[\mathrm{BR}(\mathbf{a}_{-n})]_k \triangleq a_n^{*k}$ and the coupling vector as

$$[\mathbf{C}_n(\mathbf{a}_{-n})]_k \triangleq \frac{\alpha_n^k}{F_{nn}^k} + \sum_{m \neq n} F_{mn}^k a_m^k \tag{2.78}$$

with $k \in \{1, \ldots, K\}$. We also define

$$\mathbf{F}'_{mn} \triangleq \operatorname{diag}\Big(F^1_{mn}, F^2_{mn}, \ldots, F^K_{mn}\Big) \tag{2.79}$$

and

$$\boldsymbol{\alpha}'_n \triangleq \Big[\frac{\alpha^1_n}{F^1_{nn}}, \frac{\alpha^2_n}{F^2_{nn}}, \ldots, \frac{\alpha^K_n}{F^K_{nn}}\Big]^T. \tag{2.80}$$

Therefore, the coupling vector can be alternatively rewritten as

$$\mathbf{C}_n(\mathbf{a}_{-n}) = \boldsymbol{\alpha}'_n + \sum_{m \neq n} \mathbf{F}'_{mn}\mathbf{a}_m. \tag{2.81}$$

Define a weight matrix $\mathbf{W} = [\mathbf{w}_1 \ldots \mathbf{w}_N]$ in which the element $[\mathbf{W}]_{kn}$ is chosen according to

$$[\mathbf{W}]_{kn} = [\mathbf{w}_n]_k = \frac{(F^k_{nn})^{1+\frac{1}{\alpha}}}{\sum_{k=1}^K (F^k_{nn})^{1+\frac{1}{\alpha}}}. \tag{2.82}$$

By Lemma 2.2, we know that the vector update operator $\mathrm{BR}_n(\mathbf{a}_{-n})$ in (2.19) can be interpreted as the projection of the coupling vector $-\mathbf{C}_n(\mathbf{a}_{-n})$ onto user n's action set $\mathcal{A}_n$ with respect to $\|\cdot\|_2^{\mathbf{w}_n}$, i.e.

$$\mathrm{BR}_n(\mathbf{a}_{-n}) = \big[-\mathbf{C}_n(\mathbf{a}_{-n})\big]^{\mathbf{w}_n}_{\mathcal{A}_n}. \tag{2.83}$$

Given any $\mathbf{a}^{(1)}, \mathbf{a}^{(2)} \in \mathcal{A}$, we define respectively, for each user n, the weighted Euclidean distances between these two vectors and their projected vectors using (2.83) as $e_n = \big\|\mathbf{a}^{(2)}_n - \mathbf{a}^{(1)}_n\big\|_2^{\mathbf{w}_n}$ and $e_{\mathrm{BR}_n} = \big\|\mathrm{BR}_n(\mathbf{a}^{(1)}_{-n}) - \mathrm{BR}_n(\mathbf{a}^{(2)}_{-n})\big\|_2^{\mathbf{w}_n}$. Again, we first prove the convergence of the parallel update case in (2.15). We have

$\forall n \in \mathcal{N}$,

$$
\begin{aligned}
e_{\mathrm{BR}_n} &= \Big\| \big[-\mathbf{C}_n(\mathbf{a}_{-n}^{(1)})\big]_{\mathcal{A}_n}^{\mathbf{w}_n} - \big[-\mathbf{C}_n(\mathbf{a}_{-n}^{(2)})\big]_{\mathcal{A}_n}^{\mathbf{w}_n} \Big\|_2^{\mathbf{w}_n} \\
&\leq \Big\| \mathbf{C}_n(\mathbf{a}_{-n}^{(2)}) - \mathbf{C}_n(\mathbf{a}_{-n}^{(1)}) \Big\|_2^{\mathbf{w}_n} && (2.84) \\
&= \Big\| \sum_{m \neq n} \mathbf{F}'_{mn} \mathbf{a}_m^{(2)} - \sum_{m \neq n} \mathbf{F}'_{mn} \mathbf{a}_m^{(1)} \Big\|_2^{\mathbf{w}_n} = \Big\| \sum_{m \neq n} \mathbf{F}'_{mn} \big(\mathbf{a}_m^{(2)} - \mathbf{a}_m^{(1)}\big) \Big\|_2^{\mathbf{w}_n} && (2.85) \\
&\leq \sum_{m \neq n} \Big\| \mathbf{F}'_{mn} \big(\mathbf{a}_m^{(2)} - \mathbf{a}_m^{(1)}\big) \Big\|_2^{\mathbf{w}_n} = \sum_{m \neq n} \sqrt{\sum_{k=1}^{K} [\mathbf{w}_n]_k \big([\mathbf{F}'_{mn}]_{kk}\big)^2 \Big(a_m^{(2)k} - a_m^{(1)k}\Big)^2} && (2.86) \\
&= \sum_{m \neq n} \sqrt{\sum_{k=1}^{K} [\mathbf{w}_m]_k \Big([\mathbf{F}'_{mn}]_{kk} \frac{[\mathbf{w}_n]_k}{[\mathbf{w}_m]_k}\Big)^2 \Big(a_m^{(2)k} - a_m^{(1)k}\Big)^2} && (2.87) \\
&\leq \sum_{m \neq n} \max_k \Big(\big|[\mathbf{F}'_{mn}]_{kk}\big| \cdot \frac{[\mathbf{w}_n]_k}{[\mathbf{w}_m]_k} \Big) \sqrt{\sum_{k=1}^{K} [\mathbf{w}_m]_k \Big(a_m^{(2)k} - a_m^{(1)k}\Big)^2} && (2.88) \\
&= \sum_{m \neq n} \max_k \Big(\big|[\mathbf{F}'_{mn}]_{kk}\big| \cdot \frac{[\mathbf{w}_n]_k}{[\mathbf{w}_m]_k} \Big) \big\| \mathbf{a}_m^{(2)} - \mathbf{a}_m^{(1)} \big\|_2^{\mathbf{w}_m} && (2.89) \\
&= \sum_{m \neq n} [\mathbf{S}^{\max}]_{mn} e_m, && (2.90)
\end{aligned}
$$

where (2.84) follows from the non-expansion property of the projector $[\cdot]_{\mathcal{A}_n}^{\mathbf{w}_n}$ in the norm $\|\cdot\|_2^{\mathbf{w}_n}$ (See Proposition 3.2(c) in [BT97]), (2.86) follows from the triangle inequality [HJ81], and $\mathbf{S}^{\max}$ in (2.90) is defined according to (2.20).

The rest of the proof is similar as the proof after equation (2.61) in Appendix A. Details are omitted due to space limitations. ■

2.10 Appendix D: Proof of Theorem 2.4

The beginning part of the proof is the same as the proof of Theorem 2.1. For any user n with general $f_n^k(\cdot)$, the inequalities after (2.55) become

$$\sum_{k=1}^{K}[a_n^{k,t+1}-a_n^{k,t}]^+ \le \max\{p^{n,t}(\lambda_n^t), q^{n,t}(\lambda_n^t)\}$$

$$= \max\left\{\sum_{k=1}^{K}\Big[f_n^k(\mathbf{a}_{-n}^t)-f_n^k(\mathbf{a}_{-n}^{t-1})\Big]^+, \sum_{k=1}^{K}\Big[f_n^k(\mathbf{a}_{-n}^t)-f_n^k(\mathbf{a}_{-n}^{t-1})\Big]^-\right\} \tag{2.91}$$

$$= \max\Bigg\{\sum_{k=1}^{K}\Big[\sum_{m\neq n}\sum_{k'=1}^{K}\frac{\partial f_n^k}{\partial a_m^{k'}}(\xi_{-n}^t)(a_m^{k',t}-a_m^{k',t-1})\Big]^+,$$
$$\sum_{k=1}^{K}\Big[\sum_{m\neq n}\sum_{k'=1}^{K}\frac{\partial f_n^k}{\partial a_m^{k'}}(\xi_{-n}^t)(a_m^{k',t}-a_m^{k',t-1})\Big]^-\Bigg\} \tag{2.92}$$

$$\le \max\Bigg\{\sum_{k=1}^{K}\sum_{m\neq n}\sum_{k'=1}^{K}\Big[\frac{\partial f_n^k}{\partial a_m^{k'}}(\xi_{-n}^t)(a_m^{k',t}-a_m^{k',t-1})\Big]^+,$$
$$\sum_{k=1}^{K}\sum_{m\neq n}\sum_{k'=1}^{K}\Big[\frac{\partial f_n^k}{\partial a_m^{k'}}(\xi_{-n}^t)(a_m^{k',t}-a_m^{k',t-1})\Big]^-\Bigg\} \tag{2.93}$$

$$= \max\Bigg\{\sum_{m\neq n}\sum_{k'=1}^{K}\sum_{k=1}^{K}\Big[\frac{\partial f_n^k}{\partial a_m^{k'}}(\xi_{-n}^t)(a_m^{k',t}-a_m^{k',t-1})\Big]^+,$$
$$\sum_{m\neq n}\sum_{k'=1}^{K}\sum_{k=1}^{K}\Big[\frac{\partial f_n^k}{\partial a_m^{k'}}(\xi_{-n}^t)(a_m^{k',t}-a_m^{k',t-1})\Big]^-\Bigg\} \tag{2.94}$$

$$\le \sum_{m\neq n}\left\{\max_{k'}\sum_{k=1}^{K}\Big|\frac{\partial f_n^k}{\partial a_m^{k'}}(\xi_{-n}^t)\Big|\right\}\cdot\left\{\sum_{k'=1}^{K}\Big[(a_m^{k',t}-a_m^{k',t-1})\Big]^+ + \sum_{k'=1}^{K}\Big[(a_m^{k',t}-a_m^{k',t-1})\Big]^-\right\} \tag{2.95}$$

$$= \sum_{m\neq n}2\cdot\left\{\max_{k'}\sum_{k=1}^{K}\Big|\frac{\partial f_n^k}{\partial a_m^{k'}}(\xi_{-n}^t)\Big|\right\}\cdot\sum_{k'=1}^{K}\Big[(a_m^{k',t}-a_m^{k',t-1})\Big]^+ \tag{2.96}$$

where (2.91) follows from the definition of $p^{n,t}$ and $q^{n,t}$ and the expression of $a_n^{k,t}$ and $B_n^k(\mathbf{a}_{-n},\lambda)$ in (2.15) and (2.24), (2.92) follows from the mean value theorem for vector-valued functions with $\xi^t=\alpha\mathbf{a}^t+(1-\alpha)\mathbf{a}^{t-1}$ and $\alpha\in[0,1]$. By (C4),

it is straightforward to show that the iteration is a contraction by following the same arguments in Appendix A. The rest of the proof is omitted. ■

2.11 Appendix E: Proof of Theorem 2.6

The gradient play algorithm in (2.42) is in fact a gradient projection algorithm with constant stepsize κ. In order to establish its convergence, we first need to prove that the gradient of the objective in (2.36) is Lipschitz continuous, with a Lipschitz constant given by $L > 0$, i.e.

$$\Big\| \bigtriangledown \big(\sum_{n=1}^{N} u_n(\mathbf{x}) \big) - \bigtriangledown \big(\sum_{n=1}^{N} u_n(\mathbf{y}) \big) \Big\| \leq L \big\| \mathbf{x} - \mathbf{y} \big\|, \ \forall \mathbf{x}, \mathbf{y} \in \mathcal{A}. \tag{2.97}$$

It is known that it has the property of Lipschitz continuity if it has a Hessian bounded in the Euclidean norm.

The Hessian matrix $\mathbf{H}$ of $\sum_{n=1}^{N} u_n(\mathbf{a})$ can be decomposed into two matrices: $\mathbf{H} = \mathbf{H}_1 + \mathbf{H}_2$, in which the elements of matrix $\mathbf{H}_1$ are

$$\frac{\partial^2 \Big[\sum\limits_{n=1}^{N} \sum\limits_{k=1}^{K} h_n^k \big(a_n^k + \sum\limits_{m \neq n} F_{mn}^k a_m^k \big) \Big]}{\partial a_m^k \partial a_l^j} = \begin{cases} \sum\limits_{n=1}^{N} \frac{\partial^2 h_n^k}{\partial^2 x} \big(a_n^k + \sum\limits_{m \neq n} F_{mn}^k a_m^k \big) F_{mn}^k F_{ln}^k, & \text{if } k = j \\ 0, & \text{otherwise.} \end{cases} \tag{2.98}$$

with $F_{nn}^k = 1$ and the elements of matrix $\mathbf{H}_2$ are

$$- \frac{\partial^2 \Big[\sum\limits_{n=1}^{N} \sum\limits_{k=1}^{K} g_n^k(\mathbf{a}_{-n}) \Big]}{\partial a_m^k \partial a_l^j} = - \sum_{n=1}^{N} \sum_{k=1}^{K} \frac{\partial^2 g_n^k(\mathbf{a}_{-n})}{\partial a_m^k \partial a_l^j}. \tag{2.99}$$

Recall that $g_n^k(\cdot)$ is Lipschitz continuous and it satisfies

$$\Big\| \bigtriangledown g_n^k(\mathbf{x}) - \bigtriangledown g_n^k(\mathbf{y}) \Big\| \leq L' \big\| \mathbf{x} - \mathbf{y} \big\|, \ \forall n, k, \mathbf{x}, \mathbf{y} \in \mathcal{A}_{-n}.$$

Consequently, we have $\|\mathbf{H}_2\|_2 \leq NKL'$. As a result, we can estimate the Lipschitz

constant L using the following inequalities

$$\begin{aligned}\|\mathbf{H}\|_2 &\leq \|\mathbf{H}_1\|_2 + \|\mathbf{H}_2\|_2 \leq \sqrt{\|\mathbf{H}_1\|_1\|\mathbf{H}_1\|_\infty} + NKL' \\ &\leq \sup_{x,n,k}\Big|\frac{\partial^2 h_n^k}{\partial^2 x}\Big| \cdot \max_{k,l}\sum_{m=1}^{N}\sum_{n=1}^{N}|F_{mn}^k F_{ln}^k| + NKL'.\end{aligned} \tag{2.100}$$

We can choose the RHS of (2.100) as the Lipschitz constant L . By Proposition 3.4 in [BT97], we know that if $0 < \kappa < 2/L$, the sequence $\mathbf{a}^t$ generated by the gradient projection algorithm in (2.43) and (2.44) converges to a limiting point at which the KKT conditions in (2.37)-(2.39) are satisfied. ■

2.12 Appendix F: Proof of Theorem 2.7

We know from the proof of Theorem 2.6 that, under Condition (C7), $\sum_{n=1}^{N} u_n(\mathbf{a})$ is Lipschitz continuous and the inequality in (2.97) holds. Recall that $\sum_{n=1}^{N} u_n(\mathbf{x})$ is continuously differentiable. Therefore, by the descent lemma [BT97], we have

$$\sum_{n=1}^{N} u_n(\mathbf{x}) \geq \sum_{n=1}^{N} u_n(\mathbf{y}) + (\mathbf{x}-\mathbf{y})^T \cdot \bigtriangledown\big(\sum_{n=1}^{N} u_n(\mathbf{y})\big) - \frac{L}{2}\big\|\mathbf{x}-\mathbf{y}\big\|_2^2,\ \forall \mathbf{x},\mathbf{y} \in \mathcal{A}. \tag{2.101}$$

Therefore, in order to prove $\sum_{n=1}^{N} u_n(\mathbf{a}^t) \geq \sum_{n=1}^{N} u_n(\mathbf{a}^{t-1})$, we only need to show that

$$(\mathbf{a}^t - \mathbf{a}^{t-1})^T \cdot \bigtriangledown\big(\sum_{n=1}^{N} u_n(\mathbf{a}^{t-1})\big) \geq \frac{L}{2}\big\|\mathbf{a}^t - \mathbf{a}^{t-1}\big\|_2^2 \tag{2.102}$$

for sufficiently small κ. Substituting (2.46) into (2.102), we can see that it is equivalent to

$$\sum_{n=1}^{N}\sum_{k=1}^{K}\big(B_n^{'k}(\mathbf{a}_{-n}^{t-1}) - a_n^{k,t-1}\big) \cdot \frac{\partial \sum_{n=1}^{N} u_n(\mathbf{a}^{t-1})}{\partial a_n^{k,t-1}} \geq \kappa \cdot \frac{L}{2} \cdot \sum_{n=1}^{N}\sum_{k=1}^{K}\big(B_n^{'k}(\mathbf{a}_{-n}^{t-1}) - a_n^{k,t-1}\big)^2. \tag{2.103}$$

By equation (2.45), we have

$$B_n^{'k}(\mathbf{a}_{-n}^{t-1}) - a_n^{k,t-1} = \Big\{\frac{\partial h_n^k}{\partial x}\Big\}^{-1}\big(\lambda_n + \nu_n^k - \nu_n^{'k} + \sum_{m\neq n}\pi_{mn}^{k,t-1}\big) - \sum_{m\neq n}^{N} F_{mn}^k a_m^{k,t-1} - a_n^{k,t-1} \tag{2.104}$$

and

$$\frac{\partial \sum_{n=1}^{N} u_n(\mathbf{a}^{t-1})}{\partial a_n^{k,t-1}} = \frac{\partial h_n^k}{\partial x}\big(a_n^{k,t-1} + \sum_{m\neq n}^{N} F_{mn}^k a_m^{k,t-1}\big) - \sum_{m\neq n} \pi_{mn}^{k,t-1}. \tag{2.105}$$

By the mean value theorem, there exists $\xi_n^k \in \mathcal{R}$ such that

$$\begin{aligned}
&\frac{\partial h_n^k}{\partial x}\big(a_n^{k,t-1} + \sum_{m\neq n}^{N} F_{mn}^k a_m^{k,t-1}\big) - \sum_{m\neq n} \pi_{mn}^{k,t-1} \\
&= \frac{\partial h_n^k}{\partial x}\big(a_n^{k,t-1} + \sum_{m\neq n}^{N} F_{mn}^k a_m^{k,t-1}\big) - \Big(\lambda_n + \nu_n^k - \nu_n^{'k} + \sum_{m\neq n} \pi_{mn}^{k,t-1}\Big) + \Big(\lambda_n + \nu_n^k - \nu_n^{'k}\Big) \\
&= \frac{\partial^2 h_n^k}{\partial^2 x}(\xi_n^k) \cdot \left\{ a_n^{k,t-1} + \sum_{m\neq n}^{N} F_{mn}^k a_m^{k,t-1} - \Big\{\frac{\partial h_n^k}{\partial x}\Big\}^{-1}\Big(\lambda_n + \nu_n^k - \nu_n^{'k} + \sum_{m\neq n} \pi_{mn}^{k,t-1}\Big)\right\} \\
&\quad + \lambda_n + \nu_n^k - \nu_n^{'k}.
\end{aligned}$$

Multiplying (2.104) and (2.105) leads to

$$\begin{aligned}
&\sum_{n=1}^{N}\sum_{k=1}^{K}\big(B_n^{'k}(\mathbf{a}_{-n}^{t-1}) - a_n^{k,t-1}\big) \cdot \frac{\partial \sum_{n=1}^{N} u_n(\mathbf{a}^{t-1})}{\partial a_n^{k,t-1}} \\
&= -\sum_{n=1}^{N}\sum_{k=1}^{K} \frac{\partial^2 h_n^k}{\partial^2 x}(\xi_n^k) \cdot \left\{ \Big\{\frac{\partial h_n^k}{\partial x}\Big\}^{-1}\Big(\lambda_n + \nu_n^k - \nu_n^{'k} + \sum_{m\neq n} \pi_{mn}^{k,t-1}\Big) - a_n^{k,t-1} \right. \\
&\quad \left. - \sum_{m\neq n}^{N} F_{mn}^k a_m^{k,t-1} \right\}^2 + \sum_{n=1}^{N}\sum_{k=1}^{K}\big(B_n^{'k}(\mathbf{a}_{-n}^{t-1}) - a_n^{k,t-1}\big) \cdot (\lambda_n + \nu_n^k - \nu_n^{'k})
\end{aligned} \tag{2.106}$$

In the following, we differentiate two cases in which the Lagrange multipliers $\lambda_n, \nu_n^k, \nu_n^{'k}$ take different values.

First of all, if $\lambda_n = \nu_n^k = \nu_n^{'k} = 0$ for all k, n, equation (2.106) can be simplified

as

$$\sum_{n=1}^{N}\sum_{k=1}^{K}\big(B_n^{'k}(\mathbf{a}_{-n}^{t-1})-a_n^{k,t-1}\big)\cdot\frac{\partial\sum_{n=1}^{N}u_n(\mathbf{a}^{t-1})}{\partial a_n^{k,t-1}}$$
$$=-\sum_{n=1}^{N}\sum_{k=1}^{K}\frac{\partial^2 h_n^k}{\partial^2 x}(\xi_n^k)\cdot\Bigg\{\Big\{\frac{\partial h_n^k}{\partial x}\Big\}^{-1}\Big(\lambda_n+\nu_n^k-\nu_n^{'k}+\sum_{m\neq n}\pi_{mn}^{k,t-1}\Big)-a_n^{k,t-1}$$
$$-\sum_{m\neq n}^{N}F_{mn}^k a_m^{k,t-1}\Bigg\}^2. \tag{2.107}$$

On the other hand, if $\lambda_n>0$, $\nu_n^k>0$, or $\nu_n^{'k}>0$ for some k,n. Due to complementary slackness in (2.38) and (2.39), We know that

$$\lambda_n>0\Rightarrow\sum_{k=1}^{K}B_n^{'k}(\mathbf{a}_{-n}^{t-1})=M_n\geq\sum_{k=1}^{K}a_n^{k,t-1},$$
$$\nu_n^k>0\Rightarrow B_n^{'k}(\mathbf{a}_{-n}^{t-1})=a_{n,k}^{\max}\geq a_n^{k,t-1},$$
$$\nu_n^{'k}>0,\Rightarrow B_n^{'k}(\mathbf{a}_{-n}^{t-1})=a_{n,k}^{\min}\leq a_n^{k,t-1}.$$

As a result, the last term in (2.106) satisfy

$$\sum_{n=1}^{N}\sum_{k=1}^{K}\big(B_n^{'k}(\mathbf{a}_{-n}^{t-1})-a_n^{k,t-1}\big)\cdot(\lambda_n+\nu_n^k-\nu_n^{'k})=\sum_{n=1}^{N}\lambda_n\sum_{k=1}^{K}(B_n^{'k}(\mathbf{a}_{-n}^{t-1})-a_n^{k,t-1})+$$
$$\sum_{n=1}^{N}\sum_{k=1}^{K}\nu_n^k\big(B_n^{'k}(\mathbf{a}_{-n}^{t-1})-a_n^{k,t-1}\big)+\sum_{n=1}^{N}\sum_{k=1}^{K}\nu_n^{'k}\big(a_n^{k,t-1}-B_n^{'k}(\mathbf{a}_{-n}^{t-1})\big)\geq 0. \tag{2.108}$$

Therefore, in both cases, the following inequality holds

$$\sum_{n=1}^{N}\sum_{k=1}^{K}\big(B_n^{'k}(\mathbf{a}_{-n}^{t-1})-a_n^{k,t-1}\big)\cdot\frac{\partial\sum_{n=1}^{N}u_n(\mathbf{a}^{t-1})}{\partial a_n^{k,t-1}}$$
$$\geq-\sum_{n=1}^{N}\sum_{k=1}^{K}\sup_x\frac{\partial^2 h_n^k(x)}{\partial^2 x}\cdot\Bigg\{\Big\{\frac{\partial h_n^k}{\partial x}\Big\}^{-1}\Big(\lambda_n+\nu_n^k-\nu_n^{'k}+\sum_{m\neq n}\pi_{mn}^{k,t-1}\Big)-a_n^{k,t-1}$$
$$-\sum_{m\neq n}^{N}F_{mn}^k a_m^{k,t-1}\Bigg\}^2$$
$$=-\sum_{n=1}^{N}\sum_{k=1}^{K}\sup_x\frac{\partial^2 h_n^k(x)}{\partial^2 x}\cdot\big(B_n^{'k}(\mathbf{a}_{-n}^{t-1})-a_n^{k,t-1}\big)^2. \tag{2.109}$$

Finally, we can conclude that the inequality in (2.103) holds for $\kappa \leq \frac{2}{L} \cdot (-\max_{n,k} \sup_x \frac{\partial^2 h_n^k(x)}{\partial^2 x})$. Recall that Jacobi update requires $\kappa \in (0, 1]$. The stepsize κ can be eventually chosen as $0 < \kappa \leq \min\{\frac{2}{L} \cdot (-\max_{n,k} \sup_x \frac{\partial^2 h_n^k(x)}{\partial^2 x}), 1\}$ ■

2.13 Appendix G: Upper Bound of $\rho(\mathbf{S}^k)$

Denote $\mathbf{1}^T = [1\ 1 \cdots 1]^T$. If we fix $1 - r_{m0}^k$ for $\forall m, k$, we have $\mathbf{1}^T \mathrm{R}^k = (1 - r_{m0}^k)\mathbf{1}^T$. Note that $\Upsilon^k = (\mathrm{I} - \mathrm{R}^k)^{-1} = \mathrm{I} + \sum_{i=1}^{\infty} (\mathrm{R}^k)^i$. We have $\mathbf{1}^T \Upsilon^k = \mathbf{1}^T \big(\mathrm{I} + \sum_{i=1}^{\infty} (\mathrm{R}^k)^i\big) = \mathbf{1}^T + (1 - r_{m0}^k)\mathbf{1}^T \Upsilon^k$ and $\mathbf{1}^T \Upsilon^k = \frac{1}{1 - r_{m0}^k} \mathbf{1}^T$. Therefore, $|\Upsilon^k|_1 = \frac{1}{r_{m0}^k}$. Since $F_{mn}^k = \frac{[\Upsilon^k]_{nm}}{[\Upsilon^k]_{nn}}$ and $\Upsilon^k = \mathrm{I} + \sum_{i=1}^{\infty} (\mathrm{R}^k)^i$, we know $[\Upsilon^k]_{nn} \geq 1$ for $\forall n$. Denote a diagonal matrix $\mathrm{diag}(\Upsilon^k)$ with the entries of Υ^k on the diagonal. Recall that $[\mathbf{S}^k]_{mn} = F_{mn}^k$ for $m \neq n$, and $[\mathbf{S}^k]_{nn} = 0$ for $n \in \mathcal{N}$. We can conclude that $\rho(\mathbf{S}^k) \leq |\mathbf{S}^k|_\infty \leq |(\Upsilon^k)^T - \mathrm{diag}(\Upsilon^k)|_\infty \leq |(\Upsilon^k)^T|_\infty - 1 = |\Upsilon^k|_1 - 1 = \frac{1}{r_{m0}^k} - 1$.

CHAPTER 3

Stackelberg Equilibrium in Power Control Games

The previous chapter presents the model of ACSCG and provides several sufficient conditions for various generic distributed algorithms. As a special subclass of the ACSCG, the multi-user power control problem in frequency-selective interference channels was investigated from the game-theoretic perspective in several prior works, including [YGC02, EPT07, HBH06, CYM06, YL06, CHC07]. In these multi-user wideband power control games, users are modeled as players having individual goals and strategies. They are competing or cooperating with each other until they agree on an acceptable resource allocation outcome. Existing research can be categorized into two types, *non-cooperative* games and *cooperative* games.

First, the formulation of the multi-user wideband power control problem as a non-cooperative game has appeared in several recent works [YGC02, EPT07]. An iterative water-filling (IW) algorithm was proposed to mitigate the mutual interference and optimize the performance without the need for a central controller [YGC02]. At every decision stage, selfish users deploying this algorithm try to maximize their achievable rates by water-filling across the whole frequency band until a Nash equilibrium is reached. Alternatively, self-enforcing protocols are studied in the non-cooperative scenario, in which incentive compatible

allocations are guaranteed [EPT07]. By imposing punishments in the case of misbehavior and enforcing users to cooperate, efficient, fair, and incentive compatible spectrum sharing is shown to be possible.

Second, there also have been a number of related works studying dynamic spectrum management (DSM) in the setting of cooperative games [HBH06, CYM06] [YL06, CHC07]. Two (near-) optimal but centralized DSM algorithms, the Optimal Spectrum Balancing (OSB) algorithm and the Iterative Spectrum Balancing (ISB) algorithm, were proposed to solve the problem of maximization of a weighted rate-sum across all users [CYM06, YL06]. OSB has an exponential complexity in the number of users. ISB only has a quadratic complexity in the number of users because it implements the optimization in an iterative fashion. An autonomous spectrum balancing (ASB) technique is proposed to achieve near-optimal performance autonomously, without real-time explicit information exchanges [CHC07]. These works focus on cooperative games, because it is well-known that the IW algorithm may lead to Pareto-inefficient solutions [PPR07], i.e. selfishness is detrimental in the interference channel.

In short, previous research mainly concentrates on studying the existence and performance of Nash equilibrium in non-cooperative games and developing efficient algorithms to approach the Pareto boundary in cooperative games. However, an important intrinsic dimension of this decentralized multi-user interaction still remains unexplored. Prior research does not consider the users' availability of information about other users and their potential to improve their performance when having this information. Hence, determining what is the best response strategy of a selfish user if it has the information about how the competing users respond to interference still needs to be determined. Moreover, it still needs to be established if such strategies can lead to a better performance than adopting

the IW algorithm. It is important to look at these scenarios in order to assess the significance of information availability in terms of its impact on the users' performance in non-cooperative games, and show why selfish users have incentives to learn their environment and adapt their rational response strategies [Hay05]. Intuitively, a "clever" user with more information in this non-cooperative game should be able to gain additional benefits [Hay07].

Throughout this chapter, we differentiate two types of selfish users based on their response strategies:

1) *Myopic user*: A user that always acts to maximize its immediate achievable rate. It is myopic in the sense that it treats other users' actions as fixed, ignores the dependence between its competitors' actions and its own action, and determines its response such that maximize its immediate payoff.

2) *Foresighted user*: A user that selects its transmission action by considering the long-term impacts on its performance. It anticipates how the others will react, and maximizes its performance by considering their reactions. It should be highlighted that additional information is required to assist the foresighted user in its decision making.

As opposed to previous approaches considering myopic users [YGC02], we discuss in this chapter how foresighted users should behave in non-cooperative power control games. We explicitly show that a strategic user can gain more benefit if it takes its competitors' information and response strategies into account. The concept of Stackelberg equilibrium is adopted in order to characterize the optimal power control strategy of a foresighted user by considering the response of its competing users. For the two-user case, we formulate the foresighted user's decision making to be a bi-level programming problem, show that the optimal solution is computationally prohibitive, and provide a low-complexity algorithm

based on Lagrangian duality theory.

We also note that there are already some papers applying Stackelberg equilibrium to allocate the resources in networking [ABE06]. However, the problems and the proposed solutions in these papers are completely different from this chapter. The focus here is to study the strategic behavior of selfish users, which has not been yet investigated in multi-user interference channels.

The rest of the chapter is organized as follows. Section 3.1 presents the non-cooperative game model and introduces the concept of Stackelberg equilibrium. In Section 3.2, using a simple two-user example, we formulate the foresighted user's optimal decision making as a bi-level programming problem and discuss the computational complexity of its optimal solution. Section 3.3 proposes a low-complexity dual-based approach and provides the simulation results. Section 3.3 also discusses how the required information can be obtained by the strategic users and the problem formulation in general multi-user case. Concluding remarks are drawn in Section 3.4.

3.1 System Model

In this section, we describe the mathematical model of the frequency-selective interference channel and formulate the non-cooperative multi-user power control game. We introduce the concept of Stackelberg equilibrium and prove the existence of this equilibrium in the power control game.

3.1.1 System Description

Fig. 3.1 illustrates a frequency-selective Gaussian interference channel model. There are N transmitters and N receivers in the system. Each transmitter and

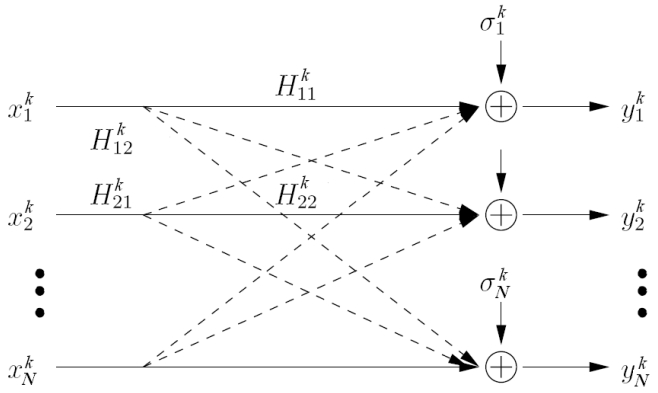

Figure 3.1: Gaussian interference channel model.

receiver pair can be viewed as a player (or user). The whole frequency band is divided into K frequency bins. In frequency bin k, the channel gain from transmitter i to receiver j is denoted as H_{ij}^k, where $k = 1, 2, \ldots, K$. Similarly, denote the noise power spectral density (PSD) that receiver n experiences as σ_n^k and player n's transmit PSD as P_n^k. For user n, the transmit PSD is subject to its power constraint:

$$\sum_{k=1}^{K} P_n^k \leq \mathbf{P_n^{max}}. \tag{3.1}$$

Define $\mathbf{P}_n = \{P_n^1, P_n^2, \ldots, P_n^K\}$ as user n's power allocation pattern. For a fixed $\mathbf{P}_n$, if treating interference as noise, user n can achieve the following data rate:

$$R_n = \sum_{k=1}^{K} \log_2 \left(1 + \frac{P_n^k |H_{nn}^k|^2}{\sigma_n^k + \sum_{j \neq n} P_j^k |H_{jn}^k|^2} \right). \tag{3.2}$$

To fully capture the performance tradeoff in the system, the concept of a rate region is defined as

$$\mathcal{R} = \Big\{ (R_1, \ldots, R_N) : \exists \, (\mathbf{P}_1, \ldots, \mathbf{P}_N) \text{ satisfying (1) and (2)} \Big\}. \tag{3.3}$$

Due to the non-convexity in the capacity expression as a function of power allocations, the computational complexity of optimal solutions (e.g., doing exhaustive search) in finding the rate region is prohibitively high. Existing works [CYM06, YL06, CHC07] aim to compute the Pareto boundary of this rate region and provide (near-) optimal performance with moderate complexity. Moreover, it is noted that cooperation among users is indispensable for this multi-user system to operate at the Pareto boundary. On the other hand, the interference channel can also be modeled as a non-cooperative game among multiple competing users. Instead of solving the optimization problem globally, the IW algorithm models the users as myopic decision makers [YGC02]. This means that they optimize their transmit PSD by water-filling and compete to increase their transmission data rates with the sole objective of maximizing their own performance regardless of the coupling among users. Under a wide range of realistic channel conditions [YGC02, SLS07], the existence and uniqueness of the competitive optimal point (Nash equilibrium) is demonstrated and it can be obtained by the IW algorithm, which significantly outperforms the static spectrum management algorithms.

Throughout this chapter, we also concentrate on the non-cooperative game setting. In the IW algorithm, users are assumed to be myopic, i.e., they update actions shortsightedly without considering the long-term impacts of taking these actions. We argue that the myopic behavior can be further improved because it neglects the coupling nature of players' actions and payoffs. In contrast with previous approaches, we study the problem of how a foresighted user should behave rather than taking myopic actions. This investigation provides us some insights to the following question: why should a strategic user sense its environment and learn the response strategies of its competitors and consequently, what is the benefit that a foresighted user can achieve compared with the myopic case?

	Left	*Right*
Up	1, 0	3, 2
Down	2, 1	4, 0

Figure 3.2: Stackelberg game: the row player's payoff is given first in each cell, with the column player's payoff following.

To illustrate the foresighted behavior, Fig. 3.2 shows a simple Stackelberg game [SPG07]. Note that in this game, the row player has a strictly dominant strategy [FT91], *Down*. Therefore, two players will end up with a (*Down, Left*) play if the row player is myopic. However, if the row player is aware of the column player's coupled reaction, they will end up with a (*Up, Right*) play, which leads to an increased payoff for both players. It is worth noticing that additional information is needed to attain this performance improvement. The row player needs to know the payoff and the response strategy of the column player. To formulate how a strategic user can take foresighted actions, we introduce the concept of Stackelberg equilibrium. The next subsection will define the Stackelberg equilibrium and show its existence in the power control game.

3.1.2 Stackelberg Equilibrium

Let $\Gamma = \langle \mathcal{N}, \mathcal{A}, u \rangle$ represent the power control game, in which user n's payoff u_n is the its achievable data rate R_n and its action set $\mathcal{A}_n$ is the set of transmit PSDs satisfying constraint (3.1). Recall that the Nash equilibrium is defined to be any $(a_1^*, \ldots, a_N^*)$ satisfying

$$u_n\left(a_n^*, a_{-n}^*\right) \geq u_n\left(a_n, a_{-n}^*\right) \text{ for all } a_n \in \mathcal{A}_n \text{ and } n = 1, \ldots, N, \tag{3.4}$$

where $a^*_{-n} = (a^*_1, \ldots, a^*_{n-1}, a^*_{n+1}, \ldots, a^*_N)$ [FT91]. The action a^*_n is a best response (BR) to actions a_{-n} if

$$u_n\left(a^*_n, a_{-n}\right) \geq u_n\left(a_n, a_{-n}\right), \ \forall\, a_n \in \mathcal{A}_n. \tag{3.5}$$

The set of user n's best response to a_{-n} is denoted as $BR_n(a_{-n})$.

The Stackelberg equilibrium is a solution concept originally defined for the cases where a hierarchy of actions exists between users [FT91]. Only one player is the *leader* and the other ones are *followers*. The leader begins the game by announcing its action. Then, the followers react to the leader's action. The Stackelberg equilibrium prescribes an optimal strategy for the leader if its followers always react by playing their Nash equilibrium strategies in the smaller sub-game. For example, in a two player game, where user 1 is the leader and user 2 is the follower, an action a^*_1 is the Stackelberg equilibrium strategy for user 1 if

$$u_1\left(a^*_1, BR_2\left(a^*_1\right)\right) \geq u_1\left(a_1, BR_2\left(a_1\right)\right), \forall a_1 \in \mathcal{A}_1. \tag{3.6}$$

For example, in Fig. 3.2, *Up* is the Stackelberg equilibrium strategy for the row player.

Next, we define Stackelberg equilibrium in the general case. Let $NE(a_n)$ be the Nash equilibrium strategy of the remaining players if player n chooses to play a_n, i.e. $NE\left(a_n\right) = a_{-n},\ \forall a_i = BR_i\left(a_{-i}\right), a_i \in \mathcal{A}_i, i \neq n$.

Definition 3.1 *The strategy profile* $\left(a^*_n, NE\left(a^*_n\right)\right)$ *is a Stackelberg equilibrium with user* n *leading iff*

$$u_n\left(a^*_n, NE\left(a^*_n\right)\right) \geq u_n\left(a_n, NE\left(a_n\right)\right), \forall a_n \in \mathcal{A}_n. \tag{3.7}$$

If multiple Nash equilibria exist in the followers' sub-game, the definition of Stackelberg equilibrium becomes more complicated. Interested readers can refer

to [ABE06, CMS05] for more details. This chapter does not consider this case and focus on the channels where a unique Nash equilibrium exists in the subgame [SLS07]. In particular, the considered channels satisfies condition (C3). It has shown that a unique Nash equilibrium for the power control game exists in these channels and it can be achieved using the IW algorithm [SPB08, SLS07].

In fact, the requirement of hierarchic actions in the original definition of Stackelberg equilibrium can be removed in our problem if we consider the repeated interaction among all the users. Regardless of the initial action order, the foresighted user can always perform the Stackelberg strategy. As long as it changes its transmit PSD, the other myopic users will water-fill with respect to their updated noise-plus-interference PSDs to gain an immediate increase in transmission rates until the system converges to an equilibrium. We are interested in the performance achieved at the steady state. Therefore, the initial action order between the foresighted user and the myopic users does not influence the final outcome of this game. Note that initially we assume that a single foresighted user exists in this game. How the users should decide to play foresightedly or myopically and the extension to the cases where there are multiple foresighted users will be discussed in Section 3.3. The following theorem establishes the existence of Stackelberg equilibrium in the considered power control game.

Theorem 3.1 *Under the considered channel conditions, the Stackelberg equilibrium always exists in the multi-user power control game.*

Proof: Suppose user 1 is the only foresighted user in this game. First, user 1's maximal achievable rate in an interference-free environment is

$$R_1^{\max} = \sum_{k=1}^{K} \log_2 \left(1 + P_1^{k*} \left|H_{11}^k\right|^2 \Big/ \sigma_1^k\right), \tag{3.8}$$

where $P_1^{k*} = (\lambda - \sigma_1^k/|H_{11}^k|^2)^+$ is the water-filling solution, $(x)^+ = \max(0, x)$, and λ is a constant satisfying the constraint in (3.1) with equality.

Second, it has been shown that in the considered channels, the existence and uniqueness of Nash equilibrium are always guaranteed [SLS07]. In the interference channel consisting of the $N-1$ followers, whatever form of $\mathbf{P}_1 \in \mathcal{A}_1$ user 1 chooses, they will regard user 1's transmit PSD as part of the fixed background noise PSD, i.e. $\tilde{\sigma}_j^k = \sigma_j^k + \left|H_{1j}^k\right|^2 P_1^k,\ j \neq 1$. Since the channel gains in the followers' subgame still satisfy the sufficient condition in [SLS07], the convergence to a unique Nash equilibrium always holds, i.e. a single $NE(a_1)$ exists for $\forall a_1 \in \mathcal{A}_1$.

To summarize, since R_1 is bounded, and for $\forall a_1 \in \mathcal{A}_1$, the remaining players' action will always lead to a Nash equilibrium, we have

$$0 \leq u_1(a_1, NE(a_1)) \leq R_1^{\max},\ \forall a_1 \in \mathcal{A}_1. \tag{3.9}$$

Therefore, there exist $a_1^* \in \mathcal{A}_1$ such that

$$u_1(a_1^*, NE(a_1^*)) = \sup_{a_1 \in \mathcal{A}_1} \{u_1(a_1, NE(a_1))\}.$$

We can conclude that Stackelberg equilibrium always exists for this power control game. ■

3.2 Problem Formulation

In this section, we study how to achieve the Stackelberg equilibrium in the two-user case, and formulate the foresighted behavior as a bi-level programming problem. We analyze the computational complexity of the optimal solution, and show that the optimum is computationally intractable for the bi-level program. We start from the simplest two-user version, because it is illustrative for understanding the interactions emerging among competing users. The extension to the

multi-user case will be discussed in Section 3.3.

3.2.1 A Bi-level Programming Formulation

The Stackelberg equilibrium applied to the two-user power control game can be represented by a bi-level mathematical problem [CMS05], in which the foresighted user acts as the leader and the other user behaves as the follower. The leader chooses a transmit PSD to maximize its own benefits by considering the response of its follower, who reacts to the leader's transmit PSD by water-filling over the entire frequency band. Hence, the Stackelberg equilibrium can be found by solving the following optimization problem:

$$\begin{cases} \textit{upper-level} \\ \textit{problem} \end{cases} \begin{cases} \max\limits_{\mathbf{P}_1} \sum\limits_{k=1}^{K} \log_2\left(1+\dfrac{P_1^k}{N_1^k+\alpha_2^k P_2^k}\right) & (a) \\ s.t. \ \sum\limits_{k=1}^{K} P_1^k \le \mathbf{P_1^{max}},\ P_1^k \ge 0, & (b) \end{cases}$$
$$\begin{cases} \textit{lower-level} \\ \textit{problem} \end{cases} \begin{cases} \mathbf{P}_2 = \arg\max\limits_{\mathbf{P}_2'} \sum\limits_{k=1}^{K} \log_2\left(1+\dfrac{P_2'^k}{N_2^k+\alpha_1^k P_1^k}\right) & (c) \\ s.t.\ P_2'^k \ge 0,\ \sum\limits_{k=1}^{N} P_2'^k \le \mathbf{P_2^{max}}, & (d) \end{cases} \tag{3.10}$$

where $N_1^k = \sigma_1^k/|H_{11}^k|^2, \alpha_1^k = |H_{12}^k|^2/|H_{22}^k|^2, N_2^k = \sigma_2^k/|H_{22}^k|^2, \alpha_2^k = |H_{21}^k|^2/|H_{11}^k|^2$. The sub-problem in (3.10.a)- (3.10.b) is called the *upper-level problem* and (3.10.c)-(3.10.d) corresponds to the *lower-level problem*. Recall that additional information is indispensable to formulate this bi-level program. This information includes the other user's channel condition N_2^k and α_2^k, maximum power constraint $\mathbf{P_2^{max}}$, and its response strategy, i.e. the IW algorithm. By letting $\mathbf{P}_1$ and $\mathbf{P}_2$ to be the transmit PSDs of the IW algorithm $\mathbf{P}_1^{NE}$ and $\mathbf{P}_2^{NE}$, we can see that the Nash equilibrium actually gives a lower bound of the problem in (3.10). Furthermore, by including the opponent's reaction into the lower-level problem, the user can

avoid the myopic IW approach and potentially improve its performance. In addition, as we will show later, user 1's foresightedness turns out to even improve the myopic user's performance. Now we make several illustrative remarks by showing two simple examples.

Remark 3.1 *The Nash equilibrium achieved by the IW algorithm may not solve the bi-level program (3.10). In other words, there exist other feasible power allocation schemes that can attain strictly better performance than that of the Nash equilibrium.*

Example 3.1 *We consider a two-user system with the parameters* $N = 2, N_1^1 = N_2^2 = 4, N_1^2 = N_2^1 = 1, \alpha_n^k = 0.5$ *for* $\forall n, k$, $\mathbf{P_1^{max}} = \mathbf{P_2^{max}} = 10$. *In this simple two-channel scenario, it is easy to derive that* $R_1 = \log_2[1 + P_1^1/(8.5 - 0.25P_1^1)] + \log_2[1 + (10 - P_1^1)/(1.5 + 0.25P_1^1)]$ *bits. Because* $\frac{\partial R_1}{\partial P_1^1} < 0$, R_1 *is maximized when* $P_1^1 = 0$. *The achievable rates attained at the Stackelberg equilibrium is* $R_1^{SE} \approx 2.939$ *bits and* $R_2^{SE} \approx 3.474$ *bits. The unique Nash equilibrium is reached by* $\mathbf{P}_1^{NE} = \{2, 8\}$ *and* $\mathbf{P}_2^{NE} = \{8, 2\}$ *and its achievable rates are* $R_1^{NE} = R_2^{NE} \approx 2.645$ *bits.*

Remark 3.2 *For some channel realizations, the Nash strategy solves the problem (3.10). If* $\alpha_n^k = 0$ *for* $\forall n, k$, *the upper-level and lower-level problems in bi-level program (3.10) are reduced to two uncoupled problems and the single user water-filling solution can achieve the upper bound in (3.8). In addition, we give a non-trivial example in which* $\alpha_n^k \neq 0$ *for* $\forall n, k$ *and the Nash strategy still solves the problem in (3.10).*

Example 3.2 *Set the parameters* N_1^1, N_2^2 *in Example 3.1 to be* 6, *and keep the remaining ones unchanged. We have* $R_1 = \log_2[1 + P_1^1/(11 - 0.25P_1^1)] + \log_2[1 +$

$(10 - P_1^1)/(1 + 0.25P_1^1)]$ *bits. In this channel realization, the Nash equilibrium coincides with the Stackelberg equilibrium. Both equilibria are reached at* $\mathbf{P}_1^{NE} = \{0, 10\}$ *and* $\mathbf{P}_2^{NE} = \{10, 0\}$ *and the resulting rates are* $R_1 = R_2 \approx 3.460$ *bits.*

Remark 3.3 *As opposed to the narrow-band case [AA03], we would like to highlight that the degrees of freedom in allocating the power across multiple bands is essential for the foresighted user to improve its performance. Consider the single-band case in which* $K = 1$*. Note that user* i*'s achievable rate* R_i *is monotonically increasing in its transmitted power* P_i*. If users selfishly maximize their achievable rates, all of them will transmit at their maximum power in the single band, which results in the unique Nash equilibrium. It is easy to check that it is also the unique Stackelberg equilibrium and it is also Pareto efficient.*

Although these examples provide us some intuition about the relationship between NE and SE, we are still interested in computing the Stackelberg equilibrium in general scenarios. The following subsection will reformulate the bi-level program into a single-level problem, which helps us to understand the computational complexity of the Stackelberg equilibrium in the multi-user power control games.

3.2.2 An Exact Single-level Reformulation

Bi-level programming problems belong to the mathematical programs having optimization problems as constraints. It is well-known they are intrinsically difficult to solve [CMS05]. To understand the computational complexity, we first transform the original bi-level program into a single-level reformulation with the form

of

$$\begin{aligned} &\max_{\mathbf{P}_1} \sum_{k=1}^{K} \log_2 \left(1 + \frac{P_1^k}{N_1^k + \alpha_2^k g_2^k \left(\mathbf{P}_1, \boldsymbol{N}_2, \boldsymbol{\alpha}_1, \mathbf{P_2^{max}}\right)}\right) \\ &s.t. \ \sum_{k=1}^{K} P_1^k \leq \mathbf{P_1^{max}}, \ P_1^k \geq 0, \end{aligned} \tag{3.11}$$

in which $g_2^k \left(\mathbf{P}_1, \boldsymbol{N}_2, \boldsymbol{\alpha}_1, \mathbf{P_2^{max}}\right)$ is a function that determines user 2's allocated power in the kth channel, $\boldsymbol{N}_2 = \left\{N_2^1, N_2^2, \ldots, N_2^K\right\}$, and $\boldsymbol{\alpha}_1 = \left\{\alpha_1^1, \alpha_1^2, \ldots, \alpha_1^K\right\}$.

Note that the lower-level problem in (3.10) is a standard convex programming problem. Its optimum is given by $g_2^k \left(\mathbf{P}_1, \boldsymbol{N}_2, \boldsymbol{\alpha}_1, \mathbf{P_2^{max}}\right) = \left(K_2 - N_2^k - \alpha_1^k P_1^k\right)^+$, where K_2 is a constant that satisfies $\sum_{k=1}^{K} P_2^k = \mathbf{P_2^{max}}$. In practice, K_2 is usually obtained using numerical (e.g. bisection) methods. In fact, an explicit expression of $g_2^k \left(\mathbf{P}_1, \boldsymbol{N}_2, \boldsymbol{\alpha}_1, \mathbf{P_2^{max}}\right)$ is needed to analytically handle single-level formulation. Towards this end, we first define a permutation $\pi : \{1, 2, \ldots, K\} \rightarrow \{1, 2, \ldots, K\}$, which ranks all the channels based on their noise plus interference PSDs and satisfies

$$\pi\left(f_1\right) < \pi\left(f_2\right), \ \text{ if } N_2^{f_1} + \alpha_1^{f_1} P_1^{f_1} < N_2^{f_2} + \alpha_1^{f_2} P_1^{f_2}. \tag{3.12}$$

Then, we can extend the results in [AAG08], and have the following closed-form expression:

$$g_2^k \left(\mathbf{P}_1, \boldsymbol{N}_2, \boldsymbol{\alpha}_1, \mathbf{P_2^{max}}\right) = \begin{cases} \frac{1}{f}\Big(\mathbf{P_2^{max}} + \sum\limits_{m=1}^{f} \big(N_2^{\pi^{-1}(m)} + \\ \alpha_1^{\pi^{-1}(m)} P_1^{\pi^{-1}(m)}\big)\Big) - N_2^k - \alpha_1^k P_1^k, & \pi(k) \leq f, \\ 0, & \pi\left(k\right) > f, \end{cases} \tag{3.13}$$

where f can be found according to the condition:

$$\begin{aligned} &f\left(N_2^{\pi^{-1}(f)} + \alpha_1^{\pi^{-1}(f)} P_1^{\pi^{-1}(f)}\right) - \sum_{m=1}^{f} \left(N_2^{\pi^{-1}(m)} + \alpha_1^{\pi^{-1}(m)} P_1^{\pi^{-1}(m)}\right) < \mathbf{P_2^{max}} \leq \\ &(f+1)\left(N_2^{\pi^{-1}(f+1)} + \alpha_1^{\pi^{-1}(f+1)} P_1^{\pi^{-1}(f+1)}\right) - \sum_{m=1}^{f+1} \left(N_2^{\pi^{-1}(m)} + \alpha_1^{\pi^{-1}(m)} P_1^{\pi^{-1}(m)}\right). \end{aligned} \tag{3.14}$$

We can see that function $g_2^k\left(\mathbf{P}_1, \boldsymbol{N}_2, \boldsymbol{\alpha}_1, \mathbf{P_2^{max}}\right)$ ranks all the frequency channels based on the channel conditions and gradually increases the water-level until the maximal power constraint is satisfied.

Even though we have the closed-form expression of $g_2^k\left(\mathbf{P}_1, \boldsymbol{N}_2, \boldsymbol{\alpha}_1, \mathbf{P_2^{max}}\right)$, the single-level problem (3.11) is still intractable due to its non-convexity. Generally speaking, the global optimum can only be found via an exhaustive search. If we define the granularity in the foresighted user's transmit power as Δ_P, then the value of P_1^k can be limited to the set $\{0, \Delta_P, \ldots, \mathbf{P_1^{max}}\}$. By searching all the possible combinations, the optimum can be found. Hence, such an exhaustive search in $\left(P_1^1, \ldots, P_1^K\right)$ has a overall complexity of $\mathcal{O}((\mathbf{P_1^{max}}/\Delta_P)^K)$.

Recently, Lagrangian duality theory has been successfully used to solve non-convex weighted sum-rate maximization in interference channel with moderate computational complexity [CYM06, YL06, CHC07]. We notice that the problem in (3.11) are similar with the problems investigated in these works in that the optimization variables $\mathbf{P}_1$ also appear in the denominators of the objective function. The following sections will revisit these dual approaches and show that these methods cannot reduce the computational complexity of problem (3.11), thereby demonstrating the challenges involved in optimally computing the Stackelberg equilibrium.

3.2.3 Lagrangian Dual Approach for Non-convex Problems

We continue studying the simple two-user scenario to introduce the dual method. In a two-user frequency-selective interference channel, the weighted sum-rate

maximization investigated in [CYM06, YL06, CHC07] is given by

$$\begin{aligned} &\max_{\mathbf{P}_1,\mathbf{P}_2} \omega \sum_{k=1}^{K} \log_2\left(1+\frac{P_1^k}{N_1^k+\alpha_2^k P_2^k}\right) + (1-\omega)\sum_{k=1}^{K}\log_2\left(1+\frac{P_2^k}{N_2^k+\alpha_1^k P_1^k}\right) \\ &s.t.\ \sum_{k=1}^{K} P_1^k \le \mathbf{P_1^{max}},\ P_1^k \ge 0,\ \sum_{k=1}^{K} P_2^k \le \mathbf{P_2^{max}},\ P_2^k \ge 0, \end{aligned} \tag{3.15}$$

in which $\omega \in [0,1]$ is a fixed weight. The dual method forms the following Lagrangian

$$\begin{aligned} L(\mathbf{P}_1,\mathbf{P}_2,\lambda_1,\lambda_2) = \sum_{k=1}^{K}\Bigg\{ &\omega\log_2\left(1+\frac{P_1^k}{N_1^k+\alpha_2^k P_2^k}\right) + \\ &(1-\omega)\log_2\left(1+\frac{P_2^k}{N_2^k+\alpha_1^k P_1^k}\right) - \lambda_1 P_1^k - \lambda_2 P_2^k\Bigg\}, \end{aligned} \tag{3.16}$$

where $\lambda_1, \lambda_2 \ge 0$ are Lagrangian dual variables. The Lagrangian dual function is defined as

$$D(\lambda_1,\lambda_2) = \max_{\mathbf{P}_1,\mathbf{P}_2 \succeq 0} L(\mathbf{P}_1,\mathbf{P}_2,\lambda_1,\lambda_2). \tag{3.17}$$

Denote the objective function of problem (3.15) as $f(\mathbf{P}_1,\mathbf{P}_2)$ and the overall complexity of exhaustive search is $\mathcal{O}((\prod_i(\mathbf{P_i^{max}}/\Delta_P))^K)$. From optimization theory [BV04], we know that, for arbitrary feasible $\mathbf{P}_1,\mathbf{P}_2$, we have $f(\mathbf{P}_1,\mathbf{P}_2) \le D(\lambda_1,\lambda_2)$. This leads to $\min_{\lambda_1,\lambda_2} D(\lambda_1,\lambda_2) \ge \max_{\mathbf{P}_1,\mathbf{P}_2} f(\mathbf{P}_1,\mathbf{P}_2)$, and $\min_{\lambda_1,\lambda_2} D(\lambda_1,\lambda_2)$ provides an upper bound of the optimal value of the problem in (3.15). Generally speaking, if $f(\mathbf{P}_1,\mathbf{P}_2)$ is non-convex, the duality gap $\min_{\lambda_1,\lambda_2} D(\lambda_1,\lambda_2) - \max_{\mathbf{P}_1,\mathbf{P}_2} f(\mathbf{P}_1,\mathbf{P}_2)$ is not zero.

Fig. 3.3 summarizes the three key steps of a dual method, the OSB algorithm [CYM06, YL06], that can efficiently find the global optimum of the problem in (3.15). First, for fixed λ_1,λ_2, the maximization of $L(\mathbf{P}_1,\mathbf{P}_2,\lambda_1,\lambda_2)$ over $\mathbf{P}_1,\mathbf{P}_2$ in (3.17) is decomposed into N uncoupled sub-problems, and each of them corresponds to a per-bin optimization. Therefore, the overall complexity of maximizing $L(\mathbf{P}_1,\mathbf{P}_2,\lambda_1,\lambda_2)$ over $\mathbf{P}_1,\mathbf{P}_2$ is only $\mathcal{O}(K\prod_i(\mathbf{P_i^{max}}/\Delta_P))$. Second, it is

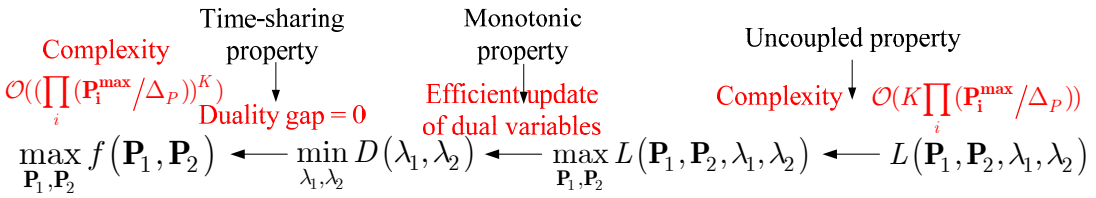

Figure 3.3: Key steps of the dual approach of non-convex weighted sum-rate maximization.

shown that, for fixed n, the sum power of user n's optimal power allocation in a multi-carrier system is a monotonic function of λ_n(Lemma 1, in [CYM06]). This property guarantees that the bi-section dual update over λ_1, λ_2 will converge to the dual optimum. Third, it is also proven that, if the number of frequency bins K is large enough and $\{H_{mn}^k\}$ and $\{\sigma_n^k\}$ are smooth in the spectral domain, the optimization problem (3.15) satisfies the so-called "time-sharing property" (Theorem 1 and 2, in [YL06]), and the duality gap of this non-convex problem is zero. Combining the three properties together, the dual approach can find the global optimum with the computational complexity of $\mathcal{O}(T_1 K \prod_i(\mathbf{P_i^{max}}/\Delta_P))$, where T_1 is the number of iterations needed for dual-update. We can see that the complexity of the dual approach is greatly reduced compared with that of the exhaustive search in the primal domain. In addition, it is found in [YL06] that, if $D(\lambda_1, \lambda_2)$ is approximated using a local maximum of $L(\mathbf{P}_1, \mathbf{P}_2, \lambda_1, \lambda_2)$, the ISB algorithm can achieve near-optimal performance with the computational complexity of $\mathcal{O}(T_1 T_2 K \sum_i(\mathbf{P_i^{max}}/\Delta_P))$, where T_2 is the number of iterations required for evaluating the local maximum.

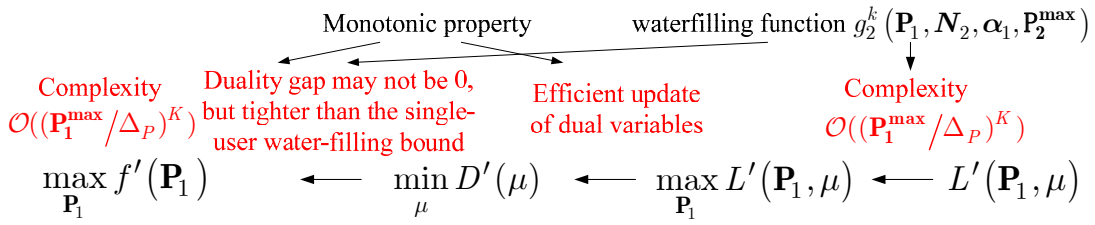

Figure 3.4: Complexity and properties of the dual approach of computing the Stackelberg equilibrium.

3.2.4 The Lagrangian Dual Approach for Computing Stackelberg Equilibrium

Now we apply the dual approach for our problem in (3.11) to understand why the Stackelberg equilibrium in our considered problem is intrinsically difficult to compute. Fig. 3.4 summarizes the key properties of the dual approach that will be addressed in the following parts. Denote the objective function of problem (3.11) as $f'(\mathbf{P}_1)$. Consider its dual objective function $D'(\mu)$ for a fixed Lagrangian dual variable μ:

$$D'(\mu) = \max_{\mathbf{P}_1 \succeq 0} L'(\mathbf{P}_1, \mu), \tag{3.18}$$

in which $L'(\mathbf{P}_1, \mu) = \sum_{k=1}^{K} \log_2\left(1 + \frac{P_1^k}{N_1^k + \alpha_2^k g_2^k\left(\mathbf{P}_1, \boldsymbol{N}_2, \boldsymbol{\alpha}_1, \mathbf{P_2^{max}}\right)}\right) + \mu\left(\mathbf{P_1^{max}} - \sum_{k=1}^{K} P_1^k\right)$. For a given μ, denote the optimal power allocation that maximizes (3.18) as $\mathbf{P}_1(\mu) = \arg\max_{\mathbf{P}_1 \succeq 0} L'(\mathbf{P}_1, \mu)$ and $P_1^k(\mu) = [\mathbf{P}_1(\mu)]_k$, The following lemma holds for $\mathbf{P}_1(\mu)$:

Lemma 3.1 *$\sum_{k=1}^{K} P_1^k(\mu)$ is monotonic decreasing in μ. In addition, we have $\lim_{\mu\to\infty} \sum_{k=1}^{K} P_1^k(\mu) = 0$ and $\sum_{k=1}^{K} P_1^k(0) = +\infty$.*

Proof: It is easy to see that $\sum_{k=1}^{K} P_1^k(0) = +\infty$. The rest of the proof is the same as in Lemma 1 in [CYM06].■

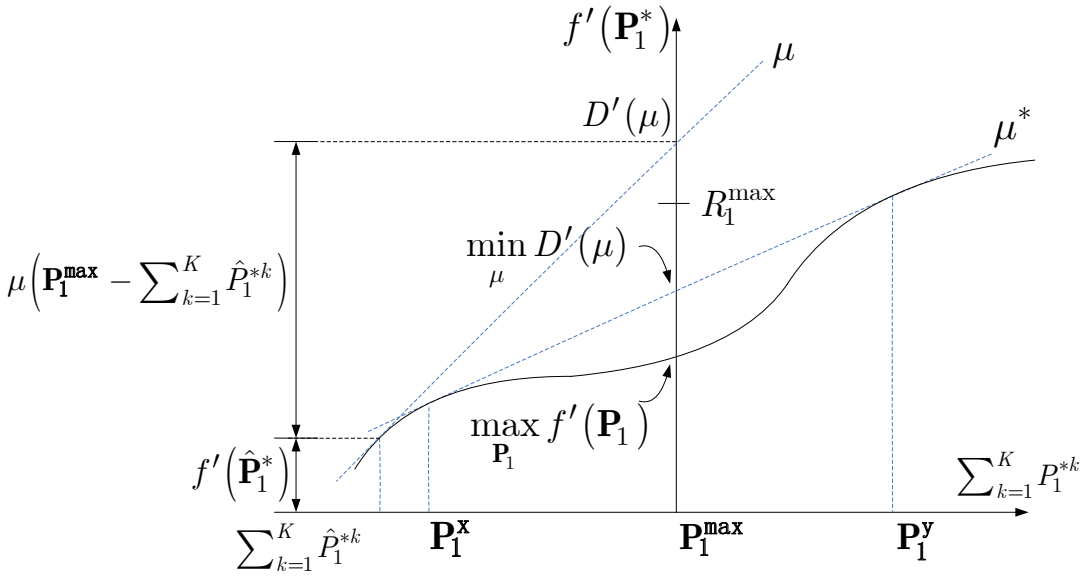

Figure 3.5: Duality gap for the problem in (3.11).

Fig. 3.5 gives a graphical illustration of the above Lemma. Consider a sequence of optimization problems similar with (3.11). These problems are parameterized by the constraint imposed over user 1's maximal sum power. The solid curve in Fig. 3.5 is a plot of the optimal value $\left(\sum_{k=1}^{K} P_1^{*k}, f'\left(\mathbf{P}_1^*\right)\right)$ as this constraint varies. The curve is plotted with $\sum_{k=1}^{K} P_1^{*f}$ on the x-axis. The y-axis is located at the point where $\sum_{k=1}^{K} P_1^{*k} = \mathbf{P_1^{max}}$. The intersection of the curve with the y-axis is the optimum of (3.11), i.e. $\max_{\mathbf{P}_1} f'\left(\mathbf{P}_1\right)$. For a fixed μ, by drawing a tangent line to the $\left(\sum_{k=1}^{K} P_1^{*k}, f'\left(\mathbf{P}_1^*\right)\right)$ curve and measuring the intersection of this tangent line with the y-axis, the value of $D'(\mu)$ can be graphically obtained. According to Lemma 3.1, as μ increases, the x-axis value of the tangent point monotonically increases. We denote $\mu^* = \arg\min_{\mu} D'(\mu)$. Recall that Lemma 3.1 does not claim the continuity of $\sum_{k=1}^{K} P_1^k(\mu)$ in μ. It is because the allocated powers in different frequency bins are coupled due to function $g_2^k\left(\mathbf{P}_1, \boldsymbol{N}_2, \boldsymbol{\alpha}_1, \mathbf{P_2^{max}}\right)$ and the time-sharing property in [YL06] is not

guaranteed for problem (3.11). The discontinuity may lead to nonzero duality gap, i.e. at least two tangent points exist on the tangent line in Fig. 3.5 and they correspond to different power constraints $\mathbf{P_1^x}$ and $\mathbf{P_1^y}$. If the duality gap is positive, the following theorem indicates that $D'(\mu^*)$ provides a tighter upper bound of the achievable rate than $R_1^{\max}$ in (3.8).

Theorem 3.2 *If the duality gap is nonzero, i.e.* $D'(\mu^*) > \max_{\mathbf{P}_1} f'(\mathbf{P}_1)$*, the dual optimum provides a tighter upper bound of user 1's maximal achievable rate than the bound in (8), i.e.* $D'(\mu^*) < R_1^{\max}$.

Proof: As shown in Fig. 3.5, the non-zero duality gap implies that there exist at least two possible values for $\sum_{k=1}^{K} P_1^k(\mu^*)$, which are denoted as $\mathbf{P_1^x}$ and $\mathbf{P_1^y}$ and they satisfy $\mathbf{P_1^x} < \mathbf{P_1^{max}} < \mathbf{P_1^y}$. Denote the optimal power allocation of having power constraints $\mathbf{P_1^x}$ and $\mathbf{P_1^y}$ as $\mathbf{P_1^-}$ and $\mathbf{P_1^+}$ respectively. We have

$$D'(\mu^*) = f'\left(\mathbf{P}_1^-\right) + \mu^*\left(\mathbf{P_1^{max}} - \sum_{k=1}^{K} P_1^{-k}\right) = f'\left(\mathbf{P}_1^+\right) + \mu^*\left(\mathbf{P_1^{max}} - \sum_{k=1}^{K} P_1^{+k}\right). \tag{3.19}$$

Moreover, since $\mathbf{P_1^x} < \mathbf{P_1^{max}} < \mathbf{P_1^y}$, there exists $0 < \upsilon < 1$ such that $\mathbf{P_1^{max}} = \upsilon\mathbf{P_1^x} + (1-\upsilon)\mathbf{P_1^y}$. Immediately, we get $D'(\mu^*) = \upsilon f'\left(\mathbf{P}_1^-\right) + (1-\upsilon) f'\left(\mathbf{P}_1^+\right)$. It corresponds to the time-sharing scenario, in which the power allocation $\mathbf{P}_1^-$ is adopted for time-fraction υ and $\mathbf{P}_1^+$ for time-fraction $1-\upsilon$. Consider the problem of allocating user 1's power subject to the maximal power constraint $\mathbf{P_1^{max}}$ in the interference-free environment. We know that the optimal solution is the single-user water-filling. Noting that $\mathbf{P_1^{max}} = \upsilon\mathbf{P_1^x} + (1-\upsilon)\mathbf{P_1^y}$ and $\mathbf{P_1^x} \neq \mathbf{P_1^y}$, the aforementioned time-sharing strategy is sub-optimal for this problem. Therefore,

we have

$$D'\left(\mu^*\right) = \upsilon f'\left(\mathbf{P}_1^-\right) + \left(1-\upsilon\right) f'\left(\mathbf{P}_1^+\right) \leq \upsilon \sum_{k=1}^{K} \log_2\left(1+\frac{P_1^{-k}\left|H_{11}^k\right|^2}{\sigma_1^k}\right) + \left(1-\upsilon\right)\sum_{k=1}^{K}\log_2\left(1+\frac{P_1^{+k}\left|H_{11}^k\right|^2}{\sigma_1^k}\right) < \sum_{k=1}^{K}\log_2\left(1+\frac{P_1^{k*}\left|H_{11}^k\right|^2}{\sigma_1^k}\right) = R_1^{\max}, \tag{3.20}$$

and this concludes the proof. ■

By Theorem 3.2, evaluating the dual function leads to a tighter upper bound of Stackelberg equilibrium than $R_1^{\max}$. However, it is unfortunate that the computational complexity of optimally maximizing $L'\left(\mathbf{P}_1, \mu\right)$ is still $\mathcal{O}((\mathbf{P_1^{max}}/\Delta_P)^K)$. This is because term $g_2^k\left(\mathbf{P}_1, \boldsymbol{N}_2, \boldsymbol{\alpha}_1, \mathbf{P_2^{max}}\right)$ in the denominator term of (3.11) is also a function of the allocated power $P_1^{k'}$ $(k' \neq k)$, which makes it impossible to decouple the maximization in (3.18) into K independent sub-problems. To conclude, the complexity of optimal solution in the dual domain is the same as the primal approach, which again highlights the fact that the Stackelberg equilibrium is difficult to compute.

3.3 Low-complexity Algorithm, Simulations, and Extensions

In this section, we propose a low-complexity dual algorithm to search the Stackelberg equilibrium and examine its achievable performance via extensive numerical simulations. We also discuss how the strategic users can obtain the required information and the extensions to general multi-user scenarios.

Table 3.1: **Algorithm** 3.1: A low-complexity dual algorithm.

Input: $\mathbf{P_1^{max}}, \mathbf{P_2^{max}}, N_1^k, N_2^k, \alpha_1^k, \alpha_2^k \; for \; \forall k$

Initialize: $\mathbf{P}_1 = \mathbf{P}_1^{NE}, \mu^{\max}, \mu^{\min}$

Repeat

$\mu = \frac{1}{2}\left(\mu^{\max} + \mu^{\min}\right).$

Repeat

for $k = 1$ to K,

set $P_1^k = \arg\max_{\mathbf{P}_1} \sum_{k=1}^{K} \left\{ \ln\left[1 + \frac{P_1^k}{N_1^k + \alpha_2^k g_2^k\left(\mathbf{P}_1, \boldsymbol{N}_2, \boldsymbol{\alpha}_1, \mathbf{P_2^{max}}\right)}\right] - \mu P_1^k \right\}$ by keeping $P_1^1, \ldots, P_1^{k-1}, P_1^{k+1}, \ldots, P_1^K$ fixed.

end

until $\left(P_1^1, \ldots, P_1^K\right)$ converges

if $\sum_{k=1}^{K} P_1^k > \mathbf{P_1^{max}}$, $\mu^{\min} = \frac{1}{2}\left(\mu^{\max} + \mu^{\min}\right)$; else $\mu^{\max} = \frac{1}{2}\left(\mu^{\max} + \mu^{\min}\right)$.

until it converges

3.3.1 A Low-Complexity Dual Approach

As we have shown, the dual approach cannot reduce the complexity of the global optimum of problem (3.11). However, inspired by the ISB algorithm [YL06], we develop an efficient dual approach, which is listed as Algorithm 3.1. The basic idea of the algorithm is to approximately evaluate $D'(\mu)$ by locally optimizing $L'(\mathbf{P}_1, \mu)$. For fixed μ, the algorithm finds the optimal P_1^k while keeping $P_1^1, \ldots, P_1^{k-1}, P_1^{k+1}, \ldots, P_1^K$ fixed, and changes the index f until it converges to a local maximum for $L'(\mathbf{P}_1, \mu)$. Then the algorithm updates μ using bi-section search and repeats the procedure above until the convergence is achieved.

As discussed in [YL06], the local optimum depends on the initial starting point and the ordering of iterations. Moreover, the proof of convergence of the whole

Table 3.2: User 1's computational complexity for different algorithms.

Algorithm	**Computational complexity**
Exhaustive search	$\mathcal{O}((\mathbf{P_1^{max}}/\Delta_P)^K)$
Algorithm 3.1	$\mathcal{O}(T_1T_2K\mathbf{P_1^{max}}/\Delta_P)$
Iterative water-filling	$\mathcal{O}(T_3K)$

algorithm becomes an issue. Algorithm 3.1 sets the Nash equilibrium as the initial starting point. In most of the experimental setting we have tested, Algorithm 3.1 has been observed to converge to a feasible solution within 10-15 iterations. The computational complexity of this iterative algorithm is only $\mathcal{O}(T_1T_2K\mathbf{P_1^{max}}/\Delta_P)$ and it reduces the complexity of the optimal exhaustive search by a factor of $\mathcal{O}((\mathbf{P_1^{max}}/\Delta_P)^{K-1}/(T_1T_2K))$, which is considerably large for small Δ_P and large K . Table 3.2 summarizes the computational complexity comparison for user 1 if it adopts different algorithms, in which T_3 is the number of iterations required in the iterative water-filling algorithm.

3.3.2 Illustrative Results

In this sub-section, we evaluate the performance of Algorithm 3.1 by comparing with the IW algorithm. We simulate a wireless system with 20 sub-carriers over the 6.25-MHz band. We assume that $\mathbf{P_1^{max}} = \mathbf{P_2^{max}} = 200$ and $\sigma_1^k = \sigma_2^k = 0.01$. To evaluate the performance, we tested 10^5 sets of frequency-selective fading channels where a unique Nash equilibrium exists, which are simulated using a four-ray Rayleigh model with the exponential power profile and 160 ns delay between two adjacent rays [Rap96]. The simulated power of each ray decreases exponentially according to its delay. The total power of all rays of H_{11}^k and H_{22}^k is normalized as one, and that of H_{12}^k and H_{21}^k is normalized as 0.5.

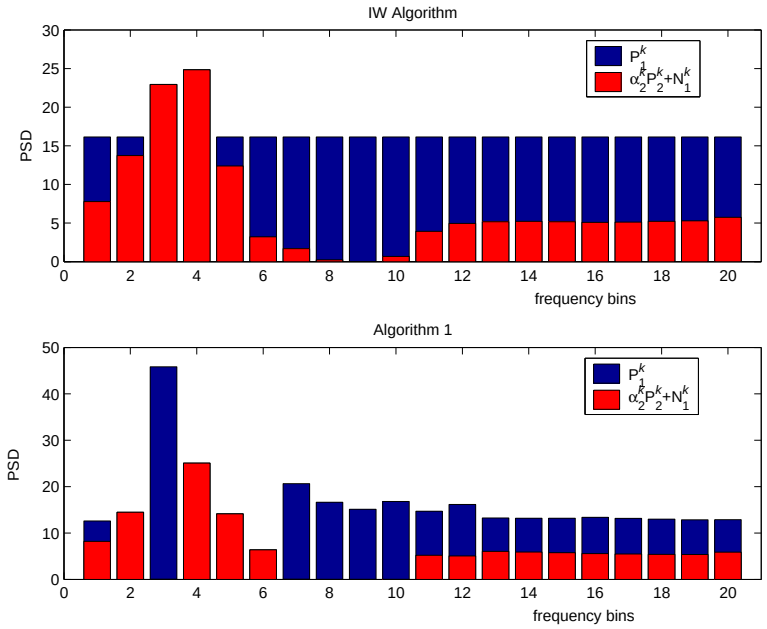

Figure 3.6: User 1's power allocation using different algorithms.

Fig. 3.6 and 3.7 show the power allocations for both users using different algorithms. In the IW algorithm, each user water-fills the whole frequency band by regarding its competitor's transmit PSD as background noise until the Nash equilibrium is achieved. In contrast, user 1 does not water-fill if it adopts Algorithm 3.1. For example, in Fig. 3.6, user 1 allocates a large amount of power in frequency bin 3 even though it can gain an immediate increase in R_1 by re-allocating some of its power in the frequency bins 5 and 6 where the noise plus interference PSD is below its water-levels in the frequency bins 7-12.

Denote user i's achieved rate by deploying Algorithm 3.1 as R_i' . Fig. 3.8 shows the simulated cumulative distribution functions (cdf) of R_i'/R_i^{NE}. From the curve, Algorithm 3.1 achieves a higher rate for the foresighted user in all the simulated realizations. The average rate improvement that Algorithm 3.1 provides over the IW algorithm is 38%. In addition, it is surprising to find that,

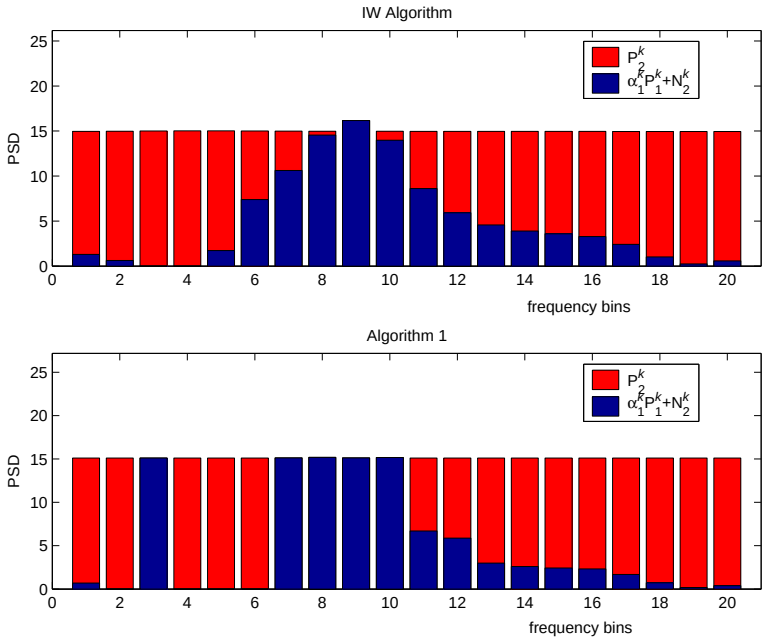

Figure 3.7: User 2's power allocation using different algorithms.

in 95% of the simulation settings, Algorithm 3.1 also results in a higher rate R_2' than R_2^{NE} for the myopic user, and the average rate improvement is 45%. This is because user 1's Stackelberg strategy mitigates its interference caused to user 2.

We also simulate the scenarios in which the total power of H_{12}^k and H_{21}^k is normalized as 0.25 and all the other parameters remain the same as above. Fig. 3.9 shows the simulated cdfs of R_i'/R_i^{NE}. The average rate improvement for user 1 is 27% and that of user 2 is 32%. It is intuitive that the average rate improvement is decreasing when the power of H_{12}^k and H_{21}^k decreases, because the interference coupling between users and the foresighted user's ability in shaping the myopic user's response are both reduced.

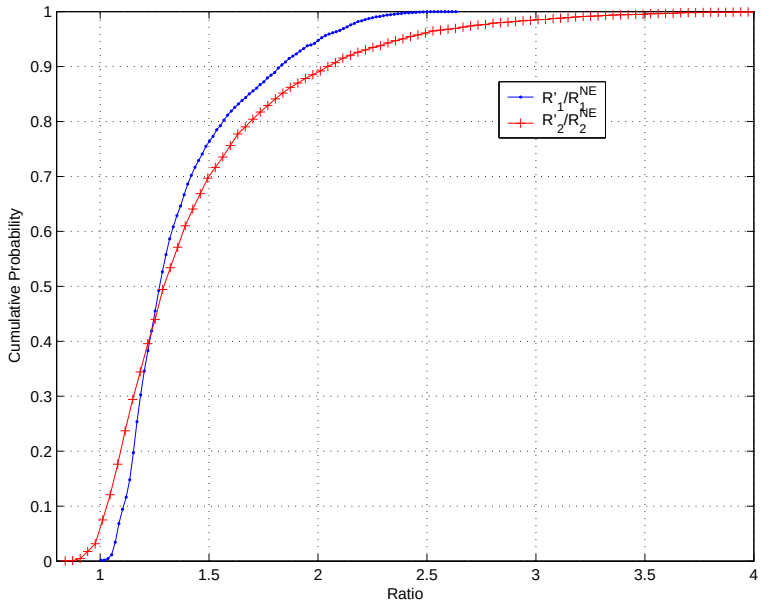

Figure 3.8: Cdfs for the ratio of R_i'/R_i^{NE} ($\sum_k \left|H_{12}^k\right|^2 = \sum_k \left|H_{21}^k\right|^2 = 0.5$).

3.3.3 Information Acquisition

Previous sections mentioned that, in order to play the Stackelberg equilibrium, the additional information about the competing user's CSI, maximum power constraint, and power allocation strategy is indispensable. In practice, there are several possible methods to acquire this required information.

First, the myopic user has the incentive to provide the required information, because its performance can be greatly improved if the foresighted player knows the myopic player's private information. In the distributed setting, users can individually decide whether or not to play the Stackelberg strategy based on their computational hardware constraints. The user that wants to behave myopically can reveal its information to the foresighted user. This can be viewed as the user's cooperative behavior to avoid mutual interference.

When no information exchanges among users are possible, the alternative

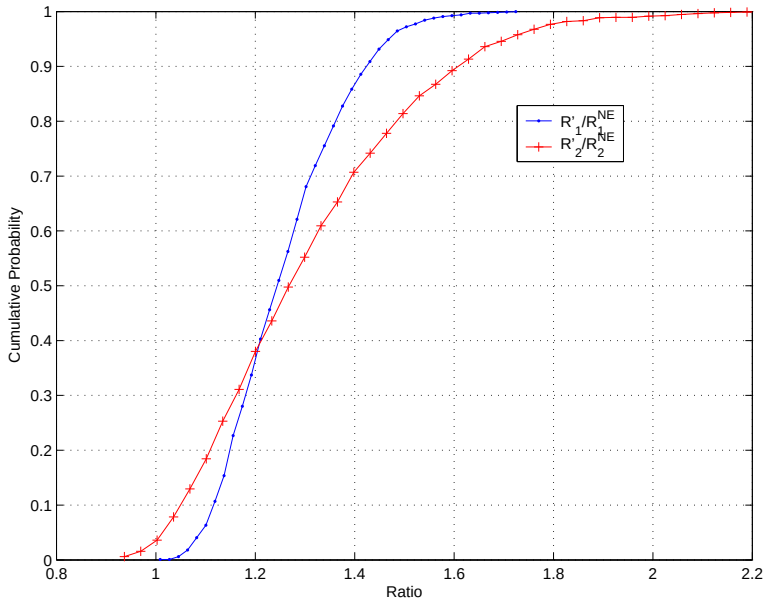

Figure 3.9: Cdfs for the ratio of R_i'/R_i^{NE} ($\sum_k \left|H_{12}^k\right|^2 = \sum_k \left|H_{21}^k\right|^2 = 0.25$).

way for users to gather this information is through predictive modeling. If the foresighted user strategically changes its power allocation, it can measure and model the resulting interference PSD, i.e. estimate the functional expression of $g_2^k\left(\mathbf{P}_1, \boldsymbol{N}_2, \boldsymbol{\alpha}_1, \mathbf{P_2^{max}}\right)$, without any information exchange among users. For instance, in the next chapter, we will show that the foresighted user can effectively model its experienced interference as a linear function of its own allocated power, formulate a local approximation of the original bi-level program, and substantially improve both users' achievable rates.

3.3.4 Extensions to Multi-user Games

The two-user formulation can be extended to the general cases in which multiple users can be myopic or foresighted. The analysis in these cases becomes much more involved. We denote the number of foresighted user as n_f and the number of myopic user as n_m. We briefly address two remaining cases as follows.

In the first case, $n_f = 1, n_m > 1$. As in (3.11), we can still have the following single-level formulation:

$$\begin{aligned} &\max_{\mathbf{P}_1} \sum_{k=1}^{K} \log_2 \left(1 + \frac{P_1^k}{N_1^k + \sum_{n=2}^{n_m+1} \alpha_{n1}^k q_n^k \left(\mathbf{P}_1, \boldsymbol{N}, \boldsymbol{\alpha}, \mathbf{P_2^{max}}, \ldots, \mathbf{P_{n_m+1}^{max}} \right)} \right) \\ &s.t. \ \sum_{k=1}^{K} P_1^k \leq \mathbf{P_1^{max}}, \ P_1^k \geq 0, \end{aligned} \tag{3.21}$$

in which $N_i^k = \sigma_i^k / |H_{ii}^k|^2$, $\boldsymbol{N} = \left\{ N_i^k : i = 2, \ldots, n_m + 1, k = 1, \ldots, K \right\}$, $\boldsymbol{\alpha} = \left\{ \alpha_{ij}^k : i = 1, \ldots, n_m + 1, \ j = 2, \ldots, n_m + 1, k = 1, \ldots, K \right\}$, and $q_n^k \left(\mathbf{P}_1, \boldsymbol{N}, \boldsymbol{\alpha}, \mathbf{P_2^{max}}, \ldots, \mathbf{P_{n_m+1}^{max}} \right)$ is the function determining user n's allocated power in channel k. As a general from of the two-user case, problem (3.21) is also non-convex. It is easy to verify that Lemma 3.1 and Theorem 3.2 still hold. Although it is difficult to analytically derive $q_n^k \left(\mathbf{P}_1, \boldsymbol{N}, \boldsymbol{\alpha}, \mathbf{P_2^{max}}, \ldots, \mathbf{P_{n_m+1}^{max}} \right)$, we are still able to numerically evaluate it. Hence, Algorithm 3.1 can be applied in this case by replacing its lines 7 with numerically finding local maxima of

$$\sum_{k=1}^{K} \left[\log_2 \left(1 + \frac{P_1^k}{N_1^k + \sum_{n=2}^{n_m+1} \alpha_{n1}^k q_n^k \left(\mathbf{P}_1, \boldsymbol{N}, \boldsymbol{\alpha}, \mathbf{P_2^{max}}, \ldots, \mathbf{P_{n_m+1}^{max}} \right)} \right) - \mu P_1^k \right].$$

We simulate some three-user scenarios in which $\sum_{k=1}^{K} \left| H_{ij}^k \right|^2 = 0.25$ for $i \neq j$, $\mathbf{P_i^{max}} = 200$, and $\sigma_i^k = 0.01$, and all the other parameters remain the same as Section 3.3.2. Fig. 3.10 shows the simulated cdfs of R_i'/R_i^{NE}. The average rate improvement for user 1 is 34% and that of user 2 and 3 is 10.5%. From Fig. 3.10, we can see that, the Stackelberg strategy also benefits the two myopic users in more than 83% of the channel realizations.

Assume now that we have multiple foresighted users, i.e. $n_f > 1, \ n_m \geq 1$. In this case, the single objective function in the original upper-level problem disappears and it becomes a multi-objective optimization problem. Using similar

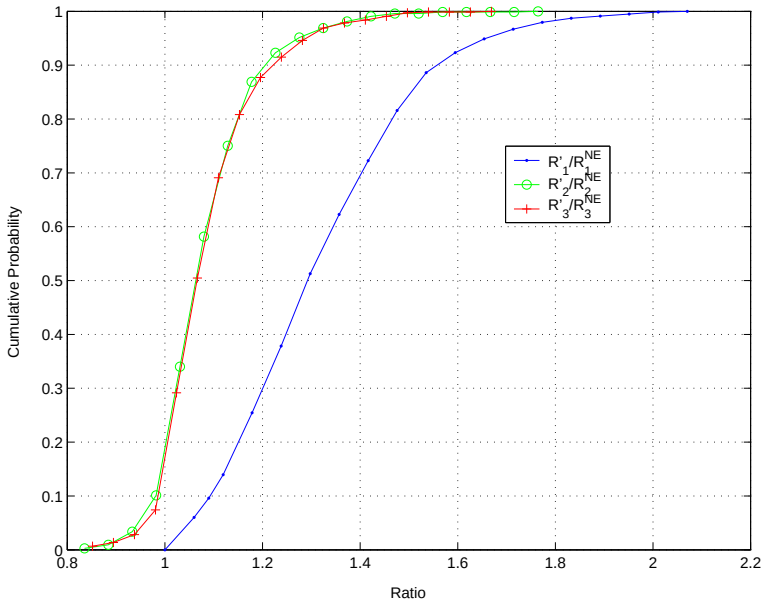

Figure 3.10: Cdfs for the ratio of R_i'/R_i^{NE} ($\sum_k \left|H_{ij}^k\right|^2$ =0.25, $i \neq j$).

arguments in Theorem 3.1, we can show that the Nash equilibrium still exists in the followers' game. For these foresighted users, a reasonable outcome is to choose an operating point in the set $\mathcal{R}^{n_f} = \left\{\left(R_1, \ldots, R_{n_f}\right) : R_i \geq R_i^{NE}, \forall i = 1, \ldots, n_f\right\}$, where R_i^{NE} is user i's achievable rate if all the users are myopic. This point can be determined based on the negotiation among the foresighted users. Cooperative game theory provides many solution concepts, e.g. bargaining, for choosing the operating point [FT91]. Note that the overall game in this scenario is a mixture of cooperation and competition in that the cooperation exists among the foresighted users while myopic players compete with each other. A possible way of achieving the boundary point on $\mathcal{R}^{n_f}$ is to let some coordinator solve the following weighted sum-rate maximization and determine the transmitted PSDs

for different foresighted users:

$$\max_{\mathbf{P}_1,\ldots,\mathbf{P}_{n_f}} \sum_{k=1}^{K} \omega_i \log_2 \left(1 + \frac{P_i^k}{N_i^k + \sum\limits_{n=n_f+1}^{n_f+n_m} \alpha_{ni}^k q_n^k \left(\mathbf{P}_1, \ldots, \mathbf{P}_{n_f}, \boldsymbol{N}, \boldsymbol{\alpha}, \mathbf{P}_{\mathbf{n_f+1}}^{\mathbf{max}}, \ldots, \mathbf{P}_{\mathbf{n_f+n_m}}^{\mathbf{max}} \right)} \right)$$

$$s.t. \quad \sum_{k=1}^{K} P_i^k \leq \mathbf{P_i^{max}},\ P_i^k \geq 0,\ R_i \geq R_i^{NE},\ \ i = 1, \ldots, n_f, \tag{3.22}$$

in which $\omega_i \geq 0$ is user i's weight. Although this problem is generally difficult to solve optimally, some low-complexity methods similar to Algorithm 3.1 can be adopted to obtain sub-optimal solutions.

3.4 Concluding Remarks

This chapter considers the strategic behavior in determining the transmit power PSD for selfish users sharing a frequency-selective interference channel. We adopt the game theoretic concept of Stackelberg equilibrium and model the two-user case as a bi-level programming problem. We show that the Stackelberg equilibrium is intrinsically difficult to compute and propose a low-complexity approach based on Lagrangian dual theory. Numerical results show the strategic user should avoid shortsighted Nash strategy and it can substantially improve both users' performance if it knows the CSI and response strategy of the competing user. Operational methods for acquiring the necessary information and extensions to multi-user scenarios are proposed. Obtaining satisfactory performance with minimal information exchange while multiple foresighted users exist is identified as a problem for further investigation.

CHAPTER 4

Conjectural Equilibrium in Power Control Games

For power control games, the previous chapter uses the Stackelberg equilibrium (SE) formulation to investigate the best response strategy of a selfish user that knows its myopic opponents' private information, including their channel state information and power constraints. It was shown that, surprisingly, a foresighted user playing the SE can improve both its performance as well as the performance of all the other users. These results highlight the significance of information availability in power control games. However, one key question remains unsolved: how should a foresighted user acquire its desired information and adapt its response?

First, as opposed to the approach in the previous chapter, which assumes a foresighted user having perfect knowledge of its competitors' responses to its actions, we discuss in this chapter how the foresighted user without any such a priori knowledge can accumulate this knowledge and improve its performance when participating in the power control game. We propose that the foresighted user can explicitly model its competitors' response as a function of its power allocation by repeatedly interacting with the environment and observing the resulting interference. Second, we introduce the concept of conjectural equilibrium (CE) proposed by Wellman and others [WH98, FJQ04] to characterize the strategic behavior of a user that models the response of its myopic competing users,

and the existence of this equilibrium in the power control game is proven. Some previously adopted solutions, including NE and SE, are shown to be special cases of the CE. The basic notion of CE was first proposed by Hahn in the context of a market model [Hah77]. A general multi-agent framework is proposed in [WH98] to study the existence of and the convergence to CE in market interactions. Specifically, a strategic user is assumed to model the market price as a linear function of its desired demand. It is observed that it may be better or worse off than without modeling, depending on its initial belief. However, we note that using the linear model is purely heuristic in [WH98]. In contrast to this heuristic belief formation, we apply CE in the power control game, because it provides a practical solution concept to approach the performance bound of SE. Finally, we show that deploying the linear model to form conjectures can suitably explore the problem structure of the power control game, and therefore, it can lead to a substantial performance improvement. Practical algorithms are developed to form accurate beliefs and select desirable power allocation strategies. It is shown that, a foresighted user without any a priori knowledge can effectively learn how the other users will respond to its actions and guide the system to an operating point having comparable performance to Algorithm 3.1, where perfect a priori knowledge is assumed.

The rest of the chapter is organized as follows. Section 4.1 introduces the concept of CE and Section 4.2 proves the existence of this CE in the power control game. Section 4.3 develops practical algorithms to form beliefs and approach CE. Numerical results are provided in Section 4.4 to show that a foresighted user can achieve substantial performance improvement if it models its competitors in the power control game. Concluding remarks are drawn in Section 4.5.

4.1 Conjectural Equilibrium

As discussed in Chapter 3, to find the SE in the power control game, we need to solve the bi-level programming problem in (3.21), where user 1 is assumed to be the foresighted user. It should be pointed out that the foresighted user needs to know the private information $\{\sigma_n^k\}, \{\alpha_{mn}^k\}, \{\mathbf{P_n^{max}}\}$ of all its competitors in order to formulate the above optimization. The approach in the previous chapter assumes that the foresighted user has the perfect knowledge of this private information. Importantly, it was shown in Chapter 3 that users' performance is substantially improved compared with that of IW algorithm if the foresighted user plays the SE strategy, even though the remaining users behave myopically. However, how such a foresighted user should accumulate this required information remains unsolved. In the remaining part of this chapter, we will show that the foresighted user can obtain this information and improve its performance by forming conjectures over the behavior of its competitors through repeated interaction with the environment.

In a game-theoretic setting, which equilibria will be played is determined based on the existing assumptions about the players' knowledge and beliefs. For example, the standard NE solution is a set of strategies where no player has a unilateral incentive to change its strategy. An implicit underlying assumption is that each Nash player takes the other players' actions as given. Therefore, it chooses to myopically maximize its own payoff [FT91]. Another example is that of a SE strategy, where the foresighted user needs to know the structure of the resulting $NE(a_n)$ for any $a_n \in \mathcal{A}_n$ and believes that all the remaining players play the NE strategy. Summarizing, the players operating at equilibrium can be viewed as decision makers behaving optimally with respect to their *beliefs* about the policies adopted by the other players.

To rigorously define the CE, we need to use the reformulation of the strategic game $\Gamma = (\mathcal{N}, \mathcal{A}, u, \mathcal{S}, s)$ defined in (1.4). $\mathcal{S} = \times_{n\in\mathcal{N}}\mathcal{S}_n$ is the *state space*, where $\mathcal{S}_n$ is the part of the state relevant to the nth user. Specifically, the state in the power control game is defined as the interference that users experience. The utility function $u = \times_{n\in\mathcal{N}}u_n$ is a map from users' state space and actions to real numbers, $u_n : \mathcal{S}_n \times \mathcal{A}_n \to \mathcal{R}$. The *state determination function* $s = \times_{n\in\mathcal{N}}s_n$ maps joint actions to states for each component $s_n : \mathcal{A} \to \mathcal{S}_n$. Each user cannot directly observe the actions chosen by the others, and each user has some belief about the state that would result from performing its available actions. The *belief function* $\tilde{s} = \times_{n\in\mathcal{N}}\tilde{s}_n$ is defined to be $\tilde{s}_n : \mathcal{A}_n \to \mathcal{S}_n$ such that $\tilde{s}_n(a_n)$ represents the state that the player n believes that would result if it selects action a_n. Notice that the beliefs are not expressed in terms of other player's actions and preferences, and the multi-user coupling in these beliefs is captured directly by individual users forming conjectures of the effects of their own actions. In non-cooperative scenarios, each user chooses the action $a_n \in \mathcal{A}_n$ if it believes this action maximizes its utility.

Definition 4.1 *In game* Γ*, a configuration of belief functions* $(\tilde{s}_1^*, \ldots, \tilde{s}_N^*)$ *and a joint action* $a^* = (a_1^*, \ldots, a_N^*)$ *constitute a conjectural equilibrium, if for each* $n \in \mathcal{N}$*,*

$$\tilde{s}_n^*(a_n^*) = s_n(a_1^*, \ldots, a_N^*) \text{ and } a_n^* = \arg\max_{a_n\in\mathcal{A}_n} u_n(\tilde{s}_n^*(a_n), a_n). \tag{4.1}$$

From the definition, we can see that, at CE, all users' expectations based on their beliefs are realized and each user behaves optimally according to its expectation. In other words, users' beliefs are consistent with the outcome of the play and they behave optimally with respect to their beliefs. CE considers the users' beliefs rather than their perfect knowledge $NE(a_n)$ as in SE, which makes

CE an appropriate solution concept when the perfect knowledge is not available. The key problem is how to configure the belief functions such that it leads to a CE having a satisfactory performance.

4.2 Existence of CE in Power Control Games

In this section, we discuss how to configure a user's belief about its experienced interference as a linear function of its transmit power, and show that such CE exists and it is a relaxation of both NE and SE. We begin by stating several fundamental assumptions used throughout the investigation hereafter.

Assumption 4.1 *There is only one foresighted user modeling its competitors' reaction as a function of its allocated power, and all the remaining users are myopic users that deploy the IW algorithm. Without loss of generality, we assume that this foresighted user is user 1.*

Assumption 4.2 *Every user is able to perfectly measure its experienced equivalent noise PSD* σ_n^k *and interference PSD* $\sum_{i=1,i\neq n}^{N} \alpha_{in}^k P_i^k$ *in all frequency channels.*

Assumption 4.3 *Users* $2,\ldots,N$ *react to any small variation in their experienced interference by setting their power allocations according to the water-filling strategy.*

Assumption 4.4 *In the lower-level problem formed by user in (3.21), there always exists a unique NE and the IW algorithm converges to this unique NE. A sufficient condition that guarantee the uniqueness of NE is condition (C3).*

Next, we formally define the concept of stationary interference.

Definition 4.2 *The stationary interference that user 1 experiences in the kth channel is the accumulated interference* $I_1^k = \sum_{i=2}^{N} \alpha_{i1}^k P_i^k$ *when best-response users* $2, \ldots, N$ *reach their NE in the lower-level problem in (3.21). Note that* I_1^k *is in fact a function of user 1's power allocation* $\mathbf{P}_1 = \left[P_1^1, \ldots, P_1^K\right]$ *in the power control game and it can also be denoted as* $I_1^k(\mathbf{P}_1)$.

4.2.1 Linear Belief of Stationary Interference

As discussed before, both the state space and belief functions need to be defined in order to investigate the existence of CE. In the market models for pure exchange economy [WH98], the market price is impacted by the other consumers' announced demand. Therefore, it is natural to define the state to be the market price in such scenarios. However, the proposed approach in [WH98] that models and updates the belief on the market price as a linear function of the excess demand is entirely heuristic. This is not the case in our setting, where forming linear conjectures fits the natural structure of the considered interference game.

In the power control game, we define state $\mathcal{S}_n$ to be the stationary interference caused to user n, because besides its own power allocation, its utility only depends on the interference that its competitors cause to it. Notice that the action available to user n is to choose the transmitted power allocations subjected to its maximum power constraint. By the definition of belief function, we need to express the stationary interference as a function of the transmitted power. As we will see later, it is natural to deploy linear belief models due to the linearity of the caused stationary interference in terms of the allocated power, and hence, forming such beliefs can lead to significant performance improvements because they capture the inherent characteristics of the actual interference coupling.

Define $\mathbf{P}_1^{k+}, \mathbf{P}_1^{k-}$ as $\mathbf{P}_1^{k+} = \left[P_1^1, \ldots, P_1^k + \varepsilon, \ldots, P_1^K\right]$, $\mathbf{P}_1^{k-} = \left[P_1^1, \ldots, P_1^k - \varepsilon,\right.$

$\ldots, P_1^K\big]$ for arbitrarily small positive variation ε in power. Given user 1's power allocation $\mathbf{P}_1$, $NE_k(\mathbf{P}_1) = \big[P_2^k, \ldots, P_N^k\big]^T$ represents the power that user $2, \ldots, N$ allocate in the kth channel at equilibrium. Vector $\boldsymbol{\alpha}^k = \left\{\alpha_{ij}^k : i \neq j\right\}$ contains channel gains in the kth frequency bin. Indicator function $\boldsymbol{y} = sign(\boldsymbol{x})$ is a mapping of $\mathcal{R}^{N-1} \rightarrow \{0,1\}^{N-1}$, which is defined to be: $y_i = 1$, if $x_i > 0$, and $y_i = 0$, otherwise. Based on these notations, the following theorem motivates us to develop linear belief functions of stationary interference.

Theorem 4.1 *If the number of frequency bins K is sufficiently large, the first derivative of the stationary interference that user 1 experiences in the kth channel with respect to its allocated power in the mth channel satisfies*

$$\frac{\partial I_1^k}{\partial P_1^k} = c\left(\boldsymbol{\alpha}^k, sign\left(NE_k(\mathbf{P}_1)\right)\right), \ if \ there \ does \ not \ exist \ n \in \{2, \ldots, N\}$$
$$satisfying \ P_n^k = 0 \ and \ \lambda_n^k = 0;$$

$$\left.\frac{\partial I_1^k}{\partial P_1^k}\right|_{P_1^k \rightarrow P_1^{k+}} = c\left(\boldsymbol{\alpha}^k, sign\left(NE_k\left(\mathbf{P}_1^{k+}\right)\right)\right),$$

$$\left.\frac{\partial I_1^k}{\partial P_1^k}\right|_{P_1^k \rightarrow P_1^{k-}} = c\left(\boldsymbol{\alpha}^k, sign\left(NE_k\left(\mathbf{P}_1^{k-}\right)\right)\right), \qquad otherwise;$$

$$\frac{\partial I_1^k}{\partial P_1^m} = 0, \ if \ m \neq k,$$

in which $\lambda_n^k \, (n \in \{2, \ldots, N\})$ is the Lagrange multiplier of $P_n^k \geq 0$ at the optimum of lower-level problem in (3.21). The function $sign(\cdot)$ is the indicator of which polyhedron the piece-wise affine water-filling function [SLS07] lies in. $c\left(\boldsymbol{\alpha}^k, \boldsymbol{y}\right)$ represents a constant determined by $\boldsymbol{\alpha}^k$ and the non-zero elements of $\boldsymbol{y}$.

Proof: By the definition of I_1^k, we have $\frac{\partial I_1^k}{\partial P_1^m} = \sum_{i=2}^{N} \alpha_{i1}^k \frac{\partial P_i^k}{\partial P_1^m}$. We differentiate two different cases:

1) If there does not exist any $n \in \{2, \ldots, N\}$ satisfying $P_n^k = 0$ and $\lambda_n^k = 0$, i.e. there is a non-zero gap between the interference that users $2, \ldots, N$ experi-

ence and their water-levels, it is straightforward to see that $sign\left(NE_k\left(\mathbf{P}_1\right)\right) = sign\left(NE_k\left(\mathbf{P}_1^{k+}\right)\right) = sign\left(NE_k\left(\mathbf{P}_1^{k-}\right)\right)$.

Without loss of generality, we temporarily assume that $P_n^k > 0$ for $n \in \{2, \ldots, N\}$. When users $2, \ldots, N$ reach the equilibrium, we have from the optimality conditions of water-filling solution:

$$\left(\boldsymbol{I} + \boldsymbol{G}\right) \cdot NE_k\left(\mathbf{P}_1\right) + \boldsymbol{g}^k P_1^k = \boldsymbol{\nu},$$

in which

$$\boldsymbol{G} = \begin{bmatrix} 0 & \alpha_{32}^k & \alpha_{42}^k & \ldots & \alpha_{N2}^k \\ \alpha_{23}^k & 0 & \alpha_{43}^k & \ldots & \alpha_{N3}^k \\ \alpha_{24}^k & \alpha_{34}^k & \ddots & \ldots & \vdots \\ \vdots & \vdots & \vdots & 0 & \alpha_{N,N-1}^k \\ \alpha_{2N}^k & \alpha_{3N}^k & \ldots & \alpha_{N-1,N}^k & 0 \end{bmatrix}, \boldsymbol{g}^k = \begin{bmatrix} \alpha_{12}^k \\ \alpha_{13}^k \\ \vdots \\ \alpha_{1N}^k \end{bmatrix}, \boldsymbol{\nu} = \begin{bmatrix} \nu_2 \\ \nu_3 \\ \vdots \\ \nu_N \end{bmatrix},$$

$\boldsymbol{\nu}_i \, (i = 2, \ldots, N)$ are the water-levels of all the myopic users. We consider the channel realizations satisfying $\left\| \boldsymbol{G} \right\|_2 < 1$, which guarantees that the power control game has a unique NE (Theorem 8 in [SLS07]). Therefore, $\boldsymbol{I} + \boldsymbol{G}$ is invertible. It then follows that

$$NE_k\left(\mathbf{P}_1\right) = \left(\boldsymbol{I} + \boldsymbol{G}\right)^{-1} \boldsymbol{\nu} - \left(\boldsymbol{I} + \boldsymbol{G}\right)^{-1} \boldsymbol{g}^k P_1^k \tag{4.2}$$

We also have $\lim\limits_{K \to \infty} \frac{\partial \nu_i}{\partial P_1^k} = 0$, because if the number of each frequency bin K is sufficiently large, the fluctuation of the water-level is negligible. As a result, we have

$$\frac{\partial I_1^k}{\partial P_1^m} = \frac{\partial \boldsymbol{h}^k \cdot NE_k\left(\mathbf{P}_1\right)}{\partial P_1^m} = \begin{cases} -\boldsymbol{h}^k \left(\boldsymbol{I} + \boldsymbol{G}\right)^{-1} \boldsymbol{g}^k, \; if \; m = k \\ 0, \qquad\qquad\qquad\qquad otherwise \end{cases} \tag{4.3}$$

in which $\boldsymbol{h}^k = \begin{bmatrix} \alpha_{21}^k & \alpha_{31}^k & \ldots & \alpha_{N1}^k \end{bmatrix}$. Note that if $P_n^k = 0$ and $\lambda_n^k > 0$, all the derivations above still apply by removing the nth column and nth row from

$\boldsymbol{G}, NE_k(\mathbf{P}_1), \boldsymbol{g}^k, \boldsymbol{\nu}$ correspondingly. Hence, we can conclude $\frac{\partial I_1^k}{\partial P_1^k}$ is a constant $c\left(\boldsymbol{\alpha}^k, sign\left(NE_k(\mathbf{P}_1)\right)\right)$ that depends on both $\boldsymbol{\alpha}^k$ and the non-zero elements of $NE_k(\mathbf{P}_1)$.

2) If there exists $n \in \{2, \ldots, N\}$ satisfying $P_n^k = 0$ and $\lambda_n^k = 0$, the stationary interference caused to user n is the same as its water-level ν_n. Therefore, a sufficiently small increment or decrement ε in user 1's allocated power P_1^k may cause $sign\left(NE_k\left(\mathbf{P}_1^{k+}\right)\right)$ and $sign\left(NE_k\left(\mathbf{P}_1^{k-}\right)\right)$ to be different, i.e. the stationary interference $NE_k(\mathbf{P}_1)$ lies on the boundary between two polyhedra that have different piece-wise affine water-filling functions [SLS07]. We need to treat the left-sided and the right-sided first derivatives respectively, and similar conclusions can be derived in the same way as in the first part. ■

Theorem 4.1 indicates that, the first derivative with respect to a foresighted user's allocated power in a certain channel is sufficient to capture how the stationary interference varies locally in that channel. We observe from equality (4.2) that

$$I_1^k = \boldsymbol{h}^k \cdot NE_k(\mathbf{P}_1) = \boldsymbol{h}^k (\boldsymbol{I} + \boldsymbol{G})^{-1} \boldsymbol{\nu} - \boldsymbol{h}^k (\boldsymbol{I} + \boldsymbol{G})^{-1} \boldsymbol{g}^k P_1^k.$$

Therefore, user 1 can define its belief function using the linear form [1] $\tilde{I}_1^k = \beta^k - \gamma^k P_1^k$, in which γ^k is the estimate of $-\frac{\partial I_1^k}{\partial P_1^k}$ and β^k is a constant representing the composite effect of user $2, \ldots, N$'s water-levels $\boldsymbol{\nu}$. This linear characterization of the stationary interference can greatly simplify the implicit functional expression $I_1^k(\mathbf{P}_1)$ given by the solution of the lower-level problem (3.21), while maintaining an accurate model of $I_1^k(\mathbf{P}_1)$ around the feasible operating point $\mathbf{P}_1$.

[1] Note that as long as the channel realization is random, for a fixed K, the probability that the left-sided and right-sided derivatives in Theorem 4.1 are not equal is zero. We will assume that the first derivative exists hereafter. If it does not exist, similar results can be derived by treating the left-sided and right-sided first derivatives separately.

Table 4.1: Comparison among NE, SE, and CE in power control games.

	User 1	User $2, \ldots, N$
Nash Equilibrium	$\max_{\mathbf{P}_n \in \mathcal{A}_n} \sum_{k=1}^{K} \log_2 \left(1 + \frac{P_n^k}{\sigma_n^k + I_n^k}\right)$	
Stackelberg Equilibrium	$\max_{\mathbf{P}_1 \in \mathcal{A}_1} \sum_{k=1}^{K} \log_2 \left(1 + \frac{P_1^k}{\sigma_1^k + I_1^k(\mathbf{P}_1)}\right)$	$\max_{\mathbf{P}_n \in \mathcal{A}_n} \sum_{k=1}^{K} \log_2 \left(1 + \frac{P_n^k}{\sigma_n^k + I_n^k}\right)$
Conjectural Equilibrium	$\max_{\mathbf{P}_n \in \mathcal{A}_n} \sum_{k=1}^{K} \log_2 \left(1 + \frac{P_n^k}{\sigma_n^k + \tilde{I}_n^k}\right)$	
	$\tilde{I}_1^k = \beta^k - \gamma^k P_1^k = I_1^k = \sum_{i=2}^{N} \alpha_{i1}^k P_i^k$	$\tilde{I}_n^k = I_n^k = \sum_{i=1, i \neq n}^{N} \alpha_{in}^k P_i^k$

4.2.2 Existence of Conjectural Equilibrium

Under the same known sufficient conditions discussed in [SLS07, SPB08] and Chapter 3 for guaranteeing the existence of NE and SE, the existence of CE can be proven by showing that the first two types of equilibrium are special cases of CE. To this end, Table 4.1 compares the optimality conditions of the three types of equilibria in the power control game.

As shown in Table 4.1, the information requirement for playing various equilibria differs. At NE, each user includes its stationary interference I_n^k as a constant in the optimization, and its action is the best response to I_n^k. To play SE, the foresighted user needs to know the functional expression of the stationary interference $I_1^k(\mathbf{P}_1')$ such that the bi-level program can be formed. Specifically, the required information includes both the system-wide channel state information $\boldsymbol{\alpha}^k$, the noise PSD σ_n^k, and the individual power constraint $\mathbf{P}_n^{max}$ for $\forall k \in \{1, \ldots, K\}, n \in \mathcal{N}$. In contrast, in the case of CE, the above information for playing SE is no longer

required and the foresighted user behaves optimally with respect to its beliefs $\tilde{I}_1^k$ on how the stationary interference changes as a function of P_1^k.

Theorem 4.2 *In the power control game, both the Nash equilibrium and the Stackelberg equilibrium are special cases of conjectural equilibrium.*

Proof: To solve the CE, the optimization solving CE in Table 4.1 is essentially

$$\begin{aligned} &\max_{\mathbf{P}_1} \sum_{k=1}^{K} \log_2\left(1+\frac{P_1^k}{\sigma_1^k+\beta^k-\gamma^k P_1^k}\right) \\ &s.t.\ \ P_1^k \geq 0\ , \beta^k-\gamma^k P_1^k \geq 0\ \text{ and }\ \sum\nolimits_{k=1}^{K} P_1^k \leq \mathbf{P_1^{max}}. \end{aligned} \tag{4.4}$$

In order to show that both NE and SE are special cases of CE, we only need to verify that at NE and SE, user 1's action is optimal with respect to its belief and its belief agrees with its state. First, clearly, NE is a trivial CE with the parameters $\beta^k = \sum\limits_{i=2}^{N} \alpha_{i1}^k P_i^k, \gamma^k = 0$ in user 1's belief functions. Next, denote $\mathbf{P}_{SE} = \left[P_{SE}^1, \ldots, P_{SE}^K\right]$ the optimal solution of the discretized version of problem (3.21). To prove SE is a CE, we need to find the corresponding β^k and γ^k and show that SE also solves problem (4.4). Consider the belief function in Table 4.1 with the parameters $\beta^k = \left(I_1^k - P_1^k \cdot \frac{\partial I_1^k}{\partial P_1^k}\right)\Big|_{\mathbf{P}_1=\mathbf{P}_{SE}}$ and $\gamma^k = -\frac{\partial I_1^k}{\partial P_1^k}\Big|_{\mathbf{P}_1=\mathbf{P}_{SE}}$. As discussed before, such parameters preserve all the local information of the objective of problem (3.21) around $\mathbf{P}_{SE}$ into problem (4.4). KKT conditions hold at $\mathbf{P}_{SE}$ since it solves problem (3.21). A sufficient condition that ensures SE to be a CE is that problem (4.4) belongs to convex optimization, because KKT conditions are necessary and sufficient for convex programming to attain its optimum. Appendix H provides a sufficient condition under which problem (4.4) is convex, thereby proving that SE is a special CE if these conditions are satisfied. ■

Theorem 4.2 indicates that the two isolating points, NE and SE, are both CE, if parameters $\boldsymbol{\beta} = \left\{\beta^k\right\}_{k=1}^K$, $\boldsymbol{\gamma} = \left\{\gamma^k\right\}_{k=1}^K$ are properly chosen. Therefore,

CE can be viewed as an operational approach to attain the SE if the system-wide information required for solving SE is not available. It is because only the local information including stationary interference I_1^k and its first derivative $\frac{\partial I_1^k}{\partial P_1^k}$ is required to formulate problem (4.4), and this information can be obtained using measurements performed at the receiver.

In addition, we are interested in the existence of other CEs besides these two points. Denote the parameters of any CE, e.g. NE or SE, as $\boldsymbol{\beta}_* = \left\{\beta_*^k\right\}_{k=1}^K$, $\boldsymbol{\gamma}_* = \left\{\gamma_*^k\right\}_{k=1}^K$, and the optimal solution of problem (4.4) given parameters $\boldsymbol{\beta}, \boldsymbol{\gamma}$ as $\mathbf{P}_1(\boldsymbol{\beta}, \boldsymbol{\gamma})$. Let $F : \mathcal{R}^K \times \mathcal{R}^K \rightarrow \mathcal{R}^K$ be a mapping defined as $F(\boldsymbol{\beta}, \boldsymbol{\gamma}) = \left\{F^k(\boldsymbol{\beta}, \boldsymbol{\gamma})\right\}_{k=1}^K$ in which

$$F^k(\boldsymbol{\beta}, \boldsymbol{\gamma}) = \boldsymbol{h}^k \cdot NE_k(\mathbf{P}_1(\boldsymbol{\beta}, \boldsymbol{\gamma})) - \beta^k - \gamma^k P_1^k(\boldsymbol{\beta}, \boldsymbol{\gamma}) \tag{4.5}$$

The following theorem gives a sufficient condition which ensures that infinite CEs exist.

Theorem 4.3 *Let Γ be a power control game that satisfies condition (C9). Suppose that all the users form conjectures according to Table 4.1. If there exist open neighborhoods $A \subset \mathcal{R}^K$ and $B \subset \mathcal{R}^K$ of $\boldsymbol{\beta}_*$ and $\boldsymbol{\gamma}_*$ respectively, such that $F(\cdot, \gamma) : A \rightarrow \mathcal{R}^K$ is locally one-to-one for any $\boldsymbol{\gamma} \in B$, then Γ admits an infinite set of conjectural equilibria.*

Proof: See Appendix I.

In summary, Theorem 4.1, 4.2, and 4.3 characterize the existence and structure of conjectural equilibrium in power control games. As shown in Fig. 4.1, NE and SE can be both special cases of CE. Open sets of CE that contain NE and SE may exist in the $\boldsymbol{\beta} - \boldsymbol{\gamma}$ plane and different conjectural equilibria correspond to different values of $\boldsymbol{\beta}$ and $\boldsymbol{\gamma}$. SE attains the maximal data rate that a foresighted

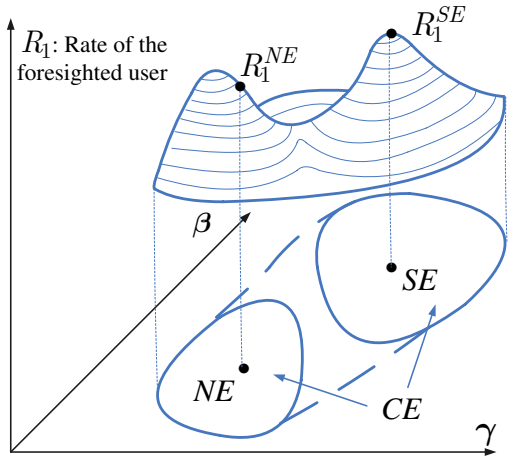

Figure 4.1: Structure of conjectural equilibria in power control games.

user can achieve. According to theorem 4.3, if the foresighted user properly sets up its parameters $\boldsymbol{\beta}, \boldsymbol{\gamma}$, the solution of CE in problem (4.4) coincides with the solution of SE in problem (3.21). More importantly, as opposed to the SE in which the knowledge of the system-wide private information is required, CE assumes that the foresighted user knows only its stationary interference and the first derivatives with respect to the allocated power, which greatly simplifies the information acquisition. Therefore, in order to approach the performance upper bound given by SE, this chapter adopts the approach of CE. The next Section will develop practical conjecture forming and updating algorithms to select out of the infinite CEs a desirable power allocation scheme that provides comparable achievable rates with SE.

4.3 Conjecture-based Rate Maximization

Since Theorem 3 shows that infinite CEs may exist and SE is the most desirable CE for a foresighted user, the parameters β^k, γ^k of belief functions should

be wisely chosen in order to attain SE as a CE. Moreover, the one-shot game formulation and declarative conclusions in the previous sections provide no hint on how to approach the CE. In practice, it is also important to construct algorithmic mechanisms to attain the desirable CE. To arrive at a CE, a multi-agent learning approach is proposed for the repeated game setting [WH98]. Let $\tilde{s}_{n,t}$ and $a_{n,t}$ denote user n's belief and action at time t. In the framework, at time t, the users update their beliefs $\tilde{s}_{n,t}$ and select their actions $a_{n,t}$ based on their past observations. If we define learning as the players' dynamic process of forming conjectures about the effects of their actions, CE captures the achieved outcome when consistency of conjectures within and across players emerges.

Similarly, this section proposes that users can update their beliefs in the repeated interaction setting and numerically examines their performance. Before going into the technical details, it should be pointed out that the pursuit of the practical solution's convergence to CE is not the principal goal of our investigation. Instead, computing power allocation strategies that require only local information and achieve comparable rates with SE (which requires global information) is the ultimate objective rather than the convergence. In other words, any power allocation strategy that lies outside the open CE set in Fig. 4.1 is favorable if it can improve the performance compared with NE.

Table 4.2 summarizes the dynamic updates of all users' states, belief functions, and optimal actions in the power control game. Specifically, at iteration t, users' states $I_{n,t}$ are determined by their opponents' power allocation. User 1 updates the parameters β_t^k, γ_t^k in its belief functions based on its state $I_{1,t}^k$ and allocated power $P_{1,t}^k$, and it also updates its power allocation $\mathbf{P}_{1,t+1}$ based on current operating points $\mathbf{P}_{1,t}$ and its belief $\tilde{\boldsymbol{I}}_{1,t}$. At the same time, myopic users $2, \ldots, N$ set their beliefs equal to their experienced interference and update their

Table 4.2: Dynamic updates of the play.

	User 1	User $2, \ldots, N$
State $I_{n,t}$	$I_{n,t}^k = \sum_{i=1, i\neq n}^{N} \alpha_{i1}^k P_{i,t}^k$	
Belief function $\tilde{s}_n : \mathcal{A}_n \to \mathcal{S}_n$	$\beta_t^k, \gamma_t^k \leftarrow \mathbf{Update_1}\left(I_{1,t}^k, P_{1,t}^k\right)$ $\tilde{I}_{1,t}^k = \beta_t^k - \gamma_t^k P_{1,t}^k$	$\tilde{I}_{n,t}^k = I_{n,t}^k = \sum_{i=1, i\neq n}^{N} \alpha_{in}^k P_{i,t}^k$
Action $a_{1,t}, \ldots, a_{N,t}$	$\mathbf{P}_{1,t+1} \leftarrow \mathbf{Update_2}\left(\mathbf{P}_{1,t}, \tilde{\boldsymbol{I}}_{1,t}\right)$	$\max_{\mathbf{P}_n \in \mathcal{A}_n} \sum_{k=1}^{K} \log_2\left(1 + \frac{P_n^k}{\sigma_n^k + \tilde{I}_{n,t}^k}\right)$

power allocation based on the water-filling strategy. Note that Table 4.2 implicitly assumes that user 1 will update after user $2, \ldots, N$'s IW algorithms converge such that user $2, \ldots, N$'s power allocations $\mathbf{P}_{n,t}$ at time t can be regarded as an equilibrium state. The outcome of this dynamic play is a CE if $\lim_{t\to\infty} \mathbf{P}_{n,t}$ exists and $\lim_{t\to\infty} \boldsymbol{I}_{n,t} = \lim_{t\to\infty} \tilde{\boldsymbol{I}}_{n,t}$. As discussed in the proof of Theorem 4.2, it is equivalent to check the convergence of user 1's updates. We can see from Table 4.2 that user 1 needs to complete two updates at each iteration. The entire procedure in Table 4.2 that enables the foresighted user to build beliefs and improve its performance is named "*Conjecture-based Rate Maximization*". Appropriate rules for updating beliefs are discussed as follows.

Update$_1$: β_t^k, γ_t^k

Note that, we have $I_1^k = \boldsymbol{h}^k \left(\boldsymbol{I} + \boldsymbol{G}\right)^{-1} \boldsymbol{\nu} - \boldsymbol{h}^k \left(\boldsymbol{I} + \boldsymbol{G}\right)^{-1} \boldsymbol{g}^k P_1^k$ from Theorem 4.1, user 1's belief function takes the form of $\tilde{I}_1^k = \beta^k - \gamma^k P_1^k$, and it satisfies $I_1^k = \tilde{I}_1^k$ at CE for any $k \in \{1, \ldots, K\}$. As discussed in the previous section, by setting the parameters $\beta^k = I_1^k - P_1^k \cdot \frac{\partial I_1^k}{\partial P_1^k}$ and $\gamma^k = -\frac{\partial I_1^k}{\partial P_1^k}$, we can preserve all the local information of the original SE problem (3.21) around current feasible operating point $\mathbf{P}_{1,t}$. Therefore, we can update β_t^k and γ_t^k using

$\beta_t^k = \left(I_1^k - P_1^k \cdot \frac{\partial I_1^k}{\partial P_1^k}\right)\Big|_{\mathbf{P}_1=\mathbf{P}_{1,t}}$ and $\gamma_t^k = -\frac{\partial I_1^k}{\partial P_1^k}\Big|_{\boldsymbol{P_1}=\mathbf{P}_{1,t}}$. By Assumption 4.3, user 1 can approximate the parameters using

$$\frac{\partial I_1^k}{\partial P_1^k} \approx \frac{I_1^k\left(\left\{P_1^k+\varepsilon\right\}\cup \mathbf{P}_1^{-k}\right) - I_1^k\left(\left\{P_1^k-\varepsilon\right\}\cup \mathbf{P}_1^{-k}\right)}{2\varepsilon}$$

for small ε in which $\mathbf{P}_1^{-k} = \left\{P_1^1, \ldots, P_1^{k-1}, P_1^{k+1}, \ldots, P_1^K\right\}$.

After $\mathbf{Update_1}$ in each iteration, user 1 needs to solve problem (4.4). If Theorem 4.2's assumption is not satisfied, problem (4.4) belongs to the class of non-convex optimization, which is generally hard to solve and standard optimization algorithms can only be used to determine local maxima [BV04]. However, in this application, we are able to show that, as long as the number of frequency bins K is sufficiently large, problem (4.4) satisfies the time-sharing condition [YL06], and its global optimum can be efficiently computed.

Definition 4.3 *Consider an optimization problem with the general form:*

$$\max \sum_{k=1}^{K} o_k\left(\mathbf{x}_k\right), \ \ s.t. \ \sum_{k=1}^{K} \mathbf{c}_k\left(\mathbf{x}_k\right) \leq \mathbf{P}, \tag{4.6}$$

where $o_k\left(\mathbf{x}_k\right)$ are objective functions that are not necessarily concave, $\mathbf{c}_k\left(\mathbf{x}_k\right)$ are constraint functions that are not necessarily convex. Power constraints are denoted by $\mathbf{P}$. Let $\mathbf{x}_k^*$ and $\mathbf{y}_k^*$ be optimal solutions to the optimization problem (4.6) with $\mathbf{P} = \mathbf{P_x}$ and $\mathbf{P} = \mathbf{P_y}$, respectively. An optimization problem of the form (4.6) is said to satisfy the time-sharing condition [YL06] if for any $0 \leq v \leq 1$, there always exists a feasible solution $\mathbf{z}_k$, such that $\sum_{k=1}^{K} \mathbf{c}_k\left(\mathbf{z}_k\right) \leq v\mathbf{P_x} + (1-v)\,\mathbf{P_y}$ and $\sum_{k=1}^{K} o_k\left(\mathbf{z}_k\right) \leq v\sum_{k=1}^{K} o_k\left(\mathbf{x}_k^*\right) + (1-v)\sum_{k=1}^{K} o_k\left(\mathbf{y}_k^*\right)$.

Theorem 4.4 *As the total number of sub-carriers K goes to infinity, problem (4.4) satisfies the time-sharing condition.*

Table 4.3: **Algorithm** 4.3: A dual method that solves problem (4.4).

Input: $\left\{\sigma_1^k\right\}, \left\{\beta_t^k\right\}, \left\{\gamma_t^k\right\}, \mathbf{P_1^{max}}$

Initialize: $\boldsymbol{\eta}_{\min}, \boldsymbol{\eta}_{\max}, \boldsymbol{\eta}_0 = \left(\boldsymbol{\eta}_{\min} + \boldsymbol{\eta}_{\max}\right)/2, i = 0$

Repeat

set $\mathbf{P}_1 = \left[P_1^1 \dots P_1^K\right]$ where

$$P_1^k = \arg \max_{P_1'^k \in dom\, f_{\sigma_1^k, \beta^k, \gamma^k}} \log_2\left(1 + \frac{P_1'^k}{\sigma_1^k + \beta_t^k - \gamma_t^k P_1'^k}\right) - \boldsymbol{\eta}_i P_1'^k$$

if $\sum_k P_1^k < \mathbf{P_1^{max}}$, $\boldsymbol{\eta}_{\max} = \boldsymbol{\eta}_i$; else $\boldsymbol{\eta}_{\min} = \boldsymbol{\eta}_i$.

$\boldsymbol{\eta}_{i+1} \leftarrow \left(\boldsymbol{\eta}_{\min} + \boldsymbol{\eta}_{\max}\right)/2,\ i = i + 1$

until $\boldsymbol{\eta}_i$ converges

Proof: Specifically, for problem (4.4), $o_k\left(\mathbf{x}_k\right) = f_{\sigma_1^k, \beta^k, \gamma^k}\left(P_1^k\right)$, $\mathbf{c}_k\left(\mathbf{x}_k\right) = P_1^k$, $\mathbf{P} = \mathbf{P_1^{max}}$. First, as the total number of sub-carriers K goes to infinity, consider σ_n^k and α_{jn}^k as $\sigma_n\left(k\right)$ and $\alpha_{jn}\left(k\right)$ that are continuous functions of k. By rule $\mathbf{Update_1}$, $\boldsymbol{\beta}_t\left(k\right)$ and $\boldsymbol{\gamma}_t\left(k\right)$ are piece-wise continuous, because Theorem 4.3 proves that $\mathbf{P}_1\left(\boldsymbol{\beta}, \boldsymbol{\gamma}\right)$ and $F\left(\boldsymbol{\beta}, \boldsymbol{\gamma}\right)$ are continuous in $\left(\boldsymbol{\beta}, \boldsymbol{\gamma}\right)$. With the piece-wise continuity of $\boldsymbol{\beta}\left(k\right), \boldsymbol{\gamma}\left(k\right)$, it is easy to check that the time-sharing condition holds by following the proof of Theorem 2 in [YL06]. ■

$\mathbf{Update_2}$: $\mathbf{P}_{1,t+1}$

It is shown in [YL06] that, if the optimization problem satisfies the time-sharing property, then it has a zero duality gap, which leads to efficient numerical algorithms that solve the non-convex problem in the dual domain. Consider the dual objective function $d\left(\boldsymbol{\eta}\right) = \sum_{k=1}^{K}\left\{\max_{P_1^k} f_{\sigma_1^k, \beta^k, \gamma^k}\left(P_1^k\right) - \boldsymbol{\eta} P_1^k\right\} + \boldsymbol{\eta}\mathbf{P_1^{max}}$. Since $d\left(\boldsymbol{\eta}\right)$ is convex, a bisection or gradient-type search over the Lagrangian dual variable $\boldsymbol{\eta}$ is guaranteed to converge to the global optimum. Specifically, Algorithm 4.3 summarizes such a dual method that solves non-convex problem

Table 4.4: Conjecture-based rate maximization.

Initialize: $t = 0, \mathbf{P}_{1,0} = \mathbf{P}_1^{NE}$

Repeat

I. $\beta_t^k, \gamma_t^k \leftarrow \mathbf{Update_1}\left(I_{1,t}^k, P_{1,t}^k\right)$

II. $\mathbf{P}_{1,t+1} \leftarrow \mathbf{Update_2}\left(\mathbf{P}_{1,t}, \tilde{\boldsymbol{I}}_{1,t}\right)$, which includes

1) Consider problem

$\max \sum_{k=1}^{K} f_{\sigma_1^k,\beta^k,\gamma^k}\left(P_1^k\right),\ s.t.\ P_1^k \in dom\ f_{\sigma_1^k,\beta^k,\gamma^k}$ and $\sum_{k=1}^{K} P_1^k \leq \mathbf{P_1^{max}}$.

2) Use Algorithm 4.3 to calculate the global optimum $\mathbf{P}_1^c$ of the above problem.

3) Search in the interval of $v\mathbf{P}_{1,t} + (1-v)\,\mathbf{P}_1^c\ \ (0 \leq v \leq 1)$ and find in the interval the power allocation $\mathbf{P}_1^s$ that maximizes user 1's actual achievable rate R_1.

4) $\mathbf{P}_{1,t+1} \leftarrow \mathbf{P}_1^s, t = t+1$.

until no improvement can be made.

(4.4) using bisection update. As long as the time-sharing condition is satisfied, Algorithm 4.3 converges to the global optimum. Hence, we can always solve problem (4.4) regardless of its convexity.

Table 4.4 summarizes the procedure of algorithm "Conjecture-based Rate Maximization" (CRM). Next, we make several remarks about this algorithm. First, since we want to achieve better performance than NE, the initial operating point $\mathbf{P}_{1,0}$ is set to be the power allocation strategy $\mathbf{P}_1^{NE}$ that user 1 will choose if it adopts the IW algorithm. Second, in $\mathbf{Update_2}$, the global optimum $\mathbf{P}_1^c$ is not directly used to update $P_{1,t+1}^k$. As shown in Fig. 4.2, this is because problem (4.4) is only a local approximation at $\mathbf{P}_{1,t}$ of the original SE problem (3.21) that we want to solve. Using $\mathbf{P}_1^c$ to update $\mathbf{P}_{1,t+1}$ may decrease the actual achievable

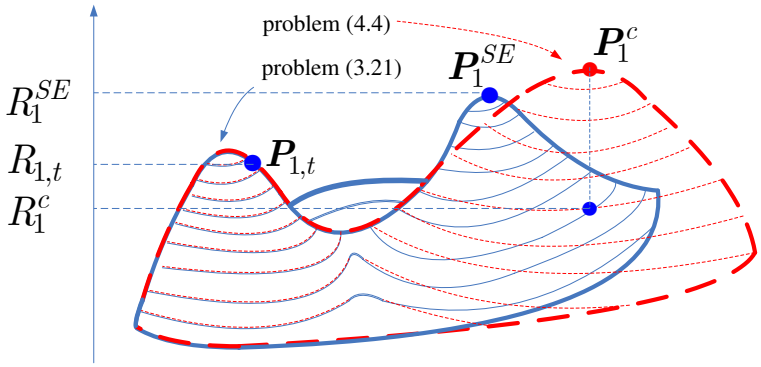

Figure 4.2: Mismatch between problem (3.21) and (4.4).

rate R_1, if a mismatch between problem (3.21) and (4.4) exists for the solution $\mathbf{P}_1^c$. Therefore, $\mathbf{Update_2}$ adopts line search and uses the transmit PSD that lies in this interval and maximizes the actual achievable rate to update $\mathbf{P}_{1,t+1}$. Therefore, it is guaranteed that the achievable rate will not decrease after each iteration. Last, CRM stops in limited iterations, but it is not guaranteed to converge to a CE. It is because the first step in $\mathbf{Update_2}$ may give $\mathbf{P}_{1,t} \neq \mathbf{P}_1^c$ but the line search returns $\mathbf{P}_{1,t+1} = \mathbf{P}_{1,t}$. However, if $\mathbf{P}_{1,t} = \mathbf{P}_1^c$, CRM converges to $\mathbf{P}_1^c$ and the resulting outcome is a CE.

4.4 Simulation Results

This section compares the performance of CRM with the IW algorithm and Algorithm 3.1 that searches SE assuming perfect knowledge of its opponent's private information. We simulate a system with 50 sub-carriers over the 15-MHz band. We consider frequency-selective channels using a four-ray Rayleigh model with the exponential power profile and 60 ns root mean square delay spread. The power of each ray is decreasing exponentially according to its delay.

We first simulate the two-user scenario with $\mathbf{P_1^{max}} = \mathbf{P_2^{max}} = 200$ and $\sigma_1^k =$

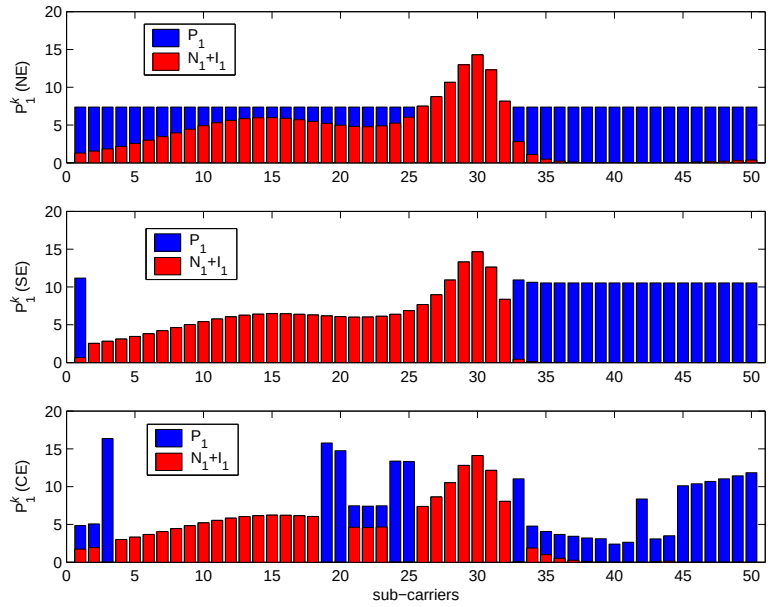

Figure 4.3: User 1's power allocation using different algorithms.

$\sigma_2^k = 0.01$. The total power of all rays of H_{11}^k and H_{22}^k is normalized as one, and that of H_{12}^k and H_{21}^k is normalized as 0.5. Fig. 4.3 shows an example of user 1's power allocations when deploying different algorithms under the same conditions. In IW algorithm, user 1 water-fills the whole frequency band by regarding its competitor's interference as background noise. In contrast, user 1 will not water-fill if choosing CRM and Algorithm 3.1. It avoids the myopic behavior and improves its performance by explicitly considering the stationary interference caused by its opponent.

To evaluate the performance, we tested 10^5 sets of frequency-selective fading channels that satisfy Assumption 4.4. Denote user i's achievable rate using CRM, IW and Algorithm 3.1 as R_i, R_i^{NE}, and $R_i^{'SE}$ respectively. Fig. 4.4 shows the simulated cumulative probability of the ratio of R_i over R_i^{NE} and $R_i^{'SE}$. The curve indicates that there is a probability of 59% that CRM returns the same power allocation strategy as IW. On the other hand, the average improvement for

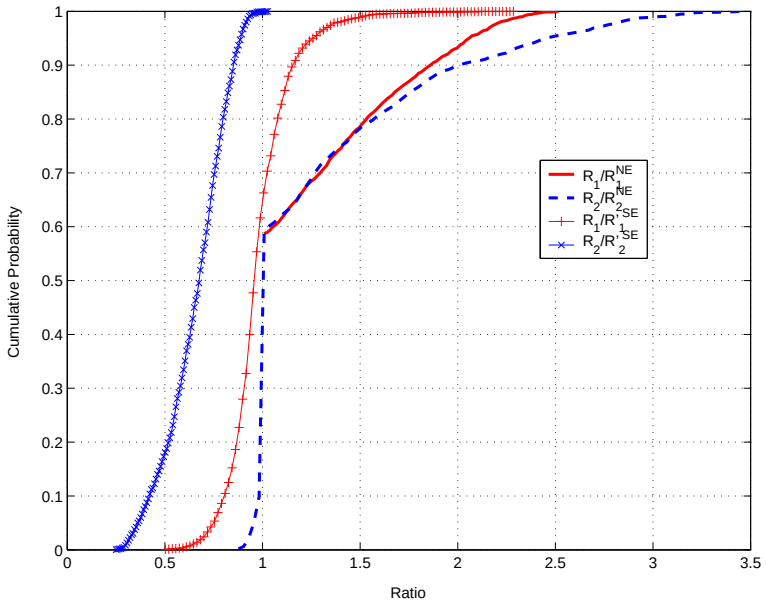

Figure 4.4: Cdfs of R_i/R_i^{NE} and $R_i/R_i^{'SE}$ $(i = 1, 2)$.

Table 4.5: Iterations required by different CRM algorithms.

Algorithm	Probability of required iterations				
	$t = 1$	$t = 2$	$t = 3$	$t = 4$	$t \geq 5$
CRM	0.59	0.29	0.06	0.04	0.02
Modified CRM	0.39	0.19	0.20	0.12	0.10

user 1 of CRM over IW is 24%, which achieves almost the same performance as Algorithm 3.1. As shown in Fig. 4.4, $R_1/R_1^{'SE}$ is distributed symmetrically with respect to $R_1 = R_1^{'SE}$. CRM improves on average user 2's data rate by 29% over IW, which is smaller than Algorithm 3.1. Similarly as in the previous chapter, in very few cases, CRM results in a rate R_2' smaller than R_2^{NE} in the IW algorithm.

The iteration time required by CRM is summarized in Table 4.5. As mentioned above, CRM stops after just one iteration with a probability of 59% due

to the problem mismatch shown in Fig. 3. In most scenarios, CRM terminates within 4 iterations and the average number of required iteration is only 1.75. To further improve the performance of CRM, we can modify the original CRM to handle the problem mismatch between (3.21) and (4.4). Notice that problem (4.4) is only a local approximation of problem (3.21) at $\mathbf{P}_{1,t}$. Additional constraints can be added in Algorithm 4.3, such that the optimum of problem (4.4) is searched only in a certain region around $\mathbf{P}_{1,t}$ rather than the whole domain of $f_{\sigma_1^k,\beta_t^k,\gamma_t^k}$. For example, $\left|P_1'^k - P_{1,t}^k\right|$ can be restricted within a certain threshold when performing Algorithm 4.3 for any $k \in \{1,\ldots,K\}$. We simulated the two-user scenarios with additional restriction of $\left|P_1'^k - P_{1,t}^k\right| \leq 1$. Fig. 4.5 shows the simulated cumulative probability of R_i/R_i^{NE} for this modified CRM. As opposed to CRM, the probability that the modified CRM returns the same power allocation strategy as IW is reduced to 39% and the average performance improvement is also increased for both users. Specifically, the average performance improvement for user 1 is 29% and that of user 2 is 31%. However, Table V shows that the improvement is achieved at the cost of more iterations.

We also tested performance of modified CRM in multi-user cases where TSA cannot be applied. We simulated the three-user scenarios with $\mathbf{P_n^{max}} = 200$ and $\sigma_n^k = 0.01$. The total power of all rays of H_{nn}^k is normalized as one, and that of H_{ij}^k $(i \neq j)$ is normalized as 0.33. Fig. 4.6 shows the simulated cumulative probability of R_i/R_i^{NE}. The average improvement for user 1 of modified CRM over IW is 29%, and that of the rest users is 8%. We can see that, it benefits on average most of the participants in the power control game if a foresighted user forms accurate conjectures and plays the conjecture equilibrium strategy.

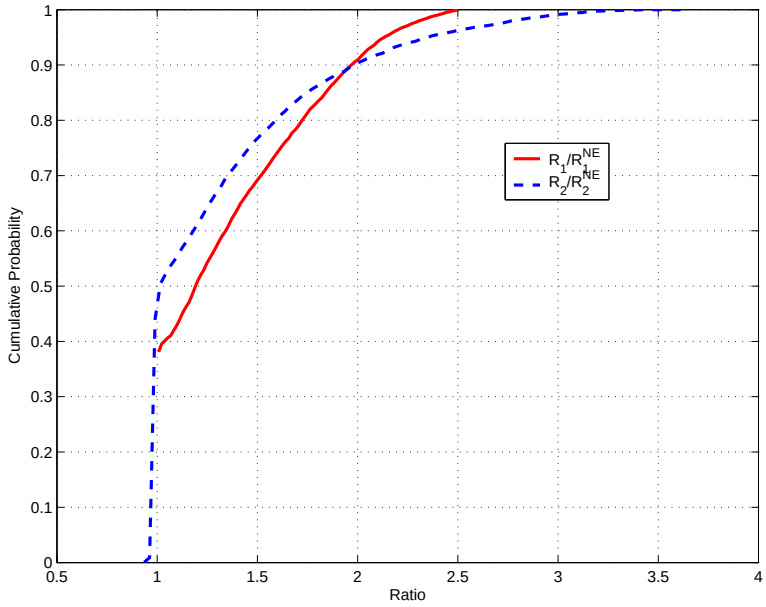

Figure 4.5: Cdfs of R_i/R_i^{NE} $(i = 1, 2)$ for modified CRM.

4.5 Concluding Remarks

This chapter introduces the concept of conjectural equilibrium in non-cooperative power control games and discusses how a foresighted user can model its experienced interference as a function of its own power allocation in order to improve its own data rate. The existence of conjectural equilibrium is proven and both game theoretic solutions, including Nash equilibrium and Stackelberg equilibrium, are shown to be special cases of this conjectural equilibrium. Practical algorithms based on conjectural equilibrium are developed to determine desirable power allocation strategies. Numerical results verify that a foresighted user forming proper conjectures can improves both its own achievable rate as well as the rates of other participants, even if it has no a priori knowledge of its competitors' private information. How to extend the framework to the scenarios in which multiple foresighted users coexist is a topic for future investigation. While this chapter

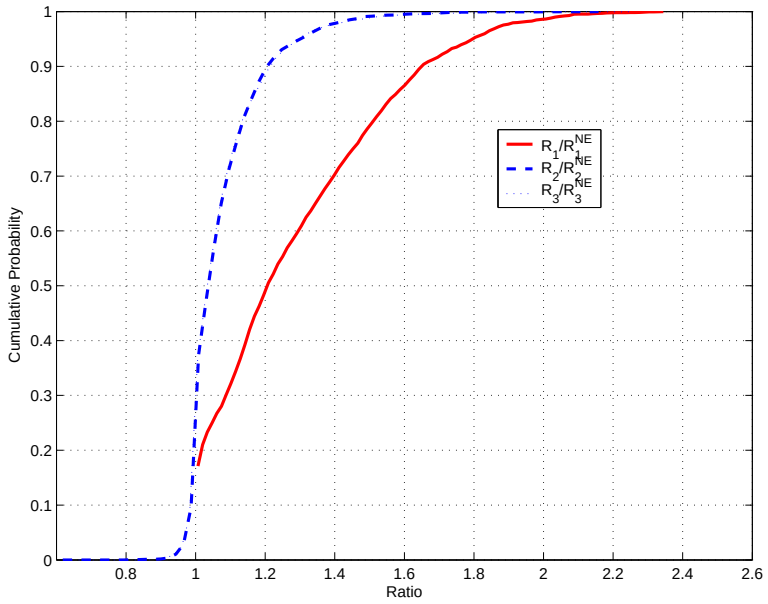

Figure 4.6: Cdfs of R_i/R_i^{NE} $(i = 1, 2, 3)$ for modified CRM.

has focused on the power control game, the idea of forming conjectures based the available local information is also applicable to any communication system where making foresighted decisions is beneficial, e.g. distributed routing in wired network [KLO95].

4.6 Appendix H: A sufficient condition for problem (4.4) to be convex

Define $f_{a_1,a_2,b}(x) = \ln\left(1 + \frac{x}{a_1+a_2-bx}\right)$ in which the term $a_1 \geq 0$ represents the noise PSD. The second derivative of $f_{a_1,a_2,b}(x)$ is

$$f''_{a_1,a_2,b}(x) = -\frac{(a_1+a_2)\left[-(a_1+a_2)(2b-1)+2b(b-1)x\right]}{(a_1+a_2-bx)^2\left[a_1+a_2-(b-1)x\right]^2}.$$

Clearly, if $b \neq 0$, $f''_{a_1,a_2,b}(x)$ is not always negative. We restrict the domain of $f_{a_1,a_2,b}$ to be $dom\ f_{a_1,a_2,b} = \{x \geq 0\} \cap \{a_2 - bx \geq 0\}$, because x is the transmitted

power and $a_2 - bx$ represents the stationary interference, both of which are non-negative. We derive a sufficient condition that guarantees $f_{a_1,a_2,b}(x)$ is concave in $dom\ f_{a_1,a_2,b}$:

$$a_2 > 0 \text{ and } b < 0.5\left(1 - \frac{a_2}{a_1}\right) \tag{4.7}$$

This condition can be simply verified by using inequality analysis. Clearly, $a_2 > 0$ leads to $a_1 + a_2 > 0$ and $b < 0.5\left(1 - \frac{a_2}{a_1}\right) < 1$. Therefore, $f''_{a_1,a_2,b}(x) < 0$ is equivalent to $-(a_1 + a_2)(2b - 1) + 2b(b - 1)x > 0$. We have

$$\begin{aligned} x \in dom\ f_{a_1,a_2,b} \Rightarrow a_2 - bx \geq 0 \Rightarrow bx - a_2 \cdot \frac{a_1 + a_2}{a_2} \cdot \frac{b - 0.5}{b - 1} < 0 \\ \Rightarrow -(a_1 + a_2)(2b - 1) + 2b(b - 1)x > 0, \end{aligned}$$

because $\frac{a_1+a_2}{a_2} \cdot \frac{b-0.5}{b-1} > 1$ when $b < 0.5\left(1 - \frac{a_2}{a_1}\right)$. Hence, the condition (4.7) leads to $f''_{a_1,a_2,b}(x) < 0$.

Based on sufficient condition (4.7), we can see, if $\beta^k > 0$ and $\gamma^k < 0.5\left(1 - \frac{\beta^k}{\sigma_1^k}\right)$ for any $k \in \{1, \cdots, K\}$, problem (4.4) belongs to convex programming. Therefore, if the following sufficient condition

$$\begin{aligned} \left(I_1^k - P_1^k \cdot \frac{\partial I_1^k}{\partial P_1^k}\right)\Big|_{\mathbf{P}_1 = \mathbf{P}_{SE}} > 0 \text{ and} \\ -\frac{\partial I_1^k}{\partial P_1^k}\Big|_{\mathbf{P}_1 = \mathbf{P}_{SE}} < \frac{1}{2} - \frac{1}{2\sigma_1^k} \cdot \left(I_1^k - P_1^k \cdot \frac{\partial I_1^k}{\partial P_1^k}\right)\Big|_{\mathbf{P}_1 = \mathbf{P}_{SE}} \end{aligned} \tag{C9}$$

holds, SE satisfies the KKT optimality condition and solves the convex programming problem (4.4), i.e. SE is also a CE.

4.7 Appendix I: Proof of Theorem 4.3

If the power control game Γ satisfies condition C9, then problem (4.4) is convex. We can use the following "maximum theorem" [SLS07, Ber97] to show that $\mathbf{P}_1(\boldsymbol{\beta}, \boldsymbol{\gamma})$ is continuous.

(***Maximum Theorem***) Let $\phi(x,y)$ be a real-valued continuous function with domain $X \times Y$, where $X \subset \mathcal{R}^m$ and $Y \subset \mathcal{R}^n$ are closed and bounded sets. Suppose that $\phi(x,y)$ is strictly concave in x for each y. The functions $\Phi(y) = \arg\max\{\phi(x,y) : x \in X\}$ is well-defined $\forall y \in Y$, and is continuous.

We can restrict the domain of parameters $\boldsymbol{\beta}$ and $\boldsymbol{\gamma}$ in closed and bounded set, e.g. $\left|\gamma^k\right| \leq M^+$, in which M^+ is a bound satisfying $M^+ \gg \max_k \boldsymbol{h}^k (\boldsymbol{I} + \boldsymbol{G})^{-1} \boldsymbol{g}^k$. Apply the maximum theorem with $\phi = R(\mathbf{P}_1, \boldsymbol{\beta}, \boldsymbol{\gamma}) = \sum_{k=1}^K f_{\sigma_1^k, \beta^k, \gamma^k}\left(P_1^k\right)$. The optimal solution $\mathbf{P}_1(\boldsymbol{\beta}, \boldsymbol{\gamma})$ of problem (4.4) is the function in the maximum theorem, and hence is a continuous function of $(\boldsymbol{\beta}, \boldsymbol{\gamma})$. As a result, $F(\boldsymbol{\beta}, \boldsymbol{\gamma})$ is also continuous in $(\boldsymbol{\beta}, \boldsymbol{\gamma})$. Note that $\mathbf{P}_1(\boldsymbol{\beta}, \boldsymbol{\gamma})$ and $F(\boldsymbol{\beta}, \boldsymbol{\gamma})$ are not necessarily continuously differentiable.

By the definition of $F(\boldsymbol{\beta}, \boldsymbol{\gamma})$ and conjectural equilibrium, we have that $F(\boldsymbol{\beta}, \boldsymbol{\gamma}) = \mathbf{0}$ implies conjectural equilibrium. Note $F(\boldsymbol{\beta}_*, \boldsymbol{\gamma}_*) = \mathbf{0}$. If there exist open neighborhoods $A \subset \mathcal{R}^K$ and $B \subset \mathcal{R}^K$ of $\boldsymbol{\beta}_*$ and $\boldsymbol{\gamma}_*$, and for $\forall \boldsymbol{\gamma} \in B$, $F(\cdot, \boldsymbol{\gamma}) : A \to \mathcal{R}^K$ is locally one-to-one, by the implicit function theorem [Kum80], there exists open neighborhoods $A_0 \subset \mathcal{R}^K$ and $B_0 \subset \mathcal{R}^K$ of $\boldsymbol{\beta}_*$ and $\boldsymbol{\gamma}_*$ such that for each $\boldsymbol{\gamma} \in B_0$, there is a unique $\boldsymbol{\beta}(\boldsymbol{\gamma})$ satisfying $F(\boldsymbol{\beta}(\boldsymbol{\gamma}), \boldsymbol{\gamma}) = \mathbf{0}$. Therefore, Γ admits an infinite set of conjectural equilibria.

Alternatively, we can view $F(\boldsymbol{\beta}, \boldsymbol{\gamma}) = \mathbf{0}$ as K equations with $2K$ unknowns, hence, the equilibrium is usually not a single point but a continuous surface. We can explore the structure of $\mathbf{P}_1(\boldsymbol{\beta}, \boldsymbol{\gamma})$ to derive the expression of this surface. Particularly, under condition (C9), the solution of convex problem (4.4) satisfies

$$\gamma^k\left(\gamma^k - 1\right)\left(P_1^k\right)^2 - \left(\sigma_1^k + \beta^k\right)\left(2\gamma^k - 1\right)P_1^k + \left(\sigma_1^k + \beta^k\right)^2 - \frac{\sigma_1^k + \beta^k}{\mu_1 - \lambda_1^k} = 0, \quad (4.8)$$

where λ_1^k and μ_1 are the Lagrange multipliers as in (4.4). The optimal $\mathbf{P}_1(\boldsymbol{\beta}, \boldsymbol{\gamma}) =$

$\left\{P_1^k(\boldsymbol{\beta},\boldsymbol{\gamma})\right\}$ is given by

$$P_1^k(\boldsymbol{\beta},\boldsymbol{\gamma}) = \frac{\left(\sigma_1^k+\beta^k\right)\left(2\gamma^k-1\right)}{2\gamma^k\left(\gamma^k-1\right)} + \frac{\sqrt{\left(\sigma_1^k+\beta^k\right)^2\left(2\gamma^k-1\right)^2 - 4\gamma^k\left(\gamma^k-1\right)\left[\left(\sigma_1^k+\beta^k\right)^2 - \frac{\sigma_1^k+\beta^k}{\mu_1-\lambda_1^k}\right]}}{2\gamma^k\left(\gamma^k-1\right)}. \tag{4.9}$$

Note that the other root of equation (4.8) is removed by checking its feasibility in $dom\ f_{\sigma_1^k,\beta^k,\gamma^k}$. By substituting (4.9) into (4.2) and (4.5), we can explicitly express $F(\boldsymbol{\beta},\boldsymbol{\gamma})$ in terms of $\boldsymbol{\beta}$ and $\boldsymbol{\gamma}$, resulting in a very complex form of the surface. ■

CHAPTER 5

Linearly Coupled Games

5.1 Introduction

In previous chapters, for ACSCG, we analyzed the sufficient condition under which there exists a unique NE and best response dynamics globally converges to such a NE. We also investigated how to improve the inefficiency of the NE. This can be accomplished by either enabling users exchange coordination information in real-time or letting one foresighted leader model the reaction of the other myopic users and play the SE or CE strategy. In this chapter, we present another game model for a particular type of non-cooperative multi-user communication scenario in which multiple users playing the CE strategy may achieve Pareto optimality without any real-time information exchange. We name it linearly coupled games, because users' utilities are linearly impacted by their competitors' actions. In particular, the main contributions of this chapter are as follows. First, based on the assumptions that we make about the properties of users' utility, we characterize the inherent structures of the utility functions for the linearly coupled games. Furthermore, based on the derived utility forms, we explicitly quantify the NE and Pareto boundary for the linearly coupled games. The price of anarchy incurred by the selfish users playing the Nash strategy is quantified. In addition, to improve the performance in the non-cooperative scenarios, we investigate the CE-based solution. Using this approach, individual users are modeled as belief-

forming agents that develop internal beliefs about their competitors and behave optimally with respect to their individual beliefs. Sufficient (and necessary) conditions that guarantee the convergence of different dynamic update mechanisms, including best response, gradient play, and Jacobi update, are addressed. We prove that these adjustment processes based on conjectures and non-cooperative individual optimization can be driven to Pareto-optimality in the linearly coupled games without the need of real-time coordination information exchange among agents. The investigated models apply to a variety of realistic applications encountered in the multiple access design, including wireless random access and flow control.

The rest of this chapter is organized as follows. Section 5.2 defines the linearly coupled games. For the investigated game models, Section 5.3 explicitly analyzes the NE and Pareto boundary of the achievable utility region and defines two basic types of linearly coupled games. We will discuss Type I games in details in Chapter 6. For Type II games, Section 5.4 quantifies the efficiency loss between NE and Pareto boundary and investigates the properties of CE under both the best response and Jacobi update dynamics. Concluding remarks are drawn in Section 5.5.

5.2 Linearly Coupled Games

Definition 5.1 *A multi-user interaction is considered a linearly coupled game if the action set $\mathcal{A}_n \subseteq \mathcal{R}_+$ is convex and the utility function u_n satisfies:*

$$u_n(\mathbf{a}) = a_n^{\beta_n} \cdot s_n(\mathbf{a}), \tag{5.1}$$

in which $\beta_n > 0$. In particular, the basic assumptions about $s_n(\mathbf{a})$ include:

Assumption 5.1 *$s_n(\mathbf{a})$ is non-negative;*

Assumption 5.2 *Denote* $s'_{nm}(\mathbf{a}) = \frac{\partial s_n(\mathbf{a})}{\partial a_m}$ *and* $s''_{nm}(\mathbf{a}) = \frac{\partial^2 s_n(\mathbf{a})}{\partial a_m^2}$. $s_n(\mathbf{a})$ *is strictly linear decreasing in* $a_m, \forall m \neq n$, *i.e.* $s'_{nm}(\mathbf{a}) < 0$ *and* $s''_{nm}(\mathbf{a}) = 0$; $s_n(\mathbf{a})$ *is non-increasing and linear in* a_n, *i.e.* $s'_{nn}(\mathbf{a}) \leq 0$ *and* $s''_{nn}(\mathbf{a}) = 0$;

Assumption 5.3 $\frac{s_n(\mathbf{a})}{s'_{nm}(\mathbf{a})}$ *is an affine function,* $\forall n \in \mathcal{N} \setminus \{m\}$;

Assumption 5.4 $\frac{s'_{nm}(\mathbf{a})}{s_n(\mathbf{a})} = \frac{s'_{km}(\mathbf{a})}{s_k(\mathbf{a})}, \forall n, k \in \mathcal{N} \setminus \{m\}$; $\frac{s'_{mm}(\mathbf{a})}{s_m(\mathbf{a})} = 0$ *or* $\frac{s'_{nm}(\mathbf{a})}{s_n(\mathbf{a})}$, $\forall n \neq m$.

Assumptions 5.1 and 5.2 indicate that increasing a_m for any $m \neq n$ within the domain of $s_n(\mathbf{a})$ will linearly decrease user n's utility. Assumptions 5.3 and 5.4 imply that a user's action has proportionally the same impact over the other users' utility. The structure of the utility functions that satisfy assumptions 5.1-5.4 will be addressed in the next section.

5.3 Structure of Utility Functions

In this section, we show that the computation of the NE and the Pareto boundary in linearly coupled games is equivalent to solving linear equations. Moreover, we investigate the inherent structures of the utility functions satisfying assumptions 5.1-5.4 and define two basic types of linearly coupled games.

5.3.1 Nash Equilibrium

We are interested in computing the NE in the linear coupled games. From equation (5.1), we have

$$\frac{\partial \log[u_n(\mathbf{a})]}{\partial a_m} = \begin{cases} \beta_n/a_n + s'_{nn}(\mathbf{a})/s_n(\mathbf{a}), & if\ m = n; \\ s'_{nm}(\mathbf{a})/s_n(\mathbf{a}), & otherwise. \end{cases} \tag{5.2}$$

On one hand, if $s'_{nn}(\mathbf{a}) = 0, \forall n \in \mathcal{N}$, since user n's utility function strictly increases in a_n, we have trivial NE at which a_n^* is the maximal element in $\mathcal{A}_n$ that lies in the domain of $s(\cdot)$, $\forall n \in \mathcal{N}$.

On the other hand, if $s'_{nn}(\mathbf{a}) \neq 0, \forall n \in \mathcal{N}$, according to assumption 5.3, since the multi-user interactions are linearly coupled, we have

$$s_n(\mathbf{a}) = f_n^m(\mathbf{a}_{-m}) + g_n^m(\mathbf{a}_{-m})a_m, \tag{5.3}$$

where $f_n^m(\mathbf{a}_{-m}), g_n^m(\mathbf{a}_{-m})$ are both polynomials and $g_n^n(\mathbf{a}_{-n}) \neq 0$. From this, it follows

$$\frac{s'_{nn}(\mathbf{a})}{s_n(\mathbf{a})} = \left[\frac{f_n^n(\mathbf{a}_{-n})}{g_n^n(\mathbf{a}_{-n})} + a_n\right]^{-1}. \tag{5.4}$$

At NE, we have

$$\frac{\partial \log[u_n(\mathbf{a})]}{\partial a_n} = 0, \forall n \in \mathcal{N}. \tag{5.5}$$

Under assumption 5.3 and 5.4, $\frac{f_n^n(\mathbf{a}_{-n})}{g_n^n(\mathbf{a}_{-n})}$ is a affine function, which enables us to explicitly characterize the NE. Denote $\frac{f_n^n(\mathbf{a}_{-n})}{g_n^n(\mathbf{a}_{-n})} = h_n(\mathbf{a}_{-n})$. Equation (5.5) can be rewritten as

$$\beta_n \cdot h_n(\mathbf{a}_{-n}) + (\beta_n + 1) \cdot a_n = 0, \forall n \in \mathcal{N}. \tag{5.6}$$

Therefore, the solutions of Equations (5.6) are the NE of the linearly coupled games and computing the NE is equivalent to solving N-dimension linear equations. The following theorem indicates the inherent structure of the utility functions $\{u_n\}_{n=1}^N$ when the requirements 5.1-5.3 are satisfied.

Theorem 5.1 *Under assumptions 5.1-5.3, the irreducible factors of $s_n(\mathbf{a})$ over the integers are affine functions and have no variables in common.*

Proof: Denote the factorization of $s_n(\mathbf{a})$ as

$$s_n(\mathbf{a}) = \prod_{i=1}^{M_n} b_n^i(\mathbf{a}), \tag{5.7}$$

in which M_n represents the number of the non-constant irreducible factors in $s_n(\mathbf{a})$. Define $\mathrm{V}(\cdot)$ as the mapping from a polynomial to the set of variables that appear in that polynomial. Based on assumption 5.2, we immediately have

$$\mathrm{V}(b_n^i(\mathbf{a})) \cap \mathrm{V}(b_n^j(\mathbf{a})) = \varnothing, \forall i, j(j \neq i), n.$$

Without loss of generality, we assume that $a_j \in \mathrm{V}(b_n^1(\mathbf{a}))$ and $b_n^1(\mathbf{a}) = f_{b_n^1}^j(\mathbf{a}_{-j}) + g_{b_n^1}^j(\mathbf{a}_{-j})a_j$. Then $f_n^j(\mathbf{a}_{-j}), g_n^j(\mathbf{a}_{-j})$ in (5.3) are given by

$$f_n^j(\mathbf{a}_{-j}) = f_{b_n^1}^j(\mathbf{a}_{-j}) \cdot \prod_{i=2}^{M_n} b_n^i(\mathbf{a}), \text{ and } g_n^j(\mathbf{a}_{-j}) = g_{b_n^1}^j(\mathbf{a}_{-j}) \cdot \prod_{i=2}^{M_n} b_n^i(\mathbf{a}).$$

Therefore, $\frac{f_n^m(\mathbf{a}_{-m})}{g_n^m(\mathbf{a}_{-m})} = \frac{f_{b_n^1}^j(\mathbf{a}_{-j})}{g_{b_n^1}^j(\mathbf{a}_{-j})}$. By assumption 5.3, we have that the degree of $\frac{f_{b_n^1}^j(\mathbf{a}_{-j})}{g_{b_n^1}^j(\mathbf{a}_{-j})}$ is less than or equal to 1. Since $b_n^1(\mathbf{a})$ is irreducible, we can conclude that $g_{b_n^1}^j(\mathbf{a}_{-j})$ is a constant and the degree of $f_{b_n^1}^j(\mathbf{a}_{-j})$ is less than or equal to 1. Note that the arguments above hold, $\forall j, n$. Therefore, the degree of $b_n^i(\mathbf{a})$ is one, $\forall n \in \mathcal{N}, i = 1, \ldots, M_n$, which concludes the proof. ■

5.3.2 Pareto Boundary

Since $\log(\cdot)$ is concave and $\log[u_n(\mathbf{a})]$ is a composition of affine functions [BV04], $u_n(\mathbf{a})$ is log-concave in $\mathbf{a}$ and the log-utility region $\log\mathcal{U}$ is convex. Therefore, we can characterize the Pareto boundary of the utility region as a set of $\mathbf{a}$ optimizing the following weighted proportional fairness objective[1]:

$$\max_{\mathbf{a}} \sum_{n=1}^{N} \omega_n \log[u_n(\mathbf{a})], \tag{5.8}$$

for all possible sets of $\{\omega_n\}$ satisfying $\omega_n \geq 0$ and $\sum_{n=1}^{N} \omega_n = 1$. Denote the optimal solution of problem (5.8) as $\mathbf{a}^{PB}$, which satisfies the following first-order

[1]Note that the utility region $\mathcal{U}$ is not necessarily convex. Therefore, its Pareto boundary may not be characterized by the weighted sum of $\{u_n(\mathbf{a})\}_{n=1}^N$.

condition:

$$\frac{\partial \sum_{k=1}^{N} \omega_k \log[u_k(\mathbf{a})]}{\partial a_n}\bigg|_{\mathbf{a}=\mathbf{a}^{PB}} = 0, \forall n \in \mathcal{N}, \tag{5.9}$$

Under assumptions 5.1-5.3, the LHS of equation (5.9) can be rewritten as

$$\frac{\partial \sum_{k=1}^{N} \omega_k \log[u_k(\mathbf{a})]}{\partial a_m} = \omega_m \left(\frac{\beta_m}{a_m} + \frac{s'_{mm}(\mathbf{a})}{s_m(\mathbf{a})} \right) + \sum_{k \neq m} \omega_k \frac{s'_{km}(\mathbf{a})}{s_k(\mathbf{a})}. \tag{5.10}$$

By Theorem 5.1 and assumption 5.4, we have

$$\frac{s'_{km}(\mathbf{a})}{s_k(\mathbf{a})} = \frac{1}{\psi_m(\mathbf{a})}, \ \forall k \in \mathcal{N} \setminus \{m\}, \tag{5.11}$$

in which $\psi_m(\mathbf{a})$ is a affine function. Therefore, equation (5.10) is equivalent to

$$\frac{\partial \sum\limits_{k=1}^{N} \omega_k \log[u_k(\mathbf{a})]}{\partial a_m} = \begin{cases} \beta_m \omega_m / a_m + (1-\omega_m)/\psi_m(\mathbf{a}), & if \ s'_{mm}(\mathbf{a}) = 0; \\ \beta_m \omega_m / a_m + 1/\psi_m(\mathbf{a}), & otherwise. \end{cases} \tag{5.12}$$

We can compute the Pareto boundary of the linearly coupled games by solving linear equations:

$$\frac{\partial \sum\limits_{k=1}^{N} \omega_k \log[u_k(\mathbf{a})]}{\partial a_m} = 0 \Rightarrow \begin{cases} \beta_m \omega_m \psi_m(\mathbf{a}) + (1-\omega_m) a_m = 0, & if \ s'_{mm}(\mathbf{a}) = 0; \\ \beta_m \omega_m \psi_m(\mathbf{a}) + a_m = 0, & otherwise. \end{cases} \tag{5.13}$$

5.3.3 Two Types of Linearly Coupled Games

Theorem 5.1 reveals the structural properties of the utility functions $\{u_n\}_{n=1}^N$ when assumption 5.1-5.3 are satisfied. Based on Theorem 5.1, the following theorem further refines these properties of $\{u_n\}_{n=1}^N$ when the additional assumption 5.4 is imposed.

Theorem 5.2 *Under assumptions 5.1-5.4, for any polynomial $b_n^i(\mathbf{a})$ in the factorization $s_n(\mathbf{a}) = \prod_{i=1}^{M_n} b_n^i(\mathbf{a})$, $\forall n \in \mathcal{N}$, if $|\mathrm{V}(b_n^i(\mathbf{a}))| \geq 2$ or $\mathrm{V}(b_n^i(\mathbf{a})) = \{a_n\}$,*

$b_n^i(\mathbf{a})$ *is an irreducible factor of* $s_m(\mathbf{a})$, $\forall m \in \mathcal{N}$; *if* $\mathrm{V}(b_n^i(\mathbf{a})) = \{a_m\}, m \neq n$, $b_n^i(\mathbf{a})$ *is an irreducible factor of* $s_j(\mathbf{a})$, $\forall j \in \mathcal{N}/\{m\}$.

Proof: By assumption 5.2, $s'_{nm}(\mathbf{a}) < 0, \forall m \neq n$, we have $|\mathrm{V}(s_n(\mathbf{a}))| \geq N - 1, \forall n \in \mathcal{N}$. By Theorem 5.1, the irreducible factors of $s_n(\mathbf{a})$ have no common variables and they are affine functions. Suppose $|\mathrm{V}(b_n^i(\mathbf{a}))| \geq 2$ and $\{a_m, a_l\} \in \mathrm{V}(b_n^i(\mathbf{a})$. By assumption 5.4, we know that $\frac{s'_{nm}(\mathbf{a})}{s_n(\mathbf{a})} = \frac{s'_{km}(\mathbf{a})}{s_k(\mathbf{a})} = \frac{b'^i_{nm}(\mathbf{a})}{b_n^i(\mathbf{a})}, \forall n, k \in \mathcal{N} \setminus \{m\}$. Therefore, it follows

$$s_k(\mathbf{a}) = \frac{s'_{km}(\mathbf{a}) b_n^i(\mathbf{a})}{b'^i_{nm}(\mathbf{a})}. \tag{5.14}$$

Since $b'^i_{nm}(\mathbf{a})$ is a constant, we can see that $b_n^i(\mathbf{a})$ is an irreducible factor of $s_k(\mathbf{a})$, $\forall k \in \mathcal{N} \setminus \{m\}$. By symmetry, we can conclude that $b_n^i(\mathbf{a})$ must also be an irreducible factor of $s_k(\mathbf{a})$, $\forall k \in \mathcal{N} \setminus \{l\}$. Therefore, $b_n^i(\mathbf{a})$ is an irreducible factor of $s_k(\mathbf{a})$, $\forall k \in \mathcal{N}$. Similarly, we can prove the remaining parts of Theorem 5.2. ■

For the linearly coupled games satisfying assumptions 5.1-5.4, suppose we factorize all users' state functions. Theorem 5.2 indicates that any factor with at least two variables must be a common factor of all the users' state functions, and any factor with a single variable a_k must be a common factor of state functions for users excluding k. In reality, it corresponds to the communication scenarios in which the state, i.e. the multi-user coupling, is impacted by a set of users that result in a similar signal to all the users.

We define two basic types of linearly coupled games satisfying the assumptions 5.1-5.4. In Type I games, user k's action linearly decreases all the users' states but itself. Hence, the utility functions take the form

$$u_n(\mathbf{a}) = a_n^{\beta_n} \cdot \prod_{m \neq n} (\mu_m - \tau_m a_m). \tag{5.15}$$

In Type II games, all the users share the same non-factorizable state function and their utility functions are given by

$$u_n(\mathbf{a}) = a_n^{\beta_n} \cdot (\mu - \sum_{m=1}^{N} \tau_m a_m). \tag{5.16}$$

5.3.4 Illustrative Examples

There are a number of multi-user communication scenarios that can be modeled as linearly coupled games. For example, in the random access scenario, the action of a node is to select its transmission probability and a node n will independently attempt transmission of a packet with transmit probability p_n. The action set available to node n is $\mathcal{A}_n = [0, 1]$ for all $n \in \mathcal{N}$. In this case, the utility function is defined as

$$u_n(\mathbf{p}) = p_n \cdot \prod_{m \neq n} (1 - p_m). \tag{5.17}$$

As an additional example, in flow control [ZD92], N Poisson streams of packets are serviced by a single exponential server with departure rate μ and each class can adjust its throughput r_n. The utility function is defined as the weighted ratio of the throughput over the average experienced delay:

$$u_n(\mathbf{r}) = r_n^{\beta_n} \cdot (\mu - \sum_{m=1}^{N} r_m), \tag{5.18}$$

in which $\beta_n > 0$ is interpreted as the weighting factor. Specifically, we can see that the state determination functions are $s_n(\mathbf{p}) = \prod_{m \in \mathcal{N} \setminus \{n\}} (1 - p_m)$ in (5.17) and $s_n(\mathbf{r}) = \mu - \sum_{m=1}^{N} r_m$ in (5.18). It is straightforward to verify that these functions satisfy assumptions 5.1-5.4 for both (5.17) and (5.18).

As special examples, the random access problem in (5.17) belongs to Type I games and the rate control problem in (5.18) belongs to Type II games. In fact, all the games that have the properties 5.1-5.4 can be viewed as compositions

of these two basic types of games. Therefore, investigating the two basic types provides us the fundamental understanding of the linearly coupled multi-user interaction. We are interested in comparing the achievable performance attained by different game-theoretic solution concepts. On one hand, it is well-known that NE is generally inefficient in games [Dub86], but it may not require explicit message exchanges, while Pareto-optimality can usually be achieved only by exchanging implicit or explicit coordination messages among the participating users. On the other hand, in previous chapters, we have applied the CE-based solution in different communication scenarios to improve the system performance in non-cooperative settings. The remaining parts of the dissertation aim to compare the solutions of NE, Pareto boundary, and CE in terms of the payoffs and informational requirements in different types of linearly coupled games. Specifically, Section 5.4 will focus on Type II games and Chapter 6 will use random access to illustrate the properties of various solutions in Type I games.

5.4 Solutions for Type II Linearly Coupled Games

5.4.1 Nash Equilibrium and Pareto Boundary

For Type II games with utility functions given in (5.16), we have

$$\frac{s'_{nn}(\mathbf{a})}{s_n(\mathbf{a})} = \frac{-\tau_n}{\mu - \sum_{m=1}^{N} \tau_m a_m}. \tag{5.19}$$

Therefore, Equation (5.6) can be reduced to

$$(1+\beta_n)\tau_n a_n + \beta_n \sum_{m \neq n} \tau_m a_m = \beta_n \mu, \forall n \in \mathcal{N}. \tag{5.20}$$

The solution of the linear equations gives the NE, and its closed form has been addressed in [DM92] for $\tau_n = 1, \forall n \in \mathcal{N}$. For the general case, it is easy to verify

that the NE is given by

$$a_n^{NE} = \frac{\beta_n \mu}{\tau_n (1 + \sum_{m=1}^{N} \beta_m)}, \forall n \in \mathcal{N}. \tag{5.21}$$

Similarly, to compute the Pareto boundary of Type II games, Equation (5.12) can be reduced to

$$(1 + \omega_n \beta_n) \tau_n a_n + \omega_n \beta_n \sum_{m \neq n} \tau_m a_m = \omega_n \beta_n \mu, \forall n \in \mathcal{N}. \tag{5.22}$$

The solution is given by

$$a_n^{PB} = \frac{\omega_n \beta_n \mu}{\tau_n (1 + \sum_{m=1}^{N} \omega_m \beta_m)}, \forall n \in \mathcal{N}. \tag{5.23}$$

From Section 5.3.2, we know that the region $\log \mathcal{U}$ is convex. Therefore, we can compare the efficiency of $\mathbf{a}^{NE}$ and $\mathbf{a}^{PB}$ using the system-utility metric $\sum_{n=1}^{N} \omega_n \log[u_n(\mathbf{a})]$. Specifically, we have

$$\sum_{n=1}^{N} \omega_n \log \frac{u_n(\mathbf{a}^{NE})}{u_n(\mathbf{a}^{PB})} = \sum_{n=1}^{N} \omega_n \beta_n \log \frac{1 + \sum_{j=1}^{N} \omega_j \beta_j}{\omega_n (1 + \sum_{j=1}^{N} \beta_j)} + \log \frac{1 + \sum_{j=1}^{N} \omega_j \beta_j}{1 + \sum_{j=1}^{N} \beta_j}. \tag{5.24}$$

Denote $w_0 = 1$, $x_0 = \frac{1 + \sum_{j=1}^{N} \omega_j \beta_j}{1 + \sum_{j=1}^{N} \beta_j}$, $w_n = \omega_n \beta_n$, and $x_n = \frac{1 + \sum_{j=1}^{N} \omega_j \beta_j}{\omega_n (1 + \sum_{j=1}^{N} \beta_j)}, \forall n \in \mathcal{N}$. Therefore,

$$\sum_{n=1}^{N} \omega_n \log \frac{u_n(\mathbf{a}^{NE})}{u_n(\mathbf{a}^{PB})} = \sum_{n=0}^{N} w_n \log x_n = \sum_{n=0}^{N} w_n \cdot \log \Big(\prod_{n=0}^{N} x_n^{w_n} \Big)^{1 / \sum_{n=0}^{N} w_n}. \tag{5.25}$$

Using the inequalities among the arithmetic, geometric and harmonic means [Spi68], we have

$$\frac{(1 + \sum\limits_{n=1}^{N} \omega_n \beta_n)^2}{(1 + \sum\limits_{n=1}^{N} \omega_n^2 \beta_n)(1 + \sum\limits_{n=1}^{N} \beta_n)} = \frac{\sum\limits_{n=0}^{N} w_n}{\sum\limits_{n=0}^{N} \frac{w_n}{x_n}} \leq \Big(\prod_{n=0}^{N} x_n^{w_n} \Big)^{\frac{1}{\sum_{n=0}^{N} w_n}} \leq \frac{\sum\limits_{n=0}^{N} x_n w_n}{\sum\limits_{n=0}^{N} w_n} = 1. \tag{5.26}$$

Both inequalities hold with equality if and only if $x_0 = x_1 = \ldots = x_N$, i.e. $\omega_1 = \ldots = \omega_N = 1$. However, since we require $\sum_{n=1}^{N} \omega_n = 1$, (5.26) holds as strict inequalities, which leads to

$$(1+\sum_{n=1}^{N}\omega_n\beta_n)\cdot\log\frac{(1+\sum\limits_{n=1}^{N}\omega_n\beta_n)^2}{(1+\sum\limits_{n=1}^{N}\omega_n^2\beta_n)(1+\sum\limits_{n=1}^{N}\beta_n)} < \sum_{n=1}^{N}\omega_n\log\frac{u_n(\mathbf{a}^{NE})}{u_n(\mathbf{a}^{PB})} < 0. \quad (5.27)$$

Based on Equation (5.27), we can make two important observations. First, due to the lack of coordination, the NE in Type II games is always strictly Pareto inefficient. Second, the efficiency loss in Type II games are lower bounded, which means that every user receives positive payoff at NE. Noticing that the performance gap between $u_n(\mathbf{a}^{NE})$ and $u_n(\mathbf{a}^{PB})$ is non-zero, we will investigate how the non-cooperative CE solution can improve the system performance for Type II games.

5.4.2 Linear Beliefs

According to the definition of CE in (4.1), all players' expectations based on their beliefs are realized and each agent behaves optimally according to its expectation. In other words, agents' beliefs are consistent with the outcome of the play and they use "conjectured best responses" in their individual optimization program. The key challenges are how to configure the belief functions such that cooperation can be sustained in such a non-cooperative setting and how to design the evolution rules such that the communication system can dynamically converge to a CE having satisfactory performance.

To define the belief functions, we need to express agent n's expected state $\tilde{s}_n$ as a function of its own action a_n. The simplest approach is to design linear

belief models for each user, i.e. player n's belief function takes the form

$$\tilde{s}_n(a_n) = \bar{s}_n - \lambda_n(a_n - \bar{a}_n), \tag{5.28}$$

for $n \in \mathcal{N}$. The values of $\bar{s}_n$ and $\bar{a}_n$ are specific states and actions, called *reference points* and λ_n is a positive scalar. In other words, user n assumes that other players will observe its deviation from its reference point $\bar{a}_n$ and the aggregate state deviates from the reference point $\bar{s}_n$ by a quantity proportional to the deviation of $a_n - \bar{a}_n$. How to configure $\bar{s}_n, \bar{a}_n$, and λ_n will be addressed in the rest of this chapter. We focus on the linear belief represented in (5.28), because this simple belief form is sufficient to drive the resulting non-cooperative equilibrium to the Pareto boundary.

The goal of user n is to maximize its expected utility $a_n^{\beta_n} \cdot \tilde{s}_n(a_n)$ taking into account the conjectures that it has made about the other users. Therefore, the optimization a user needs to solve becomes:

$$\max_{a_n \in \mathcal{A}_n} a_n^{\beta_n} \cdot \Big[\bar{s}_n - \lambda_n(a_n - \bar{a}_n)\Big]. \tag{5.29}$$

For $\lambda_k > 0$, user n believes that increasing a_n will further reduce its conjectured state $\bar{s}_n$. The optimal solution of (5.29) is given by

$$a_n^* = \frac{\beta_n(\bar{s}_n + \lambda_n \bar{a}_n)}{\lambda_n(1 + \beta_n)}. \tag{5.30}$$

In the following, we first show that forming simple linear beliefs in (5.28) can cause all the operating points in the achievable utility region to be CE.

Theorem 5.3 *For Type II games, all the positive operating points in the utility region $\mathcal{U}$ are essentially CE.*

Proof: For each positive operating point $(u_1^*, \ldots, u_N^*)$ (i.e. $u_n^* > 0, \forall n \in \mathcal{N}$) in the utility region $\mathcal{U}$, there exists at least one joint action profile $(a_1^*, \ldots, a_N^*) \in \mathcal{A}$

such that $u_n^* = u_n(\mathbf{a}^*)$, $\forall n \in \mathcal{N}$. We consider setting the parameters in the belief functions $\{\tilde{s}_n(a_n)\}_{n=1}^N$ to be:

$$\lambda_n^* = \beta_n \cdot \frac{\mu - \sum_{m=1}^N \tau_m a_m^*}{a_n^*}, \forall n \in \mathcal{N}. \tag{5.31}$$

It is easy to check that, if the reference points are $\bar{s}_n = \mu - \sum_{m=1}^N \tau_m a_m^*, \bar{a}_n = a_n^*$, we have $\tilde{s}_n(a_n^*) = s_n(a_1^*, \ldots, a_N^*)$ and $a_n^* = \arg\max_{a_n \in \mathcal{A}_n} u_n(\tilde{s}_n(a_n), a_n)$. Therefore, this belief function configuration and the joint action $\mathbf{a}^* = (a_1^*, \ldots, a_N^*)$ constitute the CE that results in the utility $(u_1^*, \ldots, u_N^*)$. ■

Theorem 5.3 establishes the existence of CE, i.e. for a particular $\mathbf{a}^* \in \mathcal{A}$, how to choose the parameters $\{\bar{s}_n, \bar{a}_n, \lambda_n\}_{n=1}^N$ such that $\mathbf{a}^*$ is a CE. However, it neither tells us how these CE can be achieved and sustained in the dynamic setting nor clarifies how different belief configurations can lead to various CE.

We consider the dynamic scenarios in which users revise their reference points based on their past local observations over time. Let $s_n^t, a_n^t, \tilde{s}_n^t, \bar{s}_n^t, \bar{a}_n^t$ be user n's state, action, belief function, and reference points at stage t, in which $s_n^t = \mu - \sum_{m=1}^N \tau_m a_m^t$. We propose a simple rule for individual users to update their reference points. At stage t, user n sets its $\bar{s}_n^t$ and $\bar{a}_n^t$ to be s_n^{t-1} and a_n^{t-1}. In other words, user n's conjectured utility function at stage t is

$$u_n^t(\tilde{s}_n^t(a_n), a_n) = a_n^{\beta_n} \cdot \Big[\mu - \sum_{m=1}^N \tau_m a_m^{t-1} - \lambda_n(a_n - a_n^{t-1})\Big]. \tag{5.32}$$

Since we have defined the users' utility function at stage t, upon specifying the rule of how user n updates its action a_n^t based on its utility function $u_n^t(\tilde{s}_n^t(a_n), a_n)$, the trajectory of the entire dynamic process is determined. The remainder of this chapter will investigate the dynamic properties of the best response and Jacobi update mechanisms and the performance trade-off among the competing users at the resulting steady-state CE. In particular, for fixed $\{\lambda_n\}_{n=1}^N$, Section 5.4.3 derives necessary and sufficient conditions for the convergence of the best

response and the Jacobi update dynamics. Section 5.4.4 quantitatively describes the limiting CE for given $\{\lambda_n\}_{n=1}^N$ and investigates how the parameters $\{\lambda_n\}_{n=1}^N$ should be properly chosen such that Pareto efficiency can be achieved.

5.4.3 Dynamic Algorithms

5.4.3.1 Best Response

In the best response algorithm, each user updates its action using the best response that maximizes its conjectured utility function in (5.32). Therefore, at stage t, user n chooses its action according to

$$a_n^t = B_n(\mathbf{a}^{t-1}) := \frac{\beta_n(\mu - \sum_{m\in\mathcal{N}\setminus\{n\}} \tau_m a_m^{t-1})}{\lambda_n(1+\beta_n)} + \frac{\beta_n(\lambda_n - \tau_n)a_n^{t-1}}{\lambda_n(1+\beta_n)}. \tag{5.33}$$

We are interested in characterizing the convergence of the update mechanism defined by (5.33) when using various λ_n to initialize the belief function $\tilde{s}_n$.

To analyze the convergence of the best response dynamics, we consider the Jacobian matrix of the self-mapping function in (5.33). Let J_{ik} denote the element at row i and column k of the Jacobian matrix $\mathbf{J}$. The elements of the Jacobian matrix $\mathbf{J}^{BR}$ of (5.33) are defined as:

$$J_{ik}^{BR} = \frac{\partial a_i^t}{\partial a_k^{t-1}} = \begin{cases} \frac{\beta_k(\lambda_k-\tau_k)}{\lambda_k(1+\beta_k)}, & \text{if } i = k, \\ -\frac{\beta_i\tau_k}{\lambda_i(1+\beta_i)}, & \text{if } i \neq k. \end{cases} \tag{5.34}$$

For Type II games, the following theorem gives a necessary and sufficient condition under which the best response dynamics defined in (5.33) converges.

Theorem 5.4 *For Type II games, a necessary and sufficient condition for the best response dynamics to converge is*

$$\sum_{n=1}^{N} \frac{\tau_n\beta_n}{\lambda_n(1+2\beta_n)} < 1. \tag{5.35}$$

Proof: The best response dynamics converges if and only if the eigenvalues $\{\xi_n^{BR}\}_{n=1}^N$ of the Jacobian matrix $\mathbf{J}^{BR}$ in (5.34) are all inside the unit circle of the complex plane [GD03], i.e. $|\xi_n^{BR}| < 1, \forall n \in \mathcal{N}$. To determine the eigenvalues of $\mathbf{J}^{BR}$, we have

$$\begin{aligned}
\det(\xi I - \mathbf{J}^{BR}) &= \begin{vmatrix} \xi - \frac{\beta_1(\lambda_1-\tau_1)}{\lambda_1(1+\beta_1)} & \frac{\beta_1\tau_2}{\lambda_1(1+\beta_1)} & \cdots & \frac{\beta_1\tau_N}{\lambda_1(1+\beta_1)} \\ \frac{\beta_2\tau_1}{\lambda_2(1+\beta_2)} & \xi - \frac{\beta_2(\lambda_2-\tau_2)}{\lambda_2(1+\beta_2)} & \cdots & \frac{\beta_2\tau_N}{\lambda_2(1+\beta_2)} \\ \vdots & \vdots & \ddots & \vdots \\ \frac{\beta_N\tau_1}{\lambda_N(1+\beta_N)} & \frac{\beta_N\tau_2}{\lambda_N(1+\beta_N)} & \cdots & \xi - \frac{\beta_N(\lambda_N-\tau_N)}{\lambda_N(1+\beta_N)} \end{vmatrix} \\
&= \begin{vmatrix} \xi - \frac{\beta_1(\lambda_1-\tau_1)}{\lambda_1(1+\beta_1)} & \frac{\tau_2}{\tau_1}\big(\frac{\beta_1}{1+\beta_1} - \xi\big) & \cdots & \frac{\tau_N}{\tau_1}\big(\frac{\beta_1}{1+\beta_1} - \xi\big) \\ \frac{\beta_2\tau_1}{\lambda_2(1+\beta_2)} & \xi - \frac{\beta_2}{1+\beta_2} & \cdots & 0 \\ \vdots & \vdots & \ddots & \vdots \\ \frac{\beta_N\tau_1}{\lambda_N(1+\beta_N)} & 0 & \cdots & \xi - \frac{\beta_N}{1+\beta_N} \end{vmatrix} \\
&= \begin{vmatrix} \big(\xi - \frac{\beta_1}{1+\beta_1}\big) \cdot \big[1 - \sum_{n=1}^N \frac{\tau_n}{\lambda_n(1-\frac{1+\beta_n}{\beta_n}\xi)}\big] & 0 & \cdots & 0 \\ \frac{\beta_2\tau_1}{\lambda_2(1+\beta_2)} & \xi - \frac{\beta_2}{1+\beta_2} & \cdots & 0 \\ \vdots & \vdots & \ddots & \vdots \\ \frac{\beta_N\tau_1}{\lambda_N(1+\beta_N)} & 0 & \cdots & \xi - \frac{\beta_N}{1+\beta_N} \end{vmatrix}.
\end{aligned}$$

Therefore, we can see that, the eigenvalues of $\mathbf{J}^{BR}$ are the roots of

$$\Big[\sum_{n=1}^N \frac{\tau_n}{\lambda_n(1 - \frac{1+\beta_n}{\beta_n}\xi)} - 1\Big] \cdot \prod_{n=1}^N \big(\xi - \frac{\beta_n}{1+\beta_n}\big) = 0. \tag{5.36}$$

Denote $q(\xi) = \sum_{n=1}^N \frac{\tau_n}{\lambda_n(1-\frac{1+\beta_n}{\beta_n}\xi)}$. First, we assume that $\beta_i \neq \beta_j, \forall i, j$. Without loss of generality, consider $\beta_1 < \beta_2 < \cdots < \beta_N$. In this case, the eigenvalues of $\mathbf{J}^{BR}$ are the roots of $q(\xi) = 1$. Note that $q(\xi)$ is a continuous function and it strictly increases in $(-\infty, \frac{\beta_1}{1+\beta_1})$, $(\frac{\beta_1}{1+\beta_1}, \frac{\beta_2}{1+\beta_2})$, $\cdots$, $(\frac{\beta_{N-1}}{1+\beta_{N-1}}, \frac{\beta_N}{1+\beta_N})$, and $(\frac{\beta_N}{1+\beta_N}, +\infty)$. We also have $\lim_{\xi\to(\frac{\beta_n}{1+\beta_n})^-} q(\xi) = +\infty$, $\lim_{\xi\to(\frac{\beta_n}{1+\beta_n})^+} q(\xi) = -\infty, n = 1, 2, \cdots, N$, and $\lim_{\xi\to-\infty} q(\xi) = \lim_{\xi\to+\infty} q(\xi) = 0$. Therefore, the

roots of $q(\xi) = 1$ lie in $(-\infty, \frac{\beta_1}{1+\beta_1})$, $(\frac{\beta_1}{1+\beta_1}, \frac{\beta_2}{1+\beta_2})$, $\cdots$, $(\frac{\beta_{N-1}}{1+\beta_{N-1}}, \frac{\beta_N}{1+\beta_N})$. Since $q(\xi)$ strictly increases in $(-\infty, \frac{\beta_1}{1+\beta_1})$, we have $|\xi_n^{BR}| < 1, \forall n \in \mathcal{N}$ if and only if $q(-1) = \sum_{n=1}^{N} \frac{\tau_n \beta_n}{\lambda_n(1+2\beta_n)} < 1$.

Second, we consider the cases in which there exists $\beta_i = \beta_j$ for certain i, j. Suppose that $\{\beta_n\}_{n=1}^N$ take K discrete values $\kappa_1, \cdots, \kappa_K$ and the number of $\{\beta_n\}_{n=1}^N$ that equal to κ_k is n_k. In this case, Equation (5.36) is reduced to

$$\Big[\sum_{n=1}^{N} \frac{\tau_n}{\lambda_n(1 - \frac{1+\beta_n}{\beta_n}\xi)} - 1\Big] \cdot \prod_{k=1}^{K} \big(\xi - \frac{\kappa_k}{1+\kappa_k}\big)^{n_k} = 0. \tag{5.37}$$

Hence, equation $q(\xi) = 1$ has $N + K - \sum_{k=1}^{K} n_k$ roots in total, and $\xi = \frac{\kappa_k}{1+\kappa_k}$ is a root of multiplicity $n_k - 1$ for Equation (5.37), $\forall k$. All these roots are the eigenvalues of matrix $\mathbf{J}^{BR}$. Similarly, the roots of $q(\xi) = 1$ lie in $(-\infty, \frac{\kappa_1}{1+\kappa_1})$, $(\frac{\kappa_1}{1+\kappa_1}, \frac{\kappa_2}{1+\kappa_2})$, $\cdots$, $(\frac{\kappa_{K-1}}{1+\kappa_{K-1}}, \frac{\kappa_K}{1+\kappa_K})$. A necessary and sufficient condition under which $|\xi_n^{BR}| < 1, \forall n \in \mathcal{N}$ is still $q(-1) < 1$, i.e. $\sum_{n=1}^{N} \frac{\tau_n \beta_n}{\lambda_n(1+2\beta_n)} < 1$. ■

Remark 5.1 *Theorem 5.4 indicates that, if the condition in (5.35) is satisfied, the best response dynamics converges linearly to the CE. The convergence rate is mainly determined by* $\max_{n\in\mathcal{N}} |\xi_n^{BR}|$. *Suppose* $\beta_1 < \beta_2 < \cdots < \beta_N$ *and* $\xi_1^{BR} < \xi_2^{BR} < \cdots < \xi_N^{BR}$. *From the proof of Theorem 5.4, we can see that, under condition (5.35),* $-1 < \xi_1^{BR} < \frac{\beta_1}{1+\beta_1} < \xi_2^{BR} < \cdots < \xi_N^{BR}$, *and* $\frac{\beta_{N-1}}{1+\beta_{N-1}} < \xi_N^{BR} < \frac{\beta_N}{1+\beta_N}$. *Therefore, the rate of convergence can be approximated by* $\max\{|\xi_1^{BR}|, |\xi_N^{BR}|\}$. *Note that choosing larger* $\{\lambda_n\}_{n=1}^N$ *increases* ξ_1^{BR}. *Hence, if* $-1 < \xi_1^{BR} < -|\xi_N^{BR}|$, *increasing* $\{\lambda_n\}_{n=1}^N$, *i.e. having more self-constraint users, accelerate the convergence rate of the best response mechanism. On the other hand, since* $\xi_N^{BR} > \frac{\beta_{N-1}}{1+\beta_{N-1}}$, *the convergence rate is lower bounded by* $\frac{\beta_{N-1}}{1+\beta_{N-1}}$. *Therefore, if more than two users associate large weighting factors* β *with their individual actions in the utility functions, we have* $\frac{\beta_{N-1}}{1+\beta_{N-1}} \to 1$ *and the best response dynamics converges slowly.*

Remark 5.2 *Theorem 5.4 generalizes the necessary and sufficient condition derived in [DM92], where users are assumed to be symmetric, i.e.* $\tau_n = 1, \forall n$ *and they adopt the Nash strategy by choosing* $\lambda_n = \tau_n, \forall n$*. Due to lack of symmetry, the derivation in [DM92] is not readily applicable to analyze the convergence of the best response dynamics. The proof of Theorem 5.4 instead directly characterizes the eigenvalues of the Jacobian matrix, and hence, provides a more general convergence analysis of the dynamic algorithms that allow users to update their actions based on their independent linear conjectures.*

Remark 5.3 *In Type II games, a locally stable CE is also globally convergent, which is purely due to the property of its utility functions specified in (5.16). From (5.34), we can see that all the elements in* $\boldsymbol{J}^{BR}$ *are independent of the joint play* $\boldsymbol{a}^{t-1}$*. This is in contrast with Type I games that will be considered in Chapter 6, where local stability of a CE may not imply its global convergence and the best response dynamics may only converge if the operating point is close enough to the steady-state equilibrium.*

5.4.3.2 Jacobi Update

We consider another alternative strategy update mechanism called Jacobi update [LA02]. In Jacobi update, every user adjusts its action gradually towards the best response strategy. At stage t, user n chooses its action according to

$$a_n^t = J_n(\mathbf{a}^{t-1}) := a_n^{t-1} + \epsilon\big[B_n(\mathbf{a}^{t-1}) - a_n^{t-1}\big], \tag{5.38}$$

in which the stepsize $\epsilon > 0$ and $B_n(\mathbf{a}^{t-1})$ is defined in (5.33). The following theorem establishes the convergence property of the Jacobi update dynamics.

Theorem 5.5 *In Type II games, for given* $\{\tau_n, \beta_n, \lambda_n\}_{n=1}^N$*, the Jacobi update dynamics converges if the stepsize* ϵ *is sufficiently small.*

Proof: The Jacobian matrix $\mathbf{J}^{JU}$ of the self-mapping function (5.38) satisfies $\mathbf{J}^{JU} = (1-\epsilon)I + \epsilon\mathbf{J}^{BR}$. Therefore, its eigenvalues $\{\xi_n^{JU}\}_{n=1}^N$ are given by $\xi_n^{JU} = 1 - \epsilon + \epsilon\xi_n^{BR}$. From the proof of Theorem 5.4, we know that $\xi_n^{BR} < 1, \forall n \in \mathcal{N}$. Therefore, if $\epsilon < \frac{2}{1-\min_n \xi_n^{BR}}$, we have $\xi_n^{JU} \in (-1,1), \forall n \in \mathcal{N}$ and the Jacobi update dynamics converges. ■

Remark 5.4 *Theorem 5.5 indicates that, for any $\{\tau_n, \beta_n, \lambda_n\}_{n=1}^N > 0$, the Jacobi update mechanism globally converges to a CE as long as the stepsize is set to be a small enough positive number. In other words, the small stepsize in the Jacobi update can compensate for the instability of the best response dynamics even though the necessary and sufficient condition in (5.35) is not satisfied.*

5.4.4 Stability of the Pareto Boundary

In order to understand how to properly choose the parameters $\{\lambda_n\}_{n=1}^N$ such that it leads to efficient outcomes, we need to explicitly describe the steady-state CE in terms of the parameters $\{\lambda_n\}_{n=1}^N$ of the belief functions. Denote the joint action profile at CE as $(a_1^*, \ldots, a_N^*)$. From Equation (5.33), we know that

$$(\lambda_n + \beta_n\tau_n)a_n^* + \sum_{m\in\mathcal{N}\setminus\{n\}} \beta_n\tau_m a_m^* = \beta_n\mu, \forall n \in \mathcal{N}. \tag{5.39}$$

The solutions of the above linear equations are

$$a_n^{CE} = \frac{\beta_n\mu}{\lambda_n(1 + \sum_{m=1}^N \frac{\tau_m\beta_m}{\lambda_m})}, \forall n \in \mathcal{N}. \tag{5.40}$$

Based on the closed-form expression of the CE, the following theorem indicates the stability of the Pareto boundary in Type II games.

Theorem 5.6 *For Type II games, all the operating points on the Pareto boundary are globally convergent CE under the best response dynamics.*

Proof: Comparing Equations (5.23) and (5.40), we can see that, $(a_1^{CE}, \ldots, a_N^{CE}) = (a_1^{PB}, \ldots, a_N^{PB})$ if and only if $\lambda_n = \tau_n/\omega_n$. Substitute it into the LHS of (5.35):

$$\sum_{n=1}^{N} \frac{\tau_n \beta_n}{\lambda_n(1+2\beta_n)} = \sum_{n=1}^{N} \frac{\omega_n \beta_n}{1+2\beta_n} < \frac{\sum_{n=1}^{N} \omega_n}{2} = \frac{1}{2}. \tag{5.41}$$

Condition (5.35) is satisfied for all the Pareto-optimal operating points. In fact, we have $\min_n \xi_n^{BR} = 0$, which is because $q(0) = \sum_{n=1}^{N} \frac{\tau_n}{\lambda_n} = \sum_{n=1}^{N} \omega_n = 1$. Therefore, under the best response dynamics, the Pareto boundary is globally convergent. ■

In addition, we also note that Theorem 5.5 already indicates the stability of the Pareto boundary under Jacobi update as long as the parameters $\{\tau_n, \beta_n, \lambda_n\}_{n=1}^N$ are properly chosen.

Remark 5.5 *Since $\sum_{n=1}^{N} \omega_n = 1$, we can see from the previous proof that, the belief configurations $\{\lambda_n\}_{n=1}^N$ lead to Pareto-optimal operating points if and only if*

$$\sum_{n=1}^{N} \frac{\tau_n}{\lambda_n} = 1. \tag{5.42}$$

Therefore, we can see that, to achieve Pareto-optimality in these non-cooperative scenarios, users need to choose the belief parameters $\{\lambda_n\}_{n=1}^N$ to be greater than or equal to the parameters $\{\tau_n\}_{n=1}^N$ in the utility function $\{u_n\}_{n=1}^N$ and the summation of $\frac{\tau_n}{\lambda_n}$ should be equal to 1. Define user n's conservativeness as $\frac{\tau_n}{\lambda_n}$, which reflects the ratio between the immediate performance degradation $-\tau_n \Delta a_n$ in the actual utility function and the long-term effect $-\lambda_n \Delta a_n$ in the conjectured utility function if user n increases its action by Δa_n. The condition in Equation (5.42) indicates that, to achieve efficient outcomes, the non-collaborative users need to jointly maintain moderate conservativeness by considering the multi-user coupling and appropriately choosing $\{\lambda_n\}_{n=1}^N$. By "moderate", we mean that users are neither too aggressive, i.e. $\lambda_n \to \tau_n$ and $\sum_{n=1}^{N} \frac{\tau_n}{\lambda_n} \to N$, nor too conservative, i.e.

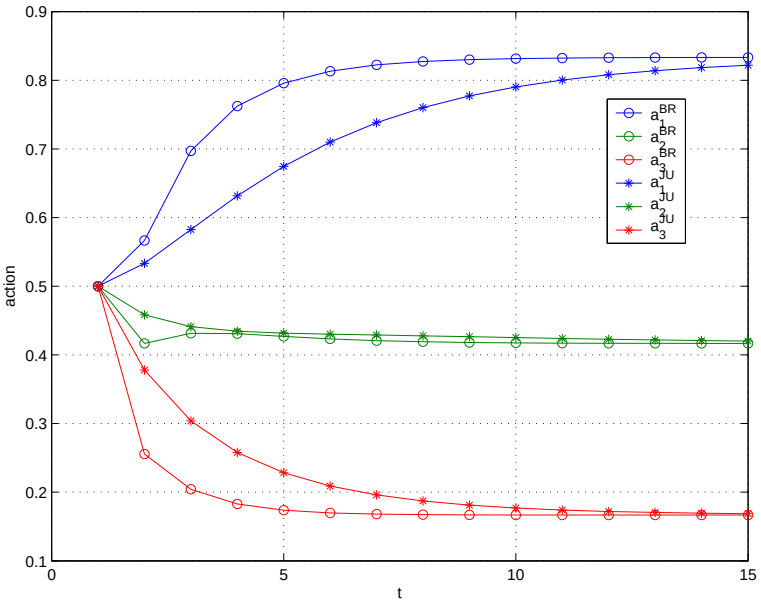

Figure 5.1: The trajectory of the best response and Jacobi update dynamics.

$\lambda_n \to +\infty$ *and* $\sum_{n=1}^{N} \frac{\tau_n}{\lambda_n} \to 0$. *If more than one user plays the Nash strategy and choose* $\lambda_n = \tau_n$, *Equation (5.42) does not hold and the resulting operating point is not Pareto-optimal. Therefore, myopic selfish behavior is detrimental.*

Similarly as in (5.24), we have

$$\sum_{n=1}^{N} \omega_n \log \frac{u_n(\mathbf{a}^{CE})}{u_n(\mathbf{a}^{PB})} = \sum_{n=1}^{N} \omega_n \beta_n \log \frac{\tau_n(1+\sum_{j=1}^{N} \omega_j \beta_j)}{\lambda_n \omega_n (1+\sum_{j=1}^{N} \frac{\tau_j \beta_j}{\lambda_j})} + \log \frac{1+\sum_{j=1}^{N} \omega_j \beta_j}{1+\sum_{j=1}^{N} \frac{\tau_j \beta_j}{\lambda_j}}. \quad (5.43)$$

Using Jensen's inequality, we can conclude that $\sum_{n=1}^{N} \omega_n \log \frac{u_n(\mathbf{a}^{CE})}{u_n(\mathbf{a}^{PB})} \leq 0$ *and* $\sum_{n=1}^{N} \omega_n \log \frac{u_n(\mathbf{a}^{CE})}{u_n(\mathbf{a}^{PB})} = 0$ *if and only if* $\omega_n = \frac{\tau_n}{\lambda_n}, \forall n$. *Therefore, if a CE is Pareto efficient, user* n*'s conservativeness* τ_n/λ_n *corresponds to the weight assigned to user* n *in the weighted proportional fairness defined in (5.8).*

As an illustrative example, we simulate a three-user system with parameters $\beta = [1.5\ 1\ 0.5]$, $\tau = [3\ 4\ 5], \mu = 10, \omega_n = \frac{1}{3}, \forall n$. In this case, the joint actions

Table 5.1: Actions and payoffs at NE and Pareto boundary.

	User 1	User 2	User 3
a_i^{NE}	1.25	0.625	0.25
u_i^{NE}	3.4939	1.5625	1.25
a_i^{PB}	0.833	0.417	0.167
u_i^{PB}	3.8036	2.0833	2.0412

and the corresponding utilities at NE and Pareto boundary are summarized in Table 5.1. The price of anarchy quantified according to (5.27) is -0.2877 and the lower bound in (5.27) is -0.5754. As discussed in Section III.C, both the upper bound and lower bound in (5.27) are not tight. Fig. 5.1 shows the trajectory of the action updates under both best response and Jacobi update dynamics, in which $a_n^0 = 0.5$, $\lambda_n = \frac{\tau_n}{\omega_n}, \forall n$, and $\epsilon = 0.5$. The best response update converges to the Pareto-optimal operating point in around 8 iterations and the Jacobi update experiences a smoother trajectory and the same equilibrium is attained after more iterations.

5.5 Concluding Remarks

We derive the structure of the utility functions in the multi-user communication scenarios where a user's action has proportionally the same impact over other users' utilities. We define two basic types of linearly coupled games and investigate the properties of Type II game. The performance gap between NE and Pareto boundary of the utility region is explicitly characterized. To improve the performance in non-cooperative cases, we investigate a CE approach which endows users with simple linear beliefs which enables them to select an equilibrium

outcome that is efficient without the need of explicit message exchanges. The properties of the CE under both the best response and Jacobi dynamic update mechanisms are characterized. We show that the entire Pareto boundary in linearly coupled games is globally convergent CE which can be achieved by both studied dynamic algorithms without the need of real-time message passing. A potential future direction is to see how to extend the CE approach to the nonlinearly coupled multi-user communication scenarios.

CHAPTER 6

Dynamic Conjectures in Random Access Networks

6.1 Introduction

As discussed in the previous chapter, the multi-user interaction in random access communication networks can be modeled as Type I linear coupled games. It is well-known that myopic selfish behavior is detrimental in random access communication networks [CGA05]. This chapter is concerned with developing distributed algorithms in random access communication networks to improve the throughput efficiency from the game-theoretic perspective. To avoid a network collapse and encourage cooperation, we adopt the conjecture-based model and enable the cognitive communication devices to build belief models about how their competitors' reactions vary in response to their own action changes. The belief functions of the wireless devices are inspired by the concept of reciprocity, which refers to interaction mechanisms in which the emergence of cooperative behavior is favored by the probability of future mutual interactions [Smi82, Now06]. Specifically, by deploying such a behavior model, devices will no longer adopt myopic, selfish, behaviors, but rather they will form beliefs about how their actions will influence the responses of their competitors and, based on these beliefs, they will try to maximize their own welfare. The steady state of such a play among

belief-forming devices can be characterized as a conjectural equilibria (CE). At the equilibrium, devices compensate for their lack of information by forming an internal representation of the opponents' behavior and preferences, and using these "conjectured responses" in their personal optimization program [FJQ04]. More importantly, we show that the reciprocity among these self-interested devices can be sustained.

In particular, the main contributions of this chapter are as follows. First, to cultivate cooperation in random access networks, we enable self-interested autonomous nodes to form independent linear beliefs about how their rival actions vary as a function of their own actions. We design two simple distributed algorithms in which all the nodes' beliefs and actions will be revised by observing the outcomes of past mutual interaction over time. Both conjecture-based algorithms require little information exchange among different nodes and the internal computation for each node is very simple. For both algorithms, we investigate the stability of different operating points and derive sufficient conditions that guarantee their global convergence, thereby establishing the connection between the dynamic belief update procedures and the steady-state CE. We prove that all the operating points in the throughput region are stable CE and reciprocity can be eventually sustained via the proposed evolution. We also provide an engineering interpretation of the proposed design to clarify the similarities and differences between the proposed algorithms and existing protocols, e.g. the IEEE 802.11 DCF.

Second, we investigate the relationship between the parameter initialization of beliefs and Pareto-efficiency of the achieved CE. In the economic market context, it has been shown that adjustment processes based on conjectures and individual optimization may sometimes be driven to Pareto-optimality [JT06]. To the best of

our knowledge, this is the first attempt in investigating the Pareto efficiency of the conjecture-based approach in communication networks. Importantly, it is shown that, regardless of the number of nodes, there always exist certain belief configurations such that the proposed distributed algorithms can operate arbitrarily close to the Pareto boundary of the throughput region while approximately maintaining the weighted fairness across the entire network. Our investigation provides useful insights that help to define convergent dynamic adaptation schemes that are apt to drive distributed random access networks towards efficient, stable, and fair configurations.

The rest of this chapter is organized as follows. Section 6.2 presents the system model of random access networks, reviews the existing game theoretic solutions, and introduces the concept of CE. Section 6.3 develops two simple distributed algorithms in which nodes form dynamic conjectures and optimize their actions based on their conjectures. The stability of different CE and the condition of global convergence are established. This section also shows that nodes' conjectures can be configured to stably operate at any point that is arbitrarily close to the Pareto frontier in throughput region. Section 6.4 addresses the topics of equilibrium selection in heterogeneous networks and presents possible extension to ad-hoc networks. Numerical simulations are provided in Section 6.5 to compare the proposed algorithms with the IEEE 802.11 DCF protocol and P-MAC protocol. We will compare the similarities and differences between Type I and II linear coupled games in Section 6.6. Concluding remarks are drawn in Section 6.7.

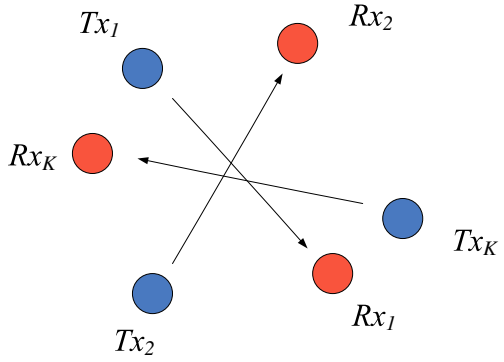

Figure 6.1: System model of a single cell.

6.2 System Description

In this section, we describe the system model of random access networks, define the investigated random access game, and discuss the existing game-theoretic solutions.

6.2.1 System Model of Random Access Networks

Following [LTH07, CCL08], we model the interaction among multiple autonomous wireless nodes in random access networks as a random access game.

As shown in Fig. 6.1, consider a set $\mathcal{K} = \{1, 2, \ldots, K\}$ of wireless nodes and each node represents a transmitter-receiver pair (link). We define Tx_k as the transmitter node of link k and Rx_k as the receiver node of link k. We first assume a single-cell wireless network, where every node can hear every other node in the network, and we will address the ad-hoc network scenario in Section 6.4.2. The system operates in discrete time with evenly spaced time slots [MM85, GS06]. We assume that all nodes always have a data packet to transmit at each time slot (i.e. we investigate the saturated traffic scenario[1]), and the network is noise

[1]This chapter focuses on the saturated system because we are interested in throughput

free and packet loss occurs only due to collision. The action of a node in this game is to select its transmission probability and a node k will independently attempt transmission of a packet with transmit probability p_k. The action set available to node k is $P_k = [0, 1]$ for all $k \in \mathcal{K}$[2]. Once the nodes decide their transmission probabilities based on which they transmit their packets, an action profile is determined. We denote the action profile in the random access game as a vector $\mathbf{p} = (p_1, \ldots, p_K)$ in $P = P_1 \times \cdots \times P_K$. Then the throughput of node k is given by[3]

$$u_k(\mathbf{p}) = p_k \prod_{i \in \mathcal{K} \setminus \{k\}} (1 - p_i). \tag{6.1}$$

To capture the performance tradeoff in the network, the throughput (payoff) region is defined as $\mathscr{T} = \{(u_1(\mathbf{p}), \ldots, u_K(\mathbf{p}))| \ \exists \ \mathbf{p} \in P\}$. The random access game can be formally defined by the tuple $\Gamma = \langle \mathcal{K}, (P_k), (u_k) \rangle$ [FT91]. Denote the transmission probability for all nodes but k by $\mathbf{p}_{-k} = (p_1, \ldots, p_{k-1}, p_{k+1}, \ldots, p_K)$. From (6.1), we can see that node k's throughput depends not only on its own transmission probability p_k, but also the other nodes' transmission probabilities $\mathbf{p}_{-k}$.

6.2.2 Existing Solutions

The throughput tradeoff and stability of random access networks have been extensively studied from the game theoretic perspective [JK02, LTH07, CCL08, CGA05]

[LCC07, MHC09, MMR09]. This subsection briefly reviews these existing results

maximization. The analysis can be extended to investigate the non-saturated networks where the incoming packets of the individual nodes' queues arrive at finite rates.

[2]The action set can be alternatively defined to be $P_k = [P_k^{\min}, P_k^{\max}]$ and the analysis in this chapter still applies.

[3]This throughput model assumes that time is slotted and all packets are of equal length. We use this model for theoretic analysis. The throughput of the scenarios in which packet lengths are not equal, e.g. the IEEE 802.11 DCF, will be addressed in Section 6.5.

and highlights the advantage and disadvantage of different approaches.

In the random access game, one of the most investigated problems is whether or not a Nash equilibrium exists. The NE of the investigated random access game has been addressed in the similar context of CSMA/CA networks where selfish nodes deliberately control their random deferment by altering their contention windows [CGA05]. Specifically, the transmission probability p_k in our model can be related to the contention window CW_k in the CSMA/CA protocol, where $p_k = \frac{2}{1+CW_k}$. It has been shown in [CGA05] that at the NE, at least one selfish node will set $CW_k = 1$ (i.e. always transmit). If more than one selfish node sets its contention window to 1, it will cause zero throughput for all the nodes in the system. This kind of result is known as *the tragedy of the commons*. We can see that, myopic selfish behavior is detrimental in random access scenarios and novel mechanisms are required to encourage cooperative behavior among the self-interested devices. In addition, the existence of and convergence to the NE in random access games have been studied also in other scenarios, where individual nodes have utility functions that are different from (6.1) [JK02, LTH07]. For example, the nodes in [JK02] adjust their transmission probabilities in an attempt to attain their desired throughputs. A local utility function is found for exponential backoff-based MAC protocols, based on which these protocols can be reverse-engineered in order to stabilize the network [LTH07]. However, due to the inadequate coordination or feedback mechanism in these protocols, Pareto optimality of the throughput performance cannot be guaranteed.

Several recent works also investigate how to design new distributed algorithms that provably converge to the Pareto boundary of the network throughput region [CGA05, LCC07, MHC09]. A distributed protocol is proposed in [CGA05] to guide multiple selfish nodes to a Pareto-optimal NE by including penalties

into their utility functions. However, the penalties must be carefully chosen. In [LCC07], the utility maximization is solved using the dual decomposition technique by enabling nodes to cooperatively exchange coordination information among each other. Furthermore, it is shown in [MHC09] that network utility maximization in random access networks can be achieved without real-time message passing among nodes. The key idea is to estimate the other nodes' transmission probabilities from local observations, which in fact increases the internal computational overhead of individual nodes.

As discussed before, the goal of this chapter is to design a simple distributed random access algorithm that requires limited information exchanges among nodes and also stabilizes the entire network. More importantly, this algorithm should be capable of achieving high efficiency and of differentiating among heterogeneous nodes carrying various traffic classes with different quality of service requirements. As we will show later, the game-theoretic concept of conjectural equilibrium defined in (4.1) provides such an elegant solution.

6.3 Distributed Algorithms

By the definition of CE, all nodes' expectations based on their beliefs are realized and each node behaves optimally according to its expectation. In other words, nodes' beliefs are consistent with the outcome of the play and they behave optimally with respect to their beliefs. The key challenges are how to configure the belief functions such that reciprocal behavior is encouraged and how to design the evolution rules such that the network can dynamically converge to a CE having satisfactory performance. In this section, to promote reciprocity, we design a prescribed rule for each node to configure its belief about its expected contention of the wireless network as a linear function of its own transmission

probability. It is shown that all the achievable operating points in the throughput region $\mathscr{T}$ are CE by deploying these belief functions. Furthermore, we propose two distributed algorithms for these nodes to dynamically achieve the CE. We provide the sufficient conditions that guarantee the stability and convergence of the CE. We also discuss the similarities and differences between the proposed algorithms and the existing well-known protocols. Finally, it is proven that any Pareto-inefficient operating point is a stable CE, i.e. we can approach arbitrarily close to the Pareto frontier of the throughput region $\mathscr{T}$.

6.3.1 Individual Behavior

As discussed before, both the state space and belief functions need to be defined in order to investigate the existence of CE. In the random access game, we define the state $s_k = \prod_{i \in \mathcal{K} \setminus \{k\}} (1 - p_i)$ to be the contention measure signal representing the probability that all nodes except node k do not transmit. This is because besides its own transmission probability, its throughput only depends on the probability that the remaining nodes do not transmit. We can see that state s_k indicates the aggregate effects of the other nodes' joint actions on node k's payoff. In practice, it is hard for wireless nodes to compute the exact transmission probabilities of their opponents [MHC09]. Therefore, we assume that s_k is the only information that node k has about the contention level of the entire network, because it is a metric that node k can easily compute based on local observations. Specifically, from user k's viewpoint, the probabilities of experiencing an idle time slot is $p_k^{idle} = (1 - p_k)s_k$. Let n_k^{idle} denote the number of time slots between any two consecutive idle time slots. n_k^{idle} has an independent identically distributed geometric distribution with probability p_k^{idle}. Therefore, we have $p_k^{idle} = 1/(1 + \bar{n}_k^{idle})$, where $\bar{n}_k^{idle}$ is the mean value of n_k^{idle} and can be locally estimated by node k

through its observation of the channel contention history. Since node k knows its own transmission probability p_k, it can estimate s_k using $s_k = 1/(1+\bar{n}_k^{idle})(1-p_k)$. Notice that the action available to node k is to choose the transmission probability $p_k \in P_k$. By the definition of belief function, we need to express the expected contention measure $\tilde{s}_k$ as a function of its own transmission probability p_k. The simplest approach is to deploy linear belief models, i.e. node k's belief function takes the form

$$\tilde{s}_k(p_k) = \bar{s}_k - a_k(p_k - \bar{p}_k), \tag{6.2}$$

for $k \in \mathcal{K}$. The values of $\bar{s}_k$ and $\bar{p}_k$ are specific states and actions, called *reference points* [JT06] and a_k is a positive scalar. In other words, node k assumes that other nodes will observe its deviation from its reference point $\bar{p}_k$ and the aggregate contention probability deviates from the referent point $\bar{s}_k$ by a quantity proportional to the deviation of $p_k - \bar{p}_k$. How to configure $\bar{s}_k, \bar{p}_k$, and a_k will be addressed in the rest of this chapter. The reasons why we focus on the linear beliefs represented in (6.2) are two-fold. First, the linear form represents the simplest model based on which a user can model the impact of its environment. As we will show later in Section 6.3.5, building and optimizing over such simple beliefs is sufficient for the network to achieve almost any operating point in the throughput region as a stable CE. Second, the conjecture functions deployed by the wireless users are based on the concept of reciprocity [Smi82, Now06], which was developed in evolutionary biology, and refers to interaction mechanisms in which the evolution of cooperative behavior is favored by the probability of future mutual interactions. Similarly, in single-hop wireless networks, the devices repeatedly interact when accessing the channel. If they disregard the fact that they have a high probability to interact in the future, they will act myopically, which will lead to a tragedy of commons (the zero-payoff Nash equilibrium). However, if they recognize that their probability of interacting in the future is

high, they will consider their impact on the network state, which is captured in the belief function by the positive a_k.

The goal of node k is to maximize its expected throughput $p_k \cdot \tilde{s}_k(p_k)$ taking into account the conjectures that it has made about the other nodes. Therefore, the optimization a node needs to solve becomes:

$$\max_{p_k \in P_k} p_k \Big[\bar{s}_k - a_k(p_k - \bar{p}_k) \Big], \tag{6.3}$$

where the second term is the expected contention measure $\tilde{s}_k(p_k)$ if node k transmits with probability p_k. The product of p_k and $\tilde{s}_k(p_k)$ gives the expected throughput for $p_k \in P_k$. For $a_k > 0$, node k believes that increasing its transmission probability will increase its experienced contention probability. The optimal solution of (6.3) is given by

$$p_k^* = \min \Big\{ \frac{\bar{s}_k}{2a_k} + \frac{\bar{p}_k}{2}, 1 \Big\}. \tag{6.4}$$

In the following, we first show that forming simple linear beliefs in (6.2) can cause all the operating points in the achievable throughput region to be CE.

Theorem 6.1 *All the operating points in the throughput region $\mathscr{T}$ are conjectural equilibria.*

Proof: For each operating point $(\tau_1, \ldots, \tau_K)$ in the throughput region $\mathscr{T}$, there exists at least a joint action profile $(p_1^*, \ldots, p_K^*) \in P$ such that $\tau_k = u_k(\mathbf{p}^*)$, $\forall k \in \mathcal{K}$. We consider setting the parameters in the belief functions to be:

$$a_k^* = \frac{\prod_{i \in \mathcal{K} \setminus \{k\}} (1 - p_i^*)}{p_k^*}. \tag{6.5}$$

It is easy to check that, if the reference points are $\bar{s}_k = \prod_{i \in \mathcal{K} \setminus \{k\}} (1 - p_i^*), \bar{p}_k = p_k^*$, we have $\tilde{s}_k(p_k^*) = s_k(p_1^*, \ldots, p_K^*)$ and $p_k^* = \arg\max_{p_k \in P_k} u_k(\tilde{s}_k(p_k), p_k)$. Therefore,

this configuration of the belief functions and the joint action $\mathbf{p}^* = (p_1^*, \ldots, p_K^*)$ constitute the CE that results in the throughput $(\tau_1, \ldots, \tau_K)$.[4] ■

Theorem 6.1 establishes the existence of CE, i.e. for a particular $\mathbf{p}^* \in P$, how to choose the parameters $\{\bar{s}_k, \bar{p}_k, a_k\}_{k=1}^K$ such that $\mathbf{p}^*$ is a CE. However, it neither tells us how these CE can be achieved and sustained in the dynamic setting nor clarifies how different belief configurations can result in various CE.

In distributed scenarios, nodes learn when they modify their conjectures based on their new observations. Specifically, we first allow the nodes to revise their reference points based on their past local observations. Let $s_k^t, p_k^t, \tilde{s}_k^t, \bar{s}_k^t, \bar{p}_k^t$ be user k's state, transmission probability, belief function, and reference points at stage t[5], in which $s_k^t = \prod_{i \in \mathcal{K} \setminus \{k\}} (1 - p_i^t)$. We propose a simple rule for individual nodes to update their reference points. At stage t, node k set its $\bar{s}_k^t$ and $\bar{p}_k^t$ to be s_k^{t-1} and p_k^{t-1}. In other words, node k's conjectured utility function at stage t is

$$u_k^t(\tilde{s}_k^t(p_k), p_k) = p_k \Big[\prod_{i \in \mathcal{K} \setminus \{k\}} (1 - p_i^{t-1}) - a_k (p_k - p_k^{t-1}) \Big]. \tag{6.6}$$

The remainder of this chapter will investigate the dynamic properties of the resulting operating points and the performance trade-off among multiple competing nodes. In particular, for fixed $\{a_k\}_{k=1}^K$, Sections 6.3.2 and 6.3.3 will embed the above individual optimization scheme in two different distributed learning processes in which all the nodes update their transmission probabilities over time. Section 6.3.5 further allows individual nodes adaptively update their parameters

[4] By the definition of CE, the configuration of the linear belief functions is a key part of CE. Since this chapter focuses on the linear belief functions defined in (6.2), we will simply state the joint action $\mathbf{p}^*$ is a CE hereafter for the ease of presentation.

[5] This chapter assumes the persistence mechanism for contention resolution except in Section 6.3.4. In the persistence mechanism, each wireless node maintains a persistence probability and accesses the channel with this probability [NKG00]. A stage contains multiple time slots. The nodes estimate the contention level in the network and update their persistence probabilities in the "stage-by-stage" manner. The superscript t in this chapter represents the numbering of the stages unless specified.

Table 6.1: **Algorithm** 6.1: A Distributed Best Response Algorithm for Random Access.

Initialize: $t = 0$, the transmission probability $p_k^0 \in [0, 1]$, and the parameter $a_k > 0$ in node k's belief function, $\forall k \in \mathcal{K}$.

procedure

Repeat

Locally at each node k, iterate through t:

Set $t \leftarrow t + 1$.

for all $k \in \mathcal{K}$ **do**

At stage t, $p_k^t \leftarrow \min\{p_k^{t-1}/2 + \prod_{i \in \mathcal{K}\setminus\{k\}}(1 - p_i^{t-1})/(2a_k), 1\}$.

end for

Node k decides if it will transmit data with a probability p_k^t (or equivalently, maintain a window size of $CW_k^t = 2/p_k^t - 1$) for all the time slots during stage t.

end procedure

$\{a_k\}_{k=1}^K$ such that desired efficiency can be attained. For given $\{a_k\}_{k=1}^K$, Section 6.4.1 will derive a quantitative description of the resulting CE $\mathbf{p}^*$.

6.3.2 A Best Response Algorithm

Our first algorithm adopts the simplest update mechanism in which each node adjusts its transmission probability using the best response that maximizes its conjectured utility function (6.6). Therefore, at stage t, node k chooses a transmission probability

$$p_k^t = \arg\max_{p_k \in P_k} u_k^t(\tilde{s}_k^t(p_k), p_k) = \min\left\{\frac{p_k^{t-1}}{2} + \frac{\prod_{i \in \mathcal{K}\setminus\{k\}}(1 - p_i^{t-1})}{2a_k}, 1\right\}. \tag{6.7}$$

The detailed description of the entire distributed best response procedure is

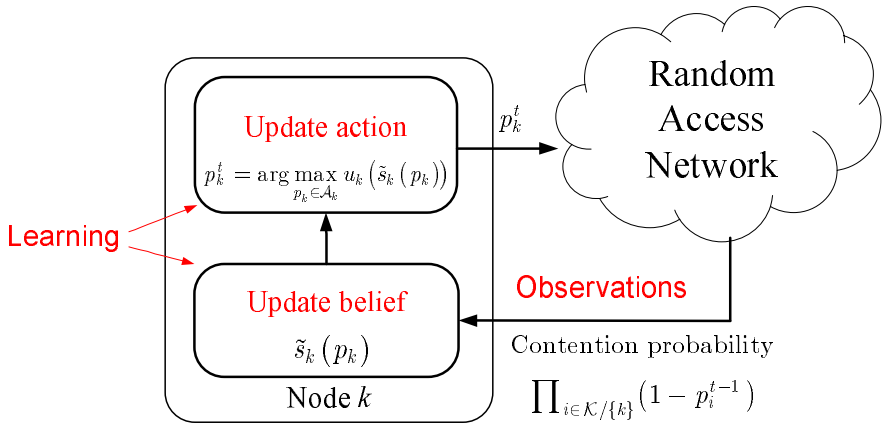

Figure 6.2: An illustration of the distributed algorithms.

summarized in Algorithm 6.1 and it is also pictorially illustrated in Fig. 6.2. Next, we are interested in deriving the limiting behavior, e.g. stability and convergence, of this algorithm. For ease of illustration, the sufficient conditions for stability and convergence throughout this chapter are expressed in terms of $\{p_k\}_{k=1}^K$ and $\{a_k\}_{k=1}^K$, respectively. The mapping from $\{p_k\}_{k=1}^K$ to $\{a_k\}_{k=1}^K$ is given in (6.5) and the mapping from $\{a_k\}_{k=1}^K$ to $\{p_k\}_{k=1}^K$ will be addressed in Section 6.4.1.

6.3.2.1 Local Stability

Although Theorem 6.1 indicates that all the points in $\mathscr{T}$ are CE, they may not be necessarily stable. An unstable equilibrium is not desirable, because any small perturbation might cause the sequence of iterates to move away from the initial equilibrium. The following theorem describes a subset in P in which all the points are stable CE.

Theorem 6.2 *For any* $\boldsymbol{p}^* = (p_1^*, \ldots, p_K^*) \in P$, *if*

$$\sum_{k=1}^{K} p_k^* < 1, \quad \text{or} \quad \sum_{i \in \mathcal{K} \setminus \{k\}} \frac{p_k^*}{1 - p_i^*} < 1, \ \forall k \in \mathcal{K}, \tag{6.8}$$

$\boldsymbol{p}^*$ is a stable CE for Algorithm 6.1.

Proof: To analyze the stability of different CE, we consider the Jacobian matrix of the self-mapping function in (6.7). Let J_{ik} denote the element at row i and column k of the Jacobian matrix $\mathbf{J}$. If $p_k^{t-1}/2+\prod_{i\in\mathcal{K}\setminus\{k\}}(1-p_i^{t-1})/(2a_k)\leq 1$, the Jacobian matrix $\mathbf{J}^{BR}$ of (6.7) is defined as:

$$J_{ik}^{BR}=\frac{\partial p_i^t}{\partial p_k^{t-1}}=\begin{cases}\frac{1}{2}, & \text{if } i=k,\\ -\frac{1}{2a_i}\prod_{j\in\mathcal{K}\setminus\{i,k\}}(1-p_j^{t-1}), & \text{if } i\neq k.\end{cases} \tag{6.9}$$

As proven in Theorem 6.1, for $\mathbf{p}^*=(p_1^*,\ldots,p_K^*)\in P$ to be a fixed point of the self-mapping function in (6.7), a_k must be set to be $a_k^*=\prod_{i\in\mathcal{K}\setminus\{k\}}(1-p_i^*)/p_k^*$. It follows that

$$J_{ik}^{BR}|_{\mathbf{p}=\mathbf{p}^*,\ \boldsymbol{a}=\boldsymbol{a}^*}=\begin{cases}\frac{1}{2}, & \text{if } i=k,\\ -\frac{p_i^*}{2(1-p_k^*)}, & \text{if } i\neq k.\end{cases} \tag{6.10}$$

$\mathbf{p}^*$ is stable if and only if the eigenvalues $\{\lambda_k\}_{k=1}^K$ of matrix $\mathbf{J}^{BR}$ in (6.10) are all inside the unit circle of the complex plane, i.e. $|\lambda_k|<1,\forall k\in\mathcal{K}$.

From Gersgorin circle theorem [HJ81], all the eigenvalues $\{\lambda_k\}_{k=1}^K$ of $\mathbf{J}^{BR}$ are located in the region

$$\bigcup_{k=1}^K\Big\{|\lambda-J_{kk}^{BR}|\leqslant\sum_{i\in\mathcal{K}\setminus\{k\}}|J_{ik}^{BR}|\Big\}\text{ and }\bigcup_{k=1}^K\Big\{|\lambda-J_{kk}^{BR}|\leqslant\sum_{i\in\mathcal{K}\setminus\{k\}}|J_{ki}^{BR}|\Big\}.$$

Note that $J_{kk}^{BR}=1/2$, these regions can be further simplified as

$$\bigcup_{k=1}^K\Big\{|\lambda-\frac{1}{2}|\leqslant\sum_{i\in\mathcal{K}\setminus\{k\}}\frac{p_i^*}{2(1-p_k^*)}\Big\}\text{ and }\bigcup_{k=1}^K\Big\{|\lambda-\frac{1}{2}|\leqslant\sum_{i\in\mathcal{K}\setminus\{k\}}\frac{p_k^*}{2(1-p_i^*)}\Big\}.$$

If either condition in (6.8) is satisfied, all the eigenvalues of $\mathbf{J}^{BR}$ must fall into the region $|\lambda-\frac{1}{2}|<\frac{1}{2}$, which is located within the unit circle $|\lambda|<1$. Therefore, $\mathbf{p}^*$ is a stable CE. ■

Remark 6.1 *$p_k^*/(1-p_i^*)$ can be interpreted as the worst case probability that node k occupies the channel given that node i does not transmit. This metric reflects from node k's perspective the impact that node i's evacuation has on the overall congestion of the channel. Therefore, the sufficient conditions in (6.8) means that if the system is not overcrowded from all the nodes' perspectives, the corresponding CE is stable. We can see from Theorem 6.2 that lowering the transmission probabilities helps to stabilize the random access network. The system can accommodate a certain degree of individual nodes' "aggressiveness" while maintaining the network stability. For example, if a node sends its packets with a probability close to 1, as long as the other nodes are conservative and they set their transmission probability small enough, the entire network can still be stabilized. However, if too many "aggressive" nodes with large transmission probabilities coexist, the system stability may collapse, leading to a tragedy of commons.*

6.3.2.2 Global Convergence

Note that Theorem 6.2 only investigates the stability for different fixed points, i.e. Algorithm 6.1 converges to these points when initial values are close enough to them. In addition to local stability, we are also interested in characterizing the global convergence of Algorithm 6.1 when using various a_k to initialize the belief function $\tilde{s}_k$.

Theorem 6.3 *Regardless of any initial value chosen for $\{p_k^0\}_{k=1}^K$, if the parameters $\{a_k\}_{k=1}^K$ in the belief functions $\{\tilde{s}_k\}_{k=1}^K$ satisfy*

$$\sum_{i\in\mathcal{K}\setminus\{k\}} \frac{1}{a_i} < 1, \forall k \in \mathcal{K}, \tag{6.11}$$

Algorithm 6.1 converges to a unique CE.

Proof: For $a_k > 1$, the self-mapping function in (6.7) can be rewritten as

$$p_k^t = \frac{p_k^{t-1}}{2} + \frac{\prod_{i\in\mathcal{K}\setminus\{k\}}(1-p_i^{t-1})}{2a_k}. \tag{6.12}$$

We can prove for Algorithm 6.1 the uniqueness of and the convergence to CE by showing that function (6.12) is a contraction map if the condition in (6.11) is satisfied.

Let $d(\cdot)$ be the induced distance function by certain vector norm in the Euclidean space. Consider two sequences of the transmission probability vectors $\{\mathbf{p}^0, \ldots, \mathbf{p}^{t-1}, \mathbf{p}^t, \ldots\}$ and $\{\hat{\mathbf{p}}^0, \ldots, \hat{\mathbf{p}}^{t-1}, \hat{\mathbf{p}}^t, \ldots\}$. We have

$$d(\mathbf{p}^t, \hat{\mathbf{p}}^t) = \|\mathbf{p}^t - \hat{\mathbf{p}}^t\| \leq \|\mathbf{J}^{BR}\| \cdot \|\mathbf{p}^{t-1} - \hat{\mathbf{p}}^{t-1}\| = \|\mathbf{J}^{BR}\| \cdot d(\mathbf{p}^{t-1}, \hat{\mathbf{p}}^{t-1}). \tag{6.13}$$

The matrix norm used here is induced by the same vector norm. Using $\|\cdot\|_1$ for the Jacobian matrix of (6.12) as given in (6.10), we have

$$\|\mathbf{J}^{BR}\|_1 = \max_{k\in\mathcal{K}} \sum_{i=1}^{K} |J_{ik}^{BR}| \leq \frac{1}{2} + \frac{1}{2} \max_{k\in\mathcal{K}} \sum_{i\in\mathcal{K}\setminus\{k\}} \frac{1}{a_i}. \tag{6.14}$$

Therefore, if the condition in (6.11) is satisfied, there exist a constant $q \in [0, 1)$ and a positive ϵ, such that $q = \|\mathbf{J}^{BR}\|_1 = 1 - \epsilon < 1$ and $\|\mathbf{p}^t - \hat{\mathbf{p}}^t\|_1 \leq q\|\mathbf{p}^{t-1} - \hat{\mathbf{p}}^{t-1}\|_1$. From the contraction mapping theorem [GD03], the self-mapping function in (6.7) has a unique fixed point and the sequence $\{\mathbf{p}^t\}_{t=0}^{+\infty}$ converges to the unique fixed point. ■

Remark 6.2 *We can also alternatively derive a sufficient condition using* $\|\cdot\|_\infty$ *for (6.13) to be a contraction map. We have*

$$\|\boldsymbol{J}^{BR}\|_\infty = \max_{k\in\mathcal{K}} \sum_{i=1}^{K} |J_{ki}^{BR}| \leq \frac{1}{2} + \frac{1}{2} \max_{k\in\mathcal{K}} \frac{K-1}{a_k}. \tag{6.15}$$

Therefore, if $a_k > K - 1, \forall k \in \mathcal{K}$*, Algorithm 6.1 also globally converges. However, it is easy to verify that it is a special case of the sufficient condition given by*

(6.11). In addition, we can see from (6.11) that, if the accumulated "aggressiveness" of the nodes in the entire networks reaches a certain threshold, the global convergence property may not hold. However, if all the nodes back off adequately by choosing their algorithm parameters $\{a_k\}_{k=1}^K$ such that condition (6.11) is satisfied, Algorithm 6.1 globally converges.

Remark 6.3 *Under the sufficient condition in (6.11), by substituting (6.5) into (6.11), the limiting points lie in the set*

$$\Big\{\boldsymbol{p}^* = (p_1^*, \ldots, p_K^*) \Big| \sum_{i \in \mathcal{K}\setminus\{k\}} \frac{p_i^*}{\prod_{l \in \mathcal{K}\setminus\{i\}}(1-p_l^*)} < 1, \forall k \in \mathcal{K}\Big\}. \tag{6.16}$$

It is easy to check that this is a subset of $\{\boldsymbol{p}^* = (p_1^*, \ldots, p_K^*) | \sum_{k=1}^K p_k^* < 1\}$ *for* $K > 2$*, which verifies the intuition that the set that Algorithm 6.1 globally converges to should be a subset of the set of locally stable CE.*

6.3.3 A Gradient Play Algorithm

The best-response based dynamics may lead to large fluctuations in the entire network, which may not be desirable if we want to avoid temporary system-wide instability. Therefore, in this subsection, we propose an alternative gradient play algorithm. At each iteration, each node updates its action gradually in the ascent direction of its conjectured utility function in (6.6). Specifically, at stage t, node k chooses its transmission probability according to

$$p_k^t = \left[p_k^{t-1} + \gamma_k \frac{\partial u_k^t(\tilde{s}_k^t(p_k), p_k)}{\partial p_k} \bigg|_{p_k = p_k^{t-1}} \right]_0^1, \tag{6.17}$$

in which $[x]_a^b$ means $\max\{\min\{x, b\}, a\}$. As long as the stepsize γ_k is small enough, the entire network will "evolve" smoothly and temporary system-wide instability will not occur. In the following, we assume that all nodes use the same stepsize

Table 6.2: **Algorithm** 6.2: A Distributed Gradient Play Algorithm for Random Access.

Initialize: $t = 0$, stepsize γ, the transmission probability $p_k^0 \in [0, 1]$, and the parameter $a_k > 0$ in node k's belief function, $\forall k \in \mathcal{K}$.

procedure

Repeat

Locally at each node k, iterate through t:

Set $t \leftarrow t + 1$.

for all $k \in \mathcal{K}$ **do**

At stage t, $p_k^t \leftarrow \left[p_k^{t-1} + \gamma \left\{ \prod_{i \in \mathcal{K} \setminus \{k\}} (1 - p_i^{t-1}) - a_k p_k^{t-1} \right\} \right]_0^1$.

end for

Node k decides if it will transmit data with a probability p_k^t (or equivalently, maintain a window size of $CW_k^t = 2/p_k^t - 1$) for all the time slots during stage t.

end procedure

$\gamma_k = \gamma, \forall k \in \mathcal{K}$ and $0 < p_k^{t-1} < 1$. If γ is sufficiently small, substituting the utility function (6.6) into (6.17), we have

$$p_k^t = p_k^{t-1} + \gamma \Big\{ \prod_{i \in \mathcal{K} \setminus \{k\}} (1 - p_i^{t-1}) - a_k p_k^{t-1} \Big\}. \tag{6.18}$$

The detailed description of the distributed gradient play learning mechanism is summarized in Algorithm 6.2. As for Algorithm 6.1, we investigate the stability and convergence of this gradient play algorithm.

6.3.3.1 Local Stability

First of all, the following theorem describes a stable CE set in P for Algorithm 6.2.

Theorem 6.4 *For any $\boldsymbol{p}^* = (p_1^*, \ldots, p_K^*) \in P$, if*

$$\sum_{k=1}^{K} p_k^* < 1, \quad \text{or} \quad \sum_{i \in \mathcal{K}\setminus\{k\}} \frac{p_k^*}{1-p_i^*} < 1, \ \forall k \in \mathcal{K}, \tag{6.19}$$

and the stepsize γ is sufficiently small, $\boldsymbol{p}^*$ is a stable CE for Algorithm 6.2.

Proof: Consider the Jacobian matrix $\mathbf{J}^{GP}$ of the self-mapping function in (6.18). We have $J_{ik}^{GP} = \partial p_i^t / \partial p_k^{t-1}$. As discussed above, for $\mathbf{p}^* = (p_1^*, \ldots, p_K^*) \in P$ to be a fixed point of the self-mapping function in (6.18), a_k must be set to be $a_k^* = \prod_{i \in \mathcal{K}\setminus\{k\}} (1-p_i^*)/p_k^*$. It follows that

$$J_{ik}^{GP}|_{\mathbf{p}=\mathbf{p}^*,\ \boldsymbol{a}=\boldsymbol{a}^*} = \begin{cases} 1 - \gamma \prod_{l \in \mathcal{K}\setminus\{k\}} (1-p_l^*)/p_k^*, & \text{if } i = k, \\ -\gamma \prod_{l \in \mathcal{K}\setminus\{i,k\}} (1-p_l^*), & \text{if } i \neq k. \end{cases} \tag{6.20}$$

$\mathbf{p}^*$ is stable if and only if the eigenvalues $\{\lambda_k\}_{k=1}^K$ of matrix $\mathbf{J}^{GP}$ are all inside the unit circle of the complex plane, i.e. $|\lambda_k| < 1, \forall k \in \mathcal{K}$. Recall that the spectral radius $\rho(\mathbf{J})$ of a matrix $\mathbf{J}$ is the maximal absolute value of the eigenvalues[HJ81]. Therefore, it is equivalent to prove that $\rho(\mathbf{J}^{GP}) < 1$.

To a vector $\boldsymbol{w} = (w_1, \cdots, w_K) \in \mathcal{R}_+^K$ with positive entries, we associate a *weighted ℓ_∞ norm*, defined as

$$\|\boldsymbol{x}\|_\infty^{\boldsymbol{w}} = \max_{k \in \mathcal{K}} \frac{|x_k|}{w_k}. \tag{6.21}$$

The vector norm $\|\cdot\|_\infty^{\boldsymbol{w}}$ induces a matrix norm, defined by

$$\|A\|_\infty^{\boldsymbol{w}} = \max_{k \in \mathcal{K}} \frac{1}{w_k} \sum_{i=1}^{K} |a_{ki}| w_i. \tag{6.22}$$

According to Proposition A.20 in [BT97], $\rho(\mathbf{J}^{GP}) \leq \|\mathbf{J}^{GP}\|_\infty^{\boldsymbol{w}}$. Consider the vector $\boldsymbol{w} = (w_1, \cdots, w_K)$ in which $w_k = p_k^*(1-p_k^*)$. We have

$$\begin{aligned} \frac{1}{w_k} \sum_{i=1}^{K} |J_{ki}^{GP}| w_i &= 1 - \frac{\gamma \prod_{l \in \mathcal{K}\setminus\{k\}} (1-p_l^*)}{p_k^*} + \sum_{i \in \mathcal{K}\setminus\{k\}} \frac{\gamma p_i^* \prod_{l \in \mathcal{K}\setminus\{k\}} (1-p_l^*)}{p_k^*(1-p_k^*)} \\ &= 1 - \frac{\gamma \prod_{l \in \mathcal{K}\setminus\{k\}} (1-p_l^*)}{p_k^*} \Big[1 - \sum_{i \in \mathcal{K}\setminus\{k\}} \frac{p_i^*}{1-p_k^*} \Big]. \end{aligned} \tag{6.23}$$

Therefore, if $\sum_{k\in\mathcal{K}} p_k^* < 1,\ \forall k \in \mathcal{K}$, there exists some $\beta > 0$ such that

$$\frac{\prod_{l\in\mathcal{K}\setminus\{k\}}(1-p_l^*)}{p_k^*}\Big[1-\sum_{i\in\mathcal{K}\setminus\{k\}}\frac{p_i^*}{1-p_k}^*\Big] \geq \beta, \quad \forall k \in \mathcal{K}. \tag{6.24}$$

If the stepsize γ satisfies $0 < \gamma < 1/\beta$, we have

$$\|\mathbf{J}^{GP}\|_\infty^{\boldsymbol{w}} = \max_{k\in\mathcal{K}}\left\{1-\frac{\gamma\prod\limits_{l\in\mathcal{K}\setminus\{k\}}(1-p_l^*)}{p_k^*}\Big[1-\sum_{i\in\mathcal{K}\setminus\{k\}}\frac{p_i^*}{1-p_k^*}\Big]\right\} \leq 1-\gamma\beta < 1. \tag{6.25}$$

Since $\rho(\mathbf{J}^{GP}) \leq \|\mathbf{J}^{GP}\|_\infty^{\boldsymbol{w}} < 1$, all the eigenvalues of $\mathbf{J}^{GP}$ must fall into the unit circle $|\lambda| < 1$. Therefore, $\mathbf{p}^*$ is a stable CE. Similarly, by choosing $\boldsymbol{w} = [1, \cdots, 1]$, we can show that, if

$$\sum_{i\in\mathcal{K}\setminus\{k\}}\frac{p_k^*}{1-p_i^*} < 1,\ \forall k \in \mathcal{K}, \tag{6.26}$$

and γ is sufficiently small, $\mathbf{p}^*$ is also stable. ■

6.3.3.2 Global Convergence

Similarly as in the previous subsection, we derive in the following theorem a sufficient condition under which Algorithm 6.2 globally converges.

Theorem 6.5 *Regardless of any initial value chosen for $\{p_k^0\}_{k=1}^K$, if the parameters $\{a_k\}_{k=1}^K$ in the belief functions $\{\tilde{s}_k\}_{k=1}^K$ satisfy*

$$\sum_{i\in\mathcal{K}\setminus\{k\}}\frac{1}{a_i} < 1, \forall k \in \mathcal{K}, \tag{6.27}$$

and the stepsize γ is sufficiently small, Algorithm 6.2 converges to a unique CE.

Proof: For the self-mapping function in (6.18), the elements of its Jacobian matrix $\mathbf{J}^{GP}$ satisfy

$$J_{ik}^{GP} = \begin{cases} 1-\gamma a_k, & \text{if } i = k, \\ -\gamma\prod_{l\in\mathcal{K}\setminus\{i,k\}}(1-p_l), & \text{if } i \neq k. \end{cases} \tag{6.28}$$

Consider the induced distance by weighted ℓ_∞ norm in the Euclidean space. We have

$$\|\mathbf{p}^t - \hat{\mathbf{p}}^t\|_\infty^{\boldsymbol{w}} \leq \|\mathbf{J}^{GP}\|_\infty^{\boldsymbol{w}} \cdot \|\mathbf{p}^{t-1} - \hat{\mathbf{p}}^{t-1}\|_\infty^{\boldsymbol{w}}. \tag{6.29}$$

Using $\boldsymbol{w} = (1/a_1, \cdots, 1/a_K)$ for (6.29), we have

$$\begin{aligned} \|\mathbf{J}^{GP}\|_\infty^{\boldsymbol{w}} &= \max_{k\in\mathcal{K}} \Bigg\{ 1 - \gamma a_k + \sum_{i\in\mathcal{K}\setminus\{k\}} \prod_{l\in\mathcal{K}\setminus\{i,k\}} \frac{\gamma a_k (1-p_l)}{a_i} \Bigg\} \\ &\leq \max_{k\in\mathcal{K}} \Bigg\{ 1 - \gamma a_k \Big(1 - \sum_{i\in\mathcal{K}\setminus\{k\}} \frac{1}{a_i} \Big) \Bigg\}. \end{aligned} \tag{6.30}$$

Therefore, if the condition in (6.27) is satisfied, there exists some $\beta > 0$ such that

$$a_k \Big(1 - \sum_{i\in\mathcal{K}\setminus\{k\}} \frac{1}{a_i} \Big) \geq \beta, \quad \forall k \in \mathcal{K}. \tag{6.31}$$

If the stepsize γ satisfies $0 < \gamma < 1/\beta$, we have

$$\|\mathbf{J}^{GP}\|_\infty^{\boldsymbol{w}} \leq \max_{k\in\mathcal{K}} \Bigg\{ 1 - \gamma a_k \Big(1 - \sum_{i\in\mathcal{K}\setminus\{k\}} \frac{1}{a_i} \Big) \Bigg\} \leq 1 - \gamma\beta < 1. \tag{6.32}$$

Therefore, there exist a constant $q \in [0, 1)$ and a positive ϵ, such that $q = \|\mathbf{J}^{GP}\|_\infty^{\boldsymbol{w}} = 1 - \epsilon < 1$ and $\|\mathbf{p}^t - \hat{\mathbf{p}}^t\|_\infty^{\boldsymbol{w}} \leq q\|\mathbf{p}^{t-1} - \hat{\mathbf{p}}^{t-1}\|_\infty^{\boldsymbol{w}}$. From the contraction mapping theorem [GD03], the self-mapping function in (6.18) has a unique fixed point and the sequence $\{\mathbf{p}^t\}_{t=0}^{+\infty}$ converges to the unique fixed point. ■

Remark 6.4 *Compare Theorem 6.4 and 6.5 with Theorem 6.2 and 6.3. We can see that, given the same target operating point $\boldsymbol{p}$ or parameters $\{a_k\}_{k=1}^K$, Algorithm 6.2 exhibits similar properties in terms of local stability and global convergence, provided that its stepsize γ is sufficiently small. In other words, the limiting behavior of these two distinct algorithms are similar. However, we need to consider some design trade-off for both algorithms and choose the desired algorithm based on the specific system requirements about the speed of convergence and the performance fluctuation. Generally speaking, the best response algorithm converges*

fast, but it may cause temporary large fluctuations during the convergence process, which is not desirable for transporting constant-bit-rate applications. On the other hand, the gradient play algorithm with small stepsize will evolve smoothly at the cost of sacrificing its convergence rate.

6.3.4 Alternative Interpretations of the Conjecture-based Algorithms

In this section, we re-interpret the proposed algorithms using the the backoff mechanism model in which the transmission probabilities change from time slot to time slot [NKG00], which helps us to understand the key difference between the proposed algorithms and 802.11 DCF. The superscript t in this subsection represents the numbering of the time slots. We define T_k^t and T_{-k}^t as the events that node k transmits data at time slot t and any node in $\mathcal{K}\backslash\{k\}$ transmits data at time slot t, respectively. If $a_k > 1$, the RHS of (6.7) equals to $\frac{p_k^{t-1}}{2} + \frac{\prod_{i\in\mathcal{K}\backslash\{k\}}(1-p_i^{t-1})}{2a_k}$, and the best response update function in (6.7) can be rewritten as

$$\begin{aligned} p_k^t = \frac{1}{2}\mathrm{E}\{p_k^{t-1}\mathbf{1}_{\{T_{-k}^{t-1}=1\}}|\mathbf{p}^{t-1}\} + \frac{1}{2a_k}\mathrm{E}\{\mathbf{1}_{\{T_{-k}^{t-1}=0\}}\mathbf{1}_{\{T_k^{t-1}=0\}}|\mathbf{p}^{t-1}\} \\ +\frac{1}{2}(1+\frac{1}{a_k})\mathrm{E}\{\mathbf{1}_{\{T_{-k}^{t-1}=0\}}\mathbf{1}_{\{T_k^{t-1}=1\}}|\mathbf{p}^{t-1}\}, \end{aligned} \tag{6.33}$$

where $\mathbf{1}_a$ is an indicator function of event a taking place, $\mathrm{E}\{a|b\}$ is the expected value of a given b, $\mathrm{E}\{\mathbf{1}_{\{T_k^{t-1}=1\}}|\mathbf{p}^{t-1}\} = p_k^{t-1}$, and $\mathrm{E}\{\mathbf{1}_{\{T_{-k}^{t-1}=1\}}|\mathbf{p}^{t-1}\} = 1 - \prod_{i\in\mathcal{K}\backslash\{k\}}(1-p_i^{t-1})$. According to (6.33), we can provide an alternative interpretation of the best-response update algorithm as follows. Consider the following update algorithm. At each time slot, if node k observes that any other node attempts to transmit, i.e. it senses a busy channel, it reduces its transmission probability by a factor 1/2. If no transmission attempt is made by any node in the system, node k sets its transmission probability to be $1/2a_k$. Otherwise, if node k makes a successful transmission, it will transmit with probability $0.5(1+1/a_k)$ in the next time slot. We can see that equation (6.33) characterizes the expected

Did other nodes transmit?	Did node k transmit? Yes	Did node k transmit? No
Yes	$p_k^t = p_k^{t-1}/2 \quad (BR)$ $p_k^t = p_k^{t-1}/2 \quad (DCF)$	$p_k^t = p_k^{t-1}/2 \quad (BR)$ $p_k^t = p_k^{t-1} \quad (DCF)$
No	$p_k^t = 0.5(1+1/a_k) \quad (BR)$ $p_k^t = P^{\max} \quad (DCF)$	$p_k^t = 1/2a_k \quad (BR)$ $p_k^t = p_k^{t-1} \quad (DCF)$

Figure 6.3: Comparison between the best response algorithm and the IEEE 802.11 DCF ($P^{\max}$ is specified in the DCF protocol).

trajectory of this alternative update mechanism. Fig. 6.3 compares this new interpretation with the IEEE 802.11 DCF [LTH07]. We can see that, node k behaves similarly in the best response algorithm and the IEEE 802.11 DCF if it made a transmission attempt in the previous time slot, and the fundamental difference between these two protocols is how node k updates its action given that it did not transmit in the previous time slot. In DCF, p_k^t is kept the same as p_k^{t-1}. However, as we can see from (6.33), the best response algorithm either performs back-off if the channel is busy or sets p_k^t to be $1/2a_k$ if the channel is free.

Remark 6.5 *Both Equation (6.5) and (6.33) intuitively explain the meaning of the algorithm parameters* $\{a_k\}_{k=1}^K$. *Note that the numerator of (6.5),* $\prod_{i\in\mathcal{K}\setminus\{k\}}(1-p_i^*)$, *represents the probability that transmitter* k *experiences a contention-free environment at* $\boldsymbol{p}^*$. *The value of* $1/a_k$, *i.e. the ratio between node* k*'s transmission probability* p_k *and its contention-free probability, indicates the "aggressiveness" of this particular node at equilibrium. In addition, according to (6.33), the transmission probability* $1/2a_k$ *also reflects node* k*'s "aggressiveness" in selecting its transmission probability after it sensed a free channel. It is straightforward to*

see the selection of $\{a_k\}_{k=1}^K$ *introduces some trade-off between the stability and throughput of the networks. First of all, large values of* $\{a_k\}_{k=1}^K$ *refrain nodes from transmitting at a higher channel access probability, and hence, it stabilizes the system at the cost of reducing the throughput. On the other hand, lowering* $\{a_k\}_{k=1}^K$ *increases the nodes' transmission probability, which may improve the throughput performance. However, it can cause the conditions in (6.8) and (6.19) to fail and the system becomes unstable. Therefore, the problems which we will investigate in the next subsection are which part of the throughput region can be achieved with stable CE and how the nodes can adaptively update their* $\{a_k\}_{k=1}^K$ *such that the system can attain efficient and stable operating points.*

Before proceeding to the next subsection, similarly as for the best response algorithm, we present an reinterpretation of the gradient play. Equation (6.18) can be rewritten as

$$p_k^t = (1-\gamma a_k)p_k^{t-1}\mathrm{E}\{\mathbf{1}_{\{T_{-k}^{t-1}=1\}}|\mathbf{p}^{t-1}\} + [p_k^{t-1}+\gamma(1-a_k p_k^{t-1})]\mathrm{E}\{\mathbf{1}_{\{T_{-k}^{t-1}=0\}}|\mathbf{p}^{t-1}\}. \tag{6.34}$$

If $a_k > 1$, the interpretation of (6.34) is that at each time slot, if node k senses a busy channel, it reduces its transmission probability by a factor $1-\gamma a_k$, otherwise it increases its transmission probability by an amount $\gamma(1-a_k p_k^{t-1})$. We can see that, this interpretation of the gradient play learning resembles the well-known AIMD (Additive Increase Multiplicative Decrease) control algorithm, which has been widely applied in the context of congestion avoidance in computer networks due to its superior performance in terms of convergence and efficiency [CJ89].

6.3.5 Stability of the Throughput Region

The results in the previous subsections describe the values of $\{p_k\}_{k=1}^K$ and $\{a_k\}_{k=1}^K$ for which local stability and global convergence can be guaranteed in both Algo-

rithm 6.1 and 6.2. This subsection directly investigates for both algorithms the stability of achievable operating points in the throughput region $\mathscr{T}$.

Lemma 6.1 *The Pareto boundary of the throughput region $\mathscr{T}$ is the set of all points $\boldsymbol{\tau} = (\tau_1, \ldots, \tau_K)$ such that $\tau_k = p_k \prod_{i \in \mathcal{K} \setminus \{k\}} (1 - p_i)$ where $\boldsymbol{p} = (p_1, \ldots, p_K)$ is a vector satisfying $\boldsymbol{p} \geq \boldsymbol{0}$ and $\sum_{k \in \mathcal{K}} p_k = 1$; and each such $\boldsymbol{\tau}$ is determined by a unique such $\boldsymbol{p}$.*

Proof: See Theorem 1 in [MM85]. ■

Theorem 6.6 *Regardless of the number of nodes in the network, for any Pareto-inefficient operating point $\boldsymbol{\tau}^*$ in the throughput region $\mathscr{T}$, there always exists a belief configuration $\{a_k\}_{k=1}^K$ stabilizing Algorithm 6.1 and 6.2, and achieve the throughput $\boldsymbol{\tau}^*$. If $K > 2$, any Pareto-optimal operating point $\{p_k^*\}_{k=1}^K$ in $\mathscr{T}$ that satisfies $p_k^* > 0, \forall k \in \mathcal{K}$ is a stable CE for Algorithm 6.1 and 6.2.*

Proof: From Theorem 6.2, we know that $\sum_{k \in \mathcal{K}} p_k < 1$ is sufficient to guarantee that the corresponding CE is stable. Therefore, it is equivalent to check that any Pareto-inefficient operating point $\boldsymbol{\tau}^*$ can be achieved with a joint transmission probability $\mathbf{p}^* \in P$ satisfying $\sum_{k \in \mathcal{K}} p_k^* < 1$.

Define the throughput region

$$\mathscr{T}(t) = \{(u_1(\mathbf{p}), \ldots, u_K(\mathbf{p})) | \ \exists \ \mathbf{p} \in P, \sum_{k \in \mathcal{K}} p_k \leq t\}, \tag{6.35}$$

in which an additional constraint $\sum_{k \in \mathcal{K}} p_k \leq t$ is imposed. We denote the Pareto boundary of $\mathscr{T}(t)$ as

$$\partial \mathscr{T}(t) = \{\boldsymbol{\tau} | \ \nexists \ \boldsymbol{\tau}' \in \mathscr{T}(t) \text{ such that } \tau_k' \geq \tau_k, \ \forall k \in \mathcal{K} \text{ and } \tau_k' > \tau_k, \ \exists k \in \mathcal{K}\}. \tag{6.36}$$

Following the proof of Lemma 6.1, we can draw a similar conclusion: all the points on $\partial\mathscr{T}(t)$ satisfy $\sum_{k\in\mathcal{K}} p_k = t$. By Lemma 6.1, $\partial\mathscr{T}(1)$ corresponds to the Pareto boundary of $\mathscr{T}$. Note that $\partial\mathscr{T}(0) = \mathbf{0}$. In other words, varying t from 1 to 0 will cause $\partial\mathscr{T}(t)$ to continuously shrink from the Pareto boundary of the throughput region $\mathscr{T}$ to the origin $\mathbf{0}$. Therefore, for any Pareto inefficient point $\boldsymbol{\tau}^* \in \mathscr{T}$, there exists $0 \le t' < 1$ such that $\boldsymbol{\tau}^*$ lie on $\partial\mathscr{T}(t')$, i.e. $\boldsymbol{\tau}^*$ can be achieved with an action profile $\mathbf{p}^*$ satisfying $\sum_{k\in\mathcal{K}} p_k^* = t < 1$.

To prove the Pareto boundary are stable CE when $K > 2$, we need to show that the eigenvalues $\{\xi_k^{BR}\}_{k=1}^K$ of the Jacobian matrices $\mathbf{J}^{BR}$ and $\mathbf{J}^{GP}$ are all inside the unit circle of the complex plane [GD03], i.e. $|\xi_k| < 1, \forall k \in \mathcal{K}$. Take the best response dynamics for example. To determine the eigenvalues of $\mathbf{J}^{BR}$, we have

$$
\begin{aligned}
\det(\xi I - \mathbf{J}^{BR}) &= \begin{vmatrix} \xi - \frac{1}{2} & \frac{p_1}{2(1-p_2)} & \cdots & \frac{p_1}{2(1-p_K)} \\ \frac{p_2}{2(1-p_1)} & \xi - \frac{1}{2} & \cdots & \frac{p_2}{2(1-p_K)} \\ \vdots & \vdots & \ddots & \vdots \\ \frac{p_K}{2(1-p_1)} & \frac{p_K}{2(1-p_2)} & \cdots & \xi - \frac{1}{2} \end{vmatrix} \\
&= \begin{vmatrix} \xi - \frac{1}{2} & \frac{p_1}{2(1-p_2)} & \cdots & \frac{p_1}{2(1-p_K)} \\ \frac{p_2}{2(1-p_1)} - \frac{p_2}{p_1}\left(\xi - \frac{1}{2}\right) & \xi - \frac{1}{2} - \frac{p_2}{2(1-p_2)} & \cdots & 0 \\ \vdots & \vdots & \ddots & \vdots \\ \frac{p_K}{2(1-p_1)} - \frac{p_K}{p_1}\left(\xi - \frac{1}{2}\right) & 0 & \cdots & \xi - \frac{1}{2} - \frac{p_K}{2(1-p_K)} \end{vmatrix} \\
&= \begin{vmatrix} \left(\xi - \frac{1}{2(1-p_1)}\right) \cdot \left[1 + \sum_{k=1}^{K} \frac{\frac{p_k}{2(1-p_k)}}{\xi - \frac{1}{2(1-p_k)}}\right] & 0 & \cdots & 0 \\ \frac{p_2}{2(1-p_1)} - \frac{p_2}{p_1}\left(\xi - \frac{1}{2}\right) & \xi - \frac{1}{2(1-p_2)} & \cdots & 0 \\ \vdots & \vdots & \ddots & \vdots \\ \frac{p_K}{2(1-p_1)} - \frac{p_K}{p_1}\left(\xi - \frac{1}{2}\right) & 0 & \cdots & \xi - \frac{1}{2(1-p_K)} \end{vmatrix}.
\end{aligned}
$$

Therefore, we can see that, the eigenvalues of $\mathbf{J}^{BR}$ are the roots of

$$\big[1+\sum_{k=1}^{K}\frac{\frac{p_k}{2(1-p_k)}}{\xi-\frac{1}{2}-\frac{p_k}{2(1-p_k)}}\big]\cdot\prod_{k=1}^{K}\big(\xi-\frac{1}{2}-\frac{p_k}{2(1-p_k)}\big)=0. \tag{6.37}$$

Denote $f(\xi)=\sum_{k=1}^{K}\frac{\frac{p_k}{2(1-p_k)}}{\xi-\frac{1}{2}-\frac{p_k}{2(1-p_k)}}$. First, we assume that $p_i\neq p_j,\forall i,j$. Without loss of generality, consider $p_1<p_2<\cdots<p_K$. In this case, the eigenvalues of $\mathbf{J}^{BR}$ are the roots of $f(\xi)=-1$. Note that $f(\xi)$ is a continuous function and it strictly decreases in $(-\infty,\frac{1}{2}+\frac{p_1}{2(1-p_1)})$, $(\frac{1}{2}+\frac{p_1}{2(1-p_1)},\frac{1}{2}+\frac{p_2}{2(1-p_2)})$, $\cdots$, $(\frac{1}{2}+\frac{p_{K-1}}{2(1-p_{K-1})},\frac{1}{2}+\frac{p_K}{2(1-p_K)})$, and $(\frac{p_K}{2(1-p_K)},+\infty)$. We also have $\lim_{\xi\to(\frac{1}{2}+\frac{p_k}{2(1-p_k)})^-}f(\xi)=-\infty$, $\lim_{\xi\to(\frac{1}{2}+\frac{p_k}{2(1-p_k)})^+}f(\xi)=+\infty, n=1,2,\cdots,K$, and $\lim_{\xi\to-\infty}f(\xi)=\lim_{\xi\to+\infty}f(\xi)=0$. Therefore, the roots of $f(\xi)=-1$ lie in $(-\infty,\frac{1}{2}+\frac{p_1}{2(1-p_1)})$, $(\frac{1}{2}+\frac{p_1}{2(1-p_1)},\frac{1}{2}+\frac{p_2}{2(1-p_2)})$, $\cdots$, $(\frac{1}{2}+\frac{p_{K-1}}{2(1-p_{K-1})},\frac{1}{2}+\frac{p_K}{2(1-p_K)})$ respectively.

For the operating points on the Pareto boundary, we have $\sum_{k=1}^{K}p_k=1$. It is easy to verify that $f(0)=-1$, i.e. $\xi_1=0$. Therefore,

$$\rho(\mathbf{J}^{BR})=\max_k|\xi_k|=\xi_K\in(\frac{1}{2}+\frac{p_{K-1}}{2(1-p_{K-1})},\frac{1}{2}+\frac{p_K}{2(1-p_K)}). \tag{6.38}$$

To see $\xi_K<1$ for $0\leq p_1<p_2<\cdots<p_K$ and $\sum_{k=1}^{K}p_k=1$. We differentiate two cases:

1) If $p_K\leq 0.5$, we have $\xi_K<\frac{1}{2}+\frac{p_K}{2(1-p_K)}\leq 1$;

2) If $p_K>0.5$, we have $\frac{1}{2}+\frac{p_{K-1}}{2(1-p_{K-1})}<1$ and $\frac{1}{2}+\frac{p_K}{2(1-p_K)}>1$. Since $f(\xi)$ strictly decreases in $(\frac{1}{2}+\frac{p_{K-1}}{2(1-p_{K-1})},\frac{1}{2}+\frac{p_K}{2(1-p_K)})$, we have $\rho(\mathbf{J}^{BR})<1$ if and only if $f(1)<-1$. In fact,

$$f(1)-(-1)=\sum_{k=1}^{K}\frac{p_k}{1-2p_k}+1=\sum_{k=1}^{K-1}p_k\big(\frac{1}{1-2p_k}-\frac{1}{1-2\sum_{m=1}^{K-1}p_m}\big)<0. \tag{6.39}$$

The inequality holds because $\frac{1}{1-2p_k}<\frac{1}{1-2\sum_{m=1}^{K-1}p_m}$ for $k=1,2,\ldots,K-1$ when $p_K>0.5$, $0\leq p_1<p_2<\cdots<p_K$, and $\sum_{k=1}^{K}p_k=1$.

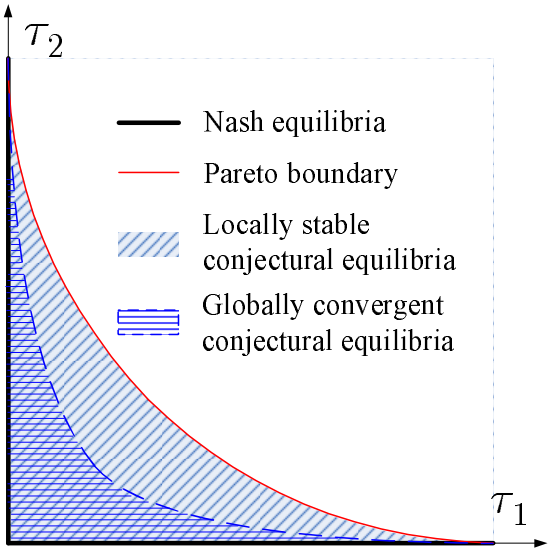

Figure 6.4: Comparison among different solution concepts.

Second, we consider the cases in which there exists $p_i = p_j$ for certain i, j. Suppose that $\{p_k\}_{k=1}^K$ take M discrete values $\kappa_1, \cdots, \kappa_M$ and the number of $\{p_k\}_{k=1}^K$ that equal to κ_m is n_m. In this case, Equation (6.37) is reduced to

$$\left[1 + \sum_{k=1}^{K} \frac{\frac{p_k}{2(1-p_k)}}{\xi - \frac{1}{2} - \frac{p_k}{2(1-p_k)}}\right] \cdot \prod_{m=1}^{M} \left(\xi - \frac{1}{2} - \frac{\kappa_m}{2(1-\kappa_m)}\right)^{n_m} = 0. \tag{6.40}$$

Hence, equation $f(\xi) = -1$ has $K + M - \sum_{k=1}^{M} n_m$ roots in total, and $\xi = \frac{1}{2} + \frac{\kappa_m}{2(1-\kappa_m)}$ is a root of multiplicity $n_m - 1, \forall m$. All these roots are the eigenvalues of matrix $\mathbf{J}^{BR}$. Similarly, the remaining roots of $f(\xi) = -1$ lie in $(-\infty, \frac{1}{2} + \frac{\kappa_1}{2(1-\kappa_1)})$, $(\frac{1}{2} + \frac{\kappa_1}{2(1-\kappa_1)}, \frac{1}{2} + \frac{\kappa_2}{2(1-\kappa_2)}), \cdots, (\frac{1}{2} + \frac{\kappa_{M-1}}{2(1-\kappa_{M-1})}, \frac{1}{2} + \frac{\kappa_M}{2(1-\kappa_M)})$. If $K > 2$, $\sum_{k=1}^{K} p_k = 1$ is still sufficient to guarantee that $f(1) < -1$. Therefore, $|\xi_k^{BR}| < 1, \forall k \in \mathcal{K}$. ■

Fig. 6.4 compares the throughput performance among various game-theoretic solution concepts, including Nash equilibria, Pareto frontier, locally stable conjectural equilibria, and globally convergent conjectural equilibria, in random access games. As proven in Theorem 6.6, Fig. 6.4 shows that, the entire space spanning between the Nash equilibria and Pareto frontier essentially consists of stable con-

jectural equilibria. In addition, as discussed in Remark 6.3, the set of globally convergent CE is a subset of the stable CE set.

In practice, it is more important to construct algorithmic mechanisms to attain the desirable CE that operate stably and closely to the Pareto boundary. To this end, we develop an iterative algorithm and summarize it as Algorithm 6.3. Specifically, this algorithm has an inner loop and an outer loop. The inner loop adopts either Algorithm 6.1 or 6.2 to achieve convergence for fixed $\{a_k\}_{k=1}^K$. This algorithm initializes $a_k > |\mathcal{K}|$ such that it initially globally converges. After converging to a stable CE, the outer loop adaptively adjusts $\{a_k\}_{k=1}^K$ until desired efficiency is attained. The outer loop updates $\{a_k\}_{k=1}^K$ in the multiplicative manner due to two reasons. First, reducing $\{a_k\}_{k=1}^K$ individually increases $\{p_k^t\}_{k=1}^K$ and $\sum_{k=1}^K p_k$ and hence, moves the operating point towards the Pareto boundary. Second, multiplying $\{a_k\}_{k=1}^K$ by the same discount factor can maintain weighted fairness among different nodes. Both reasons will be analytically explained in the Section 6.4. It is also worth mentioning that individual nodes can measure the Pareto efficiency in a fully distributed manner during the outer loop iteration. For example, individual nodes can estimate the other nodes' transmission probabilities $\{p_k^t\}_{k=1}^K$ based on its local observation and figure out whether the current operating point is close to the Pareto boundary by calculating $\sum_{k\in\mathcal{K}} p_k^t$ [MHC09]. When the network size grows bigger, individually estimating different nodes' transmission probabilities becomes challenging. An alternative solution is that individual nodes can instead monitor their common observation of the aggregate throughput $\sum_{k\in\mathcal{K}} u_k^t$ and terminate the update of $\{a_k\}_{k=1}^K$ once the aggregate throughput starts to decrease. Next, we discuss several implementation issues regarding Algorithm 3. First, it is not necessary that all the nodes update their parameters $\{a_k\}_{k=1}^K$ synchronously. However, these nodes need to maintain the same update frequency, e.g. each node will update its parameter after a cer-

Table 6.3: **Algorithm** 6.3: Adaptive Distributed Algorithm for Random Access.

Initialize: stepsize γ and δ, the transmission probability $p_k^0 \in [0,1]$, and the parameter $a_k > |\mathcal{K}|$ in node k's belief function, $\forall k \in \mathcal{K}$.

procedure

outerloop: For each node k, $a_k \leftarrow a_k(1-\delta)$.

innerloop: *Locally* at each node k, use Algorithm 6.1 or 6.2 to update p_k^t.

until it converges.

until the aggregate throughput is maximized or $\sum_{k\in\mathcal{K}} p_k^t \approx 1$.

end for

end procedure

tain number of timeslots or seconds. As long as δ is small, the performance gap between the actual CE and the intended one will not be large. Moreover, in order to guarantee fairness, the new incoming nodes need to know the real-time parameters of the old nodes in the same traffic class. This initialization only needs to be done once, when the new nodes enter the cell by tracking the evolution of the transmission probabilities of the nodes in the same traffic class.

6.4 Extensions to Heterogeneous Networks and Ad-hoc Networks

In this section, we first investigate how users with different qualify-of-service requirements should initialize their belief functions and interact in the heterogeneous network setting and show that the conjecture-based approaches approximately achieve the weighted fairness. Furthermore, we discuss how the single-cell

solution can be extended to the general ad-hoc network scenario, where only the devices within a certain neighborhood range will impact each other's throughput.

6.4.1 Equilibrium Selection for Heterogeneous Networks

Consider a network with $N > 1$ different classes of nodes. Let ϕ_n denote the parameter that class-n nodes choose for their conjectured utility functions (i.e. the parameter a_k if node k belongs to class-n) and $\mathcal{F}_n$ denote the set of nodes that set their algorithm parameters to be ϕ_n, $1 \leq n \leq N$. At equilibrium, the transmission probabilities of the same class of nodes are equal, denoted as $\tilde{p}_n$. Before we proceed, we first define the weighted fairness for the random access game [QS02]. For each traffic class n, we associate with a positive weight χ_n. Then the weighted fairness intended for the random access game satisfy

$$\forall i, j \in \{1, 2, \cdots, N\}, s \in \mathcal{F}_i, s' \in \mathcal{F}_j, \frac{\mathrm{E}\{\mathbf{1}_{\{T_{-s}=0\}}\mathbf{1}_{\{T_s=1\}}\}}{\chi_i} = \frac{\mathrm{E}\{\mathbf{1}_{\{T_{-s'}=0\}}\mathbf{1}_{\{T_{s'}=1\}}\}}{\chi_j}, \tag{6.41}$$

which means that the probability of an successful transmission attempt for traffic class n is proportional to its weight χ_n. By simple manipulation, we have the equivalent form for equation (6.41) [QS02]:

$$\forall i, j \in \{1, 2, \cdots, N\}, \frac{p_i^{WF}}{(1 - p_i^{WF})\chi_i} = \frac{p_j^{WF}}{(1 - p_j^{WF})\chi_j}. \tag{6.42}$$

Recall that Theorem 6.1 showed how to choose $\{a_k\}_{k=1}^K$ given a desired operating point $\{p_k^*\}_{k=1}^K$ such that it is a CE. The following theorem indicates the quantitative relationship between the chosen algorithm parameters $\{\phi_n\}_{n=1}^N$, the sizes of different classes $\{\mathcal{F}_n\}_{n=1}^N$, and the resulting steady-state transmission probabilities $\{\tilde{p}_n\}_{n=1}^N$. More importantly, it also shows that if the network size is large, the conjecture-based algorithms approximately achieve weighted fairness.

Theorem 6.7 *Suppose that* $\phi_n \geq 2,\ \forall 1 \leq n \leq N$. *The achieved steady-state transmission probabilities* $\{\tilde{p}_n\}_{n=1}^N$ *are given by*

$$\tilde{p}_n = \frac{1}{2}\left(1 - \sqrt{1 - \frac{4\varrho}{\phi_n}}\right), \tag{6.43}$$

where ϱ *satisfies*

$$\varrho = \frac{1}{2^K} \prod_{n=1}^{N} \left[\left(1 + \sqrt{1 - \frac{4\varrho}{\phi_n}}\right)^{|\mathcal{F}_n|}\right]. \tag{6.44}$$

Proof: As shown in Theorem 6.1, $a_k^* p_k^* = \prod_{i \in \mathcal{K}\setminus\{k\}}(1 - p_i^*)$. Denote $\varrho = \prod_{i\in\mathcal{K}}(1 - \tilde{p}_i)$. Therefore, we obtain

$$\phi_n \tilde{p}_n (1 - \tilde{p}_n) = \varrho,\ \forall\ 1 \leq n \leq N. \tag{6.45}$$

Since $\phi_n > 2$, we have $\tilde{p}_n < 0.5$. Such a root of the quadratic equation in (6.45) is given in (6.43). Note that $\varrho = \prod_{i\in\mathcal{K}}(1 - \tilde{p}_i)$. Substituting (6.43) into this equality, we get (6.44).

We can verify that a unique ϱ satisfying the equality in (6.44) exists if $\phi_n \geq 2,\ \forall 1 \leq n \leq N$. This is because the RHS of (6.44) is feasible for $\varrho \leq \min\limits_{1\leq n\leq N}\{\phi_n\}/4$ and it is a strictly decreasing function in ϱ. Meanwhile, the LHS of (6.44) is strictly increasing on $\varrho \in [0, \min\limits_{1\leq n\leq N}\{\phi_n\}/4]$. Note that when $\varrho = \min\limits_{1\leq n\leq N}\{\phi_n\}/4$,

$$\text{LHS of (6.44)} = \min_{1\leq n\leq N} \frac{\phi_n}{4} \geq \frac{1}{2} \geq \text{RHS of (6.44)}. \tag{6.46}$$

if $\phi_n \geq 2$. Therefore, a unique $\varrho \in [0, \min\limits_{1\leq n\leq N}\{\phi_n\}/4]$ satisfies (6.44) exists. ■

Remark 6.6 *There are several intuitions and observations that we can obtain from Theorem 6.7. First, the multiplicative decreasing update in Algorithm 6.3 aims to move the operating points towards Pareto boundary. A quantitative approximation between the steady-state transmission probability* $\tilde{p}_n$ *and the algorithm parameter* ϕ_n *of each traffic class can be derived if a large number of nodes*

coexist. Since $\varrho \to 0$ *when* $|\mathcal{F}_n|$ *is large, using the Taylor expansion,* $\tilde{p}_n$ *can be approximated as* ϱ/ϕ_n*, i.e. the steady-state transmission probability* $\tilde{p}_n$ *decays as the inverse first power of parameter* ϕ_n *that indicates the "aggressiveness" of traffic class* n*. Finally, we also observe from (6.45) that, if* $|\mathcal{F}_n|$ *is large,* $\tilde{p}_n \to 0$ *and* $1 - \tilde{p}_n \approx 1$*. Therefore,*

$$\forall i, j \in \{1, 2, \cdots, N\}, \phi_i \tilde{p}_i (1 - \tilde{p}_i) = \phi_j \tilde{p}_j (1 - \tilde{p}_j) \Rightarrow \frac{\phi_i \tilde{p}_i}{1 - \tilde{p}_i} \approx \frac{\phi_j \tilde{p}_j}{1 - \tilde{p}_j}. \quad (6.47)$$

Equation (6.47) indicates that Algorithm 6.1 and 6.2 approximately achieve weighted fairness given in (6.42) with weight $\chi_n = 1/\phi_n$*. Moreover, it is worth mentioning that the weighted fairness is purely an implicit by-product of the conjecture-based approach and it can be sustained with stability. Therefore, Algorithm 6.3 chooses to multiply* $\{a_k\}_{k=1}^K$ *by the same discount factor* $1 - \delta$ *such that the weighted fairness can be maintained.*

6.4.2 Extension to Ad-hoc Networks

Consider a wireless ad-hoc network with a set $\mathcal{K} = \{1, 2, \ldots, K\}$ of distinct node pairs in Fig. 6.5. Each link (node pair) consists of one dedicated transmitter and one dedicated receiver. We assume that the transmission of a link is interfered from the transmission of another link, if the distance between the receiver node of the former and the transmitter node of the latter is less than some threshold D_{th} [LZL07, LCC07]. For any node i, we define $I_i \subseteq \mathcal{K}$ as the set of nodes whose transmitters cause interference to the receiver of node i and $O_i \subseteq \mathcal{K}$ as the set of nodes whose receivers get interfered from the transmitter of node i. For example, in Fig. 6.5, $I_1 = \{K\}$ and $O_1 = \{2, K\}$. Then, the throughput of node i is

$$u_k(\mathbf{p}) = p_k \prod_{i \in I_k} (1 - p_i). \quad (6.48)$$

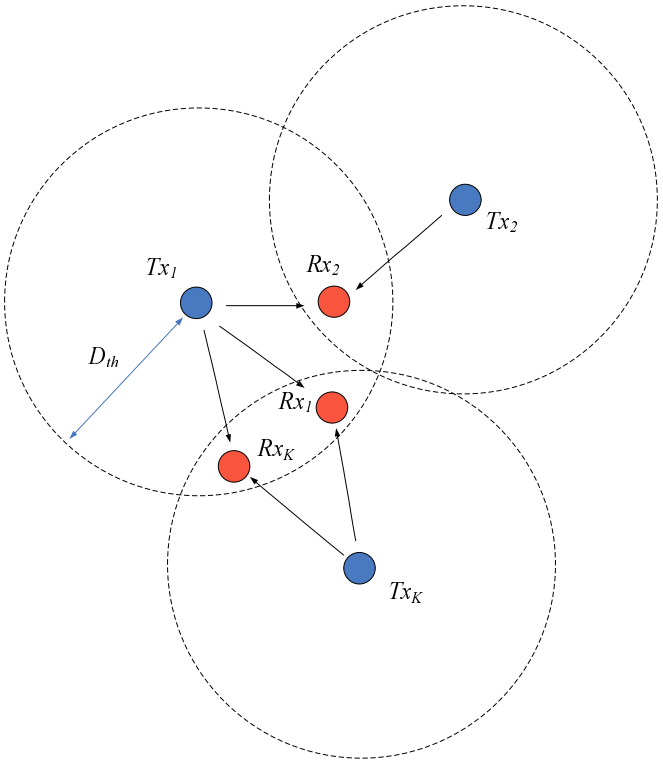

Figure 6.5: System model of ad hoc networks.

In this scenario, the state, namely, the contention measure signal, can be redefined according to $s_k = \prod_{i \in I_k}(1-p_i)$. Applying the conjecture-based approach, we have the following conjectured utility function for node k:

$$u_k^t(\tilde{s}_k^t(p_k), p_k) = p_k \Big[\prod_{i \in I_k} (1 - p_i^{t-1}) - a_k (p_k - p_k^{t-1}) \Big]. \tag{6.49}$$

Parallel to the theorems proven in Section 6.3.2 and 6.3.3, we have the following theorems on the stability and convergence of conjecture-based algorithms in ad-hoc networks. These theorems can be shown similarly as in Section 6.3, and hence, the proofs are omitted.

6.4.2.1 Stability and Convergence

Theorem 6.8 *For any* $\boldsymbol{p}^* = (p_1^*, \ldots, p_K^*) \in P$, *if*

$$\sum_{i \in O_k \cup \{k\}} p_i^* < 1, \ \forall k \in \mathcal{K}, \quad or \quad \sum_{i \in I_k} \frac{p_k^*}{1 - p_i^*} < 1, \ \forall k \in \mathcal{K}, \tag{6.50}$$

$\boldsymbol{p}^*$ *is a stable CE for Algorithm 6.1 and Algorithm 6.2 with sufficiently small* γ.

Theorem 6.9 *Regardless of any initial value chosen for* $\{p_k^0\}_{k=1}^K$, *if the parameters* $\{a_k\}_{k=1}^K$ *in the belief functions* $\{\tilde{s}_k\}_{k=1}^K$ *satisfy*

$$a_k > |O_k|, \ \forall k \in \mathcal{K}, \quad or \quad \sum_{i \in I_k} \frac{1}{a_i} < 1, \forall k \in \mathcal{K}, \tag{6.51}$$

Algorithm 6.1 and Algorithm 6.2 with sufficiently small γ *converge to a unique CE.*

Remark 6.7 *We observe that the sufficient conditions in Theorem 6.8 and 6.9 are more relaxed compared with the theorems in Section 6.3. As opposed to the single-cell case, the mutual interference is reduced in ad-hoc networks due to the large scale geographical distance, therefore, these nodes can potentially improve their throughput by increasing their transmission probabilities while still maintaining the local stability as well as global convergence.*

Remark 6.8 *In ad-hoc networks, the parameters* $\{a_k\}_{k=1}^K$ *can be determined in a distributed fashion such that the sufficient conditions in Theorem 6.9 are satisfied. For example, consider the symmetric case where transmitter* i *interferes with receiver* j *if and only if transmitter* i *can receive signals from receiver* j. *Each transmitter can listen to the channel and estimate* $|O_k|$ *by intercepting the ACK packets sent by the receivers of the nodes in set* O_k. *An alternative distributed solution is that each transmitter broadcasts its parameter* a_k, *and receiver* k *calculates* $\sum_{i \in I_k} \frac{1}{a_i}$ *and notifies the nodes in set* I_k *to adjust their parameters accordingly.*

6.4.2.2 Stability of the Throughput Region

We also extend the stability analysis of the throughput region from the single-cell scenario to the ad-hoc networks. The following lemma explicitly describes the Pareto frontier of the throughput region.

Lemma 6.2 *The Pareto boundary of the throughput region $\mathscr{T}$ can be characterized as the set of points $\boldsymbol{\tau} = (\tau_1, \ldots, \tau_K)$ optimizing the weighted proportional fairness objective [GS06]:*

$$\max_{\boldsymbol{p} \in P} \sum_{k \in \mathcal{K}} \omega_k log \tau_k, \tag{6.52}$$

in which $\tau_k = p_k \prod_{i \in I_k} (1 - p_i)$ for all possible sets of positive link "weights" $\{\omega_k\}_{k=1}^K$. Specifically, for a particular weight combination $\{\omega_k\}_{k=1}^K$, the optimal $\boldsymbol{p}'$ is given by

$$p'_k = \frac{\omega_k}{\omega_k + \sum_{i \in O_k} \omega_i}. \tag{6.53}$$

Proof: See [GS06] for details.

Based on Lemma 6.2, we derive in the following theorem the necessary and sufficient condition under which a particular Pareto-efficient operating point is a stable CE for Algorithm 6.1. Similar results can be derived for Algorithm 6.2 with sufficiently small γ.

Theorem 6.10 *Suppose $\boldsymbol{p}^* = (p_1^*, \ldots, p_K^*) \in P$ satisfies (6.53) and maximizes the problem in (6.52). The elements of the Jacobi matrix $\boldsymbol{J}$ at $\boldsymbol{p}^*$ satisfy*

$$J_{ik} = \begin{cases} \frac{1}{2}, & \text{if } i = k, \\ -\frac{p_i^*}{2(1-p_k^*)}, & \text{if } k \in I_i, \\ 0, & \text{otherwise.} \end{cases} \tag{6.54}$$

If $\rho(\boldsymbol{J}) < 1$, $\boldsymbol{p}$ is a stable CE for Algorithm 1.

Remark 6.9 *Theorem 6.10 generalizes the result in Theorem 6.6 from the single-cell scenario to the ad-hoc networks. Consider the l_1 norm for $\boldsymbol{J}$ at $\boldsymbol{p}$. We have*

$$\|\boldsymbol{J}\|_1 = \max_{k\in\mathcal{K}} \frac{\omega_k}{\omega_k + \sum_{i\in O_k}\omega_i} + \sum_{i\in O_k} \frac{\omega_i}{\omega_i + \sum_{j\in O_i}\omega_j}. \tag{6.55}$$

In the single-cell case, $O_k = \mathcal{K}\backslash\{k\}$, $\forall k \in \mathcal{K}$, and $\|\boldsymbol{J}\|_1$ equals to 1 for any Pareto-optimal operating point. Therefore, any Pareto inefficient operating point can be achieved with stability due to $\rho(\boldsymbol{J}) \leq \|\boldsymbol{J}\|_1 < 1$. However, in ad-hoc networks, the form of the Jacobi matrix $\boldsymbol{J}$ depends on the actual network topology and it is difficult to bound the spectral radius for a generic setting using certain matrix forms, such as l_1 norm or l_∞ norm. Alternatively, according to Theorem 6.10, we will numerically test the stability of the Pareto-optimal operating points in the simulation section.

6.5 Numerical Simulations

In this section, we numerically compare the performance of the existing 802.11 DCF protocol, the P-MAC protocol [QS02] and the proposed algorithms in this chapter.

We first illustrate the evolution of transmission probabilities of Algorithm 6.1 and 6.2. We simulate a single-cell network of 5 nodes. For each node, the initial transmission probability p_k^0 is uniformly distributed in $[0, 1]$ and a_k is uniformly distributed between 5 and 10. The stepsize in the gradient play is $\gamma = 0.02$. Fig. 6.6 compares the trajectory of the transmission probability updates in both Algorithm 6.1 and 6.2 in a single realization, under the assumption that node k can perfectly estimate the probability $\prod_{j\in\mathcal{K}\backslash\{k\}}(1-p_j)$, $\forall k \in \mathcal{K}$. The best response update converges in around 8 iterations and the gradient play experiences a more smooth trajectory and the same equilibrium is attained after 35 iterations. In

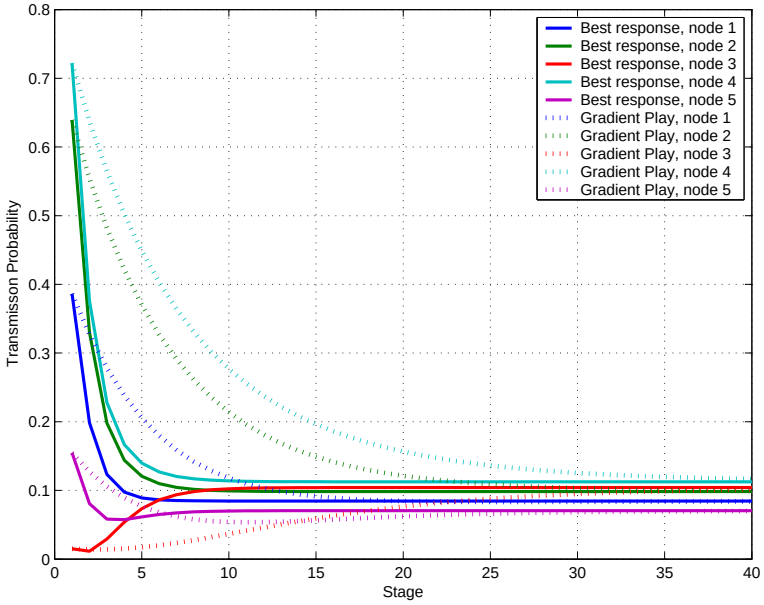

Figure 6.6: Dynamics of Algorithms 6.1 and 6.2.

addition, to illustrate how individual nodes can adaptively adjust their algorithm parameters and improve their throughput, we simulate a scenario with two traffic classes. Each traffic class consists of 5 nodes and the initial algorithm parameters of class 1 and 2 are $\phi_1 = 30$ and $\phi_2 = 60$, respectively. The discount factor in Algorithm 6.3 is $\delta = 0.05$. The blue dotted curve in Fig. 6.7 indicates that the operating point moves towards the red Pareto boundary until the outer loop detects that the desired efficiency is reached.

In practice, packet transmission over wireless links, e.g. IEEE 802.11 WLANs, involves extra protocol overheads, such as inter-frame space and packet header. Assuming these realistic communication scenarios, we compare various performance metrics, including throughput, fairness, convergence, and stability, between our proposed conjecture-based algorithms, the P-MAC protocol in [QS02], and the IEEE 802.11 DCF. To evaluate these metrics, the physical layer parameters need to be specified. In the simulation, we assume that each wireless device

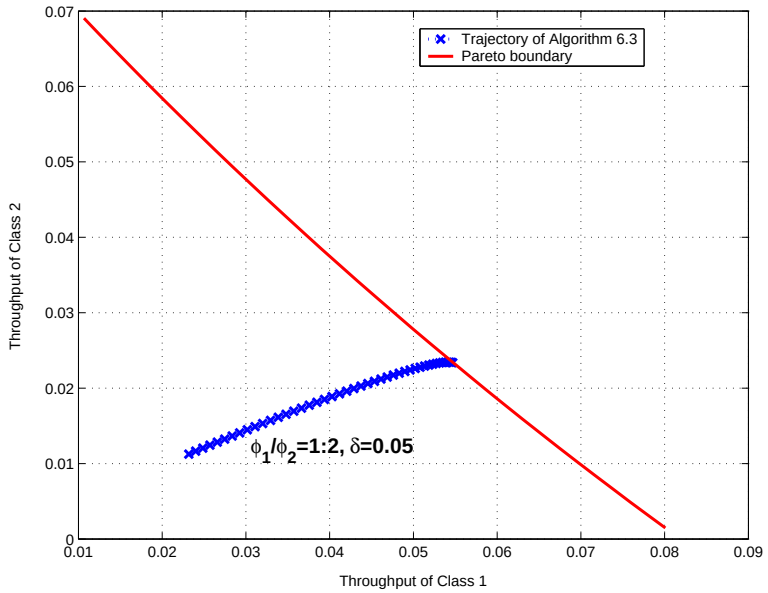

Figure 6.7: The trajectory of Algorithm 6.3.

operates at the IEEE 802.11a PHY mode-8 [80299], and the key parameters are summarized in Table 6.4. We assume no transmission errors and the RTS/CTS mechanism is disabled. The aggregate network throughput can be calculated using Bianchi's model [Bia00]

$$\mathcal{T} = \frac{P_s L_d}{(1-P_{tr})T_{slot} + P_s T_s + P_{tr} T_c - P_s T_c}, \tag{6.56}$$

where $P_s = \sum_{n=1}^{N} |\mathcal{F}_n| \cdot p_n \cdot (1-p_n)^{|\mathcal{F}_n|-1} \cdot \prod_{m \neq n} (1-p_m)^{|\mathcal{F}_n|}$ is the probability that a transmission occurring on the channel is successful, $P_{tr} = 1 - \prod_{n=1}^{N} (1-p_n)^{|\mathcal{F}_n|}$ is the probability that at least one transmission attempt happens, T_s is the average time of a successful transmission, and T_c is the average duration of a collision. The detailed derivation of T_s and T_c using the given network parameters in Table 6.4 can be found in [QS02, Bia00]. The parameters in P-MAC are set according to [QS02]. The contention window sizes in the IEEE 802.11 DCF are $CW_{min} = 16$ and $CW_{max} = 1024$. In Algorithm 6.3, individual nodes monitor the aggregate throughput to determine whether to adjust the parameter a_k. The numerical

Table 6.4: IEEE 802.11a PHY mode-8 parameters

Parameters	Value
Duration of an Idle Slot (T_{slot})	9 μs
Duration of PHY Header (T_{PHY})	20 μs
SIFS Time (T_{SIFS})	16 μs
DIFS Time (T_{DIFS})	34 μs
Propagation Delay (T_d)	1 μs
MAC Header (L_{MAC})	28 octets
Packet Payload Size (L_d)	2304 octets
ACK Frame Size (L_{ACK})	14 octets
Data Rate (R_t)	54 Mbps

results are obtained using a MAC simulation program in [Bia00]. Our comparison results are summarized as follows.

First, the throughput of the three algorithms is compared. We vary the total number of nodes K from 4 to 50, in which $\lceil K/2 \rceil$ nodes carry class-1 traffic and the remaining nodes carry class-2 traffic. The positive weights of class-1 and class-2 are $\chi_1 = 1$ and $\chi_2 = 0.5$. The initial parameters in Algorithm 6.3 are chosen to be $\phi_1 = 3K/\chi_1$ and $\phi_2 = 3K/\chi_2$. As shown in Fig. 6.8, both the conjecture-based algorithm and P-MAC significantly outperform the IEEE 802.11 DCF. The IEEE 802.11 DCF achieves the lowest throughput, because the lack of adaptation mechanism of the contention window size causes more frequent packet collisions as the number of nodes increases. Surprisingly, the performance of the conjectural equilibrium attained by Algorithm 6.3 achieves the maximum achievable throughput. It also outperforms P-MAC, because P-MAC uses approximation to derive closed-form expressions for the transmission

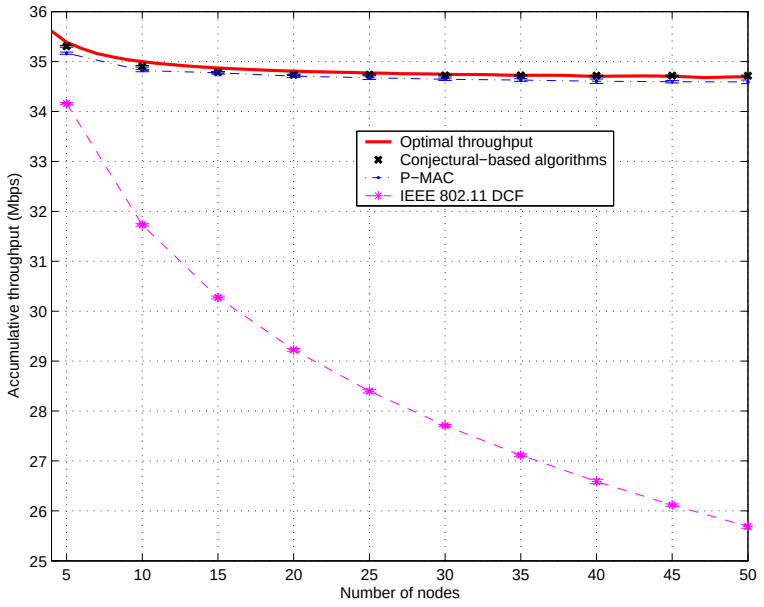

Figure 6.8: Comparison of the accumulative throughput in the IEEE 802.11 DCF, P-MAC, and conjecture-based algorithms. Error bars correspond to the standard deviation of the mean of the 100 measurements sampled at each point. The error bars in the remaining figures are as in this figure.

probabilities of different traffic class.

Next, we evaluate the short-term fairness of different protocols using the quantitative fairness index introduced in [QS02]

$$\mathbf{F} = \frac{\mu(\mathcal{T}_k/\chi_n)}{\mu(\mathcal{T}_k/\chi_n) + \sigma(\mathcal{T}_k/\chi_n)}, k \in \mathcal{F}_n \tag{6.57}$$

in which $\mathcal{T}_k$ denote the throughput of node k that belongs to traffic class n, and μ and σ are, respectively, the mean and the standard deviation of $\mathcal{T}_n/\chi_n$ over all the active data traffic flows. We simulate a transmission duration of 3 minutes. The stage duration in Algorithm 6.3 is set as 50 successful transmissions. As shown in Fig. 6.9, we can see that Algorithm 6.3 and P-MAC are comparable in their fairness performance and the achieved fairness index is always above

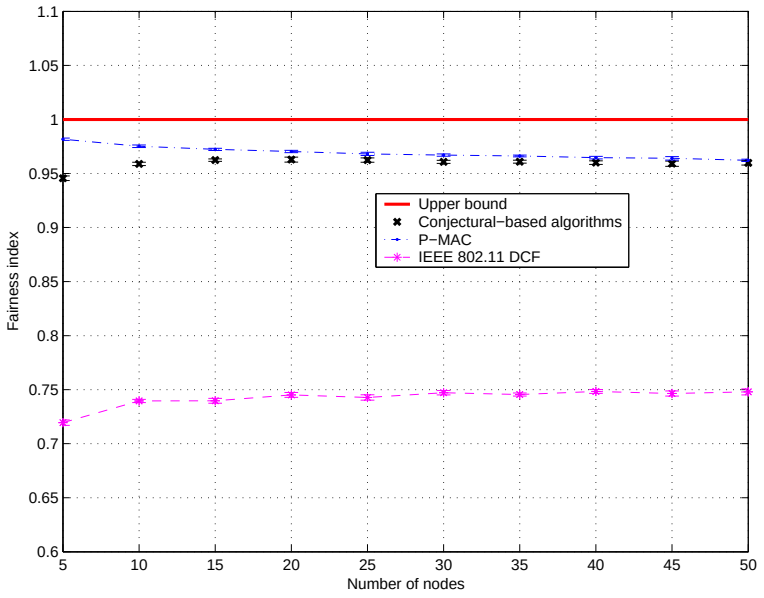

Figure 6.9: Comparison of the achieved fairness of the IEEE 802.11 DCF, P-MAC, and Algorithm 6.3.

0.95 regardless of the network configuration. On the other hand, the fairness performance of 802.11 DCF is much poorer than the previous two algorithms because the DCF protocol provides no fairness guarantee.

Last, in order to compare the convergence and the stability of different protocols for time-varying traffic, we simulate a network in which the number of active nodes fluctuates over time. In order to cope with traffic fluctuation, we slightly modify the outer loop in Algorithm 6.3. Once some nodes join or leave the network (this can be detected either by tracking the contention signal $\prod_{k\in\mathcal{K}}(1-p_k)$ or estimating the total number of nodes in the network [BT03]), the adaptation of a_k is activated. Specifically, if more nodes join the network, $a_k \leftarrow a_k(1+\delta)$, otherwise, $a_k \leftarrow a_k(1-\delta)$. At the beginning, $|\mathcal{F}_1| = |\mathcal{F}_2| = 25$. At stage 200, 15 class-1 and 15 class-2 nodes join the network. These nodes leave the network at the 400th stage. The algorithm parameter a_k is updated every 5 stages and the

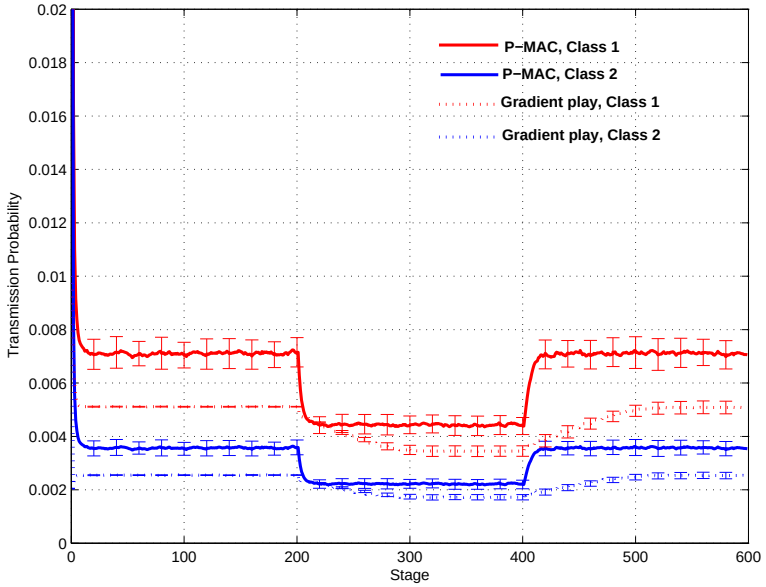

Figure 6.10: The dynamics of the transmission probabilities in P-MAC and Algorithm 6.3.

stepsize in the gradient play is $\gamma = 0.003$. Fig. 6.10 and Fig. 6.11 show the variation of the transmission probabilities for both traffic classes and the expected accumulative throughput over time. P-MAC does not converge due to the lack of feedback control, which agrees with the observation about the instability of P-MAC reported in [CCL08]. In addition, the optimal transmission probabilities computed by P-MAC and the conjecture-based algorithms are different under the same network parameters because of the approximation used in P-MAC. As shown in Fig. 6.10, nodes deploying P-MAC transmit with a higher probabilities than the conjecture-based algorithms, which creates a more congested environment. As a result, the accumulative throughput achieved by P-MAC is slightly lower than the optimal throughput. In contrast, the conjecture-based algorithms enable the nodes adaptively tune their parameters a_k to maximize the network throughput while maintaining the weighted fairness as well as the system stability. As shown in Fig. 6.10 and Fig. 6.11, during stage [200,300] and

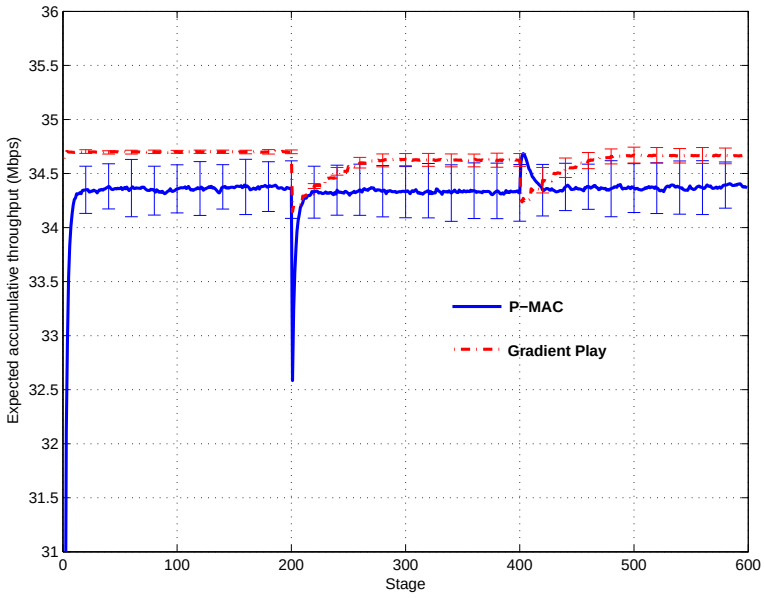

Figure 6.11: The dynamics of the accumulative throughput in P-MAC and Algorithm 6.3.

[400,470], both the best response and the gradient play autonomously adapt their parameter a_k until it converges to the optimal operating point. As discussed before, the best response learning converges faster than the gradient play learning. To give a quantitative measure of the stability, the standard deviations of the expected accumulative throughput in Fig. 6.11 for different algorithms satisfy $\sigma(\mathcal{T}_{P-MAC}^{Expected})/\sigma(\mathcal{T}_{CB}^{Expected}) \approx 7$ and the actual achieved accumulative throughput satisfy $\sigma(\mathcal{T}_{P-MAC}^{Actual})/\sigma(\mathcal{T}_{CB}^{Actual}) \approx 2$. We can see that, thanks to the inherent feedback control mechanism, both conjecture-based algorithm exhibit superior stability performance than P-MAC.

We also simulate the evolution trajectory of the transmission probabilities of the proposed Algorithm 6.1 and the algorithm in [MHC09]. Both algorithms are essentially the best-response based algorithms. Specifically, we consider a network with $K = 6$. The peak data rates for different nodes are $r_1 = 6$, $r_2 = 36$, $r_3 = 9$, $r_4 = 12$, $r_5 = 18$, and $r_6 = 54$, all in Mbps. We apply the algorithm in

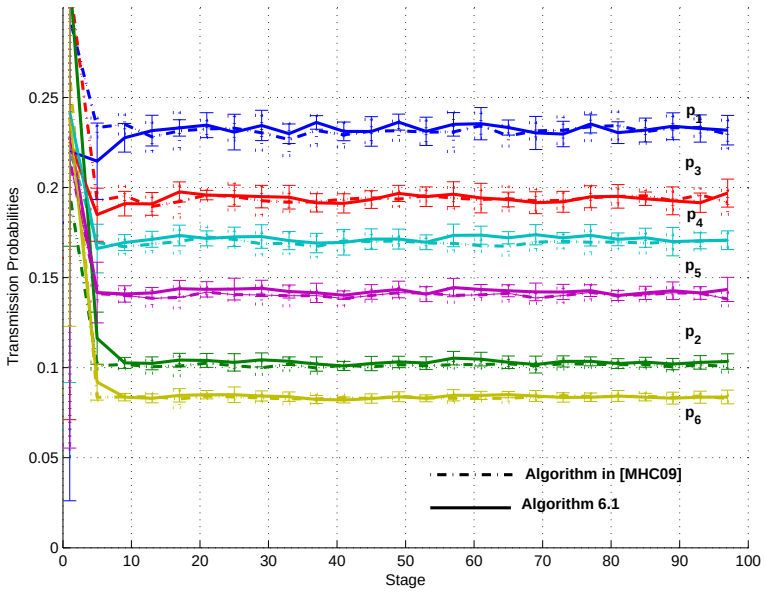

Figure 6.12: Comparison between Algorithm 6.1 and the algorithm in [MHC09].

[MHC09] to solve the following network utility maximization problem:

$$\max_{\mathbf{p}\in P} \sum_{k\in\mathcal{K}} \frac{1}{1-\alpha}\Big[r_k p_k \prod_{j\in\mathcal{K}\setminus\{k\}} (1-p_j)\Big]^{1-\alpha}, \tag{6.58}$$

in which $\alpha = 2$. The optimal solution corresponds to the belief configuration $a_1 = 2.03, a_2 = 3.93, a_3 = 2.32, a_4 = 2.55, a_5 = 2.97$, and $a_6 = 4.74$. The trajectory of both algorithms are shown in Fig. 6.12. We can see that, both algorithms converge very fast and oscillate around the neighborhood to the optimal solution after several iterations. However, as we discussed before, the algorithm in [MHC09] requires individual nodes to decode all the received packet headers and estimate the transmission probabilities of the other nodes individually, which introduces a great internal computational overhead when the network size grows large. In contrast, nodes deploying Algorithm 6.1 only have to estimate the probability of having a free channel without the need of decoding all the packets, which substantially reduces their computational efforts.

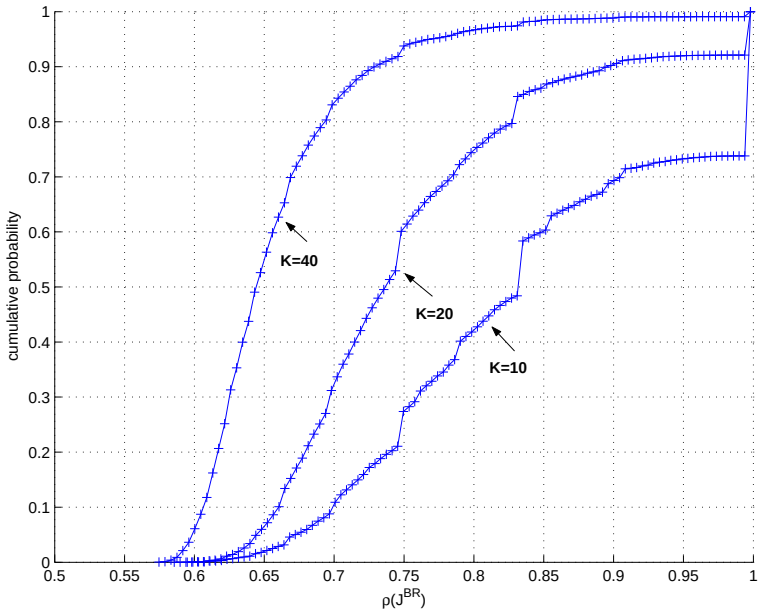

Figure 6.13: Cumulative distribution function of $\rho(\mathbf{J}^{BR})$ in ad-hoc networks.

We simulate the performance of the proposed algorithms in an ad-hoc network contained in a $100m \times 100m$ square area. Nodes in the square area are placed in the random manner. Two nodes can interfere with each other if their distance is no more than $40m$, i.e. $D_{th} = 40m$. We simulate three scenarios with the node numbers $K = \{10, 20, 40\}$. The Pareto-efficient point that we select is the associated operating point with the link weighted vector $\omega_k = 1, 1 \leq k \leq K/2$, and $0.5, K/2 < k \leq K$ in (6.53). We can see from Fig. 6.13 that, $\rho(\mathbf{J}^{BR}) \leq 1$ holds for all the simulated topologies. As shown in Fig. 6.13, in some realizations, $\rho(\mathbf{J}^{BR}) = 1$, and hence, the associate operating points are not asymptotically stable. This will occur when two nodes interfere with each other and they do not interfere and are not interfered by the remaining nodes in the entire ad-hoc network. On the other hand, the stability improves as the number of nodes increases. As long as the density of nodes is sufficiently large, the stability of the conjecture-based algorithm on the Pareto-efficient operating point can be

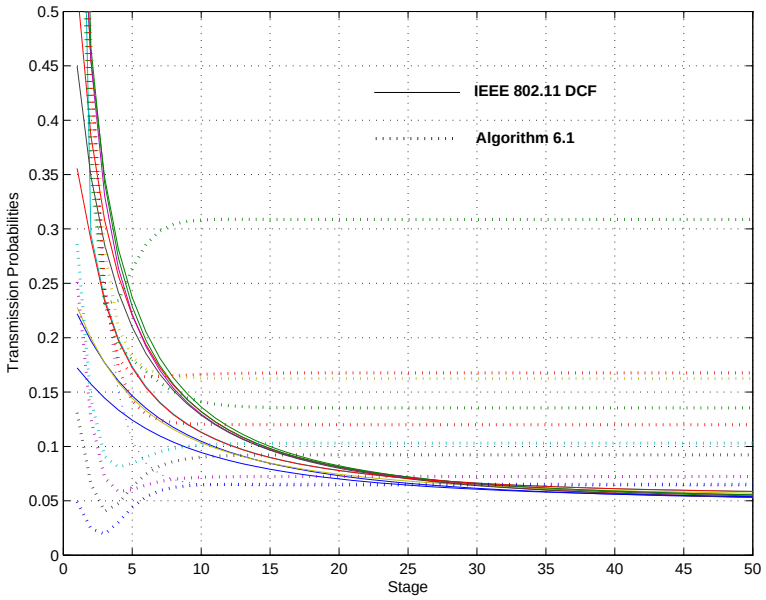

Figure 6.14: Transmission probabilities of Algorithm 6.1 and the IEEE 802.11 DCF in ad-hoc networks.

achieved. Fig. 6.14 and Fig. 6.15 show the evolution of transmission probabilities and accumulative throughput for the IEEE 802.11 DCF and Algorithm 6.1 in a 10-node ad-hoc network with a randomly generated topology. The trajectory of the IEEE 802.11 DCF is obtained using the model in [LTH07]. The parameter a_k in Algorithm 6.1 is chosen to be $|O_k|$. The intuition behind is that, if $|O_k| = 0$, node k can transmit at the maximal probability without interfering with any node. On the other hand, if $|O_k|$ is large, node k should backoff adequately such that the reciprocity can be established. As shown in the figures, Algorithm 6.1 converges faster and achieves higher throughput than DCF. Similar results have been observed in the other simulated topologies.

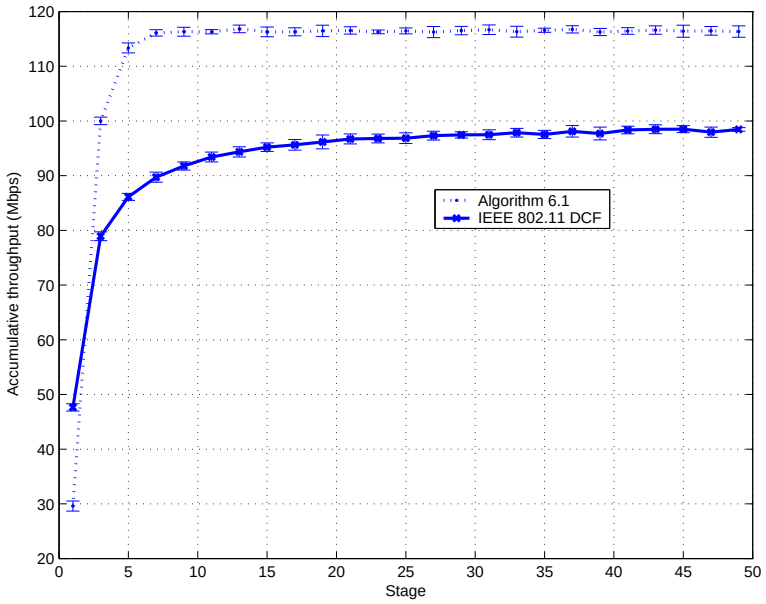

Figure 6.15: Accumulative throughput of Algorithm 6.1 and the IEEE 802.11 DCF in ad-hoc networks.

6.6 Discussions

6.6.1 Comparison between Type I and Type II games

The properties of Type II games have been investigated in the previous chapter. Table 6.5 summarizes some similarities and differences between both types of games. First, the two algorithms exhibit different properties under the best response dynamics. In Type I games, the stable CE may not be globally convergent. However, the local stability of a CE implies its global convergence in Type II games. Second, it is shown that any operating point that is arbitrarily close to the Pareto boundary of the utility region of Type I games is a stable CE. Similarly, the entire Pareto boundary of Type II games is also stable. At last, different relationships between the parameter selection and the achieved utility at equilibrium have been observed for the two types of games. In particular, in

Table 6.5: Comparison between Type I and Type II games.

Games	Best response dynamics	Stability vs. efficiency	Fairness vs. parameter selection
Type I	local stability $\Leftarrow$ global convergence	stable at near-Pareto-optimal points	$u_n \propto \tau_n/\lambda_n$
Type II	local stability $\Leftrightarrow$ global convergence	stable at Pareto boundary	$\omega_n = \tau_n/\lambda_n$ at Pareto boundary

Type I games, user k's utility u_k is approximately proportional to the inverse of the parameter λ_k in its belief function. In contrast, in Type II games, if the CE is Pareto-optimal, as addressed in Remark 5.5, the ratio τ_k/λ_k coincide with the weight ω_k assigned to user k in the proportional fairness objective function. In other words, based on the definition of proportional fairness [Kel97], we know

$$\sum_{k=1}^{K} \frac{\tau_k(u'_k - u^*_k)}{\lambda_k u^*_k} \leq 0, \tag{6.59}$$

in which $(u'_1, u'_2, \ldots, u'_K)$ is the users' achieved utility associated with any other feasible joint action and $(u^*_1, u^*_2, \ldots, u^*_K)$ is the optimal achieved utility for problem (5.8) with $\omega_k = \tau_k/\lambda_k$ and $\sum_{k=1}^{K} \omega_k = 1$.

6.6.2 Pricing Mechanism vs. Conjectural Equilibrium

In order to achieve Pareto-optimality, information exchanges among users is generally required in order to collaboratively maximize the system efficiency. The existing cooperative communication scenarios either assume that the information about all the users is gathered by a trusted moderator (e.g. access point, base station, selected network leader etc.), to which it is given the authority to centrally divide the available resources among the participating users, or, in the

distributed setting, users exchange price signals (e.g. the Lagrange multipliers for the dual problem) that reflect the "cost" for consuming per unit constrained resources to maximize the social welfare and reach Pareto-optimal allocations. As an important tool, the pricing mechanism has been applied in the distributed optimization of various communication networks [CLC07]. However, we would like to point out that, the pricing mechanism generally requires repeated coordination information exchange among users in order to determine the optimal actions and achieve the Pareto-optimality. In contrast, for the linear coupled games, since the specific structure of the utility function is explored, the CE approach is able to calculate the Pareto efficient operating point in a distributed manner, without any real-time information exchange among users. In fact, the underlying coordination is implicitly implemented when the participating users initialize their belief parameters. Once the belief parameters are properly initialized by the protocols, using the proposed dynamic update algorithms, individual users are able to achieve the Pareto-optimal CE solely based on their individual local observations on their states and no message exchange is needed during the convergence process. Therefore, the conjecture equilibrium approach is an important alternative to the pricing-based approach in the linearly coupled games.

6.7 Concluding Remarks

In this chapter, we propose distributed solutions that enable autonomous nodes to improve their throughput performance in random access networks. It has been observed in the context of random access control that a tragedy of commons might take place if nodes behave selfishly and myopically. Hence, we investigate whether forming internal belief functions and learning the impact of various actions can alter the interaction outcome among these intelligent nodes. Specifically, two

distributed mechanisms are proposed to dynamically update individual nodes' transmission probabilities. It is analytically proven that the entire throughput region essentially consist of stable conjectural equilibria. In addition, we prove that the conjecture-based approach achieves the weighted fairness for heterogeneous traffic classes and extend the distributed learning solutions to ad-hoc networks. Simulation results have shown that the proposed algorithms achieve significant performance improvement against existing protocols, including the IEEE 802.11 DCF and the P-MAC protocol, in terms of not only fairness and throughput but also convergence and stability. A potential future direction is to investigate how to detect and prevent misbehavior.

CHAPTER 7

Conclusion

This dissertation illustrates the optimal strategies for users to improve their performance in an informationally decentralized multiuser communication environment. First, we propose and investigate a new game model, which we refer to as additively coupled sum constrained games, in which each player is subject to a sum constraint and its utility is additively impacted by the remaining users' actions. We derive sufficient conditions under which a pure unique NE exist and best response dynamics converges globally and linearly to the NE without any real-time information exchange among users. Second, we investigate the multi-channel power control game to understand how to further improve the performance of inefficient NE in ACSCG. Specifically, we consider game theoretic solutions Stackelberg equilibrium and conjectural equilibrium. It is shown that if a foresighted leader can explore the inter-user coupling by considering the utility structures and model its own state (i.e. experienced interference) as a function of its own action, a leader forming proper conjectures can improves both its own utility as well as the utilities of its competitors, even if it has no a priori knowledge of their private information. Third, we propose and investigate linearly coupled games in which users' utilities are linearly impacted by their competitors' actions. For linearly coupled games, we prove that if every user is playing the CE strategy with appropriate belief configuration, the entire system can be induced to a stable Pareto-optimal operating point without exchanging any real-time information .

References

[80299] "IEEE 802.11a, Part 11: Wireless LAN Medium Access Control and Physical Layer specifications: High-speed Physical Layer in the 5 GHz Band, Supplement to IEEE 802.11 Standard.", September 1999.

[AA03] E. Altman and Z. Altman. "S-modular games and power control in wireless networks." *IEEE Transactions on. Automatic Control*, **48**:839–842, May 2003.

[AAG08] E. Altman, K. Avrachenkov, and A. Garnaev. "Closed form solutions for symmetric water filling games." In *Proceeding of IEEE Conference on Computer Communications*, pp. 673–681, April 2008.

[ABE06] E. Altman, T. Boulogne, R. El-Azouzi, T Jimenez, and L. Wynter. "A survey on networking games." *Computers and Operations Research*, **33**:286–311, February 2006.

[Ber97] C. Berge. *Topological Spaces*. Dover Publications, 1997.

[BGK85] J. Bulow, J. Geanakoplos, and P. Klemperer. "Multimarket oligopoly: strategic substitutes and strategic complements." *Journal of Political Economy*, **93**:488–511, 1985.

[Bia00] G. Bianchi. "Performance Analysis of the IEEE 802.11 Distributed Coordination Function." *IEEE Journal on Selected Areas in Communications*, **18**:535–547, March 2000.

[BT97] D. P. Bertsekas and J. N. Tsitsiklis. *Parallel and Distributed Computation*. Prentice Hall, 1997.

[BT03] G. Bianchi and I. Tinnirello. "Kalman Filter Estimation of the Number of Competing Terminals in an IEEE 802.11 Network." In *Proceedings of IEEE INFOCOM*, 2003.

[BV04] S. Boyd and L. Vandenberghe. *Convex Optimization*. Cambridge University Press, 2004.

[CCL08] T. Cui, L. Chen, and S. H. Low. "A Game-Theoretic Framework for Medium Access Control." *IEEE Journal on Selected Areas in Communications*, **7**:1116–1127, September 2008.

[CGA05] M. Cagalj, S. Ganeriwal, I. Aad, and J. P. Hubaux. "On selfish behavior in CSMA/CA networks." In *Proceeding of IEEE International Conference on Computer Communications*, March 2005.

[CHC07] R. Cendrillon, J. Huang, M. Chiang, and M. Moonen. "Autonomous spectrum balancing for digital subscriber lines." *IEEE Transactions on Signal Processing*, **55**:4241–4257, August 2007.

[CJ89] D. Chiu and R. Jain. "Analysis of the Increase/Decrease Algorithms for Congestion Avoidance in Computer Networks." *Journal of Computer Networks and ISDN*, **17**:1–14, June 1989.

[CLC07] M. Chiang, S. H. Low, A. R. Calderbank, and J. C. Doyle. "Layering as optimization decomposition." *Proceedings of the IEEE*, **95**:255–312, January 2007.

[CMS05] B. Colson, P. Marcotte, and G. Savard. "Bilevel programming: A survey." *A quarterly Journal of Operation Research*, **3**:87–107, July 2005.

[CSK03] S. T. Chung, J. L. Seung, J. Kim, and J. Cioffi. "A game-theoretic approach to power allocation in frequency-selective Gaussian interference channels." In *Proceeding of IEEE International Symposium on Information Theory*, p. 316, June 2003.

[CY01] H. Chen and D. Yao. *Fundamentals of Queueing Networks: Performance, Asymptotics, and Optimization*. Springer, 2001.

[CYM06] R. Cendrillon, W. Yu, M. Moonen, J. Verlinden, and T. Bostoen. "Optimal multiuser spectrum balancing for digital subscriber lines." *IEEE Transactions on Communications*, **54**:922–933, May 2006.

[DM92] C. Douligeris and R. Mazumdar. "A game theoretic perspective to flow control in telecommunication networks." *Journal of The Franklin Institute*, **329**:383–402, March 1992.

[Dub86] P. Dubey. "Inefficiency of Nash equilibria." *Mathematics of Operations Research*, **11**:1–8, February 1986.

[EPT07] R. Etkin, A. Parekh, and D. Tse. "Spectrum sharing for unlicensed bands." *IEEE Journal on Selected Areas in Communications*, **25**:517–528, April 2007.

[FH06] M. Felegyhazi and J. P. Hubaux. "Game theory in wireless networks: a tutorial." Technical Report LCA-REPORT-2006-002, EPFL Technical Report, February 2006.

[FJQ04] C. Figuieres, A. Jean-Marie, N. Querou, and M. Tidball. *Theory of Conjectural Variations*. World Scientific Publishing, 2004.

[FT91] D. Fudenberg and J. Tirole. *Game Theory.* MIT Press, Cambridge, MA, 1991.

[GD03] A. Granas and J. Dugundji. *Fixed Point Theory.* Springer-Verlag, 2003.

[GM80] D. Gabay and H. Moulin. *On the uniqueness and stability of Nash equilibria in noncooperative games*, pp. 271–293. North-Holland, 1980.

[GS06] P. Gupta and A. L. Stolyar. "Optimal Throughput Allocation in General Random-Access Networks." In *Proceeding of CISS*, March 2006.

[Hah77] F. H. Hahn. "Exercises in conjectural equilibrium analysis." *Scandinavian Journal of Economics*, **79**:210–226, 1977.

[Hay05] S. Haykin. "Cognitive radio: Brain-empowered wireless communications." *IEEE Journal on Selected Areas in Communications*, **23**:201–220, February 2005.

[Hay07] S. Haykin. "Cognitive dynamic systems." In *Proceeding of IEEE International Conference on Acoustics, Speech, and Signal Processing*, volume 4, pp. 1369–1372, April 2007.

[HBH06] J. Huang, R. Berry, and M. Honig. "Distributed interference compensation for wireless networks." *IEEE Journal on Selected Areas in Communications*, **24**:1074–1084, May 2006.

[HJ81] R. A. Horn and C. R. Johnson. *Matrix Analysis.* Cambridge University Press, 1981.

[JK02] Y. Jin and G. Kesidis. "Equilibria of a noncooperative game for heterogeneous users of an Aloha networks." *IEEE Communication Letters*, **6**:282–284, July 2002.

[JLL09] E. A. Jorswieck, E. G. Larsson, M. Luise, and H. V. Poor. "Game theory in signal processing and communications." *IEEE Signal Process. Magazine*, **26**, September 2009.

[JT06] A. Jean-Marie and M. Tidball. "Adapting behaviors through a learning process." *Journal of Economic Behavior and Organization*, **60**:399–422, 2006.

[Kel97] F. P. Kelly. "Charging and rate control for elastic traffic." *European Transactions on Telecommunications*, **8**:33–37, 1997.

[KLO95] Y. A. Korilis, A. A. Lazar, and A. Orda. "Architecting noncooperative networks." *IEEE Journal on Selected Areas in Communications*, **13**:1241–1251, Sep. 1995.

[Kum80] S. Kumagai. "An implicit function theorem: Comment." *Journal of Optimization Theory and Applications*, **31**:285–288, June 1980.

[LA02] R. La and V. Anantharam. "Utility based rate control in the internet for elastic traffic." *IEEE/ACM Transactions on Networking*, **10**:271–286, April 2002.

[LCC07] J. Lee, M. Chiang, and R. A. Calderbank. "Utility-optimal random-access control." *IEEE Transactions on Wireless Communications*, **6**:2741–2751, July 2007.

[LDA09] S. Lasaulce, M. Debbah, and E. Altman. "Methodologies for analyzing equilibria in wireless games." *IEEE Signal Processing Magazine*, **26**:41–52, September 2009.

[LTH07] J. Lee, A. Tang, J. Huang, M. Chiang, and A. R. Calderbank. "Reverse-engineering MAC: A non-cooperative game model." *IEEE Journal on Selected Areas in Communications*, **25**:1135–1147, August 2007.

[LZL07] C. Long, Q. Zhang, B. Li, H. Yang, and X. Guan. "Non-Cooperative Power Control for Wireless Ad Hoc Networks with Repeated Games." *IEEE Journal on Selected Areas in Communications*, **25**:1101–1112, August 2007.

[MHC09] A. Mohsenian-Rad, J. Huang, M. Chiang, and V. Wong. "Utility-Optimal Random Access: Optimal Performance Without Frequent Explicit Message Passing." *IEEE Transactions on Wireless Communications*, **8**:898–911, February 2009.

[MM85] J. Massey and P. Mathys. "The collision channel without feedback." *IEEE Transactions on Information Theory*, **31**:192–204, 1985.

[MMR09] R. T. B. Ma, V. Misra, and D. Rubenstein. "An Analysis of Generalized Slotted-Aloha Protocols." *IEEE/ACM Transactions on Networking,*, **17**:936–949, June 2009.

[MS96] D. Monderer and L. S. Shapley. "Potential games." *Games and Economic Behavior*, **14**:124–143, May 1996.

[MW00] J. Mo and J. Walrand. "Fair end-to-end window-based congestion control." *IEEE Transactions on Networking*, **8**:556–567, October 2000.

[MW01] A. MacKenzie and S. Wicker. "Game theory and the design of self-configuring, adaptive wireless networks." *IEEE Communications Magazine*, **39**:126–131, November 2001.

[NKG00] T. Nandagopal, T. E. Kim, X. Gao, and V. Bharghhavan. "Achieving MAC layer fairness in wireless packet networks." In *Proceedings of ACM Mobicom*, 2000.

[Now06] M. Nowak. "Five Rules for the Evolution of Cooperation." *Science*, **314**:1560–1563, 2006.

[NRT07] N. Nisan, T. Roughgarden, E. Tardos, and V. Vazirani. *Algorithmic Game Theory*. Cambridge University Press, September 2007.

[PC06] D. P. Palomar and M. Chiang. "A tutorial on decomposition methods for network utility maximization." *IEEE Journal on Selected Areas in Communications*, **24**:1439–1451, 2006.

[PPR07] O. Popescu, D. Popescu, and C. Rose. "Simultaneous water filling for mutually interfering systems." *IEEE Transactions on Wireless Communications*, **6**:1102–1113, March 2007.

[QS02] D. Qiao and K. G. Shin. "Achieving efficient channel utilization and weighted fairness for data communications in IEEE 802.11 WLAN under the DCF." In *Proceeding of IWQoS*, May 2002.

[Rap96] T. S. Rappaport. *Wireless Communications*. Prentice-Hall, Englewood Cliffs, NJ, 1996.

[Ros65] J. Rosen. "Existence and uniqueness of equilibrium points for concave n-person games." *Econometrica*, **33**:520–534, July 1965.

[SBH08] C. Shi, R. Berry, and M. Honig. "Distributed interference pricing for OFDM wireless networks with non-seperable utilities." In *Proceeding of Conference on Information Sciences and Systems*, pp. 19–21, 2008.

[SBP06] G. Scutari, S. Barbarossa, and D. P. Palomar. "Potential games: A framework for vector power control problems with coupled constraints." In *Proceeding of IEEE International Conference on Acoustics, Speech, and Signal Processing*, May 2006.

[Sha48] C. E. Shannon. "A mathematical theory of communication." *Bell System Technical Journal*, **27**:379423, 1948.

[SLS07] K. W. Shum, K.-K. Leung, and C. W. Sung. "Convergence of iterative waterfilling algorithm for Gaussian interference channels." *IEEE Journal on Selected Areas in Communications*, **25**:1091–1100, August 2007.

[Smi82] J. M. Smith. *Evolution and the Theory of Games*. Cambridge University Press, 1982.

[SPB08] G. Scutari, D. P. Palomar, and S. Barbarossa. "Optimal linear precoding strategies for wideband noncooperative systems based on game theory - Part II: Algorithms." *IEEE Transactions on Signal Processing*, **56**:1250–1267, Mar. 2008.

[SPG07] Y. Shoham, R. Powers, and T. Grenager. "If multi-agent learning is the answer, what is the question?" *Artificial Intelligence*, **171**:365–377, May 2007.

[Spi68] M. R. Spiegel. *Mathematical Handbook of Formulas and Tables*. McGraw-Hill, 1968.

[Top98] D. M. Topkis. *Supermodularity and Complementarity*. Princeton University Press, 1998.

[WH98] M. P. Wellman and J. Hu. "Conjectural equilibrium in multiagent learning." *Machine Learning*, **33**:179–200, 1998.

[Yao95] D. Yao. "S-modular games with queueing applications." *Queueing Systems: Theory and Applications*, **21**:449–475, 1995.

[YGC02] W. Yu, G. Ginis, and J. Cioffi. "Distributed multiuser power control for digital subscriber lines." *IEEE Journal on Selected Areas in Communications*, **20**:1105–1115, June 2002.

[YL06] W. Yu and R. Lui. "Dual methods for nonconvex spectrum optimization of multicarrier systems." *IEEE Transactions on Communications*, **54**:1310–1322, July 2006.

[ZD92] Z. Zhang and C. Douligeris. "Convergence of synchronous and asynchronous greedy algorithm in a multiclass telecommunications environment." *IEEE Transactions on Communications*, **40**:1277–1281, August 1992.